

We thank reviewer 1 for the insightful comments, and for pointing to inconsistencies. We apologize for needing more time than anticipated to address all comments, but we believe that we have been able to address most issues, and that we have significantly strengthened the manuscript.

Before addressing the comments we would like to mention that we have modified the abbreviation of the O₃ health exposure metric (6 monthly daily maximum 1-h concentration) from M6M to 6mDMA1 (and accordingly M3M to 3mDMA1) as the latter seems to be commonly used in other works.

In the following we have placed the numbered reviewer comments in boxes. Our reply to the reviewer is in **blue font**, the changes to the manuscript in **red font**.

We also attach a revised version of manuscript and supplement with tracked changes compared to the first version.

REVIEWER 1 comments:

The manuscript presents a detailed summary of the methodology and validation for the TM5-FASST screening tool. TM5-FASST is a simplified tool that uses linear source receptor relationships of air pollutant precursor species across 56 geographical source regions (plus aviation and shipping) to calculate the response in air pollutant concentrations at both the surface and 25 vertical layers in the atmosphere. The difference in concentrations can then be used to calculate the change in a number of air pollution impact metrics related to human health, climate and crop production. The tool allows for the impact from different emissions scenarios to be explored without the need to run more detailed composition climate models. The manuscript provides a through description of the underlying methodology of TM5-FASST as well as an evaluation of the air pollutant predictions and impact metrics against a number of different sources. It provides a good reference for the TM5-FASST tool for use in future studies.

Major General Comments

1) Whilst I understand that TM5-FASST is not meant to replicate full scale model simulations, it would be good to bring together the limitations together into a more coherent section, possibly within the discussion section. Throughout the manuscript specific sections of the text mention aspects that TM5-FASST will not be able to predict e.g. changing spatial distribution of emissions and chemical regime. It would make sense for the reader to have these all in one place.

REPLY: Thank you for the suggestion. We have substantially edited and extended the discussion section to address the limitations of the tool..

CHANGES TO MANUSCRIPT: *New section 4:*

4 Discussion

Although the methodology of a reduced-form air quality model, based on linearized emission – concentration sensitivities is not new and has been successfully applied in earlier studies (Alcamo et al., 1990), the concept of directly linking pollutant emission scenarios to a large set of impacts across various policy fields, in a global framework, have made TM5-FASST a highly requested tool in a broad field of applications. HTAP1 showed that TM5 source-receptor results

(for the large HTAP1 regions) were in most cases similar to the median model results of more than 10 global models, lending additional trust to the model performance (e.g. Anenberg et al., 2014; Dentener et al., 2010; Fiore et al., 2009). The results in the previous sections have outlined its strengths and weaknesses. The major strength of the tool is its mathematical simplicity allowing for a quick processing of large sets of scenarios or scenario ensembles. An extreme example is the full family of SSP scenarios delivered by all participating Integrated Assessment Models, for decadal time slices up to 2050, constituting a batch of 594 scenarios of which a selection of 124 scenarios was analysed with TM5-FASST in the study by Rao et al. (2017). Further, the tool is unique in having a broad portfolio of implemented impact modules which are evaluated consistently over the global domain from the same underlying pollutant field which creates a basis for a balanced evaluation of trade-offs and benefits attached to policy options.

On the other hand, the reduced-form approach inevitably encompasses a number of caveats and uncertainties that have to be considered with care and which are discussed in the following sections.

4.1 Issues related to the reduced-form approach

The reliability of the model output in terms of impacts depends critically on the validity of the linearity assumption for the relevant exposure metrics (in particular secondary components), which becomes an issue when evaluating emission scenarios that deviate strongly from the base and -20% perturbation on which the current FASST SRs are based. The evaluation exercise indicated that non-linearity effects in PM_{2.5} and O₃ metrics in general lead to a higher bias for stringent emission reductions (towards -80% and beyond) than for strong emission increases compared to the RCP2000 base case, but over-all remain within acceptable limits when considering impacts. Indeed, because of the thresholds included in exposure-response functions, the higher uncertainty on low (below-threshold) pollutant levels from strong emission reductions has a low weight in the quantification of most impacts. In future developments the available extended-range (-80%, +100%) emission perturbation simulations could form the basis of a more sophisticated parameterization including a bias correction based on second order terms following the approach by Wild et al. (2012) both for O₃ and secondary PM_{2.5}. The break-down of the linearity at low emission strengths is relevant for O₃ and O₃ exposure metrics as the implementation of control measures in Europe and the US has already substantially lowered NO_x levels over the past decade, gradually modifying the prevailing O₃ formation regime from NO_x-saturated (titration regime) to NO_x-limited (Jin et al., 2017). Ozone impact on agricultural crop production is deemed to be the least robustly quantified impact category included in FASST, in particular when evaluated from the threshold-based AOT40 metric, and has to be interpreted as indicative order-of-magnitude estimate. In an integrated assessment perspective of evaluating trade-offs and benefits of air pollutants scenarios, the dominant impact category however appears to be human health (Kitous et al., 2017; OECD, 2016; UNEP, 2011) where TM5-FASST provides reliable estimates. Another issue for caution relates to the FASST analysis of emission scenarios with spatial distribution that differs from the FASST reference scenario (RCP year 2000). The definition of the source regions when establishing the SR matrices implicitly freezes the spatial distribution of pollutant emissions within each region, and therefore the reduced-form model cannot deal with intra-regional spatial shifts in emissions. In practice this is not expected to introduce large errors as anthropogenic emissions are closely linked to populated areas and road networks of which the extent may change, but much less so the spatial distribution. It can be a problem when going far back in time, when large patterns of migration and land development occurred, while in RCP scenarios relatively simple expansions of emissions into the future did not assume huge shifts in regional emission patterns.

The implicitly fixed emission spatial distribution may also become relevant when making a sector apportionment of pollutant concentrations and impacts. Source-Receptor relations are indeed particularly useful to evaluate the apportionment of emission sources (in terms of economic sector as well as source regions) to pollutant levels in a given receptor. However, as

the TM5-FASST_v0 source-receptor matrices were not segregated according to economic sectors, an emission reduction of 20% for a given source region is implicitly considered as a 20% reduction in all sectors simultaneously. Although the atmospheric chemistry and transport of emissions is in principle independent of the specific source, a difference in the sector-specific SR matrices may occur due to differences in temporal and spatial (horizontal/vertical) distribution of the sources. Therefore apportionment studies on sectors which have a significantly different emission spatial distribution than other sectors in the same region should be interpreted with care. In particular impacts of off-shore flaring cannot be assessed with TM5-FASST because those emissions were not included in the RCP base emissions. This limitation however does not apply to international shipping and aviation for which specific SR matrices have been established.

Comparing to earlier studies and reference data, the performance of TM5-FASST with respect to climate metrics is satisfactory, with the exception of BC forcing which is at the low side of current best estimates. In fact, earlier TM5-FASST assessments where climate metrics were provided (UNEP, 2011; UNEP and CCAC, 2016) applied a uniform adjustment factor of 3.6 on BC forcing, in line with the observation by that many models underestimate atmospheric absorption attributable to BC with a factor of almost 3. In TM5-FASST, an adjustment factor of 3.6 leads to a global forcing by anthropogenic BC of 600 mW m⁻². This tuning factor implicitly accounts for not-considered BC forcing contributions and for a longer BC atmospheric lifetime than implemented in the TM5 model and the resulting FASST SR coefficients.

The current version of TM5-FASST is missing some source-receptor relations which may introduce a bias in estimated PM_{2.5} and O₃ responses upon emission changes. The omission of secondary organic PM in TM5 is estimated to introduce a low bias in the base concentration of the order of 0.1 µg m⁻³ as global mean however with regional levels in Central Europe and China up to 1 µg m⁻³ in areas where levels of primary organic matter are reaching 20 µg m⁻³ (Farina et al., 2010) indicating a relatively low contribution of SOA to total PM_{2.5}. O₃ formation from CO is included in the TM5 base simulations, but no SR matrices for the FASST source region definition are available. Based on the HTAP1 CO perturbation simulations with TM5, we estimate that a doubling of anthropogenic CO emissions contributes with 1 – 1.9 ppb in annual mean O₃ over Europe, 1.3 -1.9 ppb over North-America, 0.7-1.0 ppb over South Asia and 0.3 – 1.5 ppb over East-Asia. Development of CO-O₃ SRs is an important issue for the further development of the tool.

4.2 Inter-annual meteorological variability

A justified critique on the methodology applied to construct the FASST SRs relates to the use of a single and fixed meteorological year 2001, implying possible unspecified biases in pollutant concentrations and source-receptor matrices compared to using a ‘typical meteorological/climatological year’. We followed the choice of the meteorological year 2001 made for the HTAP1 exercise. As the North-Atlantic Oscillation (NAO) is an important mode of the inter-annual variability in pollutant concentrations and long range transport (Christoudias et al., 2012; Li et al., 2002; Pausata et al., 2013; Pope et al., 2018), the HTAP1 expectation was that this year was not an exceptional year for long-rang pollutant transport - e.g. for the North-Atlantic region, as indicated by a North Atlantic Oscillation (NAO) index close to zero for that year (<https://www.ncdc.noaa.gov/teleconnections/nao/>). The HTAP1 report (Dentener et al., 2010) also suggested that “Inter-annual differences in SR relationships for surface O₃ due to year-to-year meteorological variations are small when evaluated over continental-scale regions. However, these differences may be greater when considering smaller receptor regions or when variations in natural emissions are accounted for”. The role of spatial and temporal meteorological variability can thus be reduced by aggregating resulting pollutant levels and impacts as regional and annual averages or aggregates, the approach taken in TM5-FASST. The impact of the choice of this specific year on the TM5-FASST model uncertainty or possible biases in base concentrations and SR coefficients is not easily quantified. For what concerns the pollutant base concentrations, some insights in the possible relevance of meteorological variability can found in the literature. For example, Anderson et al., (2007) showed that in

Europe, the meteorological component in regional inter-annual variability of pollutant concentrations ranges between 3% and 11% for airborne pollutants (O_3 , $PM_{2.5}$), and up to 20% for wet deposition. On a global scale, Liu et al. (2007) demonstrated that the inter-annual variability in PM concentrations, related to inter-annual meteorological variability can even be up to a factor of 3 in the tropics (e.g. over Indonesia) and in the storm track regions. A sample analysis (documented in section S2.2 of the SI) of the RCP year 2000 emission scenario with TM5 at $6^\circ \times 4^\circ$ resolution of 5 consecutive meteorological years 2001 to 2005 indicates a year-to-year variability on regional $PM_{2.5}$ within 10% (relative standard deviation) and within 3% for annual mean O_3 . We find a similar variability on the magnitudes of 20% emission perturbation responses within the source region for 6 selected regions (India, China, Europe, Germany, USA and Japan). The relative share of source regions to the pollutant levels within a given receptor region shows a lower inter-annual variability (typically between 2 and 6% for $PM_{2.5}$) than the absolute contributions.

4.3 Impact of the native TM5 grid resolution on pollutant concentration and SRs

FASST base concentrations and SRs have been derived at a $1^\circ \times 1^\circ$ resolution which is a relatively fine grid for a global model, but still not optimal for population exposure estimates and health impact assessments. Previous studies have documented the impact of grid resolution on pollutant concentrations. The effect of higher grid resolution in global models is in general to decrease ozone exposure in polluted regions and to reduce O_3 long-range transport, while $PM_{2.5}$ exposure – mainly to primary species - increases (Fenech et al., 2018; Li et al., 2016; Pungler and West, 2013). Without attempting a detailed analysis, a comparison of TM5 available output for $PM_{2.5}$ and O_3 at $6^\circ \times 4^\circ$, $3^\circ \times 2^\circ$ and $1^\circ \times 1^\circ$ resolution confirms these findings, as illustrated in Fig. S2.6 of the SI. Although FASST is expected to better represent population exposure to pollutants than coarser resolution models, a resolution of $1^\circ \times 1^\circ$ may not adequately capture urban scale pollutant levels and gradients when the urban area occupies only a fraction of the grid cell. The developed sub-grid parameterization for $PM_{2.5}$, providing an order-of-magnitude correction which is consistent with a high-resolution satellite product, is subject to improvement and to extension to other primary pollutants (NO_2 , e.g. Kieseewetter et al., 2014, 2015) and O_3 . To our knowledge a workable parametrization to quantify the impact of sub-grid O_3 processes on population exposure – in particular titration due to local high NO_x concentrations in urban areas - has not been addressed in global air quality models.

The impact of grid resolution on the within-region source-receptor coefficients can be significant, in particular for polluted regions where the coarse resolution includes ocean surface, like Japan. Table S2.3 in the SI shows as an example within-region and long-range SR coefficients for receptor regions Germany, USA and Japan. A higher grid resolution increases the within-region response and decreases the contribution of long-range transport (where the contribution of China to nearby Japan behaves as a within-region perturbation). In the case of Japan, the within-region $PM_{2.5}$ response magnitude increases with a factor of 3, and the sign of the within-region O_3 response is reversed when passing from $6^\circ \times 4^\circ$ to higher resolution. Also over the USA, the population-weighted within-region response sensitivity upon NO_x perturbation increases with a factor of 5. Further, we find that in titration regimes, the magnitude of the O_3 response to NO_x emissions increases with resolution (i.e. ozone increases more when NO_x is reduced using a fine resolution) whereas the in-region ozone response is reduced in non-titration regimes (India and China, Fig. 2.7d). These indicative results are in line with more detailed studies (e.g. Wild and Prather, 2006).

- 2) Also I found little mention of how the fixed meteorological year of 2001 could potentially impact the prediction of pollutants in the future i.e. how would climate change affect predictions of future pollutants?
Also the basis for the radiative forcing calculations is from a fixed meteorological year of 2001 and could have implications for the future calculation of effects. A more detailed mention of these issues would be good, perhaps in Section 4.

REPLY: This is an issue raised by both reviewers. We agree with the reviewer that the year 2001 meteorology is somewhat outdated. The perturbation runs for constructing the SR library of FASST were performed with the TM5 model set-up defined in the first phase of HTAP1 (during the period 2008 – 2011) and because of the computational costs, an update with more recent meteorology was not possible (TM5 is not taking part in HTAP2 where meteorological year 2010 has been used). A systematic check of the representativeness of this particular year for each of the FASST regions is beyond the scope of this study, in the first place because FASST is considered to be a screening tool focussing on impacts of emission changes. However we have substantially extended the discussion on the use of a single meteorological year.

CHANGES TO MANUSCRIPT: Added to Section 2.1 P5 L10

Meteorological fields are obtained from the ECMWF operational forecast representative for the year 2001. The implications of using a single meteorological year will be discussed in section 4.2.

Discussion section 4.2 added as included above.

3) TM5-FASST and the validation of it using TM5 simulations have all been conducted using emissions inventory for the year 2000 as a baseline along with 20% perturbations from this base. How appropriate is it to use a base year of 2000 for validation purposes given the large recent changes in emissions over the last 10-15 years, particularly over East Asia where some emissions have changed by >20%. What impact would using more up to date emissions in the base scenario have the calculated source-receptor coefficients and would it significantly affect the magnitude of future predictions? It would be useful to provide information on how recent changes in emissions could impact TM5-FASST.

REPLY: This is certainly an issue of concern, but at the same time difficult to address in a quantitative way. Although an independent set of SR simulations departing from a different reference scenario is not available, in the manuscript we included a validation of the linear scaling approach beyond the -20% perturbation, based on a number of additional perturbation simulations with TM5 for selected key regions, including East-Asia. In these test cases, the emissions of individual precursors were decreased by -80% relative to the reference emissions of the year 2000, while other precursors were kept at the year 2000 emissions. These simulations are not exactly testing the emission-response sensitivity for a different reference case, but they do provide a validation of the linear approach.

A second validation method, discussed as well in the paper, uses exactly emission scenarios that are strongly different from the reference year 2000 case for all precursors simultaneously (i.e. GEA FLE2030 and MIT2030 scenarios), where FASST uses the sensitivities based on year 2000 and compares the outcome with TM5, to some extent addressing the issue raised by the reviewer. The magnitudes of these emission changes are representative for more recent scenarios. A general observation is that FASST somewhat over-predicts resulting O₃ and PM_{2.5} concentrations (compared to the full TM5 model) for large (i.e. greater than say 50%) emission perturbations in either direction, but this does not compromise its usefulness as a tool to explore air pollution scenarios in a multi-pollutant/multi-impact framework. Indeed, as demonstrated in section 3.3, regional key features and trends, as well as inter-regional differences or similarities resulting from future RCP scenarios up to 2050 are reproduced within the variability of the ACCMIP air quality model ensemble.

We dedicate more discussion on these results, including a more systematic statistical analysis of the performance of FASST versus TM5. In the final discussion we refer to the new round of perturbation simulations performed in the frame of HTAP2.

CHANGES TO MANUSCRIPT: we made substantial edits to the whole of section 3.2

3.2: TM5-FASST_v0 versus TM5 for future emission scenarios

In this section we evaluate different combinations of precursor emission changes relative to the base scenario in a global framework. We take advantage of available TM5 simulations for a set of global emission scenarios which differ significantly in magnitude from the FASST base simulation, and as such provide a challenging test case to the application of the linear source-receptor relationships used in TM5-FASST. We assume that the full TM5 model provides valid evaluations of emission scenarios, and we test to what extent these simulations can be reproduced by the linear combinations of SRs implemented in the TM5-FASST_v0 model. We use a set of selected policy scenarios prepared with the MESSAGE integrated assessment model in the frame of the Global Energy Assessment GEA (Rao et al., 2012, 2013; Riahi et al., 2012). These scenarios are the so called “frozen legislation” and “mitigation” emission variants for the year 2030 (named FLE2030, MIT2030 respectively), policy variants that describe two different policy assumptions on air pollution until 2030. These scenarios and their outcomes are described in detail in Rao et al. (2013), the scope of the present study is the inter-comparison between FASST and TM5 resulting pollutant concentration and exposure levels, as well as associated health impacts.

Major scenario features and emission characteristics are provided in section S8 of the SI. Table S8.1 shows the change in global emission strengths for the major precursors for both test scenarios, relative to the RCP2000 base, aggregated to the FASST ‘master zoom’ regions listed in Table S2.2. Emission changes for the selected scenarios mostly exceed the 20% emission perturbation amplitude from which the SRs were derived. Under the MIT2030 low emission scenario, all precursors and primary pollutants (except primary PM_{2.5} in East-Asia and NH₃ in all regions) are showing a strong decrease compared to the RCP2000 reference scenario. The strongest decrease is seen in Europe (NO_x: -83%, SO₂: -93%, BC: -89%, primary PM_{2.5} - 56%) while NH₃ is increasing by 14 to 46% across all regions. The FLE2030 scenario displays a global increase for all precursors, however with heterogeneous trends across regions. In Europe, North-America and Australia, the legislation in place, combined with use of less and cleaner fuels by 2030, leads to a decrease in pollutant emissions except for NH₃ and primary PM_{2.5}. On the other hand, very substantial emission increases are projected in East and South-East for BC, NO_x and primary PM_{2.5}. Anticipating possible linearity issues, we note that for both scenarios, in all regions, SO₂ and NO_x emissions are evolving in the same direction, although not always with similar relative changes, while NH₃ is always increasing, which may induce linearity issues in the ammonium-sulfate-nitrate system. Regarding O₃ metrics, NMVOC and NO_x are evolving in the same direction, but also here we observe possible issues due to a changing emission ratio (in particular in Russia and Asia).

We further note that not only the emission levels of these scenarios are different from the FASST base scenario (RCP year 2000), but also the spatial distribution of the emissions, at the resolution of grid cells, may differ from the reference set.

We use FASST to compute PM_{2.5} and ozone concentrations applying Eq. (2), i.e. considering the FLE2030 and MIT2030 emission scenarios as a perturbation on the FASST reference emission set (RCP year 2000).

The scope of TM5-FASST is to evaluate on a regional basis the impacts of policies that affect emissions of short-lived air pollutants and their precursors. Hence we average the resulting O₃ and PM_{2.5} concentration and O₃ exposure metric 6mDMA1 over the each of the 56 FASST regions and compare them with the averaged TM5 results for the same regions.

Further, in a policy impact analysis framework, the *change* in pollutant concentrations between two scenarios (e.g. between a reference and policy case) is often more relevant than the absolute concentrations. We therefore present absolute concentrations as well as the change (delta) between the two GEA scenarios, evaluating the benefit of a mitigation scenario versus the frozen legislation scenario.

Figure 8 shows the FASST versus TM5 regional scatter plots for absolute and delta population-weighted mean anthropogenic PM_{2.5} for all 56 FASST receptor regions while the population-

weighted means over the 9 larger zoom areas are shown in Figure 9. Similarly annual mean population-weighted O₃ and 6mDMA1 scatter plots are shown in Fig. 10, and the regional distribution in Fig. 11. The grid-cell statistics (mean, NMB, MB and R²) over larger zoom areas are given in Tables 8 and 9 for PM_{2.5} and 6mDMA1 respectively.

Figure 8 and Table 8 show that on a regional basis, the low emission scenario generally overestimates population-weighted PM_{2.5} concentrations, with the highest negative bias in Europe and Asia, while the lowest deviation is found in Latin America and Africa. The agreement between FASST and TM5 is significantly better for the high emission scenario, in line with the findings in the previous section. As shown in Table 8, averaged over the larger zoom regions, we find that the relative deviation for PM_{2.5} is within 11% for FLE2030, and within 28% for MIT2030, except for Europe where the (low) PM_{2.5} concentration is overestimated by almost a factor of 2. The policy-relevant delta between the scenarios however is for all regions reproduced within 23%.

The ozone health metric 6mDMA1 is more scattered than annual mean ozone, and also here, as expected, the low emission scenario performs worse than the high emission one. Over larger zoom areas however the agreement is acceptable for both scenarios (FASST within 22% of TM5). Contrary to PM_{2.5}, the NMB for the delta 6mDMA1 between two scenarios is higher than the NMB on absolute concentrations, with a low bias for the delta metric of -38% and -45% for Europe and North-America respectively, and a high bias of 35 to 46% in Asia. However, the MB on the delta is of the same order or lower than the absolute concentrations (Table 9). This is a consequence of the fixed background ozone in the absolute concentration reducing the weight of the anthropogenic fraction in the relative error. Figures 9 and 11 provide a general picture of the performance of FASST: despite the obvious uncertainties and errors introduced with the FASST linear approximation, a consistent result emerges both for absolute concentrations from the individual scenarios as for the policy-relevant delta.

A major issue in air pollution or policy intervention impact assessments is the impact on human health; therefore we also evaluate the TM5-FASST outcome on air pollution premature mortalities with the TM5-based outcome, applying the same methodology on both TM5 and FASST outcomes. We evaluate mortalities from PM_{2.5} using the IER functions (Burnett et al., 2014) and O₃ mortalities using the log-linear ER functions and RR's from Jerrett et al. (2009) respectively. Figure 12 (PM_{2.5}) and Fig. 13 (O₃) illustrate how FASST-computed mortalities compare to TM5, both as absolute numbers for each scenario, as well as the delta (i.e. the health benefit for MIT2030 relative to FLE2030). Regional differences in premature mortality numbers are mainly driven by population numbers. In line with the findings for the exposure metrics (PM_{2.5} and 6mDMA1) FASST in general over-predicts the absolute mortality numbers, in particular in the low-emission case. For MIT2030, global PM_{2.5} mortalities are overestimated by 19%, in Europe and North-America FASST even by 43%. In the FLE2030 case, we find a better agreement, with a global mortality over-prediction of 3% (for Europe and North-America 5% and 11% respectively). For the latter scenario, the highest deviation is found in Latin America (10 – 20%). O₃ mortalities are overestimated globally by 11% (7%) with regional agreement within 20% (14%) for MIT2030 (FLE2030). However, as shown by the error bars, the difference between FASST and TM5 is smaller than the uncertainty on the mortalities resulting from the uncertainty on RR's only. The potential health benefit of the mitigation versus the non-mitigation scenario (calculated as FLE2030 minus MIT2030 mortalities) is shown in Figs. 12c and 13c. Globally, FASST underestimates the reduction in global PM_{2.5} mortalities by 17% with regional deviations ranging between -30% for Europe and North-America, and -12% for India. The global health benefit for ozone is underestimate by 2% for O₃, however as a net result of 11% overestimation in India and 12 to 59% underestimation in the other regions. The numbers corresponding to Figs. 12 and 13 are provided in Table S8.4 and S8.5 of the SI.

The error ranges presented here are obviously linked to the choice of the test scenarios and will for any particular scenario depend on the magnitude and the relative sign of the emission changes relative to RCP2000, but given the amplitude of the emission change for the currently two selected scenarios relative to RCP2000, these results support the usefulness of TM5-FASST as a tool for quick scenario screening.

4) In Section 2.1, P4, Line 12 the manuscript mentions about the advent of finer resolution global models nearing $1^\circ \times 1^\circ$ horizontal resolution. I think it would be good to make more comment on the applicability of the $1^\circ \times 1^\circ$ resolution when calculating country scale impacts. Is this resolution along with input information at similar resolution (e.g. emissions) sufficient to capture changes in pollutants at sub 100 km scales over countries such as the UK and Belgium/Luxembourg. I think that the urban adjustment of $PM_{2.5}$ is a suitable attempt at this but I think it would be good to have some further comment on the issue of resolution and the limitations provided by other inputs at this resolution e.g. emissions and meteorology

REPLY: We agree with this critique, even if TM5 during the last decade or so has been amongst the global models with highest grid resolution that have made global studies on health impacts of air pollution. Further, the FASST source regions are defined such to include several gridboxes, e.g. Belgium/The Netherlands/Luxembourg are aggregated into a single region. We address the comment in the following ways:

- 1) Section 2.4, initially dedicated to the sub-grid adjustment for urban concentrations, has now been extended to include a quick analysis of the TM5 base simulation at resolution $6^\circ \times 4^\circ$, $3^\circ \times 2^\circ$ and $1^\circ \times 1^\circ$ to illustrate the impact of resolution on concentrations and emission-concentration response sensitivities, with more detailed information and figures provided in the SI.
- 2) The paper already included a methodology to partly address the sub-grid gradients with a parametrized approach; in the connected annex S4 in the SI we now explicitly compare FASST $PM_{2.5}$ with a high-resolution satellite product.

CHANGES TO MANUSCRIPT:
Expanded section 2.1 P5 L26

With the introduction of massive parallel computing, however, this comparative advantage is now slowly disappearing, and global model resolutions of $1^\circ \times 1^\circ$ or finer are now becoming more common (see the model descriptions in this special issue, e.g. Liang et al., 2018). The model grid resolution influences the predicted pollutant concentrations as well as the estimated population exposure, especially near urban areas where strong gradients occur in population density and pollutant levels, which cannot be resolved by the $1^\circ \times 1^\circ$ resolution. In section 2.4 we describe a methodology to improve population $PM_{2.5}$ exposure estimates by applying sub-grid concentration adjustments based on high-resolution ancillary data. The bias introduced by model resolution affects as well computed SR matrices, e.g. off-setting the share of 'local' versus 'imported' pollution in a given receptor region. We will discuss this aspect more in detail in section 4.3.

(Section 4.3: see reply to comment 1)

5) Section 2.5 on health impacts provides a lot of details and is quite long compared to some other sections where most of the details are within a supplementary section. Also I found it a bit confusing to have two options for calculating $PM_{2.5}$ health effects: the log-linear and integrated exposure-response functions (IER). I assume the output from FASST is only provided from one (Figure 15)? The paragraph on page 10 Lines 8 to 13 does not seem to provide clarity on which method is preferred and could be re-worded. Therefore Section 2.5 could be potentially made more concise by removing the details on the log-linear method to the supplementary. This would allow the main text to focus more on the IER method by Burnett et al., (2014), which is the current methodology used within the Global Burden of Disease study.

REPLY: The reason for the relatively detailed description of health impacts calculations in TM5-FASST is that most users and publications tend to focus on this aspects- and because differences in methodologies are an important reason for differences in calculated health outcomes. We agree however that most of the description could move to the SI.

Most recently published global studies on health impacts of ambient air pollution use one of the two methodologies for PM_{2.5} (i.e. log-lin and/or GBD) and both methodologies appear in WHO recommendations for Europe. We included both methods in the FASST output to facilitate comparison with other studies. The two calculations also provide an additional perspective on the uncertainty of the health impact outcome. (Upon request of Ref #2 we included an additional intercomparison of present-day mortalities with other studies, using both methodologies). However we agree with the reviewer that it was not clearly stated which method was used in Fig. 15 (now Fig. 17) – in this case, as the Silva study was based on GBD, we also used the result following the GBD methodology.

CHANGES TO MANUSCRIPT:

As suggested by the reviewer, we have moved a large part of the description of the health methodology (section 2.6) to the SI and kept only the GBD methodology in the main text, while mentioning that the tool includes the log-lin method as well.

We also mention now specifically in section 3.3.5 (Health impacts) that the methodology is based on GBD.

2.5 Health impacts

TM5-FASST provides output of annual mean PM_{2.5} and O₃ health metrics (3-monthly and 6-monthly mean of daily maximum hourly O₃ (3mDMA1, 6mDMA1), and the sum of the maximal 8-hourly mean above a threshold of 35 ppbV (SOMO35) or without threshold (SOMO0), as well as annual mean NO_x and SO₂ concentrations at grid resolution of 1°x1°. These are the metrics consistent with underlying epidemiological studies (Jerrett et al., 2009; Krewski et al., 2009; Pope et al., 2002). The population-weighted pollutant exposure metrics grid maps, in combination with any consistent population grid map, are thus available for human health impact assessment. The TM5-FASST_v0 tool provides a set of standard methodologies, including default population and health statistics, to quantify the number of air quality-related premature deaths from PM_{2.5} and O₃.

Health impacts from PM_{2.5} are calculated as the number of annual premature mortalities from 5 causes of death, following the Global Burden of Disease methodology (Lim et al., 2012): ischemic heart disease (IHD), chronic obstructive pulmonary disease (COPD), stroke, lung cancer (LC) and acute lower respiratory airways infections (ALRI) whereas mortalities from exposure to O₃ are related to respiratory disease.

Cause-specific excess mortalities are calculated at grid cell level using a population-attributable fraction approach as described in Murray et al. (2003) from $\Delta Mort = m_0 \times AF \times Pop$, where m_0 is the baseline mortality rate for the exposed population, $AF = (RR-1)/RR$ is the fraction of total mortalities attributed to the risk factor (exposure to air pollution), RR = relative risk of death attributable to a change in population-weighted mean pollutant concentration, and Pop is the exposed population (adults ≥ 30 years old, except for ALRI for which infant population <5 years old was considered). RR for PM_{2.5} exposure is calculated from the Integrated Exposure-Response functions (IER) developed by Burnett et al. (2014), and first applied in e.g. the Global Burden of Disease study (Lim et al., 2012).

In order to facilitate comparison with earlier studies, TM5-FASST provides as well mortality estimates based on a log-linear exposure response function $RR = \exp^{\beta \Delta PM_{2.5}}$ where β is the concentration–response factor (CRF; i.e., the estimated slope of the log-linear relation between concentration and mortality) and $\Delta PM_{2.5}$ is the change in concentration. More details on the health impact methodologies, as well as sources for currently implemented population and baseline mortality statistics and their projections in TM5-FASST_v0 are given in section S5 of the SI.

For O₃ exposure, $RR = e^{\beta(\Delta 6mDMA1)}$, β is the concentration–response factor, and $RR = 1.040$ [95% confidence interval (CI): 1.013, 1.067] for a 10 ppb increase in 6mDMA1 according to Jerrett et al. (2009). We apply a default counterfactual concentration of 33.3 ppbV, the minimum 6mDMA1 exposure level in the Jerrett et al. (2009) epidemiological study.

We note that the coefficients in the IER functions used in the GBD assessments have been recently updated due to methodological improvements in the curve fitting, leading to generally higher RR and mortality estimates (Cohen et al., 2017; Forouzanfar et al., 2016). In particular, the theoretical minimum risk exposure level was assigned a uniform distribution of 2.4–5.9 $\mu\text{g}/\text{m}^3$ for PM_{2.5}, bounded by the minimum and fifth percentiles of exposure distributions from outdoor air pollution cohort studies, compared to the presently used range of 5.8 - 8.8 $\mu\text{g}/\text{m}^3$ which would increase the health impact from PM_{2.5} in relatively clean areas. Further, a recent health impact assessment (Malley et al., 2017), using updated RR estimate and exposure parameters from the epidemiological study by Turner et al. (2016), estimates 1.04–1.23 million respiratory deaths in adults attributable to O₃ exposure, compared with 0.40–0.55 million respiratory deaths attributable to O₃ exposure based on the earlier (Jerrett et al., 2009) risk estimate and parameters. These recent updates have not been included in the current version of TM5-FASST. Health impacts from exposure to other pollutants (NO₂, SO₂ for example) are currently not being evaluated in TM5-FASST-v0

In section 3.3.5 P27 L19

The analysis by Silva et al. (2016) used the same methodology implemented in FASST for estimating premature mortalities from PM_{2.5} and O₃ (i.e. Burnett et al., 2014 as in the Global Burden of Disease study and Jerrett et al., 2009 respectively)

6) In section 3.1.1 when making a comparison of the additivity of emission perturbations for PM_{2.5} individual changes for SO₂, NO_x and NH₃ is shown on Figure 3 and 4 but in Figure 2 there is no effect from NH₃ emissions. Whereas, in Figure S7.1 and S7.2 the 3 individual responses are shown along with the combined response on PM_{2.5} (sum of all 3). However, the effect for combined emissions is only for SO₂ and NO_x in Figure 2 and 4 and does not include any addition from NH₃. Why has the contribution from NH₃ not been included within some of the combined emission changes in PM_{2.5}? There seems to be a bit of inconsistency here, especially when considering that NH₃ emissions can be important for NO₃ aerosol formation.

REPLY: In first instance we have evaluated separately the ‘additivity’ and ‘linearity’ issues. Figure 2 demonstrates the additivity assumption of NO_x and SO₂ perturbations. This requires model simulations for (1) SO₂ only perturbation (2) NO_x only perturbation and (3) simultaneous NO_x+SO₂ perturbation, all of the same magnitude. For each of these perturbation experiments, the effect on SO₄, NO₃ and NH₄ in PM_{2.5} is available. However due to lack of CPU resources, similar analyses for combined SO₂+NH₃ and NO_x+NH₃ perturbations have not been performed unfortunately. Because only separate NH₃ perturbations are available we cannot provide the equivalent figures for these combinations. We therefore assume additivity for the combined perturbations of NH₃ with SO₂ and NO_x respectively. To some extent one may argue that source regions of NH₃ on the one hand, and SO₂ and NO_x on the other are less aligned, and that control strategies are different/independent hence simultaneous reductions are less pertinent, but we recognize this is a caveat in the FASST methodology.

CHANGES TO MANUSCRIPT:

3.1 Validation against the full TM5 model: additivity and linearity

We recall that the TM5-FASST computes concentrations and metrics based on a perturbation approach, i.e. the linearization applies only on the difference between scenario and reference emission. Therefore we focus on evaluating the perturbation response, i.e. the second term in the right hand side of Eq. 2.

The standard set of -20% emission perturbation simulations, available for all 56 continental source regions and constituting the kernel of TM5-FASST_v0 are simulations P1 (perturbation of SO₂, NO_x, BC and POM), P2 (SO₂ only), and P4 (NH₃ and NMVOC) shown in Table 2. Additional standard -20% perturbation experiments P3 (NO_x only) and P5 (NO_x and NMVOC), as well as an additional set of perturbation simulations P1' to P5' over the range [-80%, +100%], listed in Table S3 of the SI, have been performed for a limited selection of representative source regions (Europe, USA, China, India, Japan) due to limited CPU resources. For the same reason, no combined perturbation studies are available for (SO₂ + NH₃) and (NO_x + NH₃) for a systematic evaluation of additivity and linearity. The available [-80%, +100%] perturbations are used to validate the linearized reduced-form approach against the full TM5 model, exploring chemical feedback mechanisms (additivity) and extrapolation of the -20% response sensitivity towards larger emission perturbation magnitudes (linearity). This is in particular relevant for the NO_x - NMVOC - O₃ chemistry and for the secondary PM_{2.5} components NO₃⁻ - SO₄²⁻ - NH₄⁺. These mechanisms could also be important for organic aerosol, but we remind that in this study organic aerosol formation was parameterized as pseudo-emissions.

3.1.1 Additivity and linearity of secondary inorganic PM_{2.5} response:

Experiment P1, where BC, POM, SO₂ and NO_x emissions are simultaneously perturbed by -20% relative to base simulation P0, delivers SR matrices for primary components BC and POM, and a first-order approximation for the precursors SO₂ and NO_x whose emissions do not only affect SO₂ and NO_x gas concentrations but also lead to several secondary products (SO₂ forms ammonium sulfate, NO_x leads to O₃, ammonium nitrate). Experiment P2 perturbs SO₂ only, while experiment P3 perturbs NO_x only (in this latter case, to limit the computational cost, computed for a limited set of representative source regions only).

We first test the hypothesis that the PM_{2.5} response to the combined (NO_x + SO₂) -20% perturbation (P1) can be approximated by the sum of the single precursor perturbations responses (P2 + P3). Figure 2 summarizes the resulting change in SO₄²⁻, NO₃⁻, NH₄⁺ and total inorganic PM_{2.5} respectively for the selected source regions. For Europe, the emission perturbations were applied over all European countries simultaneously, hence the responses are partly due to inter-regional transport from other countries. Following findings result from the perturbation experiments P1, P2 and P3:

1. Sulfate shows a minor response to NO_x emissions, and likewise nitrate responds only slightly to SO₂ emissions and both perturbations are additive. In general the response is one order of magnitude lower than the direct formation of SO₄²⁻ and NO₃⁻ from SO₂ and NO_x respectively (Fig. 2a, b);
2. NH₄ responds to NO_x and SO₂ emissions with comparable magnitudes and in an additive way (Fig. 2c);
3. The response of total sulfate, nitrate and ammonium to a combined NO_x and SO₂ -20% perturbation can be approximated by the sum of the responses to the individual perturbations, i.e. P1 ≈ P2+P3 (Fig. 2d). Scatterplots between P1 and P2+P3 for the regional averaged individual secondary products and total inorganic PM_{2.5} are shown in Fig. S7.1 of the SI.

From the combined [SO₂+NO_x] perturbation (P1), and the separate SO₂ perturbation simulations (P2), both available for all source regions, the missing NO_x SR matrices have been gap-filled using (P1 - P2). By lack of simulations for combined (SO₂ + NH₃) or (NO_x + NH₃) perturbations we assume additivity for simultaneous NH₃, SO₂ and NO_x perturbations, i.e. the response is computed from a linear combination of P2, P3 and P4.

7) Within section 3 on the evaluation of TM5-FASST numerous references are made to the ability of FASST to predict TM5 concentrations or other metrics using the gradient of the straight line fit as an estimate of bias. I have noticed a couple of times in the text where FASST is stated to over or under estimate the comparison but the details in the figure do not agree with this statement, which could be due to the use of the gradient. I think that a more appropriate bias statistic such as normalised mean bias (or something similar) could be used to provide an evaluation of FASST rather than this simple linear fit. This occurs throughout Section 3 and please check that all comments are appropriate to the relevant figures.

REPLY:

This point is well taken, the slope of the fit was indeed not the most appropriate choice for evaluating the performance of FASST. We have omitted the linear fit in the figures, and leave only the 1:1 line as a reference. Instead we have calculated Normalized Mean Bias (NMB), Mean Bias (MB) and correlation coefficient as validation metrics in a consistent way across sections 3.1 and 3.2 when compare FASST to the full TM5 model, where

$$\text{NMB} = (\overline{\text{FASST}} - \overline{\text{TM5}}) / \overline{\text{TM5}}$$

$$\text{MB} = (\overline{\text{FASST}} - \overline{\text{TM5}})$$

\bar{Y} = average of all grid cells in region

Further, in section 3.1 (linearization error under strong emission perturbations) we focus on evaluating the perturbation term (Δ), putting additional statistics on the total concentrations in the SI. In section 3.2 (comparison with high/low GEA emission scenarios) we show and discuss both totals for individual scenarios and Δ s in the main text.

CHANGES TO MANUSCRIPT;

New discussion in section 3.1.2 P21 L6

Figure 7 illustrates the performance of the TM5-FASST approach versus TM5 for regional-mean annual mean ozone, health exposure metric 6mDMA1 (both evaluated as population-weighted mean), and for the crop-relevant exposure metrics AOT40 and M12 (both evaluated as area-weighted mean) over the extended emission perturbation range. In most cases the response (i.e. the *change* between base and perturbed case) to emission perturbations lies above the 1:1 line across the 4 metrics, indicating that FASST tends to over-predict the resulting metric (as a sum of base concentration and perturbation). Of the four presented metrics, AOT40 is clearly the least robust one, which can be expected for a threshold-based metric that has been linearized. Tables 5 to 7 give the statistical metrics for the grid-to-grid comparison of the perturbation term between FASST and TM5 for the health exposure metric 6mDMA1, and crop exposure metrics AOT40 and M12 respectively. Statistical metrics for the total absolute concentrations (base concentration + perturbation term) are given in Tables S7.2 to S7.4 in the SI. As anticipated, the NO_x-only perturbation terms are showing the highest deviation, in particular for a doubling of emissions, however combined NO_x-NMVOC perturbations are reproduced fairly well for all regions, staying within 33% for a -80% perturbation for all 3 exposure metrics, and within 38% for an emission doubling for 6mDMA1 and M12, while the AOT40 metric is overestimated by 76 to 126% for emission doubling. The total resulting concentration over the entire perturbation range for single and combined NO_x and NMVOC perturbation agrees within 5% for 6mDMA1 and M12, and within 64% for AOT40. The mean bias is positive for both perturbations, for all metrics and over all analysed regions, except for crop metric M12 under a doubling of NMVOC emissions over Europe showing a small negative bias. The deviations for individual European receptor regions under single and combined NMVOC and NO_x perturbations for health and crop exposure metrics are shown in Figs. S7.4 to S7.6 of the SI.

8) Within Section 3 a comparison has been made with air pollutant concentrations, health and climate metrics. However, no comparison has been made to other studies on the crop relevant metrics. The comparison of crop relevant metrics seems to have been excluded from the comparison. Is it possible to compare the results from FASST to other studies that have looked at the air pollution impact on crops to provide some evaluation of these metrics?

REPLY: We now include an intercomparison with a study on present-day global and regional crop losses

CHANGES TO MANUSCRIPT:

New section 3.3.6

3.3.6 Present day O₃ – crop losses

Avnery et al. (2011) evaluate year 2000 global and regional O₃-induced crop losses for wheat, maize and soy bean, based on the same crop ozone exposure metrics as used in FASST, obtained with a global chemical transport model at 2.8°x2.8° resolution. Figure 18 compares their results (in terms of relative yield loss) with FASST (TM5) results based on RCP year 2000 for the globe and 3 selected key regions (Europe, North-America and East Asia). Despite the less-robust quantification of crop impacts from O₃ in a linearized reduced-form model set-up, we find that FASST reproduces the major features and trends across regions and crop varieties. Differences may be attributed to a variety of factors, including model resolution, model O₃ chemistry processes, emissions, definition of crop growing season and crop spatial distribution.

And new Figure 18:

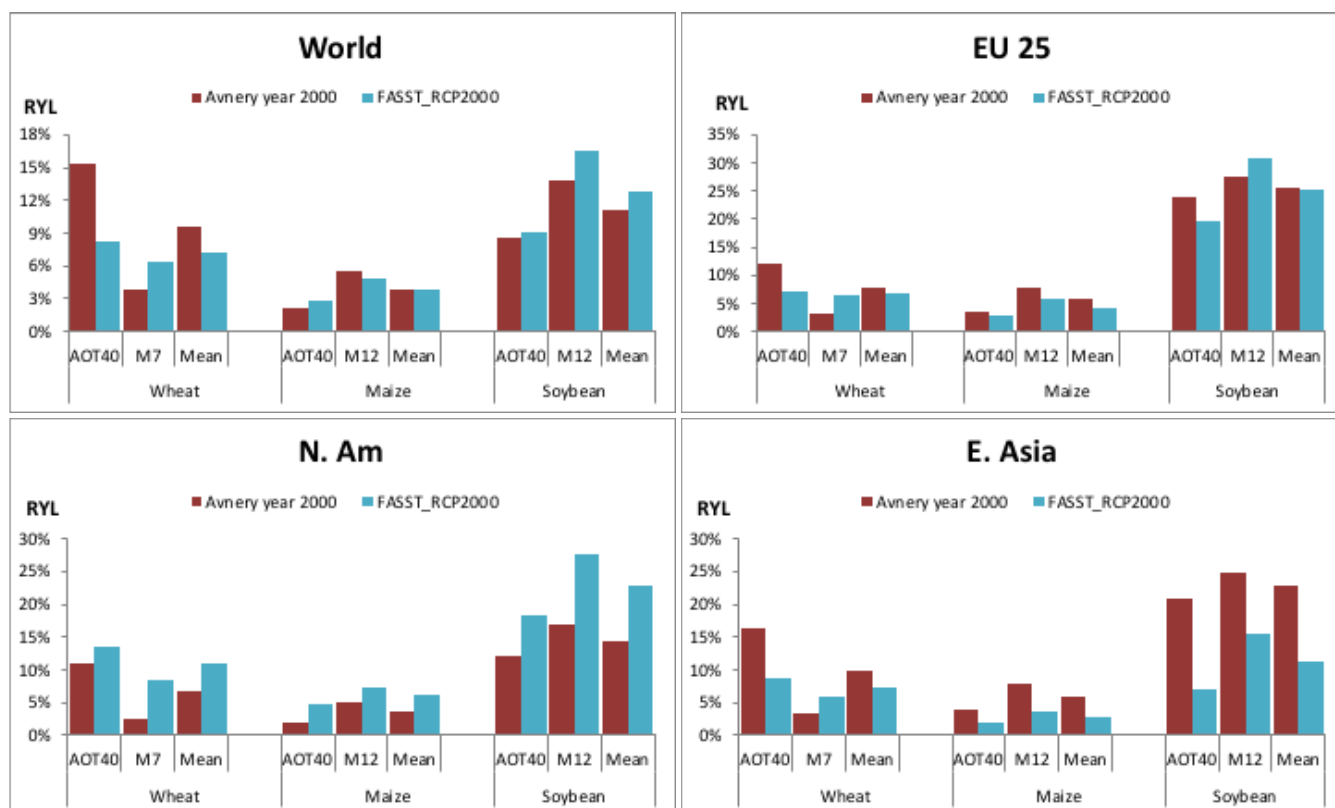


Figure 18: Year 2000 global and regional ozone-induced relative yield losses for 3 major crops, from Avnery et al. (2011) and from TM5-FASST (RCP year 2000), estimated from the 2 common exposure metrics M7 and AOT40 (see text), as well as the mean of both.

9) Please could the author make sure that all the equations provided within the manuscript are appropriately numbered. It appears that some have been but not all.

REPLY: OK, done

Minor Specific Comments:

10) Section 2.1, P3, Line 12 – Brackets needed round O3 as first time defined as ozone

REPLY: OK done

11) Section 2.1, P3, line 14 – When describing the particulate matter components I think some mention needs to be made here about Secondary Organic Aerosol (SOA). I think this comes later in the manuscript (section 2.3 P6) but I feel it would also be worth mentioning here with the initial model description

REPLY: Agree

CHANGES TO MANUSCRIPT: P4 L16

Biogenic secondary aerosol (BSOA) was included following the AEROCOM recommendation (Dentener et al., 2006; Kanakidou et al., 2005) which parameterized BSOA formation from natural VOC emissions as a fixed fraction of the primary emissions. The relative fraction compared to the anthropogenic POM emissions varied spatially, with a higher contribution in regions where the emissions of terpene emissions were higher. SOA from anthropogenic emission was not explicitly included in the current simulations.

And to the discussion: P31 L17

The omission of secondary organic PM in TM5 is estimated to introduce a low bias in the base concentration of the order of $0.1 \mu\text{g m}^{-3}$ as global mean however with regional levels in Central Europe and China up to $1 \mu\text{g m}^{-3}$ in areas where levels of primary organic matter are reaching $20 \mu\text{g m}^{-3}$ (Farina et al., 2010) indicating a relatively low contribution of SOA to total $\text{PM}_{2.5}$.

12) Section 2.1, P3, Line 26 – ‘Although for most health and ecosystem impacts only the surface level fields are required, base simulation and perturbed pollutants concentrations were calculated and stored for the 25 vertical levels of the model as monthly means, and some air quality-relevant parameters as hourly or daily fields.’ – I think some mention of the fact that to calculate climate relevant impacts requires 3D information of constituents and not just surface fields

REPLY: Agree

CHANGES TO MANUSCRIPT: *changed the relevant phrase to: (P5 L7)*

Although for most health and ecosystem impacts only the surface level fields are required, climate metrics (e.g. radiative forcing) require the full vertical column and profile information. Therefore base simulation and perturbed pollutant concentrations were calculated and stored for the 25 vertical levels of the model as monthly means, and some air quality-relevant parameters as hourly or daily fields.

13) Section 2.3, P4, Line 25 – reference should be made to the underlying effects of the particular meteorological year used i.e. 2001 in this case.

REPLY: We do not fully agree that this addition would fit in here as the phrase describes a general feature of AQ-SRM. However we added it in the 3th par where TM5-FASST_v0 is introduced.

CHANGES TO MANUSCRIPT: P6 L27

In the current version v0 of TM5-FASST the emission-concentration relationship is locally approximated by a linear function expressing the change in pollutant concentration in the receptor region upon a change in precursor emissions in the source region with the generic form $dC_y = SRC \times dE_x$ where dC_y equals the change in the pollutant concentration compared to a reference concentration in receptor region y , dE_x is the change in precursor emission compared to a reference emission in source region x , and SRC the source-receptor coefficient for the specific compound and source-receptor pair – in this case emulating atmospheric processes linked to the meteorology in 2001.

14) Section 2.3, P5, Line 4 – '(Where $j=i$ in the case of a primary component)' – maybe this could be changed to '(where the concentration of a primary pollutants is directly related to its emission)'

REPLY: We intend here that a primary component does not change chemically after its emission.

CHANGES TO MANUSCRIPT: *As the phrase is rather redundant we removed it.*

15) Section 2.3, P6, Lines 1 – 7 – There seems to be confusion between the labelling of emitted precursors and concentrations of components as in this section they both seemed to have been referred to as j . Please clarify which letter is meant to represent each

REPLY: This was indeed wrongly indexed, thanks for spotting.

CHANGES TO MANUSCRIPT: P7 L29

For each receptor point y (i.e. each model vertical level $1^\circ \times 1^\circ$ grid cell), the change in concentration of component j in receptor y resulting from a -20% perturbation of emitted precursor i in source region x , is expressed by a unique SR coefficient $A_{ij}[x, y]$:

$$A_{ij}[x, y] = \frac{\Delta C_j(y)}{\Delta E_i(x)} \text{ with } \Delta E_i(x) = 0.2 E_{i,base}(x) \quad (1)$$

The total concentration of component j in receptor region y , resulting from arbitrary emissions of *all* n_i precursors i at *all* n_x source regions x , is obtained as a perturbation on the base-simulation concentration, by summing up all the respective SR coefficients scaled with the actual emission perturbation:

$$C_j(y) = C_{j,base}(y) + \sum_{k=1}^{n_x} \sum_{i=1}^{n_i} A_{ij}[x_k, y] \cdot [E_i(x_k) - E_{i,base}(x_k)] \quad (2)$$

16) Section 2.3, P6, Equation 1 – Are these Source receptor coefficients calculated on the monthly or annual response between the precursor emission and pollutant? This needs to be stated within the description of the equation.

REPLY: Emission perturbations are implemented on annual basis, and the change in the source-receptor pollutant concentrations are evaluated on an annual basis as well. However some exposure metrics are based on seasonal values (e.g. crop growing season, human exposure to O3 during highest 6 monthly mean of hourly maximum values). We extended the paragraph, including as well additional information on the treatment of residual water in PM_{2.5} to address an issue raised by Ref #2.

CHANGES TO MANUSCRIPT: *added phrase after Eq. 1(P8 L1)*

In the present version TM5-FASST_v0, the SR coefficients for pollutant concentrations are stored as annual mean responses to annual emission changes. Individual PM_{2.5} components SRs are stored as dry mass ($\mu\text{g m}^{-3}$). PM_{2.5} residual water at 35% is optionally calculated a posteriori for sensitivity studies, assuming mass growth factors for ammonium salts of 1.27 (Tang, 1996) and for sea-salt of 1.15 (Ming and Russell, 2001). The presence of residual water in PM_{2.5} is not irrelevant: epidemiological studies establishing PM_{2.5} exposure-response functions are commonly based on monitoring data of gravimetrically determined PM_{2.5}, for which measurement protocols foresee filter conditioning at 30 – 50% RH. Therefore, although most health impact modelling studies consider dry PM_{2.5} mass, the residual water fraction should in principle be included in modelled PM_{2.5}.

We also established SR matrices linking annual emissions to specific O₃ exposure metrics that are based on seasonal or hourly O₃ concentrations (e.g. crop exposure metrics based on daytime ozone during crop growing season, human exposure to O₃ during highest 6 monthly mean of hourly maximum values).

And deleted the phrase below Eq (3):

“In TM5-FASST_v0 the monthly perturbations are aggregated to annual emission-concentration SR matrices, as the health, climate and vegetation impact metrics used in this version are also aggregated to annual values.”

17) Section 2.3, P6, Line 21 - 24 – It is unclear to me how secondary organic aerosol (SOA) is included within the TM5-FASST tool as a component of PM _{2.5} . Does it form part of the POM and what fraction of the primary emissions are used
--

REPLY: This is partly addressed in our reply to comment 10). Further we specify now that the perturbation simulations are made for anthropogenic components only.

CHANGES TO MANUSCRIPT: *Paragraph was modified as follows (P7 L14)*

The SR matrices, describing the concentration response in each receptor upon a change in emissions in each source region, have been derived from a set of simulations with the full chemical transport model TM5 by applying -20% emission perturbations for each of the 56 defined source regions (plus shipping and aviation), for all relevant anthropogenic precursor components, in comparison to a set of unperturbed simulations, hereafter denoted as ‘base simulations’. Emissions from biogenic organic components were included as a spatial/temporally varying component, but did not vary in the model emission sensitivity simulations. Consequently absolute concentrations of BSOA were identical across base and perturbation simulations and no SR coefficients are available.

18) Section 2.3, P7, Line 3 – The combination of emissions perturbation scenarios is given in Table 2. Did the base simulation not conduct emission perturbation scenarios for all 56 continental regions? I thought that this would have been essential to enable to the calculation of changes in concentrations in TM5 but Table 2 does not seem to imply this. Clarification required

REPLY: We agree that the phrase is formulated confusingly and deserves more clarification. The purpose of the perturbation simulations is indeed to obtain SR matrices for each precursor, and for each of the source regions, but it was not required to run all individual perturbations for all

regions. Table 2 explains in brief the purpose of each simulation and section 3.1 explains in detail how the various simulations are combined to get to the full set.

CHANGES TO MANUSCRIPT: *Added to section 2.3: (P9 L8)*

The -20% perturbation simulations were performed for the combination of precursors given in Table 2, with P0 the unperturbed reference simulation, and P1 through P5 -20% perturbations for combined or single precursors. Due to limited CPU availability, precursors that are expected not to interact chemically are perturbed simultaneously, with P1 combining SO₂, NO_x, BC, and POM and P4 combining NH₃ and NMVOC. P1 and P4 were computed for each of the 56 continental source regions plus shipping (P1 and P4) and aviation (P1). Additionally, a SO₂-only perturbation was computed for all individual source regions and shipping (P2) and NO_x-only for a selection of key source regions (P3). Finally a set of combined NO_x + NMVOC perturbation simulations (P5) was performed for a set of key regions.

For a limited set of representative source regions, an additional wider range of emission perturbations P'_i [-80% to +100%] has been applied to evaluate possible non-linearities in the emission-concentration relationships. The list of these additional perturbation simulations is given in Table S3 of the SI. In section 3.1 we explain how this set of perturbation runs is combined into FASST to obtain a complete set of source-receptor matrices for each precursor and source region.

Modified Section 3.1

3.1 Validation against the full TM5 model: additivity and linearity

We recall that the TM5-FASST computes concentrations and metrics based on a perturbation approach, i.e. the linearization applies only on the difference between scenario and reference emission. Therefore we focus on evaluating the perturbation response, i.e. the second term in the right hand side of Eq. 2.

The standard set of -20% emission perturbation simulations, available for all 56 continental source regions and constituting the kernel of TM5-FASST_v0 are simulations P1 (perturbation of SO₂, NO_x, BC and POM), P2 (SO₂ only), and P4 (NH₃ and NMVOC) shown in Table 2. Additional standard -20% perturbation experiments P3 (NO_x only) and P5 (NO_x and NMVOC), as well as an additional set of perturbation simulations P1' to P5' over the range [-80%, +100%], listed in Table S3 of the SI, have been performed for a limited selection of representative source regions (Europe, USA, China, India, Japan) due to limited CPU resources. For the same reason, no combined perturbation studies are available for (SO₂ + NH₃) and (NO_x + NH₃) for a systematic evaluation of additivity and linearity. The available [-80%, +100%] perturbations are used to validate the linearized reduced-form approach against the full TM5 model, exploring chemical feedback mechanisms (additivity) and extrapolation of the -20% response sensitivity towards larger emission perturbation magnitudes (linearity). This is in particular relevant for the NO_x - NMVOC - O₃ chemistry and for the secondary PM_{2.5} components NO₃⁻ - SO₄²⁻ - NH₄⁺. These mechanisms could also be important for organic aerosol, but we remind that in this study organic aerosol formation was parameterized as pseudo-emissions.

19) Section 2.3, P7, Line 15 to 18 – The change in CH₄ burden in TM5 from the HTAP1 perturbation simulations is stated as being an emission perturbation of 77 Tg/year. Could the authors provide information on how this was obtained

REPLY: The value comes from the assumption that the imposed CH₄ steady state concentration is the result of a balanced emission on the one hand and the chemical loss by oxidation by OH on the other hand (neglecting the lower-order losses to soil and stratosphere). As the TM5 model keeps track of the total amount of CH₄ oxidized, the implied change in emission is simply obtained from the difference in total amount of CH₄ oxidized in 1 year between the two runs.

We agree this could be explained better. In order to address a similar comment from Ref. #2 we have moved the details of the methodology to the SI, and modified the text as follows:

CHANGES TO MANUSCRIPT: *Main text, P9 L25:*

Annex S3 in the SI provides more details on the methodology applied to convert the CH₄ concentration perturbation into a CH₄ emission-based perturbation

Annex S3:

S3.1 CH₄ - O₃ source-receptor relations from HTAP1 perturbation experiments:

CH₄ emissions lead to a change in CH₄ concentrations with a perturbation response time of about 12 years. In order to avoid expensive transient computations, HTAP1 simulations SR1 and SR2 with prescribed fixed CH₄ concentrations (1760 ppb and 1408 ppb, see Dentener et al., 2010) were used to establish CH₄ - O₃ response sensitivities. Previous transient modeling studies have shown that a change in steady-state CH₄ abundance can be traced back to a sustained change in emissions, but the relation is not linear because an increase in CH₄ emissions removes an additional fraction of atmospheric OH (the major sink for CH₄) and prolongs the lifetime of CH₄ (Fiore et al., 2002, 2008; Prather et al., 2001).

In a steady-state situation, the CH₄ concentration is the result of balanced sources and sinks. In the HTAP1 experiments, keeping all other emissions constant, the change in the amount of CH₄ loss (mainly by OH oxidation with a lifetime of ca. 9 years, neglecting loss to soils and stratosphere with lifetimes of ca.160 and 120 years respectively (Prather et al., 2001)) under the prescribed change in CH₄ abundance should therefore be balanced by an equal and opposite source which we consider as an “effective emission”. The amount of CH₄ oxidized by OH in one year being diagnosed by the model, the resulting difference between the reference and perturbation experiment of -77 Tg sets the balancing “effective” emission rate to 77Tg/yr, which is then used to normalize the resulting O₃ and O₃ metrics response to a CH₄ emission change.

The same perturbation experiments also allow us to establish the CH₄ self-feedback factor F describing the relation between a change in emission and the change in resulting steady-state concentration:

$$\frac{C_2}{C_1} = \left(\frac{E_2}{E_1}\right)^F \quad (S3.1)$$

With CH₄ concentrations prescribed, CH₄ emissions were not included in the SR1 and SR2 experiments. The feedback factor F is derived from model-diagnosed respective CH₄ burdens (B) and total lifetimes (LT) as follows (Fiore et al., 2009; Wild and Prather, 2000):

$$F=1/(1-s)$$

$$s = \partial \ln(LT) / \partial \ln(B)$$

TM5 returns $s = 0.33$ which can be compared to a range of values between 0.25-and 0.31 in IPCC-TAR (Prather et al., 2001, Table 4.2) , resulting in a TM5-inherent calculated feedback factor $F=1.5$. This factor can be used to estimate the corresponding SR2-SR1 change in CH₄ emission in a second way. From Eq. S3.1 we find that a 20% decrease in CH₄ abundance corresponds to a 14% decrease in total CH₄ emissions. Kirschke et al. (2013) estimate total CH₄ emissions in the 2000s in the range 550 – 680 Tg yr⁻¹ from which we obtain an estimated emission change between the HTAP SR1 and SR2 experiments in the range 77 – 95 Tg yr⁻¹, in line with our steady-state loss-balancing approach.

20) Section 2.3, P7, Lines 22 to 28 – It is stated that FASST does not include impacts on O3 from perturbations in CO emissions. I am not sure why this has not been included in the development of FASST along with other O3 precursor emissions of NOx and NMVOCs. Within this section it states that there is a dedicated CO emission perturbation experiment conducted with TM5 as part of HTAP1 available and that the impacts on O3 are not insignificant. Therefore I wonder why the information from the TM5 CO experiments have not been included previously within FASST?

REPLY: This is indeed a missing link in the TM5-FASST model which we hope to address in a future version of the tool. Also here, missing CPU resources did not allow for dedicated CO perturbation simulations in each of the 56 source regions. Indeed from HTAP1, source receptor relations between large rectangular source areas (not aligned with political borders and coast lines, and including ocean) are available but we did not attempt to remap those on the FASST 56 continental regions, given expected differences in CO lifetimes for emissions from these regions. With HTAP2 source regions better aligned with the FASST ones, there may be possibilities to rely on those in future developments. This caveat has been mentioned in the discussion.

21) Section 2.4, P8 – Maybe this section should be labelled as something like ‘Urban Adjustments in PM_{2.5} for Health Calculation’ to better identify what is being done here. I am assuming that the adjusted PM_{2.5} concentrations are only used within the calculation of health impacts

REPLY: Thank you for the suggestion – indeed this is relevant for the exposure of population. As this section now also includes a discussion on the impact of grid resolution (see reply to comment 4) we have modified the title

CHANGES TO MANUSCRIPT: *Title changed to:*

2.4 PM_{2.5} adjustments in urban regions for health impact evaluation

22) Section 2.4, P8, Lines 25 -26 – Is the CIESIN population dataset the default one used within FASST as this seems to have been used to calculate the default urban increment factors in Table S4.2? Might be worth included which one is recommended for use.

REPLY: The CIESIN dataset is the one with the highest resolution and therefore most suitable for a sub-grid correction. The ‘default’ regional increment factors are indeed based on CIESIN year 2000 data, but they are static and therefore do not change with scenario years. The public web tool always uses these default factors, but the (not-public) ‘research version’ has the option to include more appropriate population data sets.

CHANGES TO MANUSCRIPT: *we added the following phrase in the conclusion section: (P33 L30)*

This version offers the possibility to explore built-in as well as user-defined scenarios, using static default urban increment correction factors and crop production data. A more sophisticated in-house research version with gridded output and flexibility in the choice of gridded ancillary data (population grid maps, scenario-specific urban increment factors, crop distribution) is under continuous development and has been applied for the assessments listed in table S1.

23) Section 2.5, P9, Line 10 – Check definition of AF here as this does not match up with what is provided further down the page, just above line 20

REPLY: In fact it does correspond: $1-1/RR = (RR-1)/RR$. But as the right-hand form is probably more legible we changed it to the latter. The part of the text above line 20 containing the larger equation has been moved to the SI following comment 4.

CHANGES TO MANUSCRIPT: *changed the phrase to: (P11 L21)*

... where m_0 is the baseline mortality rate for the exposed population, $AF = (RR-1)/RR$ is the fraction of total mortalities attributed to the risk factor (exposure to air pollution)

24) Section 2.5, P10, Lines 17 to 24 – I think a comment is required here to state how the recent updates in the epidemiological evidence for health effects could impact on the predictions in FASST i.e. will they be cause an underestimate or overestimate.

REPLY: We have added a line to clarify the impact of the new parameter on the estimated health impact for PM_{2.5}.

CHANGES TO MANUSCRIPT: *extended the phrase as follows: (P12 L6)*

In particular, the theoretical minimum risk exposure level was assigned a uniform distribution of 2.4–5.9 $\mu\text{g}/\text{m}^3$ for PM_{2.5}, bounded by the minimum and fifth percentiles of exposure distributions from outdoor air pollution cohort studies, compared to the presently used range of 5.8 - 8.8 $\mu\text{g}/\text{m}^3$ which would increase the health impact from PM_{2.5} in relatively clean areas.

25) Section 2.6, P11, Line 14 – ‘Both Mi metrics ...’ should be changed to ‘Both metrics (Mi) ...’

REPLY: OK done

26) Section 2.6, P11, Line 15 – How is the growing season defined when calculating the crop metrics?

REPLY: As reported in the text, the growing seasons for the respective crops are retrieved from the gridded GAEZ data set. To clarify this more, we have extended the description of methodology related to the definition of the crop season.

CHANGES TO MANUSCRIPT: *modified section 2.6 as follows:*

2.6 Crop impacts

The methodology applied in TM5-FASST to calculate the impacts on four crop types (wheat, maize, rice, and soy bean) is based on Van Dingenen et al. (2009). In brief, TM5 base and -20% perturbation simulations of gridded crop O₃ exposure metrics (averaged or accumulated over the crop growing season) are overlaid with crop suitability grid maps to evaluate receptor region-averaged exposure metrics SR coefficients. Gridded crop data (length and centre of growing period, as well as a gridded crop-specific suitability index, based on average climate 1961 – 1990) have been updated compared to Van Dingenen et al. (2009), using the more recent and detailed Global Agro-Ecological Zones (GAEZ) data set (IIASA and FAO, 2012, available at <http://www.gaez.iiasa.ac.at/>).

Available crop ozone exposure metrics are 3-monthly accumulated ozone above 40 ppbV (AOT40) and seasonal mean 7 hr or 12 hr day-time ozone concentration (M7, M12) for which exposure-response functions are available from the literature (Mills et al., 2007; Wang and Mauzerall, 2004). Both metrics (M_i) are calculated as the 3-monthly mean daytime (09:00 – 15:59 for M7, 08:00 – 19:59 for M12) ozone concentration, evaluated over the 3 months centred on the midpoint of the location-dependent crop-growing season provided by the GAEZ data set.

Note that in the GAEZ methodology, the theoretical growing season is determined based on prevailing temperatures and water balance calculations for a reference crop, and can range between 0 and 365 days, however our approach always considers 3 months as the standard metric accumulation or averaging period.

27) Section 2.6, P11, Line 16 – RYL is defined as the crop relative yield. Should this be the relative yield loss? Also the coefficients a,b,c within the equation for RYL need more explanation

REPLY: indeed, “RYL” was wrongly positioned in the phrase. We have included a table with the values of the coefficients in the equations. While in the Weibull function the a and b parameters are pure mathematical shape coefficients, the c coefficients sets the lower threshold value for zero impact. We included this as well.

CHANGES TO MANUSCRIPT:

Modified following section (P12 L25):

Both metrics (M_i) are calculated as the 3-monthly mean daytime (09:00 – 15:59 for M7, 08:00 – 19:59 for M12) ozone concentration, evaluated over the 3 months centred on the midpoint of the location-dependent crop-growing season.

The crop relative yield loss (RYL) is calculated as linear function from AOT40 and from a Weibull-type exposure-response as a function of M_i :

$$RYL[AOT40] = a \times AOT40 \quad (5)$$

$$RYL(M_i) = \left. \begin{array}{l} 1 - \frac{\exp\left[-\left(\frac{M_i}{a}\right)^b\right]}{\exp\left[-\left(\frac{c}{a}\right)^b\right]} \\ RYL(M_i) = 0 \end{array} \right\} \begin{array}{l} M_i \geq c \\ M_i < c \end{array} \quad (6)$$

The parameter values in the exposure response functions are given in Table 3. Note that for $M_i = c$, $RYL = 0$ hence c is the lower M_i threshold for visible crop damage. Also here, the non-linear shape of the $RYL(M_i)$ function requires the ΔRYL for 2 scenarios (S1, S2) being evaluated as $RYL(M_{i,S2}) - RYL(M_{i,S1})$, and not as $RYL(M_{i,S2} - M_{i,S1})$.

28) Section 2.7.1, P12, Lines 10 to 12 – Are these two sentences on the basic radiative properties of aerosols relevant? Including some text on the following lines would be good to discuss how the treatment of externally mixed aerosols alters the radiative forcing calculations when compared to internally mixed ones (Lesins et al., 2002; Klingmüller et al., 2014).

REPLY: We agree on the redundancy of the two sentences and removed them. We included a brief discussion on the impact of the introduced simplifications regarding mixing state as well as the use of integrated column burden instead of resolved vertical profiles. With respect to the mixing state we rather refer to Bond et al. (2013) who considered various additional processes affecting the BC absorption coefficient

CHANGES TO MANUSCRIPT: *Added following text: (P14 L15)*

Neglecting the aerosol mixing state and using column-integrated mass rather than vertical profiles introduces additional uncertainties in the resulting forcing efficiencies. Accounting for internal mixing may increase the BC absorption by 50 to 200% (Bond et al., 2013), while including the vertical profile would weaken BC forcing and increase SO4 forcing (Stjern et al.

2016). Further, the BC forcing contribution through the impact on snow and ice is not included, nor are semi- and indirect effects of BC on clouds. Our evaluation of pre-industrial to present radiative forcing in the validation section demonstrates that, in the context of the reduced-form FASST approach, the applied method however provides useful results..

29) Section 2.7.2, P12 – I think this sections needs to be made clearer. I am struggling to make the link between the output from FASST and the calculation of indirect aerosol forcing. How is done? What fields from FASST are used to calculate it? Needs to explain the methodology better for the reader.

REPLY: Apologies if the manuscript lacked clarity on this issue. Equation (7) explains how FASST SR matrices for radiative forcing are obtained: the change in forcings (both direct and indirect) for the perturbation experiments are computed from TM5-output using normalized forcing efficiencies. FASST then simply contains a SR coefficient to be multiplied with the emission change to obtain a forcing change. Sections 2.7.1 and 2.7.2. describe the underlying methodology in TM5. We have added some more clarification as follows:

CHANGES TO MANUSCRIPT: *modified section 2.7.3 as follows:*

2.7.3 Radiative forcing by O₃ and CH₄

Using TM5 output, indirect forcing is evaluated considering only the so far best studied first indirect effect, and using the method described by Boucher and Lohmann (1995). Fast feedbacks on cloud lifetimes and precipitation were not included in this off-line approach. This simplified method uses TM5 3D time-varying fields of SO₄ concentrations, cloud liquid water content, and cloud cover (the latter from the parent ECMWF meteorological data). The parameterization uses the cloud information (liquid water content and cloud cover) from the driving ECMWF re-analysis data (year 2001). Fast feedbacks on cloud lifetimes and precipitation were not included in this off-line approach. The cloud droplet number concentrations and cloud droplet effective radius were calculated following Boucher and Lohmann (1995) separating continental and maritime clouds. The equations are given in section S6 of the SI. The global indirect forcing field associated with sulfate aerosols is shown in Fig. S6.1(d) of the SI. Indirect forcing by clouds remains however highly uncertain, and although FASST evaluates its magnitude, it is often not included in our analyses.

30) Section 2.7.2, P12, Line 29 – Add year used to meteorological data

REPLY: done (see previous comment)

31) Section 2.7.2, P12, Line 30 – missing word ‘using’ between after ‘calculated’. Also it is probably worth stating here or in the supplementary section S6 the equations used to calculate cloud droplet number concentrations and cloud effective radius

REPLY: done

CHANGES TO MANUSCRIPT:

Following section was added to section S6 of the SI:

Indirect forcing:

The cloud droplet number concentrations (*CDNC*) were calculated using the following set of equations from Boucher and Lohmann (1995), separating continental and maritime clouds:

$$CDNC_{cont}^{St} = 10^{2.24+0.257\log(m_{SO_4})}$$

$$CDNC_{cont}^{Cu} = 10^{2.54+0.186\log(m_{SO_4})}$$

$$CDNC_{ocean} = 10^{2.06+0.48\log(m_{SO_4})}$$

Following Boucher and Lohmann (1995), the cloud droplet effective radius is calculated from the mean volume cloud droplet radius:

$$r_e = 1.1 \left(\frac{l\rho_{air}}{(4/3)\pi\rho_{water}CDNC} \right)^{1/3}$$

Where l = cloud liquid water content, ρ_{air} = air density, ρ_{water} = water density

32) Section 2.7.3, P13 – Like section 2.7.2. I think this section needs to be made clearer to highlight what output is being used from FASST to compute O₃ and CH₄ radiative forcings. There is a lot of details of what is included but I struggled to follow the basic principle of FASST output + forcing efficiency = radiative forcing. I think the description of what is done in FASST should come first at the start of this paragraph and then follow with the description of what it takes account of.

REPLY: We apologize for the lack of clarity. The section was indeed not very clear in explaining the methodology used in TM5 and how this is transferred into FASST. We have modified the introductory part of section 2.7 to explain the general approach: TM5 provides radiative forcing output from a built-in methodology, and the forcing SRs in FASST are simply based on emission-normalized delta's between base and perturbation experiments. The subsequent sections then explain in more detail how forcing is calculated in TM5.

Further we have shortened section 2.7.3 and moved the details of the methodology to the SI (new section S6.2)

CHANGES TO MANUSCRIPT: *we modified the introductory part of the section and the section addressing radiative forcing by O₃ and CH₄ as follows:*

2.7 Climate metrics

We make use of the available 3D aerosol and O₃ fields in the -20% emission perturbation simulations with TM5 to derive the change in global forcing for each of the perturbed emitted precursors. The region-to-global radiative forcing SR for precursor j , emitted from region k , is calculated as the emission-normalized change in global radiative forcing between the TM5 base and the corresponding -20% emission perturbation experiment:

$$SR_{RF}_k^j = \frac{RF_PERT[j,k]-RF_BASE}{0.2E_k^j} [W/m^2]/[kg/yr] \quad (7)$$

where RF_PERT and RF_BASE are the TM5 global radiative forcings for the perturbation and base simulations respectively, and E_k^j is the annual base emission of precursor j from region k . For each emitted pollutant (primary and secondary) the resulting normalized global forcing responses are then further used to calculate the global warming potential (GWP) and global temperature potential (GTP) for a series of time horizons H . In this way, a set of climate metrics is calculated with a consistent methodology as the air quality metrics, health and ecosystem impacts calculated from the concentration and deposition fields. In this section we describe in more detail the applied methodologies in TM5 to obtain the radiative forcing from aerosols, clouds and gases, as well as the derivation of the GWP and GTP metrics.

(...)

2.7.3 Radiative forcing by O₃ and CH₄

Using TM5 output, radiative forcing (RF) by ozone is approximated using the forcing efficiencies obtained by the STOCHEM model as described in Dentener et al. (2005), normalized by the ozone columns obtained in that study. Here we use annual averaged forcing based on the

RF computations provided as monthly averages by D. Stevenson (personal communication, 2004). The radiative transfer model was based on Edwards and Slingo (1996). These forcings account for stratospheric adjustment, assuming the fixed dynamical heating approximation, which reduces instantaneous forcings by ~22%.

For CH₄ the RF associated with the base simulation was taken from the equations in the IPCC-Third Assessment Report (TAR) (Table 6.2 of Ramaswamy et al., 2001). Using the HTAP1 calculated relationship between CH₄ concentration and emission, and the same equations, we evaluated a globally uniform value of 2.5 mW/m² per Tg CH₄ emitted. (Dentener et al., 2010). It includes both the direct CH₄ greenhouse gas (GHG) forcing (1.8 mW/m²) as well as the long-term feedback of CH₄ on hemispheric O₃ (0.7 mW/m²).

From the TM5 perturbation experiments we derive as well region-to-global radiative forcing SRs for precursors (NO_x, NMVOC, CO and SO₂) through their feedback on the CH₄ lifetime and subsequently on long-term hemispheric O₃ levels. Hence, the greenhouse gas radiative forcing contribution of each ozone precursor consists of 3 components: a direct effect through the production of O₃, a contribution by a change in CH₄ through modified OH levels (including a self-feedback factor accounting for the modified CH₄ lifetime), and a long-term contribution via the feedback of CH₄ on hemispheric ozone. The details of the applied methodology are given in section S6.2 of the SI.

In its current version, TM5-FASST_v0 provides the steady-state concentrations and forcing response of the long-term O₃ and CH₄ feedback of sustained precursor emissions, i.e. it does not include transient computations that take into account the time lag between emission and establishment of the steady-state concentration of the long-term O₃ and CH₄ responses.

And in the SI:

S6.2 Secondary forcing feedbacks of O₃ precursors on CH₄ and background O₃

Emissions of short-lived species (NO_x, NMVOC, CO, SO₂) influence the atmospheric OH burden and therefore the CH₄ atmospheric lifetime, which in turn contributes to long-term change in CH₄ and background ozone. Hence, the total forcing contribution from O₃ precursors consists of a short-term direct contribution from immediate O₃ formation (S-O₃), and secondary contributions from CH₄ (I-CH₄) and a long-term feedback from this CH₄ on background O₃ (M-O₃).

We apply the formulation by (Fiore et al., 2009; Prather et al., 2001; West et al., 2007) to calculate the secondary change in steady-state CH₄ from SLS emissions, using the TM5 perturbation experiments for FASST (see section S3). TM5 diagnoses the CH₄ loss by oxidation for reference and perturbation run (where the emissions of SLS are decreased with -20%), from which we calculate the CH₄ oxidation lifetime ratio between reference and perturbation:

$$\frac{LT_P}{LT_{Ref}} = \frac{CH4_{oxP}}{CH4_{oxRef}} \quad [S6.5]$$

Where LT is the CH₄ lifetime against loss by OH oxidation, and CH₄_{ox} = the amount (Tg) of CH₄ oxidized.

The new steady-state methane concentration *M* due to the changing lifetime from perturbation experiment P, induced by O₃ precursor emissions follows from (Fiore et al., 2008, 2009; Wild and Prather, 2000):

$M = M_0 \times \left(\frac{LT_P}{LT_{ref}}\right)^F$ where *M*₀ = 1760 ppb, the reference CH₄ concentration and F = 1.5, determined from the HTAP1 CH₄ perturbation experiments, as described in section S3.

The change in CH₄ forcing (I-CH₄) associated with the change to the new steady-state concentration is obtained from IPCC AR5 equations:

$$\Delta F = \alpha(\sqrt{M} - \sqrt{M_0}) - (f(M, N_0) - f(M_0, N_0)) \quad [S6.6]$$

$$f(M, N) = 0.47 \ln[1 + 2.01 \times 10^{-5} (MN)^{0.75} + 5.31 \times 10^{-15} M (MN)^{1.52}] \quad [S6.7]$$

Where M , M_0 = CH₄ concentration in ppb, N_0 = N₂O (=320 ppb)

The associated long-term O₃ forcing (M-O₃) per Tg precursor emitted is obtained by scaling linearly the change in O₃ forcing obtained in the HTAP1 CH₄ perturbation simulation (SR2–SR1), with the change in CH₄ obtained above, and normalizing by the precursor emission change (Fiore et al., 2009)

$$\Delta F = \frac{\Delta F_{O_3}[SR2-SR1]}{M_{SR2}-M_{SR1}} (M - M_0) \quad [S6.8]$$

The response of CH₄ and O₃ forcing to CO emission changes (for which no regional TM5-FASST perturbation model simulations were performed) was taken from TM5-CTM simulations performed for the HTAP1 assessment (Dentener et al., 2010) using the average forcing efficiency for North America, Europe, South-Asia and East-Asia. For regions not covered by the HTAP1 regions, the HTAP1 rest-of-the-world forcing efficiency was used.

The resulting region-to-globe emission-based forcing efficiencies are given in Tables S6.2 to S6.5 for aerosols, CO, CH₄ and other O₃ precursors respectively.

33) Section 2.7.3, P13, Lines 4 to 6 – How do these STOCHEM calculations compare to the ACCMIP multi-model mean and is it still appropriate?

REPLY: We have not made ourselves the comparison between STOCHEM and ACCMIP normalized O₃ radiative forcings. However Stevenson et al. (2013) calculated a global normalized RF of 42 mWm⁻² DU⁻¹, while two other model studies find values of about 36 mWm⁻² DU⁻¹. In this study a value 30 mWm⁻² DU⁻¹ was found, broadly in line with the global numbers above. The results of Stevenson et al. (2013) were not available when the RF module was developed, and indeed updating the radiative transfer code, including ozone vertical profiles (instead of using fixed ozone columns) would be obvious candidates for improvement.

34) Section 2.7.3, P13, Line 32 – For regions not covered by the major HTAP1 source could the ‘rest of the world’ CO forcing efficiency not be used from Table S6.3 rather than a global average?

REPLY: This is indeed a correct observation; we have corrected the text and the values in Table S6.3.

35) Section 2.7.4, P14, Line 7 – Are the emission based forcing efficiencies those in Table S6.2 to S6.5? Can a reference be put in to these in the main text?

REPLY: OK done

CHANGES TO MANUSCRIPT: *we refer to the relevant tables in the SI in the respective sections 2.7.1 (aerosols)*

(P14 L22) The regional emission-normalized forcing SRs for aerosol precursors (in W m⁻² Tg⁻¹) are given in Table S6.2 of the SI.

2.7.2 (indirect forcing)

(P15 L6) The global indirect forcing field associated with sulfate aerosols is shown in Fig. S6.1(d) of the SI an regional forcing SRs are listed in Table S6.2

and 2.7.3 (Radiative forcing by O3 and CH4)

(P15 L25) The details of the applied methodology for direct and indirect CH₄ forcing SRs are given in section S6.2 of the SI, including tables with the regional forcing efficiencies for all precursors (Tables S6.3 to S6.5).

And in the first line of section 2.7.4:

(P16 L2) The obtained emission-based forcing efficiencies (Tables S6.2 to S6.5 in the SI) are immediately useful for evaluating a set of short-lived climate pollutant climate metrics.

36) Section 3, P15, Lines 19 to 21 – Simplify point 1 to read better

REPLY: agree, we have rephrased the introduction of this section as follows

CHANGES TO MANUSCRIPT:

3 Results: validation of the reduced-form TM5-FASST

In this section we focus on the validation of regionally aggregated TM5-FASST_v0 outcomes (pollutant concentrations, exposure metrics, impacts), addressing specifically:

- 1 The additivity of individual pollutant responses as an approximation to obtain the response to combined precursor perturbations,
- 2 The linearity of the emission responses over perturbation ranges extending beyond the -20% perturbation
- 3 The FASST outcome versus TM5 for a set of global future emission scenarios that differ significantly from the reference scenario
- 4 FASST key-impact outcomes versus results from the literature for some selected case studies, with a focus on climate metrics, health impacts and crops.

37) Section 3.1, P16, Line 2 – reference is made to Annex 4 of the SI. Please clarify this reference as there is no Annex 4

REPLY: Indeed thanks for spotting.

CHANGES TO MANUSCRIPT: *reference is now correctly made to Table S3 (P17 L26)*

Additional standard -20% perturbation experiments P3 (NO_x only) and P5 (NO_x and NMVOC), as well as an additional set of perturbation simulations P1' to P5' over the range [-80%, +100%], listed in Table S3 of the SI, have been performed for a limited selection of representative source regions (Europe, USA, China, India, Japan) due to limited CPU resources.

38) Section 3.1.1, P16, Lines 12 to 14 – Is there a reason for the particular representative source regions selected in Table 2 e.g. South Africa for NO_x

REPLY: In order to optimize computing time, NO_x-only as well as the combined NO_x-NMVOC perturbation regions were selected based on their presumed relevance in terms of impact, pace of expected emission changes in the future and geographical representativeness. South Africa was included as a case of rapidly developing economy in the Southern hemisphere and a possible case where it may be “safer” to explicitly calculate the NO_x SR rather than applying gap filling.

39) Section 3.1.1, P16, Lines 19 to 22 – The explanation on these lines could be simplified

REPLY: done

CHANGES TO MANUSCRIPT: *we have rewritten the first part of section 3.1.1 as follows:*

3.1.1 Additivity and linearity of secondary inorganic PM_{2.5} response:

Experiment P1, where BC, POM, SO₂ and NO_x emissions are simultaneously perturbed by -20% relative to base simulation P0, delivers SR matrices for primary components BC and POM, and a first-order approximation for the precursors SO₂ and NO_x whose emissions do not only affect SO₂ and NO_x gas concentrations but also lead to several secondary products (SO₂ forms ammonium sulfate, NO_x leads to O₃ and ammonium nitrate). Experiment P2 perturbs SO₂ only, while experiment P3 perturbs NO_x only (in this latter case, to limit the computational cost, computed for a limited set of representative source regions only).

We first test the hypothesis that the PM_{2.5} response to the combined (NO_x + SO₂) -20% perturbation (P1) can be approximated by the sum of the single precursor perturbations responses (P2 + P3). Figure 2 summarizes the resulting change in SO₄²⁻, NO₃⁻, NH₄⁺ and total inorganic PM_{2.5} respectively for the selected source regions. For Europe, the emission perturbations were applied over all European countries simultaneously, hence the responses are partly due to inter-regional transport from other countries. Following findings result from the perturbation experiments P1, P2 and P3:

- (1) Sulfate shows a minor response to NO_x emissions, and likewise nitrate responds only slightly to SO₂ emissions and both perturbations are additive. In general the response is one order of magnitude lower than the direct formation of SO₄²⁻ and NO₃⁻ from SO₂ and NO_x respectively. (Fig. 2a, b).
- (2) NH₄ responds to NO_x and SO₂ emissions with comparable magnitudes and in an additive way (Fig. 2c)
- (3) A simultaneous -20% emission perturbation of SO₂ and NO_x behaves in an additive manner for what concerns the formation of secondary PM_{2.5}, i.e. the response of total sulfate, nitrate and ammonium to a combined NO_x and SO₂ perturbation can be approximated by the sum of the responses to the individual perturbations (Fig. 2d), i.e. P1 ≈ P2+P3. Scatterplots between P1 and P2+P3 for the regional averaged individual secondary products and total inorganic PM_{2.5} are shown in Fig. S7.1 of the SI

40) Section 3.1.1, P16, Lines 29 to 31 – Also there is a larger response to NO₃ from increasing NO_x emissions over India. Do you think that is this a particular issue for TM5 over India? Does this cause issues for future prediction of NO₃ aerosol from changes in NO_x emissions over India?

REPLY: The reviewer correctly notices the large sensitivity of aerosol nitrate formation to NO_x emissions in India. It is difficult to say whether this is a specific feature of TM5, or a more general feature of others models, as we are not aware of published sensitivity studies on NO_x - aerosol NO₃ in India. Moreover to our knowledge there are hardly any reliable NO₃ observations available from India that could corroborate the calculated sensitivity. We will however highlight this feature in our paper, with a specific recommendation to devote more multi-model studies to this.

CHANGES TO MANUSCRIPT: *Modified / added following phrases: (P19 L2)*

The figure illustrates the general near-linear behaviour of regionally aggregated responses to single precursor emission perturbations for all regions, except for India where the linearity of the response to NO_x emissions breaks down for emission reductions beyond -50%. For India we further observe a relatively strong nitrate response to NO_x emissions, with NO₃⁻ increasing by a factor of 3 for a doubling of NO_x emissions. We are not aware of reliable observations or other published NO_x-aerosol sensitivity studies from that region that could corroborate the calculated

sensitivity. Because such a feature may strongly affect projected future PM_{2.5} levels and associated impacts, we recommend devoting regional multi-model studies to this aspect.

41) Section 3.1.1, P17, Lines 8 to 11 – I don't think you can say that errors in the -80% case are larger than +100% for NO_x. They look similar to me

REPLY: This part of the section has been rewritten to comply with earlier comments on statistic metrics

CHANGES TO MANUSCRIPT: *We have rephrased the part of section 3.1.1 dealing with linearity test under the large perturbations as follows: (P18 L30)*

Next we evaluate the hypothesis that the -20% perturbation responses can be extrapolated towards any perturbation range, as an approximation of a full TM5 simulation. Figure 3 shows, for the selected regions listed in Table S3 of the SI, the TM5 computed relative change in secondary PM_{2.5} concentration versus the relative change in precursor emission in the range [-80%, +100%]. The figure illustrates the general near-linear behaviour of regionally aggregated responses to single precursor emission perturbations for all regions, except for India where the linearity of the response to NO_x emissions breaks down for emission reductions beyond -50%. For India we further observe a remarkably strong nitrate response to NO_x emissions, with NO₃⁻ increasing by a factor of 3 for a doubling of NO_x emissions, although the responses shown in Fig. 2 indicate that absolute changes (in µg m⁻³) in NO₃ are relatively low and that secondary PM_{2.5} in this region is dominated by SO₄. We are not aware of reliable observations or other published NO_x-aerosol sensitivity studies from that region that could corroborate this calculated sensitivity. Because such a feature may strongly affect projected future PM_{2.5} levels and associated impacts, we recommend regional multi-model studies devote attention this feature. Because the TM5-FASST linearization is based on the extrapolation of the -20% perturbation slope, concave-shaped trends in Fig. 3 indicate a tendency of TM5-FASST to over-predict secondary PM_{2.5} at large negative or positive emission perturbations, and opposite for convex-shaped trends. Figure 4 illustrates the error introduced in regional secondary PM_{2.5} concentrations responses when linearly extrapolating the regional -20% perturbation sensitivities to -80% (blue dots) and +100% (red dots) perturbations respectively. While the scatter plots for the single perturbations (Fig. 4 a,b,c) evaluate the linearity of the single responses, the panel showing the combined (SO₂+NO_x) perturbation (Fig. 4d) is a test for the linearity combined with additivity of SO₂ and NO_x perturbations over the considered range. In general, the linear approximation leads to a slight over-prediction of the resulting secondary PM_{2.5} (i.e. the sum of sulfate, nitrate and ammonium) for all regions considered, in either perturbation direction. Table 4 shows regional statistical validation metrics (normalized mean bias NMB [%], mean bias MB [µg m⁻³], and correlation coefficient, definitions are given in the Table Notes) for the grid-to-grid comparison between TM5-FASST and TM5-CTM of the response to the [-80%, 100%] perturbation simulations (with Europe presented as a single region). In terms of NMB, the FASST linearisation performs worst for the NO_x perturbations, with almost a factor 2 overestimate in Japan for an emission doubling. However, because of the already low NO_x emissions in this region, the absolute error (MB) remains below 0.2 µg m⁻³. In all considered perturbation cases, FASST shows a positive MB, except for the NO_x perturbation in India. In general, the highest NMB are observed for the regions where secondary PM_{2.5} shows low response sensitivity to the applied perturbations and where the impact on the total PM_{2.5} is therefore relatively low. Indeed, when considering the total resulting secondary PM_{2.5} (i.e. the full right-hand side of Eq. 2, including the PM_{2.5} base-concentration term containing primary and secondary components), regional averaged FASST secondary PM_{2.5} values stay within 15% of TM5 (see Table S7.1 of the SI). A break-down for the individual receptor regions within the European

zoom region of the linearisation error on the resulting total secondary PM_{2.5} from individual and combined precursor perturbations is shown in Fig. S7.3 of the SI.

42) Section 3.1.2, P17, Lines 18 to 19 – Can you include references to back up the fact that combined NO_x and NMVOCs emission perturbations will behave more linearly?

REPLY: We do not exactly say that combined and aligned NO_x-VOC emission changes (in general) are behaving linearly, but, seen the fact that the ratio NO_x/NMVOC determines the O₃ formation regime, combined emission changes of the same relative size and sign (in the way we applied them e.g. to establish the combined -20% perturbation responses) will not change the emission ratio and therefore preserve the O₃ formation regime implying a linear behaviour. This is an implication of the statement made in the first phrase where we provide references.

CHANGES TO MANUSCRIPT: *we adapted the phrase as follows: (P20 L5)*

Because the NO_x/NMVOC ratio determines the O₃ response to emission changes, a perturbation with simultaneous NO_x and NMVOC emission changes of the same relative size is expected to behave more linearly than single perturbations since the chemical regime remains similar.

43) Section 3.1.2, P17, Line 31 – remove ‘also here’

REPLY: done

44) Section 3.1.2, P17, Line 31 to 32 – Good agreement is found everywhere apart from China, Why?

REPLY: We presume the reviewer is referring to Fig. 5. Indeed for China the agreement between combined and sum of individual responses is – in absolute terms – slightly worse than most other regions, but in relative terms the sum of perturbations is within 10% of the combined one. We have added a scatterplot to Figure 5 to illustrate the over-all validity of additivity. The underlying reason for the small deviations between combined and sum-of-individual responses has not been investigated in detail but, as stated above, is most probably linked to the fact that changing a single precursor emission strength changes the NO_x/NMVOC ratio and could affect the O₃ emission response regime.

CHANGES TO MANUSCRIPT: *P20 L19*

As shown in Fig. 5, for the -20% perturbations we find good agreement between the combined (NO_x + NMVOC) perturbation (open circles) with the sum of the individual precursor perturbation (black dots). This occurs even in situations where titration by NO causes a reverse response in O₃ concentration as is the case in most of Europe and the USA, indicating that a -20% perturbation in individual precursors appears not to change the prevailing O₃ regime.

We also added a scatter plot to Fig. 5 to demonstrate the very good correspondence.

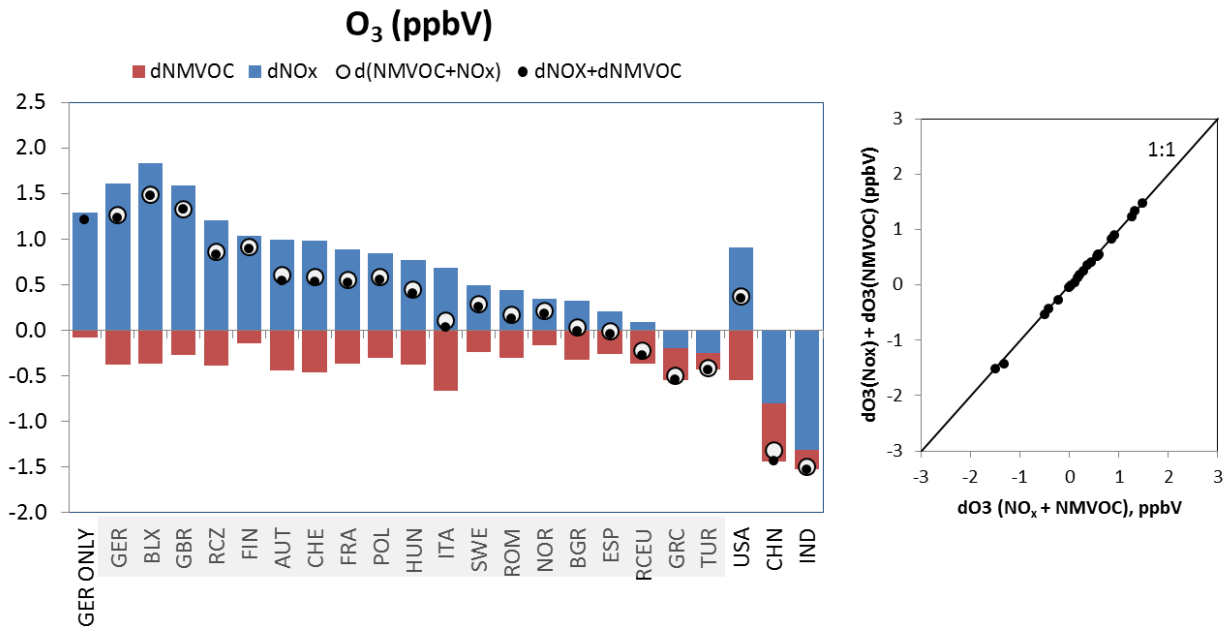


Figure 5: TM5-CTM response in annual mean population-weighted O_3 concentration (in ppbV) upon emitted precursor perturbation of -20% for selected source receptor regions. European regions were perturbed simultaneously. Red bar: response from NMVOC-only perturbation (simulation P4); blue bar: response from NO_x -only perturbation (simulation P3). Open circles: response from simultaneous (NMVOC + NO_x) perturbation (simulation P5). Black dots: sum of individual responses. Shaded regions are perturbed simultaneously as one European region. Right panel: scatter plot between O_3 response to combined and summed individual responses.

45) Section 3.1.2, P18, Line 2 – change ‘Europa’ to Europe

REPLY: done.

46) Section 3.1.2, P18, Lines 16 to 18 – If anything I would say FASST overestimates the change in TM5 (be it positive or negative) most of the time as the -80% points on the scatter plot tend to always above the 1:1 line (see major point 6 above).

REPLY: For a negative emission change, an origin-forced response slope below 1 (with points lying above the 1:1 line) indicates that the response between unperturbed and perturbed in FASST is lower than TM5, hence FASST underestimates the response upon an emission decrease and consequently overestimates the resulting concentration which is the sum of base and perturbation response (Eq. 2). A response slope larger than one for a positive emission change also corresponds to an over-prediction of the total concentration. We describe now more clearly in section 3.1 that we are evaluating the perturbation response (the change) and how an under/overestimation affects the total resulting concentration.

CHANGES TO MANUSCRIPT: *most of the section has been rewritten as follows: (P21 L6)*

Figure 7 illustrates the performance of the TM5-FASST approach versus TM5 for regional-mean annual mean ozone, health exposure metric 6mDMA1 (both evaluated as population-weighted mean), and for the crop-relevant exposure metrics AOT40 and M12 (both evaluated as area-weighted mean) over the extended emission perturbation range. In most cases the response (i.e. the *change* between base and perturbed case) to emission perturbations lies above the 1:1 line across the 4 metrics, indicating that FASST tends to over-predict the resulting metric (as a sum

of base concentration and perturbation). Of the four presented metrics, AOT40 is clearly the least robust one, which can be expected for a threshold-based metric that has been linearized. Tables 5 to 7 give the statistical metrics for the grid-to-grid comparison of the perturbation term between FASST and TM5 for the health exposure metric 6mDMA1, and crop exposure metrics AOT40 and M12 respectively. Statistical metrics for the total absolute concentrations (base concentration + perturbation term) are given in Tables S7.2 to S7.4 in the SI. As anticipated, the NO_x-only perturbation terms are showing the highest deviation, in particular for a doubling of emissions, however combined NO_x-NMVOC perturbations are reproduced fairly well for all regions, staying within 33% for a -80% perturbation for all 3 exposure metrics, and within 38% for an emission doubling for 6mDMA1 and M12, while the AOT40 metric is overestimated by 76 to 126% for emission doubling. The total resulting concentration over the entire perturbation range for single and combined NO_x and NMVOC perturbation agrees within 5% for 6mDMA1 and M12, and within 64% for AOT40. The mean bias is positive for both perturbations, for all metrics and over all analysed regions, except for crop metric M12 under a doubling of NMVOC emissions over Europe showing a small negative bias. The deviations for individual European receptor regions under single and combined NMVOC and NO_x perturbations for health and crop exposure metrics are shown in Figs. S7.4 to S7.6 of the SI.

47) Section 3.1.2, P18, Lines 21 to 22 – I am not sure that the linear fit is that good for the change in annual mean O3 in Figure 7a as there seems to be distinctive curvature in the +100% simulation for larger O3 reductions. I anticipate that this will be larger for certain months. The non-linear behaviour seems to occur to a lesser extent for other O3 metrics where a linear approximation is probably more justified. I think a change of wording for this statement is required to reflect the fact that a linear approximation does not represent the non-linear chemistry effects for large emission perturbation.

REPLY: The linear fits in Figure 7 were used as a guide to evaluate the overall correspondence of regional mean O3 metrics versus TM5, they are not the linear approximations used in FASST. (Each dot is obtained applying the region-specific SR coefficients for the respective precursors). Because this seems to cause confusion with the reader, we omitted the fittings and present the figure now only with the 1:1 line as a reference. Our statement refers to the observation that – except for AOT40 – the regional mean ozone metrics are relatively well represented by FASST (i.e. close to the 1:1 line) and in particular the FASST approximation reproduces the negative response to emission doubling (and positive response to emission reduction), typical for the titration regime.

CHANGES TO MANUSCRIPT: *We deleted the section using the slopes of the linear fits in Figs. 4 and 7– see also changes mentioned in previous comment*

48) Section 3.1.2, P18, Lines 25 to 28 – Check percentage numbers are correct as they don't appear to be the same as that shown on Figure S7.4 or in Table 3 e.g. -5 to 13% for M12 where on the Figure S7.4c I can't see anything below 0

49) Section 3.1.2, P18, Lines 28 to 30 – Same as above but for NMVOC

50) Section 3.1.2, P19, Line 1 – Same as above but for combined emission perturbation.

REPLY TO 47- 49:

The inconsistencies between values in the text and the figures were a consequence of a different statistical evaluation method, more in particular: the text vales were referring to the mean of all individual grid cell relative deviations, whereas the graphs were referring to the NMB as defined above (major comment 6). We report the values now consistently as NMB in text and figures.

51) Section 3.2, P19, Line 10 – remove ‘e’

REPLY: done

52) Section 3.2, P19, Line 25 to 26 –In both scenarios emissions can change by >80% over some regions and precursors. The ability of FASST to predict such changes over regions needs to be highlighted in the results based on the breakdown of the linear approach for O3 at such high emission perturbations.

REPLY: Indeed a valid suggestion.

CHANGES TO MANUSCRIPT:

- *First of all, we became aware that the numbers reported in Table S8 (emission % changes relative to FASST reference) were wrong for all regions except Asia and Global – they have now been corrected (this does not affect the reported results)*
- *The introductory part of section 3.2 has been rewritten/rearranged mentioning some features of the scenario emissions, pointing to possible issues with combined emission changes that could not be addressed in the dedicated additivity/linearity simulations*
- *We have added new Figures, demonstrating that FASST does capture regional features both for low and high emission scenarios*

We modified the relevant paragraph to:

3.2 TM5-FASST_v0 versus TM5 for future emission scenarios

In this section we evaluate different combinations of precursor emission changes relative to the base scenario in a global framework. We take advantage of available TM5 simulations for a set of global emission scenarios which differ significantly in magnitude from the FASST base simulation, and as such provide a challenging test case to the application of the linear source-receptor relationships used in TM5-FASST. We assume that the full TM5 model provides valid evaluations of emission scenarios, and we test to what extent these simulations can be reproduced by the linear combinations of SRs implemented in the TM5-FASST_v0 model. We use a set of selected policy scenarios prepared with the MESSAGE integrated assessment model in the frame of the Global Energy Assessment GEA (Rao et al., 2012, 2013; Riahi et al., 2012). These scenarios are the so called “frozen legislation” and “mitigation” emission variants for the year 2030 (named FLE2030, MIT2030 respectively), policy variants that describe two different policy assumptions on air pollution until 2030. These scenarios and their outcomes are described in detail in Rao et al. (2013), the scope of the present study is the inter-comparison between FASST and TM5 resulting pollutant concentration and exposure levels, as well as associated health impacts.

Major scenario features and emission characteristics are provided in section S8 of the SI. Table S8.1 shows the change in global emission strengths for the major precursors for both test scenarios, relative to the RCP2000 base, aggregated to the FASST ‘master zoom’ regions listed in Table S2.2. Emission changes for the selected scenarios mostly exceed the 20% emission perturbation amplitude from which the SRs were derived. Under the MIT2030 low emission scenario, all precursors and primary pollutants (except primary PM_{2.5} in East-Asia and NH₃ in all regions) are showing a strong decrease compared to the RCP2000 reference scenario. The strongest decrease is seen in Europe (NO_x: -83%, SO₂: -93%, BC: -89%, primary PM_{2.5} – 56%) while NH₃ is increasing by 14 to 46% across all regions. The FLE2030 scenario displays a global increase for all precursors, however with heterogeneous trends across regions. In Europe, North-America and Australia, the legislation in place, combined with use of less and cleaner fuels by 2030, leads to a decrease in pollutant emissions except for NH₃ and primary PM_{2.5}. On the other hand, very substantial emission increases are projected in East and South-East for BC, NO_x and primary PM_{2.5}. Anticipating possible linearity issues, we note that for both scenarios, in

all regions, SO₂ and NO_x emissions are evolving in the same direction, although not always with similar relative changes, while NH₃ is always increasing, which may induce linearity issues in the ammonium-sulfate-nitrate system. Regarding O₃ metrics, NMVOC and NO_x are evolving in the same direction, but also here we observe possible issues due to a changing emission ratio (in particular in Russia and Asia). We further note that not only the emission levels of these scenarios are different from the FASST base scenario (RCP year 2000), but also the spatial distribution of the emissions, at the resolution of grid cells, may differ from the reference set. We use FASST to compute PM_{2.5} and ozone concentrations applying Eq. (2), i.e. considering the FLE2030 and MIT2030 emission scenarios as a perturbation on the FASST reference emission set (RCP year 2000).

The scope of TM5-FASST is to evaluate on a regional basis the impacts of policies that affect emissions of short-lived air pollutants and their precursors. Hence we average the resulting O₃ and PM_{2.5} concentration and O₃ exposure metric 6mDMA1 over the each of the 56 FASST regions and compare them with the averaged TM5 results for the same regions.

Further, in a policy impact analysis framework, the *change* in pollutant concentrations between two scenarios (e.g. between a reference and policy case) is often more relevant than the absolute concentrations. We therefore present absolute concentrations as well as the change (delta) between the two GEA scenarios, evaluating the benefit of a mitigation scenario versus the frozen legislation scenario.

Figure 8 shows the FASST versus TM5 regional scatter plots for absolute and delta population-weighted mean anthropogenic PM_{2.5} for all 56 FASST receptor regions while the population-weighted means over the 9 larger zoom areas are shown in Figure 9. Similarly annual mean population-weighted O₃ and 6mDMA1 scatter plots are shown in Fig. 10, and the regional distribution in Fig. 11. The grid-cell statistics (mean, NMB, MB and R²) over larger zoom areas are given in Tables 8 and 9 for PM_{2.5} and 6mDMA1 respectively.

Figure 8 and Table 8 show that on a regional basis, the low emission scenario generally overestimates population-weighted PM_{2.5} concentrations, with the highest negative bias in Europe and Asia, while the lowest deviation is found in Latin America and Africa. The agreement between FASST and TM5 is significantly better for the high emission scenario, in line with the findings in the previous section. As shown in Table 8, averaged over the larger zoom regions, we find that the relative deviation for PM_{2.5} is within 11% for FLE2030, and within 28% for MIT2030, except for Europe where the (low) PM_{2.5} concentration is overestimated by almost a factor of 2. The policy-relevant delta between the scenarios however is for all regions reproduced within 23%.

The ozone health metric 6mDMA1 is more scattered than annual mean ozone, and also here, as expected, the low emission scenario performs worse than the high emission one. Over larger zoom areas however the agreement is acceptable for both scenarios (FASST within 22% of TM5). Contrary to PM_{2.5}, the NMB for the delta 6mDMA1 between two scenarios is higher than the NMB on absolute concentrations, with a low bias for the delta metric of -38% and -45% for Europe and North-America respectively, and a high bias of 35 to 46% in Asia. However, the MB on the delta is of the same order or lower than the absolute concentrations (Table 9). This is a consequence of the fixed background ozone in the absolute concentration reducing the weight of the anthropogenic fraction in the relative error.

Figures 9 and 11 provide a general picture of the performance of FASST: despite the obvious uncertainties and errors introduced with the FASST linear approximation over large emission changes compared to the RCP base run, at the level of regionally aggregated concentrations, a consistent result emerges both for absolute concentrations from the individual scenarios as for the policy-relevant delta.

And changed/added the following figures

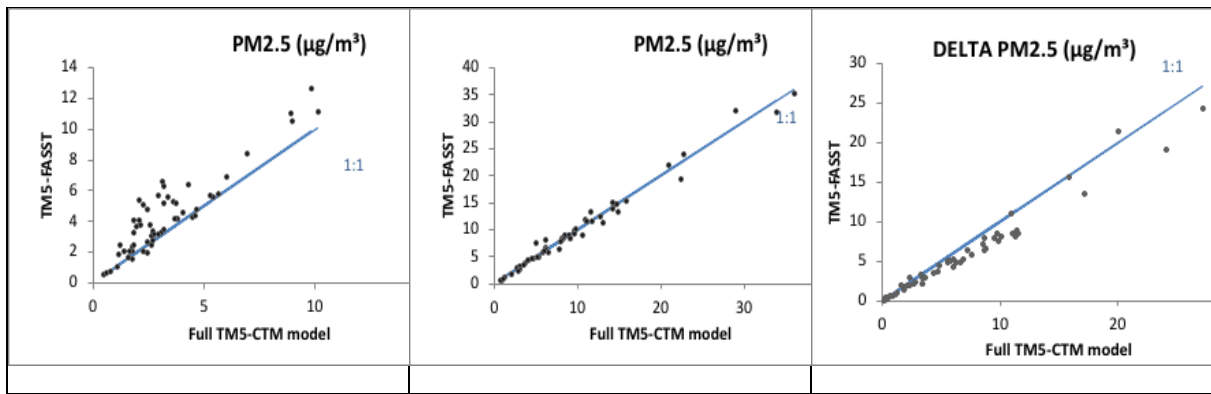


Figure 8: Population-weighted mean $PM_{2.5}$ concentration computed with TM5-FASST versus TM5-CTM for low emission scenarios MIT2030 (left), high emission scenario FLE2030 (middle) and the change between the two. Each point represents the population-weighted mean over a TM5-FASST receptor region. Blue line: 1:1 relation.

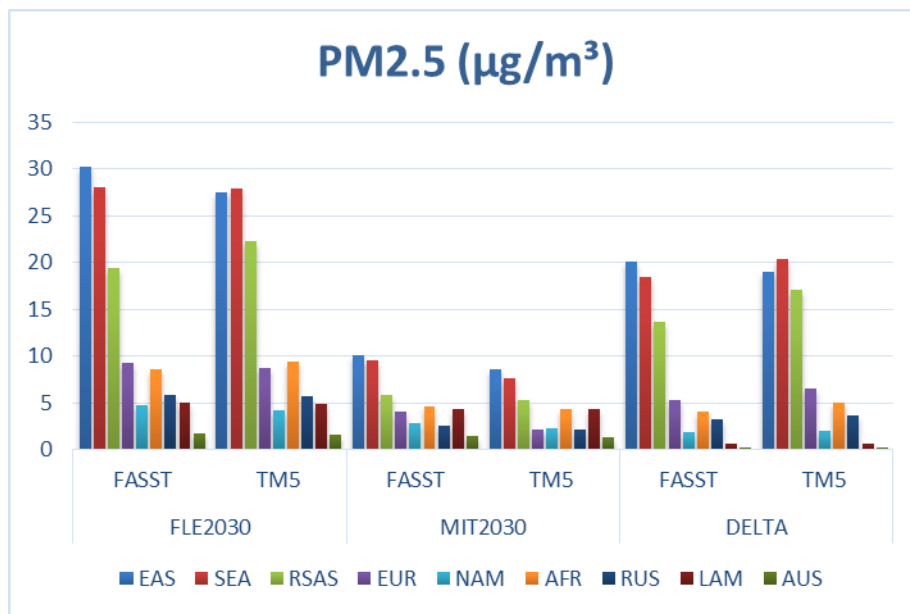


Figure 9 Total population-weighted anthropogenic $PM_{2.5}$ over larger FASST zoom areas, for the high (FLE2030) and low (MIT2030) emission scenarios, and the difference (delta) between both, computed with the full TM5 model and with FASST

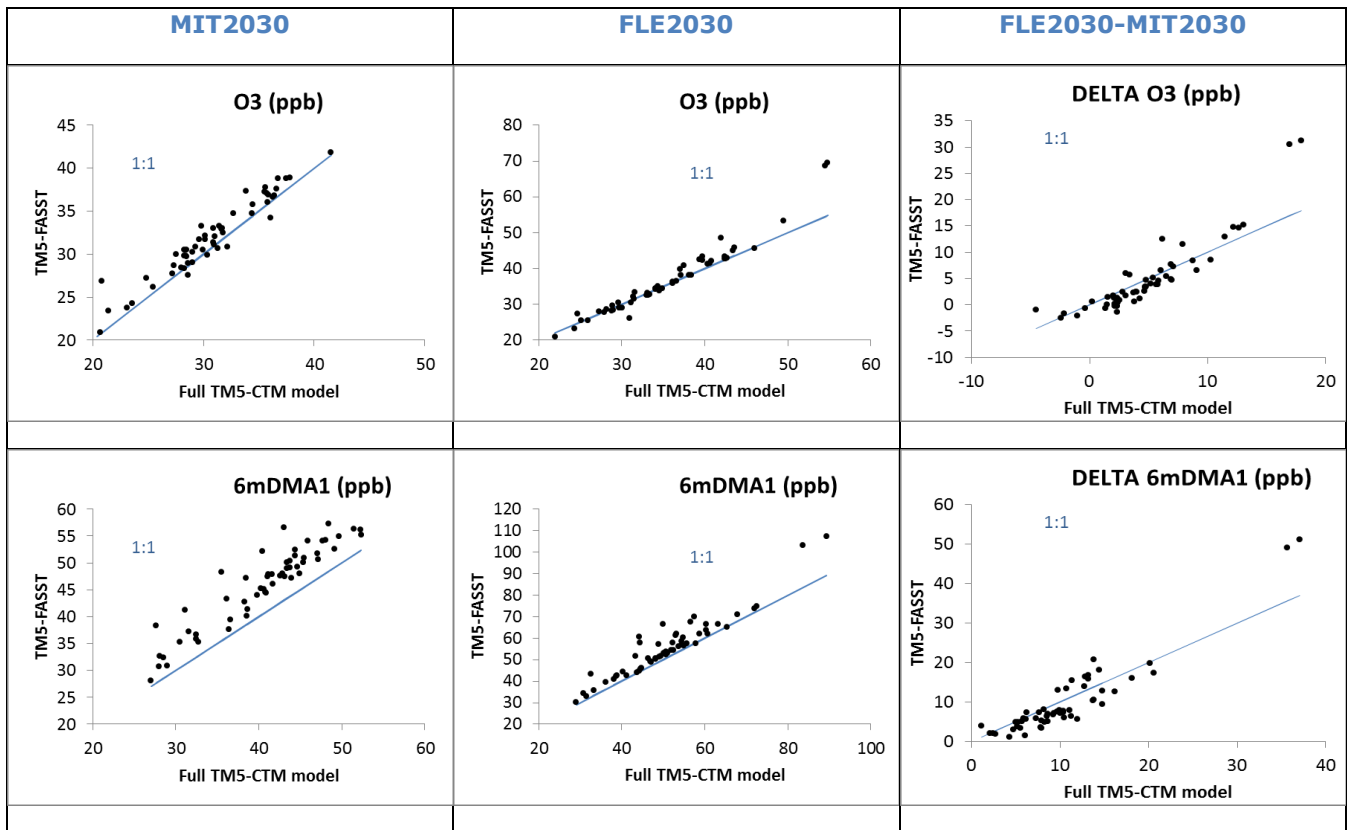


Figure 10: Population-weighted mean annual ozone (top) and ozone exposure metric 6mDMA1 (bottom) computed with TM5-FASST versus TM5-CTM for low emission scenarios MIT2030 (left), high emission scenario FLE2030 (middle) and the change between the two (right). Each point represents the population-weighted mean over a TM5-FASST receptor region. Blue line: 1:1 relation.

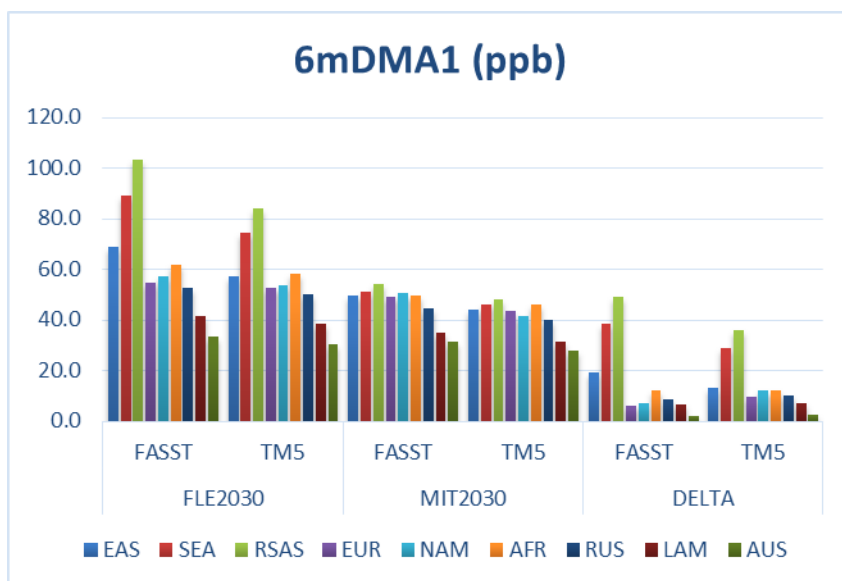


Figure 11: Total population-weighted anthropogenic PM_{2.5} over larger FASST zoom areas, for the high (FLE2030) and low (MIT2030) emission scenarios, and the difference (delta) between both, computed with the full TM5 model and with FASST

53) Section 3.2, P20, Lines 3 to 5 – If it is more policy relevant to consider the change in pollutant concentrations between two scenarios than absolute concentrations, and FASST is a tool for the assessment of policy measures, then why is the difference not shown in place of absolute concentrations? Might be worth showing the change in concentrations in the main text and the absolute concentrations in the supplementary. Also it might be better to show the change between FLE and BASE, and MIT and BASE separately rather than the different between the two future scenarios

REPLY: We agree with the comment that from policy relevance perspective, putting more emphasis on the deltas makes sense. However, using in TM5FASST the RCP reference year 2000 as a common reference scenario is not very useful as here we are looking at a different scenario family (GEA) and a different year (2030). From policy perspective, comparing a ‘policy’ case (here: MIT2030) with a ‘non-policy’ case (here: FLE2030) for a given year immediately reveals the benefits of policy action. We therefore prefer to present the delta between the two GEA scenarios (with the additional benefit that this reduces the number of figures when showing the delta).

CHANGES TO MANUSCRIPT

As mentioned in the reply to the previous comment, we have rewritten most of the section. We include and discuss now both delta and totals for the two scenarios.

54) Section 3.2, P20, Line11 to 12 – I would say that FASST tends to underestimate the magnitude of change in TM5 for both annual mean and M6M O3, as most points are below the 1:1 line. (see major point 6 above).

REPLY: The referee made a correct observation; the slope is misleading here. This has been addressed with the changes made in text and the new figures (see previous comments)

55) Section 3.2, P20, Lines 15 to 21 – Only a very small discussion on the future evaluation of health metrics. Maybe expand slightly to include different regions and that FASST always overpredicts compared to TM5

REPLY: Agree, we have expanded the discussion of the intercomparison of the health impacts and included as well the delta in mortalities as from policy perspective this is relevant.

CHANGES TO MANUSCRIPT:

- *Added additional panels c to Figs. 10 and 11 showing the delta mortalities for PM_{2.5} and O₃ respectively*
- *Modified the health impact discussion as follows: (P23 L22)*

A major issue in air pollution or policy intervention impact assessments is the impact on human health; therefore we also evaluate the TM5-FASST outcome on air pollution premature mortalities with the TM5-based outcome, applying the same methodology on both TM5 and FASST outcomes. We evaluate mortalities from PM_{2.5} using the IER functions (Burnett et al., 2014) and O₃ mortalities using the log-linear ER functions and RR's from Jerrett et al. (2009) respectively. Figure 12 (PM_{2.5}) and Fig. 13 (O₃) illustrate how FASST-computed mortalities compare to TM5, both as absolute numbers for each scenario, as well as the delta (i.e. the health benefit for MIT2030 relative to FLE2030). Regional differences in premature mortality numbers are mainly driven by population numbers. In line with the findings for the exposure metrics (PM_{2.5} and 6mDMA1) FASST in general over-predicts the absolute mortality numbers, in particular in the low-emission case. For MIT2030, global PM_{2.5} mortalities are overestimated by 19%, in Europe and North-America FASST even by 43%. In the FLE2030 case, we find a better agreement, with a global mortality over-prediction of 3% (for Europe and North-America 5% and 11% respectively). For the latter scenario, the highest deviation is found in Latin America (10 – 20%). O₃ mortalities are overestimated globally by 11% (7%) with regional agreement within 20% (14%) for MIT2030 (FLE2030). However, as shown by the error bars, the difference between FASST and TM5 is smaller than the uncertainty on the mortalities resulting from the uncertainty on RR's only. The potential health benefit of the mitigation versus the non-mitigation scenario (calculated as FLE2030 minus MIT2030 mortalities) is shown in Figs. 12c and 13c. Globally, FASST underestimates the reduction in global PM_{2.5} mortalities by 17% with regional deviations ranging between -30% for Europe and North-America, and -12% for India. The global health benefit for ozone is underestimate by 2% for O₃, however as a net result of 11% overestimation in India and 12 to 59% underestimation in the other regions. The numbers corresponding to Figs. 12 and 13 are provided in Table S8.4 and S8.5 of the SI. The error ranges presented here are obviously linked to the choice of the test scenarios and will for any particular scenario depend on the magnitude and the relative sign of the emission changes relative to RCP2000, but given the amplitude of the emission change for the currently two selected scenarios relative to RCP2000, these results support the usefulness of TM5-FASST as a tool for quick scenario screening.

56) Section 3.3.2, P22, Line 1 – relate discussion of text to labels on Figure 13 or define labels with more description in Figure 13 caption

REPLY: We presume this refers in particular to the labels in the b-panel (SLS M-O3 etc...). We have added the explanation in the figure caption.

CHANGES TO MANUSCRIPT: *changed the relevant section to: (P24 L2)*

Figure 15b shows the break-down by forcing component, including the direct contributions by aerosols, by short-lived precursors to O₃ (SLS S-O₃), their indirect effect on CH₄ (SLS I-CH₄) and associated long-term O₃ (SLS M-O₃), as well as CH₄ forcing from direct CH₄ emissions and its associated feedback on background ozone (CH₃ O₃). Fig. 15a separates the contributions by emission sector..

And similar in the caption of Fig. 13 modified to:

Figure 13: Year 2000 radiative forcing from Unger et al. (2010), based on EDGAR year 2000 emissions and from TM5-FASST applied to RCP year 2000 (a) break-down by sector and by forcing component. Biomass burning includes both large scale fires and savannah burning; (b) total over all sectors. SLS S-O₃: direct contribution of short-lived species (SLS) to O₃; SLS I-CH₄: indirect contribution from SLS to CH₄; SLS M-O₃: indirect feedback from SLS on background ozone via the CH₄ feedback. CH₄ O₃: feedback of emitted CH₄ on background O₃

57) Section 3.3.3, P22, Line 13 – replace ‘were’ with ‘where’ and remove ‘and’.

REPLY: done

58) Section 3.3.4, P22, Line 22 – remove ‘implemented in FASST

REPLY: done

59) Section 3.3.4, P22, Line 24 – replace ‘death cause’ with ‘a cause of death’.

REPLY: done

60) Section 3.3.4, P22, Line 25 to 27 – Could the difference in population and mortality rates between the two studies lead to some of the differences in Figure 14?

REPLY: This is unlikely for Figure 14 (now Figure 16) as it shows concentration changes, not mortalities. If the referee intends to refer to Fig. 15 (now 17), we mention in the text that Silva et al. use indeed different population and base mortality projections. In particular – as mentioned - the projection for respiratory base mortality rates (which is relevant only for the O₃ health impact and not for PM_{2.5}) for 2050 in Silva et al. is very different from the values used in FASST (where they are constant compared to 2030 base mortality rates). The discrete dots in the O₃ mortality graph are a simple attempt to demonstrate the impact in FASST of using these different mortality rates.

61) Section 3.3.4, P23, Line 9 to 11 – How can FASST account for inter-model variability in its results? I think that this is mentioned as a future development so needs to be linked to that here.

REPLY: We intend to say that the difference between FASST and the ACCMIP model ensemble for what concerns O₃, is probably not due to a poor performance of FASST (which is a fairly good approximation of TM5) but rather a consequence of generally occurring differences between models.

CHANGES TO MANUSCRIPT: *modified the phrase as follows: (P28 L7)*

The ozone exposure metric 6mDMA1 falls within the range of the ACCMIP model ensemble for 2030 - 2050, but the slope between 2030 and 2050 is lower than for the ACCMIP ensemble mean, i.e. FASST shows a much lower response sensitivity for O₃ to changing emissions between 2030 and 2050 than the ACCMIP models (-1ppb from 2030 to 2050 in FASST, versus -3ppb for the ACCMIP mean). Given our previous observation that FASST reproduces TM5 relatively well, this indicates that inter-model variability is a stronger factor in the model uncertainty than the reduced-form approach.

62) Section 3.3.4, P23, Line 17 – replace ‘While also’ with ‘Whilst calculated’

REPLY: It seems the use of “while” or “whilst” is interchangeable in English language. As non-native English speaker it feels more comfortable to use “while”.

63) Section 3.3.4, P23, Line 18 to 21 – Why does the different baseline mortality and population statistics have such a big impact on O3 mortality rates but not PM2.5?

REPLY: The reason is that respiratory mortality is not considered a cause of death from PM2.5; the GBD methodology includes COPD, LC, IHD and Stroke for PM_{2.5} and respiratory disease for O3.

CHANGES TO MANUSCRIPT: *added the following phrase: (P28 L25)*

Respiratory mortality is not considered as a cause of death for PM_{2.5}, which explains why a similar disagreement is not observed in the PM_{2.5} mortality trend in Fig. 17b.

64) Section 3.3.4, P23, Line 27 to 31 – Could a little more discussion on regional mortality burdens be put into the main text. Interesting differences between regions and for RCP2.6 vs RCP8.5.

REPLY: Although the scope of this paper is not to make a scenario analysis or assess trends and impacts across regions, but rather to validate the FASST model, we agree that some more discussion is useful.

CHANGES TO MANUSCRIPT: *paragraph has been rewritten as follows: (P28 L28)*

A regional break-down of mortality burden from PM_{2.5} in 2030 and 2050, relative to exposure to year 2000 concentrations, for major world regions and for the globe is shown in Figures S9.1 and S9.2 of the SI. Compared to Fig. 17 which shows the global mortality trends as a combined effect of changing population, mortality rates and pollution level, here the effect of changing population and baseline mortality is eliminated by exposing the evaluated year’s population to pollutant levels of the relevant year and to RCP year 2000 levels respectively, and calculating the change between the two resulting mortality numbers. FASST reproduces the over-all observed trends across the regions: we see substantial reductions in North America and Europe in 2030, while in East Asia significant improvements in air quality impacts are realized after 2030. For the India region, all scenarios project a worsening of the situation. The global trend is dominated by the changes in East Asia. The observed differences between FASST and ACCMIP ensemble are not insignificant and partly due to different mortality and population statistics in particular for the year 2050, still they are consistent with the findings in the previous section: FASST tends to overestimate absolute PM_{2.5} concentrations for emission scenarios different from RCP2000, and consequently tends to under-predict the benefit of emission reductions, while over-predicting the impact of increasing emissions.

65) Section 4, P24, Line 17 to 18 – Make statement in this sentence less strong by inserting ‘tend to’ between ‘metrics’ and ‘remain’.

REPLY: done

66) Section 4, P24, Lines 21 to 23 – I think the first two sentences could be re-written to simply specify that because the emissions and meteorology are fixed the source receptor matrices remain fixed. Also I think the work ‘arbitrary’ should be removed.

REPLY: we have rephrased the sentences

CHANGES TO MANUSCRIPT: (P30 L22)

Another issue for caution relates to the FASST analysis of emission scenarios with spatial distribution that differs from the FASST reference scenario (RCP year 2000). The definition of the source regions when establishing the SR matrices implicitly freezes the spatial distribution of pollutant emissions within each region, and therefore the reduced-form model cannot deal with intra-regional spatial shifts in emissions.

67) Section 4, P24, Lines 25 – remove repetitive statement of ‘compared to the base simulation year 2000’.

REPLY: done

68) Section 4, P24, Lines 27 – remove ‘be

REPLY: done

69) Section 4, P24, Lines 30 to 31 – reword sentence to ‘It can be expected that errors will be larger for the newer generation scenarios with dynamic allocation of emission across countries and macro-regions’

REPLY: done

70) Section 4, P25, Lines 5 to 7 – Sectors are mentioned that can’t be assessed but little has been mentioned about shipping and aviation which can be assessed and are specifically included as a source region in FASST. I think it is worth mentioning these source regions in this section

REPLY: Thank you for bringing this up – indeed worth mentioning.

CHANGES TO MANUSCRIPT: *added in discussion P31 L7:*

This limitation however does not apply to international shipping and aviation for which specific SR matrices have been established.

71) Section 5, P25, Line 32 – removal of ‘...’ at end of page

REPLY: done

72) Section 5, P26, Line 6 – subscripts for O₃ and PM_{2.5} required

REPLY: done

73) Section 5, P26, Line 19 – Slightly more detail could be provided on how the HTAP2 modelling exercise will inform/improve TM5-FASST, especially as TM5 was not a model that participated in HTAP2.

REPLY: The FASST architecture makes it possible to include new or additional SR matrices, even when they have been obtained from different models and with different regional definitions. SR simulations are now available from various models participating in HTAP2, but the ‘required’ and ‘desired’ simulations have not been fully completed by all participating models, and gapfilling method has been proposed (Turnock et al., 2018). Therefore a tool like FASST which

could bring this knowledge in a common structure, synthesizing the available data in an ensemble approach and make it accessible and applicable for interested users, would create a great added value. In the context of the UNECE/CLRTAP TF HTAP such a tool is already under development.

CHANGES TO MANUSCRIPT: added the paragraph P34 L22

The FASST architecture allows for an implementation of new or additional SR matrices, for instance new HTAP2 model ensemble mean matrices, each one accompanied by an ensemble standard deviation matrix to include the model variability in the results. Efforts are now underway to create a new web-based and user-friendly HTAP-FASST version, operating under the same principles as TM5-FASST, but based on an up-to-date reference simulation and underlying meteorology, thus creating a link between the knowledge generated by the HTAP scientific community and interested policy-oriented users. Indeed, similar to how the development of TM5-FASST was built upon extending the HTAP1 experiments in a single model context, the regional definitions and sector definitions used in HTAP2 (Galmarini et al., 2017; Koffi et al., 2016) were largely synchronized with the TM5-FASST set-up, increasing the community's capacity for multi-model assessments of hemispheric pollution. It is intended that the lessons-learned are informing the HTAP2 exercise

74) Figure 14 – I find that the grey lines mask out the black lines in some instances and I think the Figure would look better if the grey lines could be made less bold or more transparent. Also I am not sure why there is a different number of grey lines on each part of the Figure. Did a different number of models submit results for each experiment?

REPLY: Indeed, in ACCMIP not all models participated in each experiment, hence the different numbers. We have modified the figure to make the black lines more visible, and added information to the legenda.

CHANGES TO MANUSCRIPT: modified Fig. 14 (now 16) into

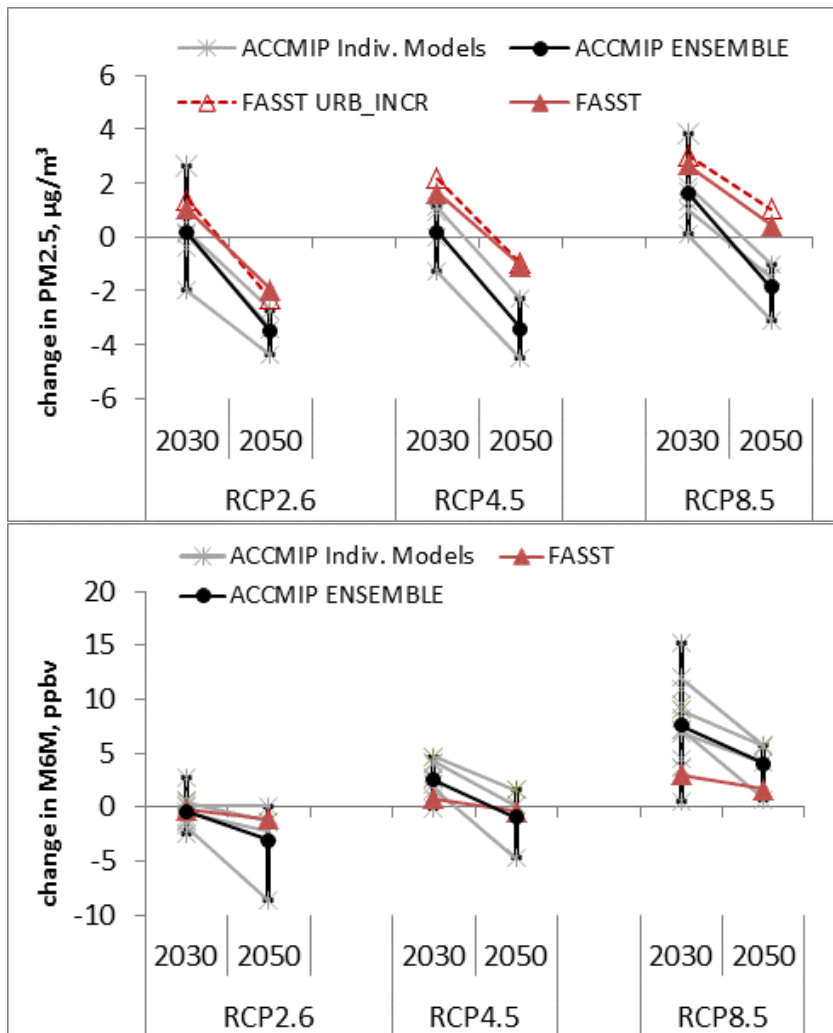


Figure 16: Global population-weighted differences (scenario year minus year 2000) (a) in annual mean PM_{2.5} concentrations and (b) in O₃ exposure metric 6mDMA1 for 3 RCP scenarios in each future year, from the ACCMIP model ensemble (Silva et al., 2016) (black symbols and lines) and TM5-FASST_v0 (red symbols and lines). FASST_URB_INCR: including the urban increment correction. Grey symbols: results from individual ACCMIP models. Grey lines connect results from a single model. Not all models have provided data for all scenarios. ACCMIP error bars represent the range (min, max) across the ACCMIP ensemble.

75) Table S3 – Certain lines in the table seem to be missing any information. e.g. P5 Germany, P4 USA, P5 Japan.

REPLY: That's a correct observation, in fact in those cases the experiments were not performed.

CHANGES TO MANUSCRIPT: *we removed the irrelevant lines, added a prime to the Pi' to distinguish from the -20% perturbations and added a line for the additional P1' simulations that were performed as well.*

76) Figure S3.3 – Why has the sign been reversed? For a 20% reduction in CH₄ you would expect a decrease in O₃ concentrations but the figure shows positive changes. This seems confusing

REPLY: Apologies for the confusion. The SR response field were stored as a positive change to a positive perturbation (although the perturbation runs were performed as negative perturbations resulting in a negative response)..

CHANGES TO MANUSCRIPT: *The caption has now been modified to:*

Figure S3.3 Decrease in annual mean surface O₃ for a 20% decrease in year 2000 CH₄ concentration, i.e. 1760 to 1408 ppb (TF-HTAP1 SR1-SR2 scenarios)

77) Section S4.1, Equation 4.4 – I am not sure I can follow how the INCR formulation was derived and why it includes the (f_{up})² terms.

REPLY: we added one intermediate step in the calculation that explains how the quadratic terms in f_{up} are obtained.

CHANGES TO MANUSCRIPT: *added*

The population-weighted concentration is calculated as

$$C_{BC, TM5}^{POP} = f_{up} C_{BC, URB} + (1 - f_{up}) C_{BC, RUR} \quad [4.3]$$

78) Figure S5 – hard to decipher the different lines on the graph. Cannot see red lines most of the time. Please make clearer

REPLY: we have decreased the size of the dots and increased the line width so it is better visible

CHANGES TO MANUSCRIPT: *figures modified in the following way:*

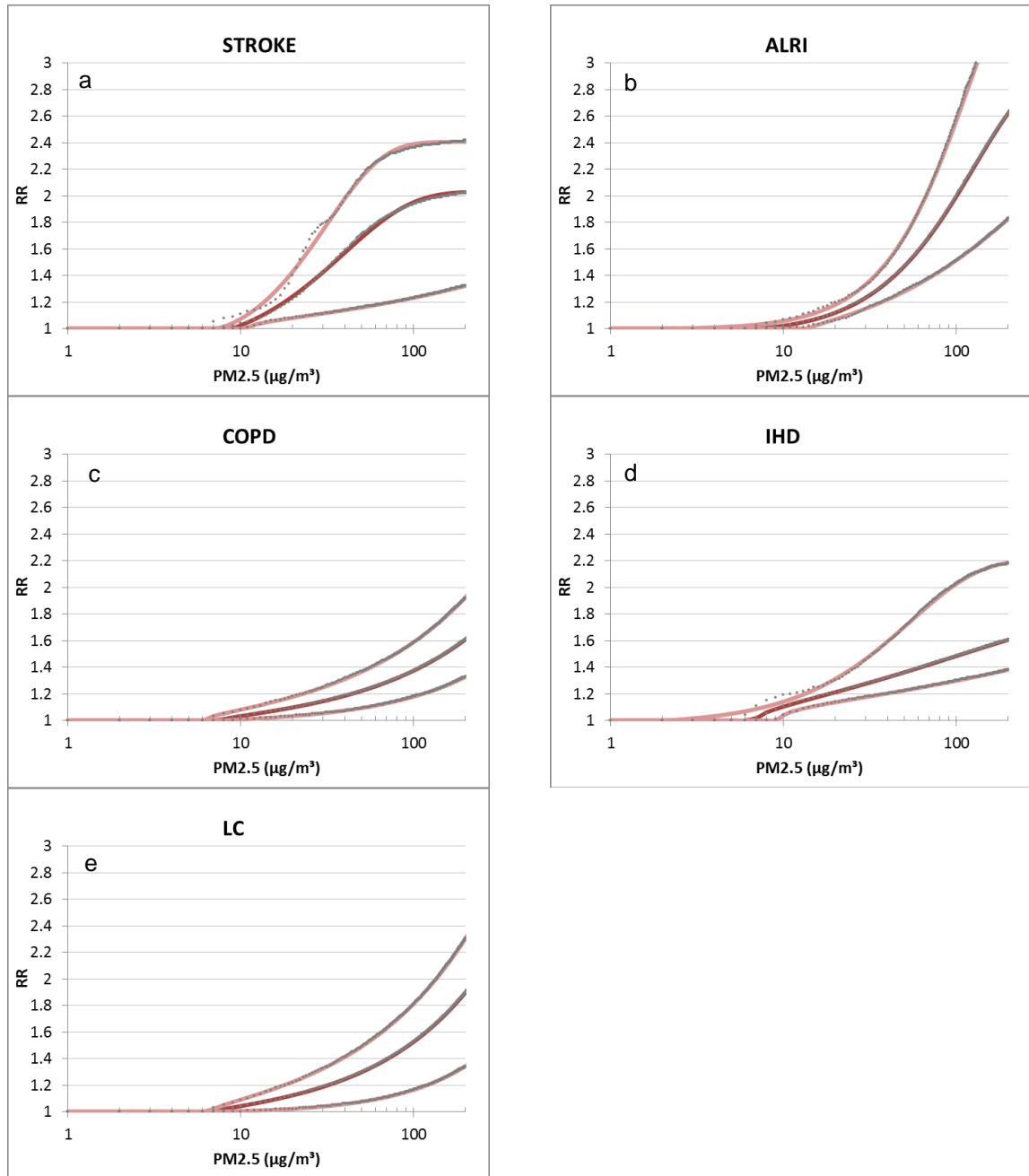


Figure S5.1: Dashed line: Median and 95% CI of the relative risk (RR) as a function of exposure to PM_{2.5} from 1000 Monte Carlo samples provided by Burnett et al. (2014). Red lines: fitted curves for all-age IER functions for 5 mortality causes, using the parameters listed in Table S6.1 (this work). (a): Stroke, (b): Acute Lower Respiratory Airways Infections (c) Chronic Obstructive Pulmonary Disease (d) Ischaemic Heart Disease (e) Lung Cancer

79) Section S6.1, P24, Line 166 – ‘Table S7.1’ should be Table S6.1.

REPLY: OK done

References:

- Andersson, C., Langner, J. and Bergström, R.: Interannual variation and trends in air pollution over Europe due to climate variability during 1958–2001 simulated with a regional CTM coupled to the ERA40 reanalysis, *Tellus B*, 59(1), 77–98, doi:10.1111/j.1600-0889.2006.00196.x, 2007.
- Avnery, S., Mauzerall, D. L., Liu, J. and Horowitz, L. W.: Global crop yield reductions due to surface ozone exposure: 1. Year 2000 crop production losses and economic damage, *Atmos. Environ.*, 45(13), 2284–2296, doi:10.1016/j.atmosenv.2010.11.045, 2011.
- Boucher, O. and Lohmann, U.: The sulfate-CCN-cloud albedo effect: a sensitivity study with two general circulation models, *Tellus Ser. B*, 47 B(3), 281–300, 1995.
- Burnett, R. T., Pope, C. A., III, Ezzati, M., Olives, C., Lim, S. S., Mehta, S., Shin, H. H., Singh, G., Hubbell, B., Brauer, M., Anderson, H. R., Smith, K. R., Balmes, J. R., Bruce, N. G., Kan, H., Laden, F., Prüss-Ustün, A., Turner, M. C., Gapstur, S. M., Diver, W. R. and Cohen, A.: An Integrated Risk Function for Estimating the Global Burden of Disease Attributable to Ambient Fine Particulate Matter Exposure, *Environ. Health Perspect.*, doi:10.1289/ehp.1307049, 2014.
- Cohen, A. J., Brauer, M., Burnett, R., Anderson, H. R., Frostad, J., Estep, K., Balakrishnan, K., Brunekreef, B., Dandona, L., Dandona, R., Feigin, V., Freedman, G., Hubbell, B., Jobling, A., Kan, H., Knibbs, L., Liu, Y., Martin, R., Morawska, L., Pope, C. A., III, Shin, H., Straif, K., Shaddick, G., Thomas, M., van Dingenen, R., van Donkelaar, A., Vos, T., Murray, C. J. L. and Forouzanfar, M. H.: Estimates and 25-year trends of the global burden of disease attributable to ambient air pollution: an analysis of data from the Global Burden of Diseases Study 2015, *The Lancet*, 389(10082), 1907–1918, doi:10.1016/S0140-6736(17)30505-6, 2017.
- Dentener, F., Stevenson, D., Cofala, J., Mechler, R., Amann, M., Bergamaschi, P., Raes, F. and Derwent, R.: The impact of air pollutant and methane emission controls on tropospheric ozone and radiative forcing: CTM calculations for the period 1990–2030, *Atmos Chem Phys*, 5(7), 1731–1755, doi:10.5194/acp-5-1731-2005, 2005.
- Dentener, F., Kinne, S., Bond, T., Boucher, O., Cofala, J., Generoso, S., Ginoux, P., Gong, S., Hoelzemann, J. J., Ito, A., Marelli, L., Penner, J. E., Putaud, J.-P., Textor, C., Schulz, M., Van, D. W. and Wilson, J.: Emissions of primary aerosol and precursor gases in the years 2000 and 1750 prescribed data-sets for AeroCom, *Atmospheric Chem. Phys.*, 6(12), 4321–4344, 2006.
- Dentener, F., Keating, T., Akimoto, H., Pirrone, N., Dutchak, S., Zuber, A., Convention on Long-range Transboundary Air Pollution, United Nations and UNECE Task Force on Emission Inventories and Projections, Eds.: Hemispheric transport of air pollution 2010: prepared by the Task Force on Hemispheric Transport of Air Pollution acting within the framework of the Convention on Long-range Transboundary Air Pollution, United Nations, New York ; Geneva., 2010.
- Edwards, J. M. and Slingo, A.: Studies with a flexible new radiation code. I: Choosing a configuration for a large-scale model, *Q. J. R. Meteorol. Soc.*, 122(531), 689–719, 1996.
- Farina, S. C., Adams, P. J. and Pandis, S. N.: Modeling global secondary organic aerosol formation and processing with the volatility basis set: Implications for anthropogenic secondary organic aerosol, *J. Geophys. Res. Atmospheres*, 115(D9), doi:10.1029/2009JD013046, 2010.
- Fenech, S., Doherty, R. M., Heaviside, C., Vardoulakis, S., Macintyre, H. L. and O’Connor, F. M.: The influence of model spatial resolution on simulated ozone and fine particulate matter for Europe: implications for health impact assessments, *Atmospheric Chem. Phys.*, 18(8), 5765–5784, doi:10.5194/acp-18-5765-2018, 2018.

- Fiore, A. M., Jacob, D. J., Field, B. D., Streets, D. G., Fernandes, S. D. and Jang, C.: Linking ozone pollution and climate change: The case for controlling methane, *Geophys. Res. Lett.*, 29(19), 25–1, 2002.
- Fiore, A. M., West, J. J., Horowitz, L. W., Naik, V. and Schwarzkopf, M. D.: Characterizing the tropospheric ozone response to methane emission controls and the benefits to climate and air quality, *J. Geophys. Res. Atmospheres*, 113(8), doi:10.1029/2007JD009162, 2008.
- Fiore, A. M., Dentener, F. J., Wild, O., Cuvelier, C., Schultz, M. G., Hess, P., Textor, C., Schulz, M., Doherty, R. M., Horowitz, L. W., MacKenzie, I. A., Sanderson, M. G., Shindell, D. T., Stevenson, D. S., Szopa, S., Van Dingenen, R., Zeng, G., Atherton, C., Bergmann, D., Bey, I., Carmichael, G., Collins, W. J., Duncan, B. N., Faluvegi, G., Folberth, G., Gauss, M., Gong, S., Hauglustaine, D., Holloway, T., Isaksen, I. S. A., Jacob, D. J., Jonson, J. E., Kaminski, J. W., Keating, T. J., Lupu, A., Marmer, E., Montanaro, V., Park, R. J., Pitari, G., Pringle, K. J., Pyle, J. A., Schroeder, S., Vivanco, M. G., Wind, P., Wojcik, G., Wu, S. and Zuber, A.: Multimodel estimates of intercontinental source-receptor relationships for ozone pollution, *J. Geophys. Res. Atmospheres*, 114(D4), doi:10.1029/2008JD010816, 2009.
- Forouzanfar, M. H., Afshin, A., Alexander, L. T., Biryukov, S., Brauer, M., Cercy, K., Charlson, F. J., Cohen, A. J., Dandona, L., Estep, K., Ferrari, A. J., Frostad, J. J., Fullman, N., Godwin, W. W., Griswold, M., Hay, S. I., Kyu, H. H., Larson, H. J., Lim, S. S., Liu, P. Y., Lopez, A. D., Lozano, R., Marczak, L., Mokdad, A. H., Moradi-Lakeh, M., Naghavi, M., Reitsma, M. B., Roth, G. A., Sur, P. J., Vos, T., Wagner, J. A., Wang, H., Zhao, Y., Zhou, M., Barber, R. M., Bell, B., Blore, J. D., Casey, D. C., Coates, M. M., Cooperrider, K., Cornaby, L., Dicker, D., Erskine, H. E., Fleming, T., Foreman, K., Gakidou, E., Haagsma, J. A., Johnson, C. O., Kemmer, L., Ku, T., Leung, J., Masiye, F., Millea, A., Mirarefin, M., Misganaw, A., Mullany, E., Mumford, J. E., Ng, M., Olsen, H., Rao, P., Reinig, N., Roman, Y., Sandar, L., Santomauro, D. F., Slepak, E. L., Sorensen, R. J. D., Thomas, B. A., Vollset, S. E., Whiteford, H. A., Zipkin, B., Murray, C. J. L., Mock, C. N., Anderson, B. O., Futran, N. D., Anderson, H. R., Bhutta, Z. A., Nisar, M. I., Akseer, N., Krueger, H., Gotay, C. C., Kisson, N., Kopec, J. A., Pourmalek, F., Burnett, R., Abajobir, A. A., Knibbs, L. D., Veerman, J. L., Lalloo, R., Scott, J. G., Alam, N. K. M., Gouda, H. N., Guo, Y., McGrath, J. J., Charlson, F. J., Erskine, H. E., Jeemon, P., Dandona, R., Goenka, S., Kumar, G. A., et al.: Global, regional, and national comparative risk assessment of 79 behavioural, environmental and occupational, and metabolic risks or clusters of risks, 1990–2015: a systematic analysis for the Global Burden of Disease Study 2015, *The Lancet*, 388(10053), 1659–1724, doi:10.1016/S0140-6736(16)31679-8, 2016.
- Galmarini, S., Koffi, B., Solazzo, E., Keating, T., Hogrefe, C., Schulz, M., Benedictow, A., Jurgen, G., Janssens-Maenhout, G., Carmichael, G., Fu, J. and Dentener, F.: Technical note: Coordination and harmonization of the multi-scale, multi-model activities HTAP2, AQMEII3, and MICS-Asia3: Simulations, emission inventories, boundary conditions, and model output formats, *Atmospheric Chem. Phys.*, 17(2), 1543–1555, doi:10.5194/acp-17-1543-2017, 2017.
- IIASA and FAO: Global Agro-Ecological Zones V3.0, [online] Available from: <http://www.gaez.iiasa.ac.at/> (Accessed 11 November 2016), 2012.
- Jerrett, M., Burnett, R. T., Arden, P. I., Ito, K., Thurston, G., Krewski, D., Shi, Y., Calle, E. and Thun, M.: Long-term ozone exposure and mortality, *N. Engl. J. Med.*, 360(11), 1085–1095, doi:10.1056/NEJMoa0803894, 2009.
- Kanakidou, M., Seinfeld, J. H., Pandis, S. N., Barnes, I., Dentener, F. J., Facchini, M. C., Dingenen, R. V., Ervens, B., Nenes, A., Nielsen, C. J., Swietlicki, E., Putaud, J. P., Balkanski, Y., Fuzzi, S., Horth, J., Moortgat, G. K., Winterhalter, R., Myhre, C. E. L., Tsigaridis, K., Vignati, E., Stephanou, E. G. and Wilson, J.: Organic aerosol and global climate modelling: a review, *Atmospheric Chem. Phys.*, 5(4), 1053–1123, doi:10.5194/acp-5-1053-2005, 2005.
- Kirschke, S., Bousquet, P., Ciais, P., Saunoy, M., Canadell, J. G., Dlugokencky, E. J., Bergamaschi, P., Bergmann, D., Blake, D. R., Bruhwiler, L., Cameron-Smith, P., Castaldi, S., Chevallier, F.,

- Feng, L., Fraser, A., Heimann, M., Hodson, E. L., Houweling, S., Josse, B., Fraser, P. J., Krummel, P. B., Lamarque, J.-F., Langenfelds, R. L., Le Quéré, C., Naik, V., O'Doherty, S., Palmer, P. I., Pison, I., Plummer, D., Poulter, B., Prinn, R. G., Rigby, M., Ringeval, B., Santini, M., Schmidt, M., Shindell, D. T., Simpson, I. J., Spahni, R., Steele, L. P., Strode, S. A., Sudo, K., Szopa, S., van der Werf, G. R., Voulgarakis, A., van Weele, M., Weiss, R. F., Williams, J. E. and Zeng, G.: Three decades of global methane sources and sinks, *Nat. Geosci.*, 6(10), 813–823, doi:10.1038/ngeo1955, 2013.
- Koffi, B., Dentener, F., Janssens-Maenhout, G., Guizzardi, D., Crippa, M., Diehl, T., Galmarini, S. and Solazzo, E.: Hemispheric Transport Air Pollution (HTAP): Specification of the HTAP2 experiments, Publications Office of the European Union, Luxembourg. [online] Available from: <http://publications.jrc.ec.europa.eu/repository/bitstream/JRC102552/lbna28255enn.pdf> (Accessed 14 December 2017), 2016.
- Krewski, D., Jerrett, M., Burnett, R. T., Ma, R., Hughes, E. and Shi, Y.: Extended Follow-Up and Spatial Analysis of the American Cancer Society Study Linking Particulate Air Pollution and Mortality., Research Report, Health Effects Institute, Boston., 2009.
- Li, Y., Henze, D. K., Jack, D. and Kinney, P. L.: The influence of air quality model resolution on health impact assessment for fine particulate matter and its components, *Air Qual. Atmosphere Health*, 9(1), 51–68, doi:10.1007/s11869-015-0321-z, 2016.
- Lim, S. S., Vos, T., Flaxman, A. D., Danaei, G., Shibuya, K., Adair-Rohani, H., Amann, M., Anderson, H. R., Andrews, K. G., Aryee, M., Atkinson, C., Bacchus, L. J., Bahalim, A. N., Balakrishnan, K., Balmes, J., Barker-Collo, S., Baxter, A., Bell, M. L., Blore, J. D., Blyth, F., Bonner, C., Borges, G., Bourne, R., Boussinesq, M., Brauer, M., Brooks, P., Bruce, N. G., Brunekreef, B., Bryan-Hancock, C., Bucello, C., Buchbinder, R., Bull, F., Burnett, R. T., Byers, T. E., Calabria, B., Carapetis, J., Carnahan, E., Chafe, Z., Charlson, F., Chen, H., Chen, J. S., Cheng, A. T.-A., Child, J. C., Cohen, A., Colson, K. E., Cowie, B. C., Darby, S., Darling, S., Davis, A., Degenhardt, L., Dentener, F., Des Jarlais, D. C., Devries, K., Dherani, M., Ding, E. L., Dorsey, E. R., Driscoll, T., Edmond, K., Ali, S. E., Engell, R. E., Erwin, P. J., Fahimi, S., Falder, G., Farzadfar, F., Ferrari, A., Finucane, M. M., Flaxman, S., Fowkes, F. G. R., Freedman, G., Freeman, M. K., Gakidou, E., Ghosh, S., Giovannucci, E., Gmel, G., Graham, K., Grainger, R., Grant, B., Gunnell, D., Gutierrez, H. R., Hall, W., Hoek, H. W., Hogan, A., Hosgood III, H. D., Hoy, D., Hu, H., Hubbell, B. J., Hutchings, S. J., Ibeanusi, S. E., Jacklyn, G. L., Jasrasaria, R., Jonas, J. B., Kan, H., Kanis, J. A., Kassebaum, N., Kawakami, N., Khang, Y.-H., Khatibzadeh, S., Khoo, J.-P., Kok, C., et al.: A comparative risk assessment of burden of disease and injury attributable to 67 risk factors and risk factor clusters in 21 regions, 1990-2010: A systematic analysis for the Global Burden of Disease Study 2010, *The Lancet*, 380(9859), 2224–2260, doi:10.1016/S0140-6736(12)61766-8, 2012.
- Liu, X., Penner, J. E., Das, B., Bergmann, D., Rodriguez, J. M., Strahan, S., Wang, M. and Feng, Y.: Uncertainties in global aerosol simulations: Assessment using three meteorological data sets, *J. Geophys. Res.*, 112(D11), doi:10.1029/2006JD008216, 2007.
- Malley, C. S., Henze, D. K., Kuylenstierna, J. C. I., Vallack, H., Davila, Y., Anenberg, S. C., Turner, M. C. and Ashmore, M.: Updated Global Estimates of Respiratory Mortality in Adults ≥ 30 Years of Age Attributable to Long-Term Ozone Exposure., *Environ. Health Perspect.*, 125(8), 087021, doi:10.1289/EHP1390, 2017.
- Mills, G., Buse, A., Gimeno, B., Bermejo, V., Holland, M., Emberson, L. and Pleijel, H.: A synthesis of AOT40-based response functions and critical levels of ozone for agricultural and horticultural crops, *Atmos. Environ.*, 41(12), 2630–2643, doi:10.1016/j.atmosenv.2006.11.016, 2007.
- Ming, Y. and Russell, L. M.: Predicted hygroscopic growth of sea salt aerosol, *J. Geophys. Res. Atmospheres*, 106(D22), 28259–28274, 2001.

- Murray, C. J., Ezzati, M., Lopez, A. D., Rodgers, A. and Vander Hoorn, S.: Comparative quantification of health risks: conceptual framework and methodological issues, *Popul. Health Metr.*, 1(1), 1, 2003.
- Pope, C. A., III, Burnett, R. T., Thun, M. J., Calle, E. E., Krewski, D., Ito, K. and Thurston, G. D.: Lung Cancer, Cardiopulmonary Mortality, and Long-term Exposure to Fine Particulate Air Pollution, *JAMA*, 287(9), 1132–1141, doi:10.1001/jama.287.9.1132, 2002.
- Prather, M., Ehhalt, D., Dentener, F., Derwent, R., Dlugokencky, E., Holland, E., Isaksen, I., Katima, J., Kirchhoff, V., Matson, P., Midgley, P., Wang, M., Berntsen, T., Bey, I., Brasseur, G., Buja, L., Pitari, G. and Et, A.: Chapter 4: Atmospheric Chemistry and Greenhouse Gases, Cambridge University Press. [online] Available from: <https://ricerca.univaq.it/handle/11697/24359#.Wltxbn0XGao> (Accessed 27 January 2017), 2001.
- Punger, E. M. and West, J. J.: The effect of grid resolution on estimates of the burden of ozone and fine particulate matter on premature mortality in the United States, *Air Qual. Atmosphere Health*, 6(3), doi:10.1007/s11869-013-0197-8, 2013.
- Ramaswamy, V., Boucher, O., Haigh, J., Hauglustaine, D., Haywood, J., Myhre, G., Nakajima, T., Shi, G., Solomon, S., Betts, R. E., Charlson, R., Chuang, C. C., Daniel, J. S., Del Genio, A. D., Feichter, J., Fuglestedt, J., Forster, P. M., Ghan, S. J., Jones, A., Kiehl, J. T., Koch, D., Land, C., Lean, J., Lohmann, U., Minschwaner, K., Penner, J. E., Roberts, D. L., Rodhe, H., Roelofs, G.-J., Rotstain, L. D., Schneider, T. L., Schumann, U., Schwartz, S. E., Schwartzkopf, M. D., Shine, K. P., Smith, S. J., Stevenson, D. S., Stordal, F., Tegen, I., van Dorland, R., Zhang, Y., Srinivasan, J. and Joos, F.: Radiative Forcing of Climate Change, Pacific Northwest National Laboratory (PNNL), Richland, WA (US). [online] Available from: <https://www.osti.gov/scitech/biblio/899821> (Accessed 27 January 2017), 2001.
- Rao, S., Chirkov, V., Dentener, F., Van Dingenen, R., Pachauri, S., Purohit, P., Amann, M., Heyes, C., Kinney, P., Kolp, P., Klimont, Z., Riahi, K. and Schoepp, W.: Environmental Modeling and Methods for Estimation of the Global Health Impacts of Air Pollution, *Environ. Model. Assess.*, 17(6), 613–622, doi:10.1007/s10666-012-9317-3, 2012.
- Rao, S., Pachauri, S., Dentener, F., Kinney, P., Klimont, Z., Riahi, K. and Schoepp, W.: Better air for better health: Forging synergies in policies for energy access, climate change and air pollution, *Glob. Environ. Change*, 23(5), 1122–1130, doi:10.1016/j.gloenvcha.2013.05.003, 2013.
- Riahi, K., Dentener, F., Gielen, D., Grubler, A., Jewell, J., Klimont, Z., Krey, V., McCollum, D., Pachauri, S., Rao, S., van Ruijven, B., van Vuuren, D. P. and Wilson, C.: The Global Energy Assessment - Chapter 17 - Energy Pathways for Sustainable Development, in *Global Energy Assessment - Toward a Sustainable Future*, pp. 1203–1306, Cambridge University Press, Cambridge, UK and New York, NY, USA and the International Institute for Applied Systems Analysis, Laxenburg, Austria. [online] Available from: www.globalenergyassessment.org, 2012.
- Silva, R. A., West, J. J., Lamarque, J. F., Shindell, D. T., Collins, W. J., Dalsoren, S., Faluvegi, G., Folberth, G., Horowitz, L. W., Nagashima, T., Naik, V., Rumbold, S. T., Sudo, K., Takemura, T., Bergmann, D., Cameron-Smith, P., Cionni, I., Doherty, R. M., Eyring, V., Josse, B., MacKenzie, I. A., Plummer, D., Righi, M., Stevenson, D. S., Strode, S., Szopa, S. and Zengast, G.: The effect of future ambient air pollution on human premature mortality to 2100 using output from the ACCMIP model ensemble, *Atmospheric Chem. Phys.*, 16(15), 9847–9862, doi:10.5194/acp-16-9847-2016, 2016.
- Stevenson, D. S., Young, P. J., Naik, V., Lamarque, J.-F., Shindell, D. T., Voulgarakis, A., Skeie, R. B., Dalsoren, S. B., Myhre, G., Berntsen, T. K., Folberth, G. A., Rumbold, S. T., Collins, W. J., MacKenzie, I. A., Doherty, R. M., Zeng, G., Van, N., Strunk, A., Bergmann, D., Cameron-Smith, P., Plummer, D. A., Strode, S. A., Horowitz, L., Lee, Y. H., Szopa, S., Sudo, K., Nagashima, T., Josse, B., Cionni, I., Righi, M., Eyring, V., Conley, A., Bowman, K. W., Wild, O. and Archibald, A.: Tropospheric ozone changes, radiative forcing and attribution to

- emissions in the Atmospheric Chemistry and Climate Model Intercomparison Project (ACCMIP), *Atmospheric Chem. Phys.*, 13(6), 3063–3085, doi:10.5194/acp-13-3063-2013, 2013.
- Stjern, C. W., Samset, B. H., Myhre, G., Bian, H., Chin, M., Davila, Y., Dentener, F., Emmons, L., Flemming, J., Haslerud, A. S., Henze, D., Jonson, J. E., Kucsera, T., Lund, M. T., Schulz, M., Sudo, K., Takemura, T. and Tilmes, S.: Global and regional radiative forcing from 20 % reductions in BC, OC and SO₄ - An HTAP2 multi-model study, *Atmospheric Chem. Phys.*, 16(21), 13579–13599, doi:10.5194/acp-16-13579-2016, 2016.
- Tang, I. N.: Chemical and size effects of hygroscopic aerosols on light scattering coefficients, *J. Geophys. Res. Atmospheres*, 101(14), 19245–19250, 1996.
- Turner, M. C., Jerrett, M., Pope, C. A., Krewski, D., Gapstur, S. M., Diver, W. R., Beckerman, B. S., Marshall, J. D., Su, J., Crouse, D. L. and Burnett, R. T.: Long-Term Ozone Exposure and Mortality in a Large Prospective Study, *Am. J. Respir. Crit. Care Med.*, 193(10), 1134–1142, doi:10.1164/rccm.201508-1633OC, 2016.
- Wang, X. and Mauzerall, D. L.: Characterizing distributions of surface ozone and its impact on grain production in China, Japan and South Korea: 1990 and 2020, *Atmos. Environ.*, 38(26), 4383–4402, doi:10.1016/j.atmosenv.2004.03.067, 2004.
- West, J. J., Fiore, A. M., Naik, V., Horowitz, L. W., Schwarzkopf, M. D. and Mauzerall, D. L.: Ozone air quality and radiative forcing consequences of changes in ozone precursor emissions, *Geophys. Res. Lett.*, 34(6), doi:10.1029/2006GL029173, 2007.
- Wild, O. and Prather, M. J.: Excitation of the primary tropospheric chemical mode in a global three-dimensional model, *J. Geophys. Res. Atmospheres*, 105(D20), 24647–24660, 2000.
- Wild, O. and Prather, M. J.: Global tropospheric ozone modeling: Quantifying errors due to grid resolution, *J. Geophys. Res. Atmospheres*, 111(D11), doi:10.1029/2005JD006605, 2006.

We thank reviewer 2 for the insightful comments, and for pointing to inconsistencies. We apologize for needing more time than anticipated to address all comments, but we believe that we have been able to address most issues, and that we have significantly strengthened the manuscript.

Before addressing the comments we would like to mention that we have modified the abbreviation of the O₃ health exposure metric (6 monthly daily maximum 1-h concentration) from M6M to 6mDMA1 (and accordingly M3M to 3mDMA1) as the latter seems to be commonly used in other works.

In the following we have placed the numbered reviewer comments in boxes. Our reply to the reviewer is in **blue font**, the changes to the manuscript in **red font**.

We also attach a revised version of manuscript and supplement with tracked changes compared to the first version.

REVIEWER 2 comments:

The manuscript by Van Dingenen et al. presents and evaluates TM5-FASST, a reduced form air quality assessment tool. The manuscript is long, but does a thorough job of both presenting the computational methods used for formulating the FASST tool and the types of impacts that it calculates (from health impacts to climate) as well as evaluating the tool against simulations from the full TM5 model as well as results in the literature. I have some additional questions in a few areas, described below, but in general was satisfied / impressed with the evaluation and performance. The writing could use a bit more editing for grammar and some of the figures need clarification on units, axis, etc. Addressing these will amount to moderate revisions and some additional evaluations.

1) However my only main concern about would be if this article should be moved to GMD instead of ACP, as the emphasis really is on the tool development and evaluation; there is not any content on application of the tool to new science or policy questions. It may not thus fit the scope of ACP.

REPLY:

We agree that this paper would have been also suited for GMD. However, due to high relevancy of this publication for the work of the TF HTAP, we decided that thematically the paper also fitted very well in this ACP special issue. Unfortunately, for this special issue, it was decided not to have a joint special issue between GMD and ACP (or other Copernicus journals), which would have been the perfect solution. We are confident that the interested reader will also find this publication in ACP.

2) 2.1-8: Why are reduced form or source-receptor models needed in the first place? I think there's a significant point to be made here about the complexity of air quality modeling vs the level of sophistication and computational intensity that can be acceptable to the decision-making community. But the article as presently writing misses this point, so the justification for the tool isn't readily apparent

REPLY:

Thank you for making this point, it is indeed important to introduce these issues to a general readership. This comment is closely related to the next one, so we address both in the introduction which has been expanded.

1. Introduction

A host of policies influence the emissions to air. In principle any policy that influences the economy and use of resources will also impact emissions into the atmosphere. Specific air pollution policies aim to mitigate the negative environmental impacts of anthropogenic activities, some of which may be affected by other policies, like climate mitigation actions, transport modal shifts or agricultural policies. Further, air quality policies may impact outside their typical environmental target domains (human and ecosystem health, vegetation and building damage,...) for instance through the role played by short-lived pollutants in the Earth's radiation balance (Myhre et al., 2011; Shindell et al., 2009). Insight into the impacts of policies in a multi-disciplinary framework through a holistic approach could contribute to a more efficient and cost-effective implementation of control measures (e.g. Amann et al., 2011; Maione et al., 2016; Shindell et al., 2012).

Several global chemical transport models are available for the evaluation of air pollutants levels from emissions, sometimes in combination with off-line computed climate relevant metrics such as optical depth or instantaneous radiative forcing (e.g. Lamarque et al., 2013; Stevenson et al., 2013). These models provide detailed output, but are demanding in terms of computational and human resources for preparing input, running the model, and analyzing output. Further they often lack flexibility to evaluate ad-hoc a series of scenarios, or perform swift what-if analysis of policy options. Therefore there is a need for computationally-efficient methods and tools that provide an integrated environmental assessment of air quality and climate policies, which have a global dimension with sufficient regional detail, and evaluate different impact categories in an internally consistent way. Reduced-form source-receptor models are a useful concept in this context. They are typically constructed from pre-computed emission-concentration transfer matrices between pollutant source regions and receptor regions. These matrices emulate underlying meteorological and chemical atmospheric processes for a pre-defined set of meteorological and emission data, and have the advantage that concentration responses to emission changes are obtained by a simple matrix multiplication, avoiding expensive numerical computations. Reduced-form source-receptor models (SRM) are increasingly being used, not only to compute atmospheric concentrations (and related impacts) from changes in emissions but they have also proven to be very useful in cost optimization and cost-benefit analysis because of their low computational cost (Amann et al., 2011). Further, because of the detailed budget information embedded in the source-receptor matrices, they are applied for apportionment studies, as a complementary approach to other techniques such as adjoint models (Zhang et al., 2015) and chemical tagging (e.g. Grewe et al., 2012).

Although the computational efficiency of SRMs comes at a cost of accuracy, regional detail and flexibility in spatial arrangement of emissions, they have been successfully applied in regional studies (Foley et al., 2014; Li et al., 2014; Liu et al., 2017; Porter et al., 2017) and have demonstrated their key role in policy development (Amann et al., 2011).

3) Intro: Overall the introduction is rather brief. There are other reduced form models on regional scales that are used for different purposes (in the US and Asia, in particular). There are also theoretical advantages (quick) and disadvantages (approximations of linearity; enforced aggregation at pre-defined scales; outdated emissions inventories or old atmospheric conditions) of reduced form models. A lot more thought could be put into discussion and introducing these issues. This is ACP, not GMD, so more than just a model description is expected

REPLY: see previous comment

4) 3.18: This sentence is a bit too vague to be useful. The authors should mention what type of model updates have been made (emissions? aerosols? etc) and why they are deemed to not be relevant for this current work.

REPLY: We have added some more text to this paragraph to explain the major differences. The choice of emissions is not relevant in this context as emission datasets are external to the model framework, and in general chosen by the user depending on scientific issue.

CHANGES TO MANUSCRIPT: *Added to Section 2.1 (P4 L24)*

TM5 results used in the present study allow comparison with a range of other global model results in HTAP1, but ignore subsequent updates and improvements in TM5 as for instance described in Huijnen et al. (2010), which we consider not critical for this study. The most recent TM5 model does no longer consider zoom regions, but recoded the model into a Massive Parallel framework, enabling efficient execution on modern computers. While global horizontal resolution (1°x1°) is similar to the resolution of the most refined zoom region in TM5, vertical resolution was increased. Further, the model also uses vertical mass fluxes from the parent ECMWF meteorological model, not available at the time of development of TM5-cy2-ipcc, which could lead to somewhat different mixing characteristics. The gas phase chemical module has been updated to a modified version of CMB5.

5) This does raise the question of uncertainties introduced in this tool owing to use of a single year (was 2001 an average year, in terms of temp, precipitation, etc.?) to approximate a reasonable climatology, as well as this use of a year that is significantly older than most present applications, considering decadal-scale climate change.

REPLY: This is an issue raised by both reviewers. We agree with the reviewer that the year 2001 meteorology is somewhat outdated. The perturbation runs for constructing the SR library of FASST were performed with the TM5 model set-up defined in the first phase of HTAP1 (during the period 2008 – 2011) and because of the computational costs, an update with more recent meteorology was not possible (TM5 is not taking part in HTAP2 where meteorological year 2010 has been used). A systematic check of the representativeness of this particular year for each of the FASST regions is beyond the scope of this study, in the first place because FASST is considered to be a screening tool focussing on impacts of emission changes. However we have substantially extended the discussion on the use of a single meteorological year.

CHANGES TO MANUSCRIPT: *Added to Section 2.1 P5 L10*

Meteorological fields are obtained from the ECMWF operational forecast representative for the year 2001. The implications of using a single meteorological year will be discussed in section 4.2.

Discussion section 4.2 added (P31 L25)

4.2 Inter-annual meteorological variability

A justified critique on the methodology applied to construct the FASST SRs relates to the use of a single and fixed meteorological year 2001, implying possible unspecified biases in pollutant concentrations and source-receptor matrices compared to using a ‘typical meteorological/climatological year’. We followed the choice of the meteorological year 2001 made for the HTAP1 exercise. As the North-Atlantic Oscillation (NAO) is an important mode of the inter-annual variability in pollutant concentrations and long range transport (Christoudias

et al., 2012; Li et al., 2002; Pausata et al., 2013; Pope et al., 2018), the HTAP1 expectation was that this year was not an exceptional year for long-rang pollutant transport - e.g. for the North-Atlantic region, as indicated by a North Atlantic Oscillation (NAO) index close to zero for that year (<https://www.ncdc.noaa.gov/teleconnections/nao/>). The HTAP1 report (Dentener et al., 2010) also suggested that “Inter-annual differences in SR relationships for surface O₃ due to year-to-year meteorological variations are small when evaluated over continental-scale regions. However, these differences may be greater when considering smaller receptor regions or when variations in natural emissions are accounted for”. The role of spatial and temporal meteorological variability can thus be reduced by aggregating resulting pollutant levels and impacts as regional and annual averages or aggregates, the approach taken in TM5-FASST. The impact of the choice of this specific year on the TM5-FASST model uncertainty or possible biases in base concentrations and SR coefficients is not easily quantified. For what concerns the pollutant base concentrations, some insights in the possible relevance of meteorological variability can be found in the literature. For example, Anderson et al., (2007) showed that in Europe, the meteorological component in regional inter-annual variability of pollutant concentrations ranges between 3% and 11% for airborne pollutants (O₃, PM_{2.5}), and up to 20% for wet deposition. On a global scale, Liu et al. (2007) demonstrated that the inter-annual variability in PM concentrations, related to inter-annual meteorological variability can even be up to a factor of 3 in the tropics (e.g. over Indonesia) and in the storm track regions. A sample analysis (documented in section S2.2 of the SI) of the RCP year 2000 emission scenario with TM5 at 6°x4° resolution of 5 consecutive meteorological years 2001 to 2005 indicates a year-to-year variability on regional PM_{2.5} within 10% (relative standard deviation) and within 3% for annual mean O₃. We find a similar variability on the magnitudes of 20% emission perturbation responses within the source region for 6 selected regions (India, China, Europe, Germany, USA and Japan). The relative share of source regions to the pollutant levels within a given receptor region shows a lower inter-annual variability (typically between 2 and 6% for PM_{2.5}) than the absolute contributions.

6) 4.29: There is extensive research on the chemical oxidation of elemental carbon and the role this plays on the lifetime of this species in the atmosphere. Comment on why this is not included.

REPLY: The referee is right, also primary pollutants can undergo chemical conversion – however we feel this comment relates rather to 6.15 where we state that in TM5 (and FASST) the lifetime of BC and POM is not changing. The statement in 4.29 was intended to point out the difference between primary and secondary pollutants where in the latter case a completely new chemical compound is formed from precursors via chemical reactions, while for primary pollutants, dispersion and deposition are the primary process affecting their atmospheric concentration. Since the development of TM5, in literature two approaches have been developed towards parameterizing 'ageing' of elemental carbon. Ageing through condensation of hydrophobic species such as SO₄ (and in the real world also other soluble components) is considered in e.g. the HAM aerosol physics model (Stier et al., 2005). The second approach considers oxidation of carbonaceous aerosol by O₃ following Tsigaridis and Kanakidou (2003). More recent work (e.g. Huang et al., 2012) analyses the joint impact of the two approaches, explicitly including the chemical-physical ageing processes. In general including the explicit processes tends to lengthen the atmospheric residence time of EC/BC compared to the earlier simple parameterisation in CTMs. The reason of not including these processes at the time of the release of TM5-JRC-Cy2-IPCC was that at that time none of the approaches was robustly anchored in improved performance at multiple observational sites, while at the same time the uncertainties in the wet removal parameterization were (and still are) also highly uncertain.

CHANGES TO MANUSCRIPT: *We feel this comment addresses original 6.15 rather than 4.29*

Original 6.15

BC and POM emissions are assumed not to interact with other pollutants and their atmospheric lifetimes are assumed not to be affected by mixing with other soluble species like sulfate, nitrate or ammonium salts

modified to (P8 L22):

BC and POM are assumed not to interact with other pollutants and their atmospheric lifetimes are prescribed and assumed neither to be affected by mixing with other soluble species like sulfate, nitrate or ammonium salts, nor to undergo oxidation by O₃. Recent work (e.g. Huang et al., 2012) indicates that a parametrized approach, as applied in TM5, tends to underestimate BC and POM atmospheric lifetimes, leading to a low concentration bias. When explicitly modelled, including the combined impact of both mechanisms, Huang et al., 2012 find that the global atmospheric residence times of BC and POM are lengthened by 9% and 3% respectively.

7) 5.1: I'm not sure what is a "parameter" in this context – please explain.

REPLY: Thank you for pointing out, this is a typo that has been corrected

CHANGES TO MANUSCRIPT: replaced 'parameters' by 'pollutants'

8) 5.1 - 14: It seems like some discussion of the fact that this functional relationship is only approximate is warranted. Instead, it is presented here as if the actual functional relationship is known, where in fact just a local linear approximation is used. This must have some limitations. For example, what is the basis for the statement later on this page that -20% perturbation is small enough to evaluate sensitivities and large enough for extrapolation? I recognize that -20% is a commonly used modeling experiment, but it is also commonly known that this approach has limitations for source attribution that are well documented in the literature (compared to tagging, 2nd order methods, or other).

REPLY: The referee makes a good point here, obviously the linear approach is approximate and has both advantages and limitations. We have already addressed most of this discussion in the introduction. We also modified the relevant phrase in the text.

CHANGES TO MANUSCRIPT:

Replaced:

In the current version v0 of TM5-FASST the function is a linear relation expressing the change in pollutant concentration in the receptor region upon a change in precursor emissions in the source region...

By (P6 L27):

In the current version v0 of TM5-FASST the emission-concentration relationship is locally approximated by a linear function expressing the change in pollutant concentration in the receptor region upon a change in precursor emissions in the source region...

9) The notation in equations (1) and (2) is not correct. In equation 1, there is an inconsistency between the description of the notation for the concentrations vs emissions species (i and j) and what is written in the equation. Assuming the equation is correct, the text should refer to change in concentration of component j (not i) owing to emitted precursor i (not j).

REPLY: Indeed, thanks for spotting.

CHANGES TO MANUSCRIPT:

Replaced:

For each receptor point y (i.e. each model vertical level $1^\circ \times 1^\circ$ grid cell), the change in concentration of component i in receptor y resulting from a -20% perturbation of emitted precursor j in source region x , ...

By (P7 L29):

For each receptor point y (i.e. each model vertical level $1^\circ \times 1^\circ$ grid cell), the change in concentration of component j in receptor y resulting from a -20% perturbation of emitted precursor i in source region x , ...

10) In equation (2), the notation on the summations is not complete nor correct. The first sum should be from $x = 1$ (below the sum) to n_x (written above the sum), and the second should be for $i = 1$ (below the sum) to $n_i(j)$ (above the sum). It's also not clear why y would be bold in this equation. As explained in the text, the number of precursor pollutants (n_i) depends on the pollutant response in consideration, hence n_i is $n_i(j)$. So the pollutant responses are dry aerosol concentrations? At what T,P,RH?

REPLY:

Indexing has been corrected and bold face removed.

The stored SR matrices for each component are indeed the dry mass, as obtained from the TM5 model lower layer (or as column density for radiative properties), using the meteorological data for year 2001.

For comparison with measurements and for health impact assessment FASST provides an estimate of $PM_{2.5}$ residual H₂O at 35% RH and 25°C using mass growth factors for ammonium salts of 1.27 (Tang, 1996) and sea-salt of 1.15 (Ming and Russell, 2001). This allows for a calculation of $PM_{2.5}$ mass simulating the protocol for determination of gravimetric $PM_{2.5}$ mass in monitoring networks, and these are also the values on which epidemiological studies are based. Radiative forcing obviously takes into account atmospheric RH conditions.

CHANGES TO MANUSCRIPT:

Added below Eq. (1) (P8 L1):

In the present version TM5-FASST_v0, the SR coefficients for pollutant concentrations are stored as annual mean responses to annual emission changes. Individual $PM_{2.5}$ components SRs are stored as dry mass ($\mu\text{g m}^{-3}$). $PM_{2.5}$ residual water at 35% is optionally calculated a posteriori for sensitivity studies, assuming mass growth factors for ammonium salts of 1.27 (Tang, 1996) and for sea-salt of 1.15 (Ming and Russell, 2001). The presence of residual water in $PM_{2.5}$ is not irrelevant: epidemiological studies establishing $PM_{2.5}$ exposure-response functions are commonly based on monitoring data of gravimetrically determined $PM_{2.5}$, for which measurement protocols foresee filter conditioning at 30 – 50% RH. As many health impact modelling studies consider dry $PM_{2.5}$ mass or do not provide information on the inclusion of residual water we use dry $PM_{2.5}$ for health impact assessment in this study for consistency, unless mentioned differently.

Correcting indexing (P8 L11):

The total concentration of component (or metric) j in receptor region y , resulting from arbitrary emissions of *all* n_i precursors i at *all* n_x source regions x , is obtained as a perturbation on the base-simulation concentration, by summing up all the respective SR coefficients scaled with the actual emission perturbation:

$$C_j(y) = C_{j,base}(y) + \sum_{k=1}^{n_x} \sum_{i=1}^{n_i} A_{ij}[x_k, y] \cdot [E_i(x_k) - E_{i,base}(x_k)] \quad (2)$$

11) 6.21: This equation needs to be corrected following suggestions for equation (2).

REPLY: Correct, done.

12) 6.23: It is oxymoronic to refer to secondary biogenic POM. This would just be secondary biogenic OM.

REPLY: Apologies for the confusion, but in this case POM actually stands for particulate organic matter.

CHANGES TO MANUSCRIPT: *changed P4 L16 to “Biogenic secondary organic aerosol (BSOA)”*

13) 6.24: Can the authors comment on how neglect of anthropogenic SOA might be biasing the results of this tool?

REPLY:

This is a difficult question, which may be worthy of an entire review. The main reason for ignoring anthropogenic SOA at the time of development of TM5- cy2-ipcc was that in the version of the CMB4 chemical scheme implemented in the model, Benzene and toluene chemistry was not included, as it was considered of local importance. In addition reliable global inventories were not available. Having said this, the importance of anthropogenic SOA will strongly depend on local emission strength and atmospheric chemistry conditions. For instance a recent study conducted in China (Hu et al., 2017) suggest that in summer biogenic SOA is larger in summer (75 %) than in winter (25 %) 5 and over 35 $\mu\text{g}/\text{m}^3$ in 4 Chinese cities.

A global modelling study by (Farina et al., 2010) based on the volatility approach suggests that SOA formation from monoterpenes, sesquiterpenes, isoprene, and anthropogenic precursors is estimated as 17.2, 3.9, 6.5, and 1.6 Tg yr^{-1} , respectively. While in that study global levels of SOA were low (annual average 0.02 $\mu\text{g}/\text{m}^3$)- in particular in Europe and China levels up to 1 $\mu\text{g}/\text{m}^3$ were calculated, where levels of primary organic aerosol were reaching 20 $\mu\text{g}/\text{m}^3$. Although this back-off the envelop assessment suggest that for larger regions the impact is less than 5-10 %, in urban regions with high anthropogenic VOC emissions the impact may be larger.

CHANGES TO MANUSCRIPT:

We added following phrase to the discussion section 4.1 (P31 L17):

The omission of secondary organic PM in TM5 is estimated to introduce a low bias in the base concentration of the order of 0.1 $\mu\text{g m}^{-3}$ as global mean however with regional levels in Central Europe and China up to 1 $\mu\text{g m}^{-3}$ in areas where levels of primary organic matter are reaching 20 $\mu\text{g m}^{-3}$ (Farina et al., 2010) indicating a relatively low contribution of SOA to total $\text{PM}_{2.5}$

14) 6.25: Just because the impacts are annual in nature doesn't mean the emissions contributions to the impacts are seasonally consistent. Surely the impact of NO_x on ammonium nitrate and O_3 is quite different in different seasons; it's not clear why one would have access to this information but not use it.

REPLY: It is certainly true that there are seasonal differences in emission-concentration sensitivities. However, when relevant, these seasonal trends are implicitly included in the exposure metrics and impacts. Several metrics are in fact based on detailed temporal ozone trends, e.g. considering only the daily maximal hourly value, or hourly values exceeding a 40 ppb threshold during the crop growing season. These responses – seasonal in nature – are stored to be scaled with annual emissions. Health impacts from $\text{PM}_{2.5}$ are based on annual averaged values and are not evaluated on a seasonal basis. Hence, although there may be scientific (process understanding) interest in elaborating seasonal trends, from a health/crop/climate impact assessment perspective, there is not much added value storing temporal trends in the source-receptor matrices which would come at a high computational cost (multiplying the number of SR matrices with 12).

15) 7.7-21: I got a bit lost in this discussion of the way CH₄ concentrations responses are treated. It would be good if this section could be expanded and formalized a bit better, using equations where useful, such that the approach could be evaluated and replicated.

REPLY: This was indeed not explained in an optimal way. As there are two instances in the paper where CH₄ responses are treated (O₃ response from CH₄ emissions, and indirect forcing from short-lived precursors on CH₄ and background ozone – see next comment) we have moved and expanded the description of the methodology, which is based on our interpretation of published work, in the SI (S3)

CHANGES TO MANUSCRIPT: added *section S3 in the SI*:

S3.1 CH₄ – O₃ source-receptor relations from HTAP1 perturbation experiments:

CH₄ emissions lead to a change in CH₄ concentrations with a perturbation response time of about 12 years. In order to avoid expensive transient computations, HTAP1 simulations SR1 and SR2 with prescribed fixed CH₄ concentrations (1760 ppb and 1408 ppb, see Dentener et al., 2010) were used to establish CH₄ – O₃ response sensitivities. Previous transient modeling studies have shown that a change in steady-state CH₄ abundance can be traced back to a sustained change in emissions, but the relation is not linear because an increase in CH₄ emissions removes an additional fraction of atmospheric OH (the major sink for CH₄) and prolongs the lifetime of CH₄ (Fiore et al., 2002, 2008; Prather et al., 2001).

In a steady-state situation, the CH₄ concentration is the result of balanced sources and sinks. In the HTAP1 experiments, keeping all other emissions constant, the change in the amount of CH₄ loss (mainly by OH oxidation with a lifetime of ca. 9 years, neglecting loss to soils and stratosphere with lifetimes of ca.160 and 120 years respectively (Prather et al., 2001)) under the prescribed change in CH₄ abundance should therefore be balanced by an equal and opposite source which we consider as an “effective emission”. The amount of CH₄ oxidized by OH in one year being diagnosed by the model, the resulting difference between the reference and perturbation experiment of -77 Tg sets the balancing “effective” emission rate to 77Tg/yr, which is then used to normalize the resulting O₃ and O₃ metrics response to a CH₄ emission change.

The same perturbation experiments also allow us to establish the CH₄ self-feedback factor F describing the relation between a change in emission and the change in resulting steady-state concentration:

$$\frac{c_2}{c_1} = \left(\frac{E_2}{E_1}\right)^F \quad (S3.1)$$

With CH₄ concentrations prescribed, CH₄ emissions were not included in the SR1 and SR2 experiments. The feedback factor F is derived from model-diagnosed respective CH₄ burdens (B) and total lifetimes (LT) as follows (Fiore et al., 2009; Wild and Prather, 2000):

$$F=1/(1-s) \quad (S3.2)$$

$$s = \partial \ln(LT) / \partial \ln(B) \quad (S3.3)$$

TM5 returns $s = 0.33$ which can be compared to a range of values between 0.25-and 0.31 in IPCC-TAR (Prather et al., 2001, Table 4.2) , resulting in a TM5-inherent calculated feedback factor $F=1.5$. This factor can be used to estimate the corresponding SR2-SR1 change in CH₄ emission in a second way. From Eq. S3.1 we find that a 20% decrease in CH₄ abundance corresponds to a 14% decrease in total CH₄ emissions. Kirschke et al. (2013) estimate total CH₄ emissions in the 2000s in the range 550 – 680 Tg yr⁻¹ from which we obtain an estimated

emission change between the HTAP SR1 and SR2 experiments in the range 77 – 95 Tg yr⁻¹, in line with our steady-state loss-balancing approach.

16) It also wasn't clear to me – is NO_x allowed to impact CH₄, particularly for the purposes of climate impacts?

REPLY: It is, as are all short-lived ozone precursors. We have added an extensive description in the SI on how the emission – forcing contributions in terms of (1) direct O₃ (2) indirect CH₄ and (3) CH₄-induced long-term O₃

CHANGES TO MANUSCRIPT: *added section S6.2 to the SI*

S6.2 Secondary forcing feedbacks of O₃ precursors on CH₄ and background O₃

Emissions of short-lived species (NO_x, NMVOC, CO, SO₂) influence the atmospheric OH burden and therefore the CH₄ atmospheric lifetime, which in turn contributes to long-term change in CH₄ and background ozone. Hence, the total forcing contribution from O₃ precursors consists of a short-term direct contribution from immediate O₃ formation (S-O₃), and secondary contributions from CH₄ (I-CH₄) and a long-term feedback from this CH₄ on background O₃ (M-O₃). We apply the formulation by (Fiore et al., 2009; Prather et al., 2001; West et al., 2007) to calculate the secondary change in steady-state CH₄ from SLS emissions, using the TM5 perturbation experiments for FASST (see section S3). TM5 diagnoses the CH₄ loss by oxidation for reference and perturbation run (where the emissions of SLS are decreased with -20%), from which we calculate the CH₄ oxidation lifetime ratio between reference and perturbation:

$$\frac{LT_P}{LT_{Ref}} = \frac{CH4_{oxP}}{CH4_{oxRef}} \quad [S6.5]$$

Where LT is the CH₄ lifetime against loss by OH oxidation, and CH₄_{ox} = the amount (Tg) of CH₄ oxidized.

The new steady-state methane concentration M due to the changing lifetime from perturbation experiment P, induced by O₃ precursor emissions follows from (Fiore et al., 2008, 2009; Wild and Prather, 2000):

$$M = M_0 \times \left(\frac{LT_P}{LT_{ref}} \right)^F \quad \text{where } M_0 = 1760 \text{ ppb, the reference CH}_4 \text{ concentration and } F = 1.5,$$

determined from the HTAP1 CH₄ perturbation experiments, as described in section S3.

The change in CH₄ forcing (I-CH₄) associated with the change to the new steady-state concentration is obtained from IPCC AR5 equations:

$$\Delta F = \alpha(\sqrt{M} - \sqrt{M_0}) - (f(M, N_0) - f(M_0, N_0)) \quad [S6.6]$$

$$f(M, N) = 0.47 \ln[1 + 2.01 \times 10^{-5}(MN)^{0.75} + 5.31 \times 10^{-15}M(MN)^{1.52}] \quad [S6.7]$$

Where M, M₀ = CH₄ concentration in ppb, N₀ = N₂O (=320 ppb)

The associated long-term O₃ forcing (M-O₃) per Tg precursor emitted is obtained by scaling linearly the change in O₃ forcing obtained in the HTAP1 CH₄ perturbation simulation (SR2–SR1), with the change in CH₄ obtained above, and normalizing by the precursor emission change (Fiore et al., 2009)

$$\Delta F = \frac{\Delta F_{O_3}[SR2-SR1]}{M_{SR2}-M_{SR1}}(M - M_0) \quad [S6.8]$$

The response of CH₄ and O₃ forcing to CO emission changes (for which no regional TM5-FASST perturbation model simulations were performed) was taken from TM5-CTM simulations performed for the HTAP1 assessment (Dentener et al., 2010) using the average forcing

efficiency for North America, Europe, South-Asia and East-Asia. For regions not covered by the HTAP1 regions, the HTAP1 rest-of-the-world forcing efficiency was used. The resulting region-to-globe emission-based forcing efficiencies are given in Tables S6.2 to S6.5 for aerosols, CO, CH₄ and other O₃ precursors respectively.

17) Many of the studies in the table are a bit out-of-date, as they would be around atmospheric conditions / emissions levels that are rather old, or in comparison to datasets that have greatly matured (for example comparison to satellite-based NO₂ retrievals, which are now much more accurate and consistent across retrievals than in the study of van Noije 2006.

REPLY: This is indeed the case. However, the TM5 version used in this study was developed and evaluated in the studies shown in the table. Since then no new developments and evaluation studies have been performed on the version used in this work. As in this study we are focusing on an evaluation of TM5-FASST, using TM5 as a reference, it is beyond the scope of this study to re-evaluate TM5 with new data sets, which would be worth one or more new papers on its own.

CHANGES TO MANUSCRIPT: *added following phrase to section S2.1 in the SI:*

We are aware of recent more accurate observational data have become available for the validation of the model since the validation studies listed in Table S2.1, in particular from satellite-based retrievals. However here we focus on the validation of FASST, using TM5 as a reference, and it is beyond the scope of this study to re-evaluate the TM5 model itself.

18) 8.3-4: Statements like this could be supported by reference many articles on the topic, including evaluation of how much this matters for different species at different scales.

REPLY:

We agree with this point. We address this now in a dedicated section in the discussion where we refer to exemplary studies that have specifically addressed the issue of grid resolution on exposure. They indicate in general that O₃ tends to be overestimated and (primary) PM_{2.5} tends to be underestimated compared to higher resolution models. Further we have included in the SI a quick analysis of the TM5 base simulation at resolution 6°x4°, 3°x2° and 1°x1° to illustrate the impact of resolution on concentrations and emission-concentration response sensitivities.

CHANGES TO MANUSCRIPT:

Modified last part of section 2.1 (P5 L28):

The model grid resolution influences the predicted pollutant concentrations as well as the estimated population exposure, especially near urban areas where strong gradients occur in population density and pollutant levels, which cannot be resolved by the 1°x1° resolution. In section 2.4 we describe a methodology to improve population PM_{2.5} exposure estimates by applying sub-grid concentration adjustments based on high-resolution ancillary data. The bias introduced by model resolution affects as well computed SR matrices, e.g. off-setting the share of 'local' versus 'imported' pollution in a given receptor region. We will discuss this aspect more in detail in section 4.3.

Added section 4.3 to the discussion section (P32 L20):

4.3 Impact of the native TM5 grid resolution on pollutant concentration and SRs

FASST base concentrations and SRs have been derived at a 1°x1° resolution which is a relatively fine grid for a global model, but still not optimal for population exposure estimates and health

impact assessments. Previous studies have documented the impact of grid resolution on pollutant concentrations. The effect of higher grid resolution in global models is in general to decrease ozone exposure in polluted regions and to reduce O₃ long-range transport, while PM_{2.5} exposure – mainly to primary species - increases (Fenech et al., 2018; Li et al., 2016; Punger and West, 2013). Without attempting a detailed analysis, a comparison of TM5 available output for PM_{2.5} and O₃ at 6°x4°, 3°x2° and 1°x1° resolution confirms these findings, as illustrated in Fig. S2.6 of the SI. Although FASST is expected to better represent population exposure to pollutants than coarser resolution models, a resolution of 1°x1° may not adequately capture urban scale pollutant levels and gradients when the urban area occupies only a fraction of the grid cell. The developed sub-grid parameterization for PM_{2.5}, providing an order-of-magnitude correction which is consistent with a high-resolution satellite product, is subject to improvement and to extension to other primary pollutants (NO₂, e.g. Kiesewetter et al., 2014, 2015) and O₃. To our knowledge a workable parametrization to quantify the impact of sub-grid O₃ processes on population exposure – in particular titration due to local high NO_x concentrations in urban areas - has not been addressed in global air quality models.

The impact of grid resolution on the within-region source-receptor coefficients can be significant, in particular for polluted regions where the coarse resolution includes ocean surface, like Japan. Table S2.3 in the SI shows as an example within-region and long-range SR coefficients for receptor regions Germany, USA and Japan. A higher grid resolution increases the within-region response and decreases the contribution of long-range transport (where the contribution of China to nearby Japan behaves as a within-region perturbation). In the case of Japan, the within-region PM_{2.5} response magnitude increases with a factor of 3, and the sign of the within-region O₃ response is reversed when passing from 6°x4° to higher resolution. Also over the USA, the population-weighted within-region response sensitivity upon NO_x perturbation increases with a factor of 5. Further, we find that in titration regimes, the magnitude of the O₃ response to NO_x emissions increases with resolution (i.e. ozone increases more when NO_x is reduced using a fine resolution) while the in-region ozone response is reduced in non-titration regimes (India and China, Fig. 2.7d). These indicative results are in line with more detailed studies (e.g. Wild and Prather, 2006).

19) Is there a reason why primary PM_{2.5} from industrial sources would also not be expected to contribute to the local urban increment? Or is this source just not very large?

REPLY: The choice of including only transport and residential sectors contributing to the urban increment is mainly motivated by the fact that these are the sectors for which the emissions correlate best with urban population. In developed countries, industrial emissions are typically somewhat away from densely populated areas in city centres, and elevated stack heights avoid direct exposure of the population. Nevertheless we recognize that depending on the local context, and especially in developing countries, these conditions may not or not completely be fulfilled. We further note that the intercomparison with satellite data (S4 in the SI) seems to indicate that the present sub-grid incremental factor is already at the high side, and including more industrial sources for primary PM_{2.5} increments would worsen the bias.

CHANGES TO MANUSCRIPT:

Modified the original phrase

Indeed, secondary PM_{2.5} is formed over longer time scales and therefore deemed to be more homogeneously distributed at the regional scale

To (P10 L23):

Indeed, secondary PM_{2.5} is formed over longer time scales and therefore deemed to be more homogeneously distributed at the regional scale, while primary PM_{2.5} emissions from other

sources than the residential and transport sector are assumed to occur more remotely from urban areas.

20) Section 2.4 and SIS4 are useful in understanding the urban increment, and some evaluation of improvement in performance compared to satellite-derived PM_{2.5} is included. However, the evidence is a bit indirect. I'd like to see a comparison of native 1x1 and urban downscaled BC concentration to in situ measurements from urban monitoring sites, such as are available in the US.

REPLY: The referee is correct in stating that the evidence is indirect and that improvements are possible. However we feel that an intercomparison with BC from monitoring stations is not the most appropriate way, because

- there are large uncertainties with BC mass measurements
- BC in TM5 really represent Elemental Carbon (excluding observation that are based on optical measurements),
- not in the least TM5, like many other models, has a low-bias towards observations.

Further, the urban-incremented FASST mean 1°x1° concentration is not directly comparable to point measurements of monitoring stations in particular when placed in urban locations. To address the reviewer's comment, we have instead elaborated the recent data set of van Donkelaar et al. (2016) which integrates a PM_{2.5} satellite product for anthropogenic PM_{2.5} with data from monitoring stations. The data set is available at a 0.1°x0.1° resolution, allowing for an aggregation at population-weighted 1°x1° grid mean that can directly be compared to FASST native as well as urban-incremented concentrations at grid cell or regional level.

CHANGES TO MANUSCRIPT:

We have significantly extended section S4 of the SI with additional text, figures and tables. We include here the new text of the section and refer to the revised SI for the figures.

S4.2 Comparison of TM5-FASST urban incremented PM_{2.5} with observations

We use the year 2010 0.1°x0.1° resolution global satellite product from the Dalhousie University Atmospheric Composition Analysis group (available at http://fizz.phys.dal.ca/~atmos/martin/?page_id=140), which includes ground-based observations via a Geographically Weighted Regression, while mineral dust and seasalt have been removed, as described in van Donkelaar et al., (2016).

The high-resolution satellite data (SAT) contain the sub-grid population and concentration gradients that we try to simulate with parametrization described above. Creating a SAT population-weighted average at 1°x1° resolution makes it possible to evaluate the TM5-FASST native and urban-incremented 1°x1° output. We convert the 0.1°x0.1° SAT resolution to the 2.5'x2.5' resolution of the CIESIN (year 2000) population dataset i.e. 24 sub-grid cells for each 1°x1° cell, to be overlaid with the satellite dataset. FASST PM_{2.5} 1°x1° grid maps are calculated from the HTAP2 year 2010 emission inventory, including the GFED v3 biomass burning emission inventor (REF). To remain consistent with the SAT product, residual water at 35% has been included. Fig. S4.1 shows global gridmaps of FASST and SAT PM_{2.5} (with dust and sea salt removed), and with the sub-grid increment included in the FASST result.

We evaluate both FASST native and urban incremented 1°x1° grid cell concentrations, using the parameterization described in the previous section. We calculate the following 1°x1° grid mean concentrations from the 2.5'x2.5' SAT PM_{2.5} and population sub-grid cells

$$SAT_{AREA} = \frac{1}{24} \sum_{i=1}^{24} PM_{2.5,i}$$

$$SAT_{POP} = \frac{\sum_{i=1}^{24} PM_{2.5,i} \cdot POP_i}{\sum_{i=1}^{24} POP_i}$$

SAT_{AREA} is the equivalent of the native FASST $1^\circ \times 1^\circ$ grid cell concentration, while SAT_{POP} represents the population-weighted mean $1^\circ \times 1^\circ$ concentration considering sub-grid gradients, to be compared with the FASST urban-incremented value, hereafter referred to as incremented concentrations. Regional and global mean population exposure to $PM_{2.5}$ (Table S4.3) is calculated using population-weighting on the $1^\circ \times 1^\circ$ grid cells, for both native (area-mean) and incremented concentrations.

Table S4.3 and Fig. S4.2 show that for all regions, except for MEA (Mediterranean + Middle East), we find an over-all good agreement in regional mean $PM_{2.5}$ exposure between FASST and SAT, both for the native and incremented values. Figure S4.3 shows the absolute regional-mean increment in $PM_{2.5}$ exposure. We find that applying the FASST sub-grid parameterization increases global mean exposure with $1.4 \mu\text{g m}^{-3}$ (FASST), versus an increase of 1.1 from SAT, corresponding to a global population-weighted mean 5% increase for both methods. The FASST urban increment parameterization generates a regional-mean increase in $PM_{2.5}$ exposure from $0.6 \mu\text{g/m}^3$ (Latin America) to $3.4 \mu\text{g/m}^3$ (Russia and former Soviet Union states). In Europe and North-America the regional increase is around $1 \mu\text{g/m}^3$. Except for East-Asia and Latin America, the regional FASST increment exceeds the SAT value. SAT regional increments range between $0.3 \mu\text{g/m}^3$ for Russia and former Soviet Union states and $1.8 \mu\text{g/m}^3$ in East-Asia. Although we don't find a direct correlation between the SAT and FASST computed increments, it is encouraging that without applying any fitting procedure, and using two completely different approaches, increments from FASST and SAT are in the same order of magnitude.

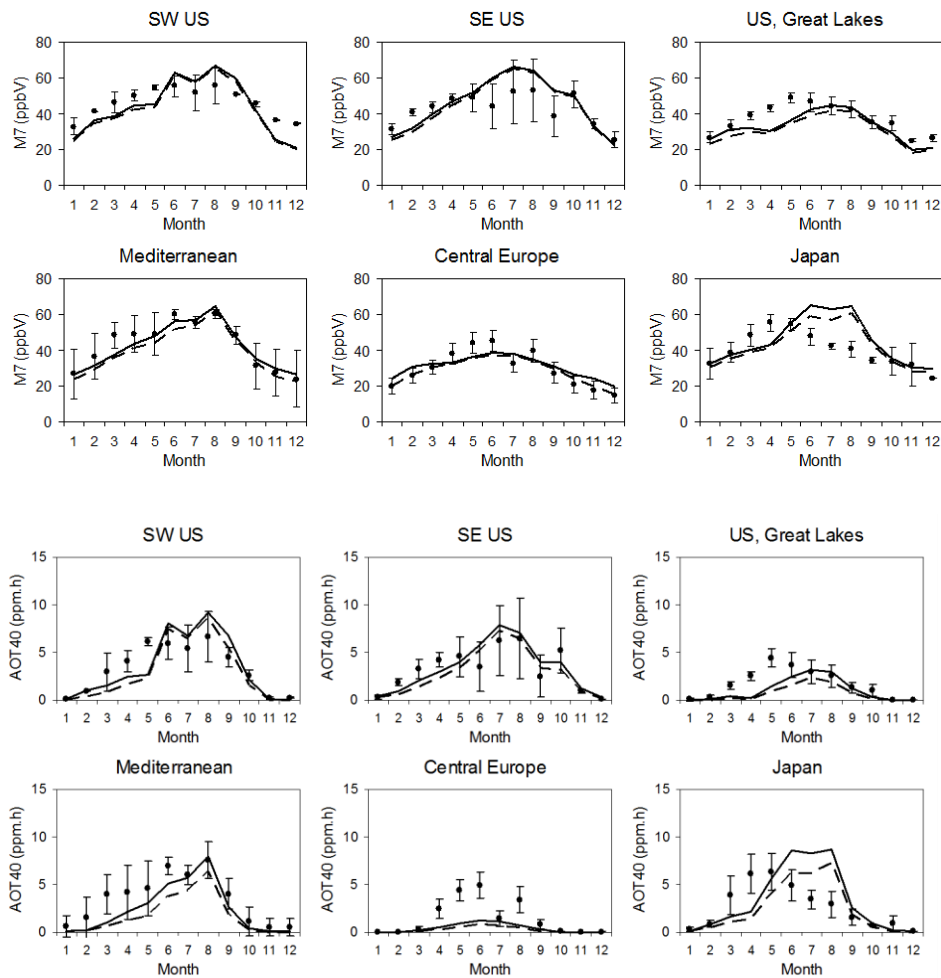
Figs. S4.4 (Europe and North-America), S4.5 (China and India) and S4.6 (Africa and Latin America) show a detailed grid-to-grid comparison for selected key regions between native and incremented FASST on the one hand and SAT_{POP} on the other. In general, individual grid cells are reproduced within a factor of two. The FASST increment parameterization slightly improves the correspondence with SAT_{POP} compared to the native data except for China where the native FASST concentrations already exceed SAT_{POP} . Although an agreement at grid cell level is not the ambition of FASST, these results indicate that our crude approach is roughly performing, but that a more sophisticated approach in the urban increment may be warranted.

Finally, seen the large uncertainties on absolute $PM_{2.5}$ concentrations, one may wonder if the implementation of an urban increment parameterization is worth the effort. A FASST RCP2000 analysis of global mortalities with and without the generic urban increment factors (given in Table S4.2) shows that the global 5% increase in $PM_{2.5}$ exposure due to the urban increment accounts for an increase in total mortality numbers with 14% when dry $PM_{2.5}$ is considered, and with 11% when $PM_{2.5}$ is humidified at 35% RH. The difference is due to the threshold in the exposure-response functions (see section S5 in this SI). In areas where the native grid concentration is just below threshold, a small increase in $PM_{2.5}$ will have a strong response in mortalities while areas with native $1^\circ \times 1^\circ$ concentrations above the threshold will respond more proportional to the subgrid increment. Including hygroscopic growth at 35% from the onset reduces the cases where native resolution $PM_{2.5}$ remains below the threshold which explains the lower impact of the subgrid increment factor.

21) 11.25-27: This justification would be improved if the authors were a bit more quantitative. Also, if the lowest model level O_3 compares favorably to the surface O_3 measurements, this begs the question then of why the modeled O_3 thought the lower atmosphere in TM5 is biased low (as surface-level concentrations would be lower than 30 m concentrations).

REPLY: As can be seen in the paper by Van Dingenen et al. (2009), which uses the same TM5 model versions, but slightly different emissions (see their figures 6 and 7 copied below, but not used in the current manuscript) during the summer months (i.e. crop growing season), the daytime a vertical gradient between 30 m (model centre) and 10 m (standard height of

observations) is nearly absent – presumably due to higher atmospheric instability. The TM5 value at 30m is generally reproducing well the observations, and when it does not, the vertical gradient in TM5 is not the dominant factor causing discrepancies.



CHANGES TO MANUSCRIPT:

Changed phrase

However comparing TM5 simulated gridbox-centre ozone metrics with observations from 99 monitoring stations 25 worldwide, Van Dingenen et al. (2009) find that, averaged over the horizontal resolution of the grid cells, the TM5 simulated 30m monthly O₃ and O₃ metrics represent the observed values within their variability range.

To (P13 L10):

However comparing TM5 simulated gridbox-centre ozone metrics with observations from 99 monitoring stations worldwide, Van Dingenen et al. (2009) find that, when averaged at the regional scale, TM5 simulated crop metrics obtained from the grid box centre are reproducing the observations within their standard deviations, and that the monthly 10m TM5 metric values do not significantly improve the bias between model value and observations. Therefore we use the standard model output at 30m.

22) 12.21: The authors evaluate their approach to calculating direct aerosol radiative forcing by providing plots of the species specific forcings in Fig S6.1 and noting they are “reliable results.” However, I don’t have any sense of what makes these results reliable. What features of the distributions shown in these plots are those that we would expect, easily explain, or could compare to observations or other modeling studies? The BC RF in the eastern part of Antarctica exhibits a strange horizontal strip that I’m not sure about. Also, the figure legend on S6.1 is redundant and the units on both of the color bars are incorrect.

REPLY:

The reviewer correctly questions our use of the word reliable, which overstates our confidence in the uncertainty associated with the whole computational chain from emissions to concentrations and aerosol columns, and the scaling with normalized radiative forcing patterns. All these steps come with intrinsic uncertainties, and the radiative forcing uncertainty at grid basis is inevitably associated with relatively large uncertainties. The statement on 'reliability' is based on comparison with other globally aggregated results with an independent study performed by Unger et al, which gives remarkably similar source specific RF results. The 'strip' at the South Pole is likely due a numerical issue related the polar singularity and the necessary grid-size inflation in TM5 to deal with the singularity in a lon-lat projection.

CHANGES TO MANUSCRIPT: *Modified the phrase to (P14 L19):*

Our evaluation of pre-industrial to present radiative forcing in the validation section demonstrates that, in the context of the reduced-form FASST approach, the applied method however provides useful results. Figure S6.1 (a, b, c) in the SI shows the resulting global radiative forcing fields for sulfate, POM and BC. The regional emission-normalized forcing SRs for aerosol precursors (in $W m^{-2} Tg^{-1}$) are given in Table S6.2 of the SI.

Figure S6.1 has been modified to display the proper legend next to each graph, and units have been corrected to $W mg^{-1}$.

23) Section 2.7.2: The tool does not include the substantial non-direct cloud interactions for BC, nor the impact of BC on snow/ ice albedo. These factors contribute significantly to the targeting of BC-rich sources for SLCP mitigation. Comment on how omission would affect TM5-FASST results.

REPLY:

This is a correct observation, and indeed worth mentioning. Surface albedo effects (snow and sea-ice) is estimated to contribute with (+0.04 to +0.33) W/m^2 , cloud interaction with (-0.47 to +1.0) W/m^2 on a total estimated forcing of (0.17 to 2.1) W/m^2 (Bond et al., 2013) where FASST estimates a total anthropogenic BC forcing of +0.15 W/m^2 hence all these contributions are significant. As mentioned in the conclusions, future developments could indeed include these effects, in particular changes in the surface albedo, seen the fact that BC deposition is computed by FASST. Nevertheless, we note that TM5, like other global models, has large uncertainties associated with the calculation of BC depositions.

CHANGES TO MANUSCRIPT:

In section 2.7.1 (P14 L15):

Neglecting the aerosol mixing state and using column-integrated mass rather than vertical profiles introduces additional uncertainties in the resulting forcing efficiencies. Accounting for internal mixing may increase the BC absorption by 50 to 200% (Bond et al., 2013), while including the vertical profile would weaken BC forcing and increase SO_4 forcing (Stjern et al. 2016). Further, the BC forcing contribution through the impact on snow and ice is not included, nor are semi- and indirect effects of BC on clouds. Our evaluation of pre-industrial to present

radiative forcing in the validation section demonstrates that, in the context of the reduced-form FASST approach, the applied method however provides useful results.

In section 3.3.1(P24 L25):

However, comparing to another widely used literature source (Bond et al., 2013), the TM5-FASST_v0 BC forcing estimate still falls within the 90% CI (0.08, 1.27) W/m² direct radiative forcing given for the year 2005, with a comparable global BC emission rate. Our low-end BC forcing estimate can be partly explained by the simplified treatment as externally mixed aerosol, without accounting for the enhancement of the mass absorption cross-section when BC particles become mixed or coated with scattering components. Not-included snow albedo and indirect cloud effects would contribute with +0.13 (+0.04 to +0.33) W/m² and +0.23 (-0.47 to +1.0) W/m² respectively (Bond et al., 2013).

24) Fig 2: What is the mechanism by which the perturbation in NO_x emissions causes a reduction in SO₄ in IND (as opposed to an increase in all other regions)?

REPLY: This is indeed an interesting observation, which could be linked to the oxidative capacity of the atmosphere in that region, and/or to the thermodynamic properties of the ammonium-sulfate-nitrate system and the specific meteorological conditions in that area. Indeed, India has the particular feature that sulfate is dominating the inorganic aerosol fraction, and NH₃ may be in excess. Answering this question would require a deeper analysis of TM5 budget data and the particular thermodynamic aerosol regimes for this case, where we notice that especially above India there are no reliable observations that could shed light on model discrepancies. Therefore we think that further analysis of this interesting model result is beyond the scope of this work where we focus on documenting and validating the linearity approach of FASST. However, in the text we point to this results for further multi-model analysis.

CHANGES TO MANUSCRIPT: *the paragraph has been expanded as follows: (P19 L4)*

For India we further observe a relative strong nitrate response to NO_x emissions, with NO₃⁻ increasing by a factor of 3 for a doubling of NO_x emissions, although the responses shown in Fig. 2 indicate that absolute changes (in µg m⁻³) in NO₃ are relatively low and that secondary PM_{2.5} in this region is dominated by SO₄. We are not aware of reliable observations or other published NO_x-aerosol sensitivity studies from that region that could corroborate this calculated sensitivity. Because such a feature may strongly affect projected future PM_{2.5} levels and associated impacts, we recommend regional multi-model studies devote attention this feature.

25) 18.1-2: It seems NO_x levels in the US and Europe are much lower now, and I'm not sure these titrations still exist; they are at least less persistent in the summer. See for example recent article by Jin, Fiore, et al., JGR, 2017.

REPLY: Thank you for pointing to this interesting paper. Indeed NO_x emissions have been decreasing in the last two decades and indeed, the FASST SR relations were established for year 2000 conditions favouring a NO_x-saturation regime over W-Europe and NE-US. The fixed O₃ emission-response slopes are a major caveat for the evaluation of future scenarios, however, as already pointed out in the paper, while annual O₃ displays the typical reverse NO_x-O₃ response because of the winter-time titration, the slope reverses to positive in most cases when considering seasonal metrics centred on summer (Figure 6 in our paper). This being said, further reduction in NO_x and NMVOC is likely to change the O₃ (metric) response sensitivity, and indeed the fixed and linear SRs are a limitation of the tool. A possible, but non-trivial implementation, way to address this trend is to introduce higher order terms in the SRs and/or

to update the year 2000 SRs with more recent ones obtained in the frame of HTAP2 (e.g. based on Turnock et al., 2018).

CHANGES TO MANUSCRIPT:

This issue is now introduced in the discussion section 4.1 (P30 L4)

The reliability of the model output in terms of impacts depends critically on the validity of the linearity assumption for the relevant exposure metrics (in particular secondary components), which becomes an issue when evaluating emission scenarios that deviate strongly from the base and -20% perturbation on which the current FASST SRs are based. The evaluation exercise indicated that non-linearity effects in PM_{2.5} and O₃ metrics in general lead to a higher bias for stringent emission reductions (towards -80% and beyond) than for strong emission increases compared to the RCP2000 base case, but over-all remain within acceptable limits when considering impacts. Indeed, because of the thresholds included in exposure-response functions, the higher uncertainty on low (below-threshold) pollutant levels from strong emission reductions has a low weight in the quantification of most impacts. In future developments the available extended-range (-80%, +100%) emission perturbation simulations could form the basis of a more sophisticated parameterization including a bias correction based on second order terms following the approach by Wild et al. (2012) both for O₃ and secondary PM_{2.5}. The break-down of the linearity at low emission strengths is relevant for O₃ and O₃ exposure metrics as the implementation of control measures in Europe and the US has already substantially lowered NO_x levels over the past decade, gradually modifying the prevailing O₃ formation regime from NO_x-saturated (titration regime) to NO_x-limited (Jin et al., 2017).

26) 18.6: The statement that the sensitivities of impact-relevant O₃ metrics (M6M and M12) are more linear than for annual average pop-weighted O₃ is not supported by the results shown in Fig 6. The responses to NO_x emission changes seem to be more nonlinear for M6M or M12 in some cases, such as GBR as well as others. The text should be revised accordingly.

REPLY: This is indeed wrongly formulated; this should rather refer to the changing sign of the slope.

CHANGES TO MANUSCRIPT: *changed phrase*

However, the impact-relevant O₃ metrics, both health and crop related, are based on summertime and daytime values and are expected to behave more linearly (Wu et al., 2009).

To (P20 L27):

On the other hand, the impact-relevant O₃ metrics, both health and crop related, are based on summertime and daytime values and are expected to be less affected by titration and consequently to maintain a positive emission-response slope (Wu et al., 2009).

27) 18.20: AOT40 would focus on high O₃ values. It's not clear to my, chemically speaking, why this would be expected to response more nonlinearly than other metrics. Presumably larger O₃ values are occurring more in the summer. Earlier it was claimed that summer sensitivities would be more linear ... so I'm a bit confused here.

REPLY:

AOT40 is a threshold-based metric accumulating only values above 40ppb, and this built-in step function makes it difficult to approximate it with a linear function over a large perturbation range. For instance, in regions where ozone levels are just above 40ppb, a small decrease in O₃ can cause a big decrease in AOT40, while a similar small increase would cause a smaller AOT40 response (in absolute terms). Similarly, a SR sensitivity established from a perturbation at high O₃ levels will behave rather linearly in the high O₃ range, but cannot be extrapolated to very

strong reductions where it will lead to an overestimation of AOT40. Therefore the SR sensitivity based on the 20% decrease is less likely to be generally applicable over a large perturbation range.

This is less the case of metrics like M12 which are based on 3-monthly means of daytime ozone and behave more linearly with respect to emission perturbations.

28) 18.31: Why is that the case, chemically speaking?

REPLY: In this case – without investigating the underlying chemical mechanism - the larger deviation is a consequence of the slight convex shape of the O₃ response to NO_x for these countries, combined with the extrapolation of the -20% slope to larger perturbations.

CHANGES TO MANUSCRIPT:

With the major revision of sections 3.1.2 this particular phrase and the figures it was referring to have been removed. However we do mention (P19 L10):

Because the TM5-FASST linearization is based on the extrapolation of the -20% perturbation slope, concave-shaped trends in Fig. 3 indicate a tendency of TM5-FASST to over-predict secondary PM_{2.5} at large negative or positive emission perturbations, and opposite for convex-shaped trends.

29) 20.4-14: I find it interesting that the change in PM_{2.5} is predicted by FASST better than absolute concentrations (which I would expect) but that the change in O₃ metrics is predicted more poorly than absolute concentrations (would not expect). Do the authors have any thoughts about the reasons behind the latter?

REPLY:

Ozone behaves in general less linearly than PM_{2.5}, i.e. the perturbation term in Eq. 2 is more robust for PM_{2.5} than for O₃. For strong perturbations, either side of the reference case, total PM_{2.5} is overpredicted, hence making the difference between the high and low emission case cancel out some of the bias compared to absolute total PM_{2.5}.

For O₃, one must consider that the relative contribution of the “base” term in Eq. 2 is relatively high, even for strong anthropogenic perturbations because it contains the natural background. Roughly speaking, setting all anthropogenic emissions to 0 would still leave about 30 ppb of 6mDMA1. Therefore, this fixed contribution in the total reduces the weight of the relative error of the perturbation term, but when making the delta it does not contribute anymore.

Note that we have introduced statistical metrics Normalized Mean Bias (NMB) and Mean Bias (MB) to evaluate the agreement between FASST and TM5 with

Normalized Mean Bias = $(FASST - TM5) / TM5$ and

Mean Bias = $(FASST - TM5)$

CHANGES TO MANUSCRIPT:

We included the following phrase in the re-written discussion in section 3.2 (P23 L13):

Contrary to PM_{2.5}, the NMB for the delta 6mDMA1 between two scenarios is higher than the NMB on absolute concentrations, with a low bias for the delta metric of -38% and -45% for Europe and North-America respectively, and a high bias of 35 to 46% in Asia. However, the MB on the delta is of the same order or lower than the absolute concentrations (Table 9). This is a consequence of the fixed background ozone in the absolute concentration reducing the weight of the anthropogenic fraction in the relative error.

30) 20.15-22: That's a reasonable comparison. I also wonder though what is the total number of estimated premature deaths associated with PM_{2.5} and O₃, and how these numbers compare to those in the literature (from e.g. GBD), for present day conditions. This would help evaluate the accuracy of the absolute estimates in addition to estimates of changes.

REPLY: We have now included a table with some values from literature (both for PM_{2.5} and O₃) in section 3.3 which is dedicated to a comparison with other published work, also illustrating the various assumptions that are involved making a direct comparison quite difficult.

CHANGES TO MANUSCRIPT: *Included a new section under section 3.3.4 Health impacts (P26 L24):*

Present-day health impacts

Table 14 gives an overview of recent global PM_{2.5} health impact studies, together with FASST estimates for the year 2000 (RCP) and year 2010 (HTAP2 scenario). The studies differ in emission inventories and year evaluated, in applied methodologies to estimate PM_{2.5} exposure, in model resolution, as well as in the choice of the exposure response functions, the value of the minimum exposure threshold, and mortality statistics. Studies excluding natural dust from the exposure are mostly applying the log-lin exposure response function and RR from Krewski et al. (2009), and estimate between 1.6 and 2.7 million annual premature mortalities from PM_{2.5} in scenario years 2000 to 2004. FASST returns 2.1 and 2.5 million deaths using the GBD and log-lin exposure functions respectively. Studies including mineral dust are mostly applying the GBD integrated exposure-response functions and a non-zero threshold to avoid unrealistically high relative risk rates at high PM_{2.5} levels in regions frequently exposed to dust. Depending on the choice of the exposure-response function and scenario year, FASST obtains 2.6 to 4.1 million global deaths, comparable with the range 1.7 to 4.2 million from previous studies.

Global ozone mortalities reported in Table 15 have been commonly based on the Jerrett et al. (2009) methodology, implemented in FASST. FASST obtains 197 thousand and 340 thousand deaths for RCP 2000 and HTAP2 2010 scenarios respectively, while the earlier studies find 380 to 470 thousand deaths in 2000, and 140 to 250 thousand in 2010 – 2015. Differences can be attributed to model chemical and meteorological processes, emission inventories, and the use of different sources for respiratory base mortality statistics.

Both for PM_{2.5} and O₃, the difference between the different studies falls within the combined RR uncertainty and model variability range.

Table 14 Overview of previous studies on health impact of PM_{2.5}, together with FASST results for 2 different scenarios. Uncertainty ranges are as reported in the respective studies. The uncertainty range on FASST results includes the RR uncertainty only (Fig. S5.1 in the SI)

Reference	Year evaluated	Method	threshold	Exposure - response function	Global deaths (millions)
Excluding mineral dust					
Fang et al., 2013	2000	CTM	no	K2009 ^(a)	1.6 (1.2 – 1.9)
Silva et al., 2013	2000	CTM	no	K2009	2.1 (1.3 -3.0)
Anenberg et al., 2010	2000	CTM	5.8µg m ⁻³	K2009	2.7 (2.0 -3.4)
Evans et al., 2013	2004	SAT	5.8µg m ⁻³	K2009	2.7 (1.9 - 3.5)
Lelieveld et al., 2013	2005	CTM	no	K2009	2.2 (2.1 - 2.3)
FASST (RCP)	2000	FASST	~7.3µg m⁻³	K2009	2.5 (1.2 – 3.6)
FASST (RCP)	2000	FASST	~7.3µg m⁻³	B2014^(b)	2.1 (1.0 – 3.0)
Including mineral dust					
Silva et al., 2016	2000	ACCMIP CTM ensemble	~7.3µg m ⁻³	B2014	1.7 (1.3 – 2.1)
Evans et al. 2013	2004	SAT	5.8µg m ⁻³	K2009	4.3 (2.9 – 5.4)
Lelieveld et al., 2015	2010	CTM	~7.3µg m ⁻³	B2014	3.2 (1.5 - 4.6)
GBD2010 (Lim et al., 2012)	2010	Fused (FASST + SAT + ground based)	~7.3µg m ⁻³	B2014	3.2 (2.8 -3.6)
GBD2013 (Forouzanfar et al., 2015)	2013	Fused (FASST + SAT + ground based)	~7.3µg m ⁻³	B2014	2.9 (2.8 – 3.1)
GBD2015 (Cohen et al., 2017)	2015	Fused (FASST + SAT + ground based)	~4.1µg m ⁻³	B2014	4.2 (3.7 – 4.8)
FASST (RCP)	2000	FASST	~7.3µg m⁻³	K2009	3.6 (2.7 -4.5)
FASST (RCP)	2000	FASST	~7.3µg m⁻³	B2014	2.6 (1.2 – 3.8)
FASST (HTAP2)	2010	FASST	~7.3µg m⁻³	B2014	4.1 (2.0 - 5.9)

(a) Krewski et al., 2009

(b) Burnett et al., 2014

Table 15 Overview of previous studies on long-term health impact of ozone, together with FASST results for 2 different scenarios

Ref	year	Method	threshold	Exposure-response function	Global deaths (thousands)
Anenberg et al., 2010	2000	CTM	33.3	J2009 ^(a)	470 (182 - 758)
Silva et al., 2013	2000	ACCMIP CTM ensemble	33.3	J2009	380 (117 -750)
Lelieveld et al., 2015	2010	CTM	~37.6	J2009	142 (90 -208)
GBD 2010 (Lim et al., 2012)	2010	FASST	~37.6	J2009	152 (52 – 270)
GBD 2013 (Forouzanfar et al., 2015)	2013	FASST	~37.6	J2009	217 (161 – 272)
GBF 2015 (Cohen et al., 2017)	2015	FASST	~37.6	J2009	254 (97 – 422)
FASST (RCP)	2000	FASST	33.3	J2009	197 (66 – 315)
FASST (HTAP2)	2010	FASST	33.3	J2009	340 (116 – 544)

(a) Jerrett et al., 2009

31) 20.25 - 21.7: I'm I incorrect in thinking that many of the pre-industrial to present IPCC RF's also include an 80% reduction in biomass burning sources? If so, this might further explain why the IPCC values are on the higher side. Also, IPCC estimates and those in Bond include RF of BC on snow, which I don't see as being accounted for in FASST.

REPLY:

We do not have the information on what reductions in biomass burning were assumed in IPCC models, but note that most recent studies point to smaller reductions, subject to large uncertainty. Large scale biomass burning is more prominent for OC emissions, than for BC. For instance, in the RCP2000 emission inventory, BC from large scale forest fires account for 15% of the total BC forcing, hence including BB does not make a large (absolute) difference on the already low BC forcing (from 0.15 to 0.17 W/m²) and cannot account for the low bias. Other missing contributions could indeed be more relevant, like the BC mixing state and residence time, snow and ice albedo impacts and cloud interactions (see also our reply to comment 23).

32) 21.22: How do they know it's owing to different OH levels and lifetimes rather than to different emissions (line 21.14)?

REPLY: The reviewer makes a correct point. We cannot be certain about this statement. However, the Stevenson ACCMIP study was based on the same emissions database described by Lamarque et al. (2013) as used in this model study, which seems to point to differences in oxidation chemistry and resulting ozone production with respect to CO and NMVOC emissions. We also spotted an error in our data treatment and corrected the data in Table 10 which changes slightly the discussion.

CHANGES TO MANUSCRIPT (P25 L6):

Table 10 compares the contribution of anthropogenic O₃ precursors CH₄, NO_x, NMVOC and CO to the O₃ and CH₄ radiative forcing with earlier work (Shindell et al., 2005, 2009; Stevenson et al., 2013). Except for NO_x which shows a large scatter across the studies, the FASST computed contributions to global O₃ and CH₄ forcing - using the same year 1850 to 2000 emission changes as in Stevenson et al. (2013) - are in good agreement with the model ensemble range in

the latter study. FASST NO_x forcing contributions are a factor 3 lower than in the Stevenson et al. study and more in line with Shindell et al. (2005, 2009) values (based on the period 1750 – 2000), however the latter obtain a NMVOC contribution to O₃ forcing which is a factor of 5 to 6 lower than the other estimates. Differences across the studies are likely due to differences in oxidation chemistry and lifetimes across models.

33) Section 3.3.2: The evaluation of global sector and species specific RF looks good. A key feature of FASST is regional specificity; could they also compare to some studies in the literature that have evaluation the RF of regionally specific emissions by species or sector?

REPLY: We note that FASST does not contain sector-specific SRs, hence global forcing efficiencies (expressed as mW/m²/Tg) for a single FASST source region are valid for the aggregated contributions of the regional sectors.

The most relevant studies to compare aerosol global forcing responses to regional emissions are the HTAP1 exercise (Yu et al., 2013) and the similar multi-model HTAP2 study (Stjern et al., 2016). For the NH regions considered in these studies, our results correspond well (within 1 stdev) with older Yu et al. study (based on a single model, using similar emission and meteorological year as FASST base simulation), whereas the multi-model ensemble mean of Stjern et al. gives higher forcing efficiencies, although in the latter case the model variability is large, and our results stays within 2 stdv (95% confidence interval).

CHANGES TO MANUSCRIPT:

We have included an additional subsection under 3.3 (Comparison of TM5-FASST_v0 impact estimates with published studies) (P25 L15):

3.2.2 Regional forcing efficiencies by emitted component

Earlier work in the frame of HTAP1 (Fry et al., 2012; Yu et al., 2013) and HTAP2 (Stjern et al., 2016) evaluated regional forcing efficiencies for larger regions than the ones defined for FASST. For a comparison we aggregate the FASST forcing efficiencies (as listed in section S6.3 of the SI) by making an emission-weighted averages over Europe (EUR), North-America (NAM), South-Asia (SAS), East-Asia (EAS), Mediterranean and Middle East (MEA) and Russia, Belarus and Ukraine (RBU). Tables 11 (PM precursors) and 12 (NO_x and NMVOC) show the earlier studies along with the FASST results. The FASST forcing efficiencies for PM precursors confirm our earlier observation that FASST is particularly biased low for BC, in particular compared to Stjern et al. (2016), but further compares relatively well with the earlier work, in particular with Yu et al. (2013) which was based on a year 2001 baseline, similar to conditions of our base scenario. A similar observation is made for NMVOC for which FASST efficiencies agree well with the study by Fry et al. (2012). The forcing efficiency for ozone precursor NO_x has a high uncertainty. While for East-Asia, North-America and South-Asia the FASST result falls within 1 standard deviation of the HTAP1 model ensemble the FASST NO_x forcing efficiency for Europe shows a larger deviation. Without going into the details of the underlying mechanisms, ozone titration effects, which are better resolved with the higher TM5 model resolution, could be a contributing factor.

New tables 11 and 12:

Table 11. Regional-to-global direct radiative forcing efficiencies for PM_{2.5} precursors (mW/m²/Tg of annual emissions) for the larger source-receptor regions in earlier studies, and from FASST, aggregated to similar regional definitions. Values in brackets represent 1 standard deviation from the respective reported model ensembles.

		NAM	EUR	SAS	EAS	RUS	MEA
Stjern et al., 2016	BC	52 (±21)	55 (±22)	94 (±38)	55 (±16)	78 (±47)	202 (±323)
	POM	-8 (±6)	-7 (±4)	-10 (±6)	-5 (±3)	-2 (±5)	-18 (±7)
	SO4 (SO2)	-5 (±2)	-6 (±2)	-8 (±4)	-4 (±1)	-4 (±1)	-10 (±7)
Yu et al., 2013	BC	27 (±15)	37 (±19)	25 (±15)	28 (±20)		
	POM	-4 (±2)	-4 (±2)	-4 (±2)	-4 (±2)		
	SO4 (SO2)	-4 (±1)	-4 (±1)	-4 (±1)	-3 (±1)		
FASST (RCP2000)	BC	17	19	19	16	25	43
	POM	-6	-4	-6	-5	-4	-9
	SO4 (SO2)	-3	-3	-4	-2	-2	-7

Table 12. Regional-to-global direct radiative forcing efficiencies for O₃ precursors (mW/m²/Tg of annual emissions) for the larger source-receptor regions in earlier work, and from FASST, aggregated to similar regional definitions, including feedbacks on CH₄. Values in brackets represent reported 1 standard deviation from the model ensemble in the earlier work.

		EAS	EUR	NAM	SAS
Fry et al., 2010	NO _x	-0.22 (±0.6)	-1.20 (±0.5)	-0.48 (±0.6)	-1.70 (±2.2)
	NMVOG	0.42 (±0.2)	0.46 (±0.2)	0.42 (±0.2)	0.72 (±0.2)
FASST (RCP200)	NO _x	-0.44	-0.33	-0.35	-1.43
	NMVOG	0.60	0.57	0.61	0.74

34) 23.25: Does including this correction for changing mortality rates though lead to worse agreement between ACCMIP and FAST for PM_{2.5} related deaths (Fig 15)?

REPLY:

It does not because according to the GBD methodology, respiratory mortality is not considered in the PM_{2.5} related causes of death (which are: COPD, LC, IHD and Stroke), it contributes only to the O₃ health impact. The ACCMIP projections of PM-relevant base mortalities are much more in line with the ones used in FASST.

CHANGES TO MANUSCRIPT: *added the following phrase (P28 L25):*

Respiratory mortality is not considered as a cause of death for PM_{2.5}, which explains why a similar disagreement is not observed in the PM_{2.5} mortality trend in Fig. 17b.

35) Section 4: Good discussion. Some caveats about missing accurate treatment of SOA? Or carbonaceous aerosol aging? And possibly being a bit more clear about the limits of the emissions perturbations magnitudes that should be used with this tool (e.g., x2? x5? x10?).

REPLY:

Thank you for the positive feedback and the suggestions. We have extended some of the discussion making a wrap-up of the major caveats of the tool. Regarding the limits of the emission perturbations magnitudes, this depends on many parameters such as the region of

emission, on the emission ratio between various precursors, so it is not possible to set an overall validity range. We believe that the MIT and FLE scenarios explore the domain boundaries in which 'reasonable' emission changes for the next decades (until 2030) and that TM5-FASST behaves sufficiently well to be used as a screening tool to explore scenarios further out in the future.

CHANGES TO MANUSCRIPT

New discussion section 4.1 is – amongst other caveats - addressing the issues mentioned (P31 L16)

The current version of TM5-FASST is missing some source-receptor relations which may introduce a bias in estimated PM_{2.5} and O₃ responses upon emission changes. The omission of secondary organic PM in TM5 is estimated to introduce a low bias in the base concentration of the order of 0.1 µg m⁻³ as global mean however with regional levels in Central Europe and China up to 1 µg m⁻³ in areas where levels of primary organic matter are reaching 20 µg m⁻³ (Farina et al., 2010) indicating a relatively low contribution of SOA to total PM_{2.5}. O₃ formation from CO is included in the TM5 base simulations, but no SR matrices for the FASST source region definition are available. Based on the HTAP1 CO perturbation simulations with TM5, we estimate that a doubling of anthropogenic CO emissions contributes with 1 – 1.9 ppb in annual mean O₃ over Europe, 1.3 -1.9 ppb over North-America, 0.7-1.0 ppb over South Asia and 0.3 – 1.5 ppb over East-Asia. Development of CO-O₃ SRs is an important issue for the further development of the tool.

References

- Amann, M., Bertok, I., Borcken-Kleefeld, J., Cofala, J., Heyes, C., Höglund-Isaksson, L., Klimont, Z., Nguyen, B., Posch, M., Rafaj, P., Sandler, R., Schöpp, W., Wagner, F. and Winiwarter, W.: Cost-effective control of air quality and greenhouse gases in Europe: Modeling and policy applications, *Environ. Model. Softw.*, 26(12), 1489–1501, doi:10.1016/j.envsoft.2011.07.012, 2011.
- Andersson, C., Langner, J. and Bergström, R.: Interannual variation and trends in air pollution over Europe due to climate variability during 1958–2001 simulated with a regional CTM coupled to the ERA40 reanalysis, *Tellus B*, 59(1), 77–98, doi:10.1111/j.1600-0889.2006.00196.x, 2007.
- Anenberg, S. C., Horowitz, L. W., Tong, D. Q. and West, J. J.: An estimate of the global burden of anthropogenic ozone and fine particulate matter on premature human mortality using atmospheric modeling, *Environ. Health Perspect.*, 118(9), 1189–1195, doi:10.1289/ehp.0901220, 2010.
- Anon: Estimates of global mortality attributable to particulate air pollution using satellite imagery, *Environ. Res.*, 120, 33–42, doi:10.1016/j.envres.2012.08.005, 2013.
- Bond, T. C., Doherty, S. J., Fahey, D. W., Forster, P. M., Berntsen, T., DeAngelo, B. J., Flanner, M. G., Ghan, S., Kärcher, B., Koch, D., Kinne, S., Kondo, Y., Quinn, P. K., Sarofim, M. C., Schultz, M. G., Schulz, M., Venkataraman, C., Zhang, H., Zhang, S., Bellouin, N., Guttikunda, S. K., Hopke, P. K., Jacobson, M. Z., Kaiser, J. W., Klimont, Z., Lohmann, U., Schwarz, J. P., Shindell, D., Storelvmo, T., Warren, S. G. and Zender, C. S.: Bounding the role of black carbon in the climate system: A scientific assessment, *J. Geophys. Res. Atmospheres*, 118(11), 5380–5552, doi:10.1002/jgrd.50171, 2013.
- Burnett, R. T., Pope, C. A., III, Ezzati, M., Olives, C., Lim, S. S., Mehta, S., Shin, H. H., Singh, G., Hubbell, B., Brauer, M., Anderson, H. R., Smith, K. R., Balmes, J. R., Bruce, N. G., Kan, H., Laden, F., Prüss-Ustün, A., Turner, M. C., Gapstur, S. M., Diver, W. R. and Cohen, A.: An Integrated Risk Function for Estimating the Global Burden of Disease Attributable to Ambient Fine Particulate Matter Exposure, *Environ. Health Perspect.*, doi:10.1289/ehp.1307049, 2014.
- Christoudias, T., Pozzer, A. and Lelieveld, J.: Influence of the North Atlantic Oscillation on air pollution transport, *Atmospheric Chem. Phys.*, 12(2), 869–877, doi:https://doi.org/10.5194/acp-12-869-2012, 2012.
- Cohen, A. J., Brauer, M., Burnett, R., Anderson, H. R., Frostad, J., Estep, K., Balakrishnan, K., Brunekreef, B., Dandona, L., Dandona, R., Feigin, V., Freedman, G., Hubbell, B., Jobling, A., Kan, H., Knibbs, L., Liu, Y., Martin, R., Morawska, L., Pope, C. A., III, Shin, H., Straif, K., Shaddick, G., Thomas, M., van Dingenen, R., van Donkelaar, A., Vos, T., Murray, C. J. L. and Forouzanfar, M. H.: Estimates and 25-year trends of the global burden of disease attributable to ambient air pollution: an analysis of data from the Global Burden of Diseases Study 2015, *The Lancet*, 389(10082), 1907–1918, doi:10.1016/S0140-6736(17)30505-6, 2017.
- Dentener, F., Keating, T., Akimoto, H., Pirrone, N., Dutchak, S., Zuber, A., Convention on Long-range Transboundary Air Pollution, United Nations and UNECE Task Force on Emission Inventories and Projections, Eds.: Hemispheric transport of air pollution 2010: prepared by the Task Force on Hemispheric Transport of Air Pollution acting within the framework of the Convention on Long-range Transboundary Air Pollution, United Nations, New York ; Geneva., 2010.
- van Donkelaar, A., Martin, R. V., Brauer, M., Hsu, N. C., Kahn, R. A., Levy, R. C., Lyapustin, A., Sayer, A. M. and Winker, D. M.: Global Estimates of Fine Particulate Matter using a Combined Geophysical-Statistical Method with Information from Satellites, Models, and Monitors, *Environ. Sci. Technol.*, 50(7), 3762–3772, doi:10.1021/acs.est.5b05833, 2016a.
- van Donkelaar, A., Martin, R. V., Brauer, M., Hsu, N. C., Kahn, R. A., Levy, R. C., Lyapustin, A., Sayer, A. M. and Winker, D. M.: Global Estimates of Fine Particulate Matter using a Combined Geophysical-Statistical Method with Information from Satellites, Models, and Monitors, *Environ. Sci. Technol.*, 50(7), 3762–3772, doi:10.1021/acs.est.5b05833, 2016b.
- Fang, Y., Naik, V., Horowitz, L. W. and Mauzerall, D. L.: Air pollution and associated human mortality: the role of air pollutant emissions, climate change and methane concentration increases from the preindustrial period to present, *Atmospheric Chem. Phys.*, 13(3), 1377–1394, doi:https://doi.org/10.5194/acp-13-1377-2013, 2013.
- Farina, S. C., Adams, P. J. and Pandis, S. N.: Modeling global secondary organic aerosol formation and processing with the volatility basis set: Implications for anthropogenic secondary organic aerosol, *J. Geophys. Res. Atmospheres*, 115(D9), doi:10.1029/2009JD013046, 2010.
- Fenech, S., Doherty, R. M., Heaviside, C., Vardoulakis, S., Macintyre, H. L. and O'Connor, F. M.: The influence of model spatial resolution on simulated ozone and fine particulate matter for Europe:

- implications for health impact assessments, *Atmospheric Chem. Phys.*, 18(8), 5765–5784, doi:10.5194/acp-18-5765-2018, 2018.
- Fiore, A. M., Jacob, D. J., Field, B. D., Streets, D. G., Fernandes, S. D. and Jang, C.: Linking ozone pollution and climate change: The case for controlling methane, *Geophys. Res. Lett.*, 29(19), 25–1, 2002.
- Fiore, A. M., West, J. J., Horowitz, L. W., Naik, V. and Schwarzkopf, M. D.: Characterizing the tropospheric ozone response to methane emission controls and the benefits to climate and air quality, *J. Geophys. Res. Atmospheres*, 113(8), doi:10.1029/2007JD009162, 2008.
- Fiore, A. M., Dentener, F. J., Wild, O., Cuvelier, C., Schultz, M. G., Hess, P., Textor, C., Schulz, M., Doherty, R. M., Horowitz, L. W., MacKenzie, I. A., Sanderson, M. G., Shindell, D. T., Stevenson, D. S., Szopa, S., Van Dingenen, R., Zeng, G., Atherton, C., Bergmann, D., Bey, I., Carmichael, G., Collins, W. J., Duncan, B. N., Faluvegi, G., Folberth, G., Gauss, M., Gong, S., Hauglustaine, D., Holloway, T., Isaksen, I. S. A., Jacob, D. J., Jonson, J. E., Kaminski, J. W., Keating, T. J., Lupu, A., Marmer, E., Montanaro, V., Park, R. J., Pitari, G., Pringle, K. J., Pyle, J. A., Schroeder, S., Vivanco, M. G., Wind, P., Wojcik, G., Wu, S. and Zuber, A.: Multimodel estimates of intercontinental source-receptor relationships for ozone pollution, *J. Geophys. Res. Atmospheres*, 114(D4), doi:10.1029/2008JD010816, 2009.
- Foley, K. M., Napelenok, S. L., Jang, C., Phillips, S., Hubbell, B. J. and Fulcher, C. M.: Two reduced form air quality modeling techniques for rapidly calculating pollutant mitigation potential across many sources, locations and precursor emission types, *Atmos. Environ.*, 98, 283–289, doi:10.1016/j.atmosenv.2014.08.046, 2014.
- Forouzanfar, M. H., Alexander, L., Anderson, H. R., Bachman, V. F., Biryukov, S., Brauer, M., Burnett, R., Casey, D., Coates, M. M., Cohen, A., Delwiche, K., Estep, K., Frostad, J. J., KC, A., Kyu, H. H., Moradi-Lakeh, M., Ng, M., Slepak, E. L., Thomas, B. A., Wagner, J., Aasvang, G. M., Abbafati, C., Ozgoren, A. A., Abd-Allah, F., Abera, S. F., Aboyans, V., Abraham, B., Abraham, J. P., Abubakar, I., Abu-Rmeileh, N. M. E., Aburto, T. C., Achoki, T., Adelekan, A., Adofo, K., Adou, A. K., Adsuar, J. C., Afshin, A., Agardh, E. E., Al Khabouri, M. J., Al Lami, F. H., Alam, S. S., Alasfoor, D., Albittar, M. I., Alegretti, M. A., Aleman, A. V., Alemu, Z. A., Alfonso-Cristancho, R., Alhabib, S., Ali, R., Ali, M. K., Alla, F., Allebeck, P., Allen, P. J., Alsharif, U., Alvarez, E., Alvis-Guzman, N., Amankwaa, A. A., Amare, A. T., Ameh, E. A., Ameli, O., Amini, H., Ammar, W., Anderson, B. O., Antonio, C. A. T., Anwari, P., Cunningham, S. A., Arnlöv, J., Arsenijevic, V. S. A., Artaman, A., Asghar, R. J., Assadi, R., Atkins, L. S., Atkinson, C., Avila, M. A., Awuah, B., Badawi, A., Bahit, M. C., Bakfalouni, T., Balakrishnan, K., Balalla, S., Balu, R. K., Banerjee, A., Barber, R. M., Barker-Collo, S. L., Barquera, S., Barregard, L., Barrero, L. H., Barrientos-Gutierrez, T., Basto-Abreu, A. C., Basu, A., Basu, S., Basulaiman, M. O., Rualcaba, C. B., Beardsley, J., Bedi, N., Bekele, T., Bell, M. L., Benjet, C., Bennett, D. A., et al.: Global, regional, and national comparative risk assessment of 79 behavioural, environmental and occupational, and metabolic risks or clusters of risks in 188 countries, 1990–2013: a systematic analysis for the Global Burden of Disease Study 2013, *The Lancet*, 386(10010), 2287–2323, doi:10.1016/S0140-6736(15)00128-2, 2015.
- Fry, M. M., Naik, V., West, J. J., Schwarzkopf, M. D., Fiore, A. M., Collins, W. J., Dentener, F. J., Shindell, D. T., Atherton, C., Bergmann, D., Duncan, B. N., Hess, P., MacKenzie, I. A., Marmer, E., Schultz, M. G., Szopa, S., Wild, O. and Zeng, G.: The influence of ozone precursor emissions from four world regions on tropospheric composition and radiative climate forcing, *J. Geophys. Res. Atmospheres*, 117(7), doi:10.1029/2011JD017134, 2012.
- Grewe, V., Dahlmann, K., Matthes, S. and Steinbrecht, W.: Attributing ozone to NO_x emissions: Implications for climate mitigation measures, *Atmos. Environ.*, 59, 102–107, doi:10.1016/j.atmosenv.2012.05.002, 2012.
- Hu, J., Wang, P., Ying, Q., Zhang, H., Chen, J., Ge, X., Li, X., Jiang, J., Wang, S., Zhang, J., Zhao, Y. and Zhang, Y.: Modeling biogenic and anthropogenic secondary organic aerosol in China, *Atmospheric Chem. Phys.*, 17(1), 77–92, doi:https://doi.org/10.5194/acp-17-77-2017, 2017.
- Huang, Y., Wu, S., Dubey, M. and French, N. H. F.: Impact of aging mechanism on model simulated carbonaceous aerosols, *Atmospheric Chem. Phys. Print*, 12, 10.5194/acpd-12-28993–2012, doi:10.5194/acpd-12-28993-2012, 2012.
- Huijnen, V., Williams, J., van Weele, M., van Noije, T., Krol, M., Dentener, F., Segers, A., Houweling, S., Peters, W., de Laat, J., Boersma, F., Bergamaschi, P., van Velthoven, P., Le Sager, P., Eskes, H., Alkemade, F., Scheele, R., Nédélec, P. and Pätz, H.-W.: The global chemistry transport model TM5: description and evaluation of the tropospheric chemistry version 3.0, *Geosci. Model Dev.*, 3(2), 445–473, doi:10.5194/gmd-3-445-2010, 2010.

- Jerrett, M., Burnett, R. T., Arden, P. I., Ito, K., Thurston, G., Krewski, D., Shi, Y., Calle, E. and Thun, M.: Long-term ozone exposure and mortality, *N. Engl. J. Med.*, 360(11), 1085–1095, doi:10.1056/NEJMoa0803894, 2009.
- Jin, X., Fiore, A. M., Murray, L. T., Valin, L. C., Lamsal, L. N., Duncan, B., Folkert, B., De, S., Abad, G. G., Chance, K. and Tonnesen, G. S.: Evaluating a Space-Based Indicator of Surface Ozone-NO_x-VOC Sensitivity Over Midlatitude Source Regions and Application to Decadal Trends, *J. Geophys. Res. Atmospheres*, 122(19), 10439–10461, doi:10.1002/2017JD026720, 2017.
- Kiesewetter, G., Borken-Kleefeld, J., Schöpp, W., Heyes, C., Thunis, P., Bessagnet, B., Terrenoire, E., Gsella, A. and Amann, M.: Modelling NO₂ concentrations at the street level in the GAINS integrated assessment model: projections under current legislation, *Atmospheric Chem. Phys.*, 14(2), 813–829, doi:https://doi.org/10.5194/acp-14-813-2014, 2014.
- Kiesewetter, G., Borken-Kleefeld, J., Schöpp, W., Heyes, C., Thunis, P., Bessagnet, B., Terrenoire, E., Fagerli, H., Nyiri, A. and Amann, M.: Modelling street level PM 10 concentrations across Europe: source apportionment and possible futures, *Atmospheric Chem. Phys.*, 15(3), 1539–1553, 2015.
- Kirschke, S., Bousquet, P., Ciais, P., Saunois, M., Canadell, J. G., Dlugokencky, E. J., Bergamaschi, P., Bergmann, D., Blake, D. R., Bruhwiler, L., Cameron-Smith, P., Castaldi, S., Chevallier, F., Feng, L., Fraser, A., Heimann, M., Hodson, E. L., Houweling, S., Josse, B., Fraser, P. J., Krummel, P. B., Lamarque, J.-F., Langenfelds, R. L., Le Quéré, C., Naik, V., O'Doherty, S., Palmer, P. I., Pison, I., Plummer, D., Poulter, B., Prinn, R. G., Rigby, M., Ringeval, B., Santini, M., Schmidt, M., Shindell, D. T., Simpson, I. J., Spahni, R., Steele, L. P., Strode, S. A., Sudo, K., Szopa, S., van der Werf, G. R., Voulgarakis, A., van Weele, M., Weiss, R. F., Williams, J. E. and Zeng, G.: Three decades of global methane sources and sinks, *Nat. Geosci.*, 6(10), 813–823, doi:10.1038/ngeo1955, 2013.
- Krewski, D., Jerrett, M., Burnett, R. T., Ma, R., Hughes, E. and Shi, Y.: Extended Follow-Up and Spatial Analysis of the American Cancer Society Study Linking Particulate Air Pollution and Mortality., Research Report, Health Effects Institute, Boston., 2009.
- Lamarque, J.-F., Shindell, D. T., Josse, B., Young, P. J., Cionni, I., Eyring, V., Bergmann, D., Cameron-Smith, P., Collins, W. J., Doherty, R., Dalsoren, S., Faluvegi, G., Folberth, G., Ghan, S. J., Horowitz, L. W., Lee, Y. H., MacKenzie, I. A., Nagashima, T., Naik, V., Plummer, D., Righi, M., Rumbold, S. T., Schulz, M., Skeie, R. B., Stevenson, D. S., Strode, S., Sudo, K., Szopa, S., Voulgarakis, A. and Zeng, G.: The Atmospheric Chemistry and Climate Model Intercomparison Project (ACCMIP): overview and description of models, simulations and climate diagnostics, *Geosci Model Dev*, 6(1), 179–206, doi:10.5194/gmd-6-179-2013, 2013.
- Lelieveld, J., Barlas, C., Giannadaki, D. and Pozzer, A.: Model calculated global, regional and megacity premature mortality due to air pollution, *Atmospheric Chem. Phys.*, 13(14), 7023–7037, doi:https://doi.org/10.5194/acp-13-7023-2013, 2013.
- Li, J., Yang, W., Wang, Z., Chen, H., Hu, B., Li, J., Sun, Y. and Huang, Y.: A modeling study of source–receptor relationships in atmospheric particulate matter over Northeast Asia, *Atmos. Environ.*, 91, 40–51, doi:10.1016/j.atmosenv.2014.03.027, 2014.
- Li, Q., Jacob, D. J., Bey, I., Palmer, P. I., Duncan, B. N., Field, B. D., Martin, R. V., Fiore, A. M., Yantosca, R. M., Parrish, D. D., Simmonds, P. G. and Oltmans, S. J.: Transatlantic transport of pollution and its effects on surface ozone in Europe and North America, *J. Geophys. Res. Atmospheres*, 107(D13), ACH 4-1-ACH 4-21, doi:10.1029/2001JD001422, 2002.
- Li, Y., Henze, D. K., Jack, D. and Kinney, P. L.: The influence of air quality model resolution on health impact assessment for fine particulate matter and its components, *Air Qual. Atmosphere Health*, 9(1), 51–68, doi:10.1007/s11869-015-0321-z, 2016.
- Lim, S. S., Vos, T., Flaxman, A. D., Danaei, G., Shibuya, K., Adair-Rohani, H., Amann, M., Anderson, H. R., Andrews, K. G., Aryee, M., Atkinson, C., Bacchus, L. J., Bahalim, A. N., Balakrishnan, K., Balmes, J., Barker-Collo, S., Baxter, A., Bell, M. L., Blore, J. D., Blyth, F., Bonner, C., Borges, G., Bourne, R., Boussinesq, M., Brauer, M., Brooks, P., Bruce, N. G., Brunekreef, B., Bryan-Hancock, C., Bucello, C., Buchbinder, R., Bull, F., Burnett, R. T., Byers, T. E., Calabria, B., Carapetis, J., Carnahan, E., Chafe, Z., Charlson, F., Chen, H., Chen, J. S., Cheng, A. T.-A., Child, J. C., Cohen, A., Colson, K. E., Cowie, B. C., Darby, S., Darling, S., Davis, A., Degenhardt, L., Dentener, F., Des Jarlais, D. C., Devries, K., Dherani, M., Ding, E. L., Dorsey, E. R., Driscoll, T., Edmond, K., Ali, S. E., Engell, R. E., Erwin, P. J., Fahimi, S., Falder, G., Farzadfar, F., Ferrari, A., Finucane, M. M., Flaxman, S., Fowkes, F. G. R., Freedman, G., Freeman, M. K., Gakidou, E., Ghosh, S., Giovannucci, E., Gmel, G., Graham, K., Grainger, R., Grant, B., Gunnell, D., Gutierrez, H. R., Hall, W., Hoek, H. W., Hogan, A., Hosgood III, H. D., Hoy, D., Hu, H., Hubbell, B. J., Hutchings, S. J., Ibeanusi, S. E., Jacklyn, G. L., Jarasaria, R.,

- Jonas, J. B., Kan, H., Kanis, J. A., Kassebaum, N., Kawakami, N., Khang, Y.-H., Khatibzadeh, S., Khoo, J.-P., Kok, C., et al.: A comparative risk assessment of burden of disease and injury attributable to 67 risk factors and risk factor clusters in 21 regions, 1990-2010: A systematic analysis for the Global Burden of Disease Study 2010, *The Lancet*, 380(9859), 2224–2260, doi:10.1016/S0140-6736(12)61766-8, 2012.
- Liu, X., Penner, J. E., Das, B., Bergmann, D., Rodriguez, J. M., Strahan, S., Wang, M. and Feng, Y.: Uncertainties in global aerosol simulations: Assessment using three meteorological data sets, *J. Geophys. Res.*, 112(D11), doi:10.1029/2006JD008216, 2007.
- Liu, Y., Hong, Y., Fan, Q., Wang, X., Chan, P., Chen, X., Lai, A., Wang, M. and Chen, X.: Source-receptor relationships for PM_{2.5} during typical pollution episodes in the Pearl River Delta city cluster, China, *Sci. Total Environ.*, 596–597, 194–206, doi:10.1016/j.scitotenv.2017.03.255, 2017.
- Maione, M., Fowler, D., Monks, P. S., Reis, S., Rudich, Y., Williams, M. L. and Fuzzi, S.: Air quality and climate change: Designing new win-win policies for Europe, *Environ. Sci. Policy*, 65, 48–57, doi:10.1016/j.envsci.2016.03.011, 2016.
- Ming, Y. and Russell, L. M.: Predicted hygroscopic growth of sea salt aerosol, *J. Geophys. Res. Atmospheres*, 106(D22), 28259–28274, 2001.
- Myhre, G., Fuglestad, J. S., Berntsen, T. K. and Lund, M. T.: Mitigation of short-lived heating components may lead to unwanted long-term consequences, *Atmos. Environ.*, 45(33), 6103–6106, doi:10.1016/j.atmosenv.2011.08.009, 2011.
- Pausata, F. S. R., Pozzoli, L., Dingenen, R. V., Vignati, E., Cavalli, F. and Dentener, F. J.: Impacts of changes in North Atlantic atmospheric circulation on particulate matter and human health in Europe, *Geophys. Res. Lett.*, 40(15), 4074–4080, doi:10.1002/grl.50720, 2013.
- Pope, R. J., Chipperfield, M. P., Arnold, S. R., Glatthor, N., Feng, W., Dhomse, S. S., Kerridge, B. J., Latter, B. G. and Siddans, R.: Influence of the wintertime North Atlantic Oscillation on European tropospheric composition: an observational and modelling study, *Atmospheric Chem. Phys.*, 18(11), 8389–8408, doi:10.5194/acp-18-8389-2018, 2018.
- Porter, P. S., Rao, S. T., Hogrefe, C. and Mathur, R.: A reduced form model for ozone based on two decades of CMAQ simulations for the continental United States, *Atmospheric Pollut. Res.*, 8(2), 275–284, doi:10.1016/j.apr.2016.09.005, 2017.
- Prather, M., Ehhalt, D., Dentener, F., Derwent, R., Dlugokencky, E., Holland, E., Isaksen, I., Katima, J., Kirchhoff, V., Matson, P., Midgley, P., Wang, M., Berntsen, T., Bey, I., Brasseur, G., Buja, L., Pitari, G. and Et, A.: Chapter 4: Atmospheric Chemistry and Greenhouse Gases, Cambridge University Press. [online] Available from: <https://ricerca.univaq.it/handle/11697/24359#.WItxbn0XGao> (Accessed 27 January 2017), 2001.
- Punger, E. M. and West, J. J.: The effect of grid resolution on estimates of the burden of ozone and fine particulate matter on premature mortality in the United States, *Air Qual. Atmosphere Health*, 6(3), doi:10.1007/s11869-013-0197-8, 2013.
- Shindell, D., Kuylenstierna, J., Vignati, E., van Dingenen, R., Amann, M., Klimont, Z., Anenberg, S., Muller, N., Janssens-Maenhout, G., Raes, F., Schwartz, J., Faluvegi, G., Pozzoli, L., Kupiainen, K., Hoglund-Isaksson, L., Emberson, L., Streets, D., Ramanathan, V., Hicks, K., Oanh, N., Milly, G., Williams, M., Demkine, V. and Fowler, D.: Simultaneously Mitigating Near-Term Climate Change and Improving Human Health and Food Security, *Science*, 335(6065), 183–189, doi:10.1126/science.1210026, 2012.
- Shindell, D. T., Faluvegi, G., Bell, N. and Schmidt, G. A.: An emissions-based view of climate forcing by methane and tropospheric ozone: EMISSIONS-BASED CLIMATE FORCING, *Geophys. Res. Lett.*, 32(4), n/a-n/a, doi:10.1029/2004GL021900, 2005.
- Shindell, D. T., Faluvegi, G., Koch, D. M., Schmidt, G. A., Unger, N. and Bauer, S. E.: Improved Attribution of Climate Forcing to Emissions, *Science*, 326(5953), 716–718, doi:10.1126/science.1174760, 2009.
- Silva, R. A., West, J. J., Zhang, Y., Anenberg, S. C., Lamarque, J.-F., Shindell, D. T., Collins, W. J., Dalsoren, S., Faluvegi, G., Folberth, G., Horowitz, L. W., Tatsuya Nagashima, Naik, V., Rumbold, S., Skeie, R., Sudo, K., Takemura, T., Daniel Bergmann, Cameron-Smith, P., Cionni, I., Doherty, R. M., Eyring, V., Josse, B., MacKenzie, I. A., Plummer, D., Righi, M., Stevenson, D. S., Strode, S., Szopa, S. and Zeng, G.: Global premature mortality due to anthropogenic outdoor air pollution and the contribution of past climate change, *Environ. Res. Lett.*, 8(3), 034005, doi:10.1088/1748-9326/8/3/034005, 2013.
- Silva, R. A., West, J. J., Lamarque, J. F., Shindell, D. T., Collins, W. J., Dalsoren, S., Faluvegi, G., Folberth, G., Horowitz, L. W., Nagashima, T., Naik, V., Rumbold, S. T., Sudo, K., Takemura, T., Bergmann, D., Cameron-Smith, P., Cionni, I., Doherty, R. M., Eyring, V., Josse, B., MacKenzie, I. A., Plummer, D.,

- Righi, M., Stevenson, D. S., Strode, S., Szopa, S. and Zengast, G.: The effect of future ambient air pollution on human premature mortality to 2100 using output from the ACCMIP model ensemble, *Atmospheric Chem. Phys.*, 16(15), 9847–9862, doi:10.5194/acp-16-9847-2016, 2016.
- Stevenson, D. S., Young, P. J., Naik, V., Lamarque, J.-F., Shindell, D. T., Voulgarakis, A., Skeie, R. B., Dalsoren, S. B., Myhre, G., Berntsen, T. K., Folberth, G. A., Rumbold, S. T., Collins, W. J., MacKenzie, I. A., Doherty, R. M., Zeng, G., Van, N., Strunk, A., Bergmann, D., Cameron-Smith, P., Plummer, D. A., Strode, S. A., Horowitz, L., Lee, Y. H., Szopa, S., Sudo, K., Nagashima, T., Josse, B., Cionni, I., Righi, M., Eyring, V., Conley, A., Bowman, K. W., Wild, O. and Archibald, A.: Tropospheric ozone changes, radiative forcing and attribution to emissions in the Atmospheric Chemistry and Climate Model Intercomparison Project (ACCMIP), *Atmospheric Chem. Phys.*, 13(6), 3063–3085, doi:10.5194/acp-13-3063-2013, 2013.
- Stier, P., Feichter, J., Kinne, S., Kloster, S., Vignati, E., Wilson, J., Ganzeveld, L., Tegen, I., Werner, M., Balkanski, Y., Schulz, M., Boucher, O., Minikin, A. and Petzold, A.: The aerosol-climate model ECHAM5-HAM, *Atmospheric Chem. Phys.*, 5(4), 1125–1156, doi:https://doi.org/10.5194/acp-5-1125-2005, 2005.
- Stjern, C. W., Samset, B. H., Myhre, G., Bian, H., Chin, M., Davila, Y., Dentener, F., Emmons, L., Flemming, J., Haslerud, A. S., Henze, D., Jonson, J. E., Kucsera, T., Lund, M. T., Schulz, M., Sudo, K., Takemura, T. and Tilmes, S.: Global and regional radiative forcing from 20 % reductions in BC, OC and SO₄ - An HTAP2 multi-model study, *Atmospheric Chem. Phys.*, 16(21), 13579–13599, doi:10.5194/acp-16-13579-2016, 2016.
- Tang, I. N.: Chemical and size effects of hygroscopic aerosols on light scattering coefficients, *J. Geophys. Res. Atmospheres*, 101(14), 19245–19250, 1996.
- Turnock, S., Wild, O., Dentener, F., Davila, Y., Emmons, L., Flemming, J., Folberth, G., Henze, D., Jonson, J., Keating, T., Kengo, S., Lin, M., Lund, M., Tilmes, S. and O'Connor, F.: The Impact of Future Emission Policies on Tropospheric Ozone using a Parameterised Approach, *Atmospheric Chem. Phys. Discuss.*, 1–41, doi:https://doi.org/10.5194/acp-2017-1220, 2018.
- Van Dingenen, R., Dentener, F. J., Raes, F., Krol, M. C., Emberson, L. and Cofala, J.: The global impact of ozone on agricultural crop yields under current and future air quality legislation, *Atmos. Environ.*, 43(3), 604–618, doi:10.1016/j.atmosenv.2008.10.033, 2009.
- West, J. J., Fiore, A. M., Naik, V., Horowitz, L. W., Schwarzkopf, M. D. and Mauzerall, D. L.: Ozone air quality and radiative forcing consequences of changes in ozone precursor emissions, *Geophys. Res. Lett.*, 34(6), doi:10.1029/2006GL029173, 2007.
- Wild, O. and Prather, M. J.: Excitation of the primary tropospheric chemical mode in a global three-dimensional model, *J. Geophys. Res. Atmospheres*, 105(D20), 24647–24660, 2000.
- Wild, O., Fiore, A. M., Shindell, D. T., Doherty, R. M., Collins, W. J., Dentener, F. J., Schultz, M. G., Gong, S., MacKenzie, I. A., Zeng, G. and others: Modelling future changes in surface ozone: a parameterized approach, *Atmospheric Chem. Phys.*, 12(4), 2037–2054, 2012.
- Wu, S., Duncan, B. N., Jacob, D. J., Fiore, A. M. and Wild, O.: Chemical nonlinearities in relating intercontinental ozone pollution to anthropogenic emissions, *Geophys. Res. Lett.*, 36(5), doi:10.1029/2008GL036607, 2009.
- Yu, H., Chin, M., West, J. J., Atherton, C. S., Bellouin, N., Bergmann, D., Bey, I., Bian, H., Diehl, T., Forberth, G., Hess, P., Schulz, M., Shindell, D., Takemura, T. and Tan, Q.: A multimodel assessment of the influence of regional anthropogenic emission reductions on aerosol direct radiative forcing and the role of intercontinental transport, *J. Geophys. Res. Atmospheres*, 118(2), 700–720, doi:10.1029/2012JD018148, 2013.
- Zhang, L., Liu, L., Zhao, Y., Gong, S., Zhang, X., Henze, D. K., Capps, S. L., Fu, T.-M., Zhang, Q. and Wang, Y.: Source attribution of particulate matter pollution over North China with the adjoint method, *Environ. Res. Lett.*, 10(8), 084011, 2015.

TM5-FASST: a global atmospheric source-receptor model for rapid impact analysis of emission changes on air quality and short-lived climate pollutants

5 Rita Van Dingenen¹, Frank Dentener¹, Monica Crippa¹, Joana Leitao^{1,2}, Elina Marmer^{1,3}, Shilpa Rao⁴,
Efisio Solazzo¹, Luana Valentini⁵

¹ European Commission, Joint Research Centre (JRC), Ispra (VA), Italy

² Now at IASS – Institute for Advanced Sustainability Studies, Potsdam, Germany

³ Now at University of Hamburg, Germany

⁴ Norwegian Institute for Public Health, PO Box 4404 Nydalen, N-0403 Oslo, Norway,

10 ⁵ GFT Italia S.r.l., Via Sile, 18 20139 Milan, Italy

Correspondence to: Rita Van Dingenen (rita.van-dingenen@ec.europa.eu)

Abstract This paper describes, documents and validates the TM5-Fast Scenario Screening Tool (TM5-FASST), a global reduced-form air quality source-receptor model that has been designed to compute ambient pollutant concentrations as well as a broad range of pollutant-related impacts on human health, agricultural crop production, and short-lived pollutant climate metrics, taking as input annual pollutant emission data aggregated at the national or regional level. The TM5-FASST tool, providing a trade-off between accuracy and applicability, is based on linearized emission-concentration sensitivities derived with the full chemistry-transport model TM5. The tool has been extensively applied in various recent critical studies. Although informal and fragmented validation has already been performed in various publications, this paper provides a comprehensive documentation of all components of the model and a validation against the full TM5 model. We find that the simplifications introduced in order to generate immediate results from emission scenarios do not compromise the validity of the output and as such TM5-FASST is proven to be a useful tool in science-policy analysis. Furthermore, it constitutes a suitable architecture for implementing the ensemble of source-receptor relations obtained in the frame of the HTAP modelling exercises, thus creating a link between the scientific community and policy-oriented users.

Deleted: , related to

Deleted: are

Deleted: compromising

1 Introduction

A host of policies influence the emissions to air. In principle any policy that influences the economy and use of resources will also impact emissions into the atmosphere. Specific air pollution policies aim to mitigate the negative environmental impacts of anthropogenic activities, some of which may be affected by other policies, like climate mitigation actions, transport modal shifts or agricultural policies. Further, air quality policies may impact outside their typical environmental target domains (human and ecosystem health, vegetation and building damage,...) for instance through the role played by short-lived pollutants in the Earth's radiation balance (Myhre et al., 2011; Shindell et al., 2009). Insight into the impacts of policies in a multi-disciplinary framework through a holistic approach could contribute to a more efficient and cost-effective implementation of control measures (e.g. Amann et al., 2011; Maione et al., 2016; Shindell et al., 2012).

Several global chemical transport models are available for the evaluation of air pollutants levels from emissions, sometimes in combination with off-line computed climate relevant metrics such as optical depth or instantaneous radiative forcing (e.g. Lamarque et al., 2013; Stevenson et al., 2013). These models provide detailed output, but are demanding in terms of computational and human resources for preparing input, running the model, and analyzing output. Further they often lack flexibility to evaluate ad-hoc a series of scenarios, or perform swift what-if analysis of policy options. Therefore there is a need for computationally-efficient methods and tools that provide an integrated environmental assessment of air quality and climate policies, which have a global dimension with sufficient regional detail, and evaluate different impact categories in an internally consistent way. Reduced-form source-receptor models are a useful concept in this context. They are typically constructed from pre-computed emission-concentration transfer matrices between pollutant source regions and receptor regions. These matrices emulate underlying meteorological and chemical atmospheric processes for a pre-defined set of

Deleted: Increasingly,

5 meteorological and emission data, and have the advantage that concentration responses to emission changes are obtained by a simple matrix multiplication, avoiding expensive numerical computations. Reduced-form source-receptor models (SRM) are increasingly being used, not only to compute atmospheric concentrations (and related impacts) from changes in emissions, but they have also proven to be very useful in cost optimization and cost-benefit analysis because of their low computational cost (Amann et al., 2011). Further, because of the detailed budget information embedded in the source-receptor matrices, they are applied for apportionment studies, as a complementary approach to other techniques such as adjoint models (e.g. Zhang et al., 2015) and chemical tagging (e.g. Grewe et al., 2012).

10 Although the computational efficiency of SRMs comes at a cost of accuracy, regional detail and flexibility in spatial arrangement of emissions, they have been successfully applied in regional studies (Foley et al., 2014; Li et al., 2014; Liu et al., 2017; Porter et al., 2017) and have demonstrated their key role in policy development (Amann et al., 2011).

15 An extensive collaborative global chemistry modelling effort evaluated local and long-range pollutant responses to emission reductions in 4 world regions in the first phase of HTAP (Dentener et al., 2010; Fiore et al., 2009), hereafter referred to as HTAP1. The resulting ensemble source-receptor relations between those regions have been used to evaluate the driving factors behind regional ozone changes in 5 world regions (Wild et al., 2012). Similarly, Yu et al. (2013) evaluated aerosol radiative forcing (RF) from HTAP1 results, whereas Fry et al. (2012) assessed the RF effects by ozone. Several papers in this special issue (e.g. Stjern et al., 2016) are devoted to advance the HTAP analysis with new models and methodologies.

20 One of the participating global models in the HTAP1 assessment was the 2-way nested global chemical transport model TM5, applied with 1°x1° resolution over the continents (Krol et al., 2005). In order to address the need for swift scenario analysis, we used TM5 to develop a reduced-form global source-receptor (SR) model, with the capability to assess in a single framework a broad portfolio of short-lived pollutants environmental impacts at the global scale, including their interaction with climate, impact on human health, on vegetation and on ecosystems. The reduced-form version was named “TM5-Fast Scenario Screening Tool” (TM5-FASST). The TM5-FASST approach refines and extends the one developed in the HTAP1 assessment by defining source-receptor regions at a finer resolution and by implementing a direct emission-based calculation of pollutant concentrations and their impacts. To our knowledge such a comprehensive global source-receptor model for a variety of components and impacts (primary and secondary particulate matter, trace gases, wet and dry deposition, climate and health metrics) is at this moment not available for fast impact assessments. The need for models like TM5-FASST is demonstrated by its extensive application in various critical studies (OECD, 2016; Rao et al., 2016; The World Bank, The International Cryosphere Climate Initiative, 2013; UNEP, 2011). An overview of earlier studies with TM5-FASST, in which fragmented and informal validation has already been performed, is given in section S1 of the Supplemental Information (SI).

30 The tool is undergoing continuous developments and updates regarding metrics and impact evaluations. Hereafter we will refer to the native chemical transport model and the derived SR model as TM5 and TM5-FASST_v0 (or its shortcuts TM5-

Deleted: . Source-receptor model studies are available on a regional scale (e.g. GAINS EUROPE, based on the EMEP chemistry-transport model , GAINS-ASIA, based on the TM5 chemistry-transport model and have been

Deleted: while

Deleted: .

Deleted: which addresses the issues above, opting for a trade-off between accuracy and speed.

FASST and FASST) respectively, with version number v0 referring to the features and methodologies described in this paper and as applied in the earlier assessments. The present paper is a comprehensive documentation of the model and its validation against TM5, to ensure credibility and future applications.

In section 2, we describe the methods implemented in TM5-FASST to evaluate in a single framework a broad portfolio of short-lived air pollutants (including CH₄) and their environmental impacts, such as interaction with climate, impact on human health, on natural vegetation and crops. Section 3 focuses on how the derived reduced-form TM5-FASST replicates the full native TM5 model in terms of linearity, additivity and application to a realistic set of future scenarios. We also evaluate the performance of TM5-FASST against some case studies from the literature. We finish with a discussion (section 4) of the limitations of the methodology, future development paths and possible ways forward for the best-use of such modelling systems for future policy assessments.

2 Methods

2.1 The native TM5 model.

The Tracer Model version 5 (TM5) is a 3-dimensional global atmospheric chemical transport model that simulates the transport, chemical processes, as well as wet and dry deposition of chemically active atmospheric trace gases (e.g. ozone (O₃), SO₂, NO_x, VOCs, NH₃), and particulate matter components, including SO₄²⁻, NO₃⁻, NH₄⁺, primary PM_{2.5} and its components black carbon, organic carbon, sea salt, and mineral dust. Biogenic secondary organic aerosol (BSOA) was included following the AEROCOM recommendation (Dentener et al., 2006a; Kanakidou et al., 2005) which parameterized BSOA formation from natural VOC emissions as a fixed fraction of the primary emissions. The relative fraction compared to the anthropogenic POM emissions varies spatially, with a higher contribution in regions where the emissions of terpene emissions are higher. SOA from anthropogenic emission was not explicitly included in the current simulations.

Model version TM5-JRC-cy2-ipc (abbreviated TM5) was used to compute the source receptor relationships as first described by Krol et al. (2005). This model version was used in the PhotoComp scenario studies (e.g. Dentener et al., 2006b; Stevenson et al., 2006) and in the HTAP1 multi-model source receptor assessment (e.g. Anenberg et al., 2009; Fiore et al., 2009; Wild et al., 2012). TM5 results used in the present study allow comparison with a range of other global model results in HTAP1, but ignore subsequent updates and improvements in TM5 as for instance described in Huijnen et al. (2010), which we consider not critical for this study. The most recent TM5 model does no longer consider zoom regions, but recoded the model into a Massive Parallel framework, enabling efficient execution on modern computers. While global horizontal resolution (1°x1°) is similar to the resolution of the most refined zoom region in TM5, vertical resolution was increased. Further, the model also uses vertical mass fluxes from the parent ECMWF meteorological model, not available at

Deleted: discussing

Deleted: Indeed, like the development of TM5-FASST was building on and extending the HTAP1 experiments in a single model context, the regional definitions and sector definitions used in HTAP2 were largely synchronized with the TM5-FASST set-up, increasing the community's capacity for multi-model assessments of hemispheric pollution. It is intended that the lessons-learned are informing the HTAP2 exercise.

Deleted: ,

Deleted: ,

Moved (insertion) [1]

Deleted: TM5

Deleted: TM5-JRC-cy2-ipc (abbreviated TM5)

the time of development of TM5-cy2-ipcc, which could lead to somewhat different mixing characteristics. The gas phase chemical module has been updated to a modified version of CMB5.

The TM5 model operates with offline meteorology from the European Centre for Medium range Weather Forecasts (ECMWF; 6 hours IFS forecast). These data are stored at a 6-hourly horizontal resolution of $1^\circ \times 1^\circ$ for large-scale 3D fields, and 3-hourly resolution for parameters describing exchange processes at the surface. Of the 60 vertical layers in the operational (OD) ECMWF model (status ca. 2008), a subset of 25 layers is used within TM5, including 5 in the boundary layer, 10 in the free troposphere, and 10 stratospheric layers. Although for most health and ecosystem impacts only the surface level fields are required, climate metrics (e.g. radiative forcing) require the full vertical column and profile information. Therefore base simulation and perturbed pollutant concentrations were calculated and stored for the 25 vertical levels of the model as monthly means, and some air quality-relevant parameters as hourly or daily fields. Meteorological fields are obtained from the ECMWF operational forecast representative for the year 2001. The implications of using a single meteorological year will be discussed in section 4.2.

TM5 utilizes a so-called two-way nested approach, which introduces refinements in both space and time in predefined regions. The nesting comprises a regional high resolution 'zoom' ($1^\circ \times 1^\circ$) within relatively coarse global resolution ($6^\circ \times 4^\circ$), and a transitional grid of $3^\circ \times 2^\circ$, as illustrated in Fig. S2.1 of the SI. A pre-processing software aggregated the 3D $1^\circ \times 1^\circ$ meteorological fields into the abovementioned coarser resolutions in a fully mass-conserving way. TM5 has a flexible choice of regional extent and amount of zoom regions. For instance, the HTAP1 simulation setup utilized a set of 4 simultaneous $1^\circ \times 1^\circ$ zooms nested over Europe, North America, South and East Asia. Since hundreds of simulations are needed to drive the TM5-FASST Source-Receptor model, due to computational constraints, it was decided to use single zoom regions, covering the countries and regions for which emission perturbation studies were carried out. For example, the European zoom would contain all European countries, the East Asian zoom region countries like China and Korea, etc. An overview of zoom regions and their regional extent is given in SI section S2. Post-processing software merged the outputs of base and sensitivity simulations into uniform $1^\circ \times 1^\circ$ fields.

We note that at the time of development of the 'zoom' model, the TM5 specific model set-up allowed to perform photochemistry and aerosol calculations with a relatively high $1^\circ \times 1^\circ$ resolution in the source regions, whereas other global models were operating at much coarser resolutions (typically $2.8^\circ \times 2.8^\circ$). With the introduction of massive parallel computing, however, this comparative advantage is now slowly disappearing, and global model resolutions of $1^\circ \times 1^\circ$ or finer are now becoming more common (see the model descriptions in this special issue, e.g. Liang et al., 2018). The model grid resolution influences the predicted pollutant concentrations as well as the estimated population exposure, especially near urban areas where strong gradients occur in population density and pollutant levels, which cannot be resolved by the $1^\circ \times 1^\circ$ resolution. In section 2.4 we describe a methodology to improve population $PM_{2.5}$ exposure estimates by applying sub-grid concentration adjustments based on high-resolution ancillary data. The bias introduced by model resolution affects as well

Deleted: pollutants

Deleted: The

Deleted: °.

Deleted: Some numerical inconsistencies of this merging procedure did occur, but were evaluated to be generally small and occurring over ocean regions, or regions with low population density.

Deleted: this

Deleted: while

Deleted: of

Deleted: T42 (

Deleted: resolution of $1^\circ \times 1^\circ$ or finer are now becoming more common (see model descriptions in this special issue). More details on TM5, together an overview of earlier validation efforts is provided in Section S2 of the SI

computed SR matrices, e.g. off-setting the share of ‘local’ versus ‘imported’ pollution in a given receptor region. We will discuss this aspect more in detail in section 4.3.

More details on the TM5 model, together with an overview of earlier validation efforts is provided in Section S2 of the SI.

2.2 Base emissions

5 As base simulation emissions we use the community generated representative concentration pathways (RCP) pollutant emissions for the year 2000 at 1°x1° resolution, prepared for IPCC 5th Assessment (Lamarque et al., 2010). Relevant emitted anthropogenic pollutants include SO₂, NO_x, NH₃, black carbon (BC), organic carbon (OC), NMVOC, CO and CH₄. (Semi-) natural emissions (sea-salt, mineral dust, volcanoes, lightning, vegetation, biomass burning, and terrestrial and oceanic DMS) for the base simulations were included following the recommendations for the AEROCOM study (Dentener et al., 10 2006a) but they are not affected in the perturbation simulations where we consider only perturbations of anthropogenic emissions.

2.3 Air pollutants source-receptor relations

In general, air quality source-receptor models (AQ-SRM) link emissions of pollutants in a given source region with downwind concentrations and related impacts, implicitly including the underlying effects of meteorology and atmospheric chemical and physical processes. The source region is any point or area from which emissions are considered; the receptor is 15 any point or area at which the pollutant concentration and impact is to be evaluated. Primary pollutants concentrations are primarily affected by dry and wet removal from the atmosphere (e.g. elemental carbon, seasalt and mineral dust) after being emitted. Secondary pollutants are formed from reactions of primary emissions, e.g. NO₂ forms nitrate aerosol but also leads to the formation of O₃; emitted SO₂ is transformed into sulfate aerosols.

20 A change of pollutant emissions has the potential to change the chemical formation of other secondary species, e.g. NO₂ affects the oxidative capacity of the atmosphere and therefore influences the lifetime of methane. In summary, a specific secondary component and related impact can be influenced from one or more emitted precursors, and an emitted precursor can change the impact from one or more pollutants. An AQ-SRM will need to include a functional relationship between each precursor and each relevant pollutant or pollutant metric, for each source region and each receptor region.

25 TM5-FASST_v0 has been designed as a reduced-form SRM: the relation between the emissions of compound i from source x and resulting concentration (or burden) of pollutant j at receptor y is expressed by a simple functional relation that mimics the underlying meteorological and chemical processes. In the current version v0 of TM5-FASST the emission-concentration relationship is locally approximated by a linear function expressing the change in pollutant concentration in the receptor region upon a change in precursor emissions in the source region with the generic form $dC_y = SRC \times dE_x$ where dC_y equals 30 the change in the pollutant concentration compared to a reference concentration in receptor region y , dE_x is the change in precursor emission compared to a reference emission in source region x , and SRC the source-receptor coefficient for the specific compound and source-receptor pair – in this case emulating atmospheric processes linked to the meteorology in

Deleted: do not undergo chemical transformation during their atmospheric lifetime and

Deleted: only

Deleted:).

Deleted: parameters

Deleted: (where $j = i$ in case of a primary component)

Deleted: function

Deleted: relation

Deleted: .

2001. The source-receptor coefficients are implemented as matrices with dimension $[n_x, n_y]$ with n_x and n_y the number of source and receptor regions respectively. A single SR matrix is available for each precursor and for each resulting component from that precursor. Table 1 gives an overview of all precursor – pollutant links that have been included.

For TM5-FASST_v0 we defined 56 source regions, as shown in Fig. 1. A detailed break-down of regions by country is given in Section S2 of the SI. The choice of regions has been made to obtain an optimal match with integrated assessment models such as IMAGE (Eickhout et al., 2004; van Vuuren et al., 2007), MESSAGE (Riahi et al., 2007), GAINS (Höglund-Isaksson and Mechler, 2005) as well as the POLES model (Russ et al., 2007; Van Aardenne et al., 2007). Most European countries are defined as individual source regions, except for the smallest countries, which have been aggregated. In the current version v0, the USA, China and India are treated as a single emission regions each, i.e. without break-down in states or provinces. Although most integrated assessment models cover Africa, South America, Russia and South-East Asia as a single socio-economic entity, it was decided to sub-divide these regions, to account for climatological difference in these vast continents. Apart from the 56 regions, source-receptor coefficients were calculated between global international shipping and aviation as sources, and the global grid as receptor, resulting in $n_x = 58$ source functions.

The SR matrices, describing the concentration response in each receptor upon a change in emissions in each source region, have been derived from a set of simulations with the full chemical transport model TM5 by applying -20% emission perturbations for each of the 56 defined source regions (plus shipping and aviation), for all relevant anthropogenic precursor components, in comparison to a set of unperturbed simulations, hereafter denoted as 'base simulations'. Emissions from biogenic organic components were included as a spatial/temporally varying component, but did not vary in the model sensitivity simulations. Consequently, absolute concentrations of BSOA were identical across base and perturbation simulations and no SR coefficients are available.

A 15 to 20% emission perturbation is commonly used to establish source-receptor emission-concentration sensitivities (Alcamo et al., 1990; Amann et al., 2011; Dentener et al., 2010). The applicability of the established SRs for larger emission perturbations - e.g. in future emission scenario studies - depends on the linearity of the emission-concentration responses, and will be evaluated in detail in section 3.

As elucidated in the previous section, base and perturbed simulations are available on a $1^\circ \times 1^\circ$ global resolution. Figures S3.1 and S3.2 in the SI shows some examples of emission perturbation - concentration response grid maps for $PM_{2.5}$, O_3 metrics, deposition and column burden for source regions China, India and USA, illustrating clearly the difference in long-range transport characteristics between different species.

For each receptor point y (i.e. each model vertical level $1^\circ \times 1^\circ$ grid cell), the change in concentration of component j in receptor y resulting from a -20% perturbation of emitted precursor i in source region x , is expressed by a unique SR coefficient $A_{ij}[x, y]$:

$$A_{ij}[x, y] = \frac{\Delta C_j(y)}{\Delta E_i(x)} \text{ with } \Delta E_i(x) = 0.2 E_{i,base}(x) \quad (1)$$

Deleted: A

Deleted: of -

Deleted: consistent with the approach in HTAP1. It is small enough to evaluate

Deleted: under present day conditions, while still allowing an extrapolation to

Deleted: changes in scenarios of the future.

Deleted: SR

Deleted: i

Deleted: j

In the present version TM5-FASST_v0, the SR coefficients for pollutant concentrations are stored as annual mean responses to annual emission changes. Individual PM_{2.5} components SRs are stored as dry mass (μg m⁻³). PM_{2.5} residual water at 35% is optionally calculated a posteriori for sensitivity studies, assuming mass growth factors for ammonium salts of 1.27 (Tang, 1996) and for sea-salt of 1.15 (Ming and Russell, 2001). The presence of residual water in PM_{2.5} is not irrelevant: epidemiological studies establishing PM_{2.5} exposure-response functions are commonly based on monitoring data of gravimetrically determined PM_{2.5}, for which measurement protocols foresee filter conditioning at 30 – 50% RH. As many health impact modelling studies consider dry PM_{2.5} mass or do not provide information on the inclusion of residual water we use dry PM_{2.5} for health impact assessment in this study for consistency, unless mentioned differently.

We also established SR matrices linking annual emissions to specific O₃ exposure metrics that are based on seasonal or hourly O₃ concentrations (e.g. crop exposure metrics based on daytime ozone during crop growing season, human exposure to O₃ during highest 6 monthly mean of hourly maximum values). The total concentration of component (or metric) j in receptor region y , resulting from arbitrary emissions of all n_i precursors i at all n_x source regions x , is obtained as a perturbation on the base-simulation concentration, by summing up all the respective SR coefficients scaled with the actual emission perturbation:

$$C_j(y) = C_{j,base}(y) + \sum_{k=1}^{n_x} \sum_{i=1}^{n_i} A_{ij}[x_k, y] \cdot [E_i(x_k) - E_{i,base}(x_k)] \quad (2)$$

Pollutants C_j include particulate matter components (SO₄, NO₃, NH₄, BC, particulate organic matter – POM), trace gases (SO₂, NO, NO₂, NH₃, O₃), and deposition fluxes of BC, N and S species. In the case of ozone, the n_i precursors in equation (2) would comprise [NO_x, NMVOC, CO, CH₄]. The set of linear equations (2) with associated source-receptor matrices (1) for all components and all source and receptor regions thus emulates the ‘full’ TM5-CTM, and constitutes the ‘kernel’ of TM5-FASST_v0. When OC emissions are provided in mass units C, the OC mass is multiplied with a factor 1.3 to obtain Particulate Organic Matter (POM) (Kanakidou et al., 2005).

BC and POM are assumed not to interact with other pollutants and their atmospheric lifetimes are prescribed and assumed neither to be affected by mixing with other soluble species like sulfate, nitrate or ammonium salts, nor to undergo oxidation by O₃. Recent work (e.g. Huang et al., 2012), indicates that a parameterized approach, as applied in TM5, tends to underestimate BC and POM atmospheric lifetimes, leading to a low concentration bias. When explicitly modelled, including the combined impact of both mechanisms, Huang et al., 2012 find that the global atmospheric residence times of BC and POM are lengthened by 9% and 3% respectively.

We note that, unlike many other inventories, the RCP emission scenarios do not include a separate inventory for total primary PM_{2.5} which includes besides BC and POM other non-specified primary particulates (e.g. primary sulfate, fly-ash). When specific scenario studies require so, TM5-FASST_v0 treats this ‘other’ primary PM_{2.5} (OPP = Primary PM_{2.5} – BC – POM) as BC in Eq. (2), where both $C_{OPP,base}$ and $E_{OPP,base}$ are zero.

$$C_{OPP}(y) = \sum_{n_x} \sum_{n_i} A_{BC}[x, y] \cdot E_{OPP}(x) \quad (3)$$

Deleted: The total concentration of component

Deleted: $(y) = C_{j,base}(y) + \sum_{n_x} \sum_{n_i} A_{ij}[x, y] \cdot [E_i(x) - E_{i,base}(x)]$

Deleted: emissions

Deleted: lifetime

Deleted: not

Deleted: .

5 ~~TM5 Surface ozone (and NO₂) fields from base and perturbation experiments~~, were stored at hourly intervals allowing for the calculation of specific vegetation and health related O₃ metrics, often based on thresholds of hourly O₃ concentrations, or concentrations during daytime. The hourly O₃ surface fields were converted into specific O₃ metrics responses to annual emissions, including accumulated hourly ozone above a threshold of 40 ~~ppb~~ during a 3 months crop growing season (AOT40), 3-monthly mean of 7 hr or 12 hr daytime ozone during crop growing season (M7, M12), maximum 6-monthly running average of daily maximum hourly O₃ (~~6mDMA1~~), the sum of daily maximal 8hr ozone mean concentrations above 35ppbV (SOMO35).

10 ~~The -20% perturbation simulations were performed for the combination of precursors given in Table 2, with P0 the unperturbed reference simulation, and P1 through P5 -20% perturbations for combined or single precursors. Due to limited CPU availability, precursors that are expected not to interact chemically are perturbed simultaneously, with P1 combining SO₂, NO_x, BC, and POM and P4 combining NH₃ and NMVOC. P1 and P4 were computed for each of the 56 continental source regions plus shipping (P1 and P4) and aviation (P1). Additionally, a SO₂-only perturbation was computed for all individual source regions and shipping (P2) and NO_x-only for a selection of key source regions (P3). Finally a set of combined NO_x + NMVOC perturbation simulations (P5) was performed for a set of key regions.~~

15 For a limited set of representative source regions, an additional wider range of emission perturbations P'_i [-80% to +100%] has been applied to evaluate possible non-linearities in the emission-concentration relationships. The list of these additional perturbation simulations is given in Table S3 of the SI. ~~In section 3.1 we explain how this set of perturbation runs is combined into FASST to obtain a complete set of source-receptor matrices for each precursor and source region.~~

20 We did not perform dedicated perturbation simulations on CH₄ as O₃ precursor, but implemented TM5 results obtained in the frame of the first phase of the Hemispheric Transport of Air Pollutants (HTAP1) assessment (Dentener et al., 2010; Fiore et al., 2008). In one of the prescribed experiment set-up, models evaluated how surface ozone levels are responding when the global steady-state CH₄ concentration decreases with 20% from 1760 ppbv (the global mean CH₄ concentration in the year 2000) to 1408 ppbv. The outcome of this experiment is a set of global grid maps with hourly O₃ concentration responses from which all relevant O₃ metrics can be obtained. As an example, the annual mean O₃ concentration response to the CH₄ concentration perturbation is shown in Fig. S3.3 in the SI. ~~Annex S3 in the SI provides more details on the methodology applied to convert the CH₄ concentration perturbation into a CH₄ emission-based perturbation.~~

25 Because of its long life time compared to short-lived ozone precursors, CH₄ source-receptor coefficients are considered independent on the location of emission and are therefore provided as global emission-to-regional (or gridded) concentration responses.

30 Because of the mismatch between the HTAP1 source - receptor regions and the FASST ones, the current version of TM5-FASST does not include source-receptor relations between CO and O₃ concentration (or O₃ exposure metrics), only impacts

Moved up [1]: SOA from anthropogenic emission was not explicitly included in the current simulations.

Deleted: Secondary biogenic POM (SOA) was included following the AEROCOM recommendation which parameterized SOA formation from natural VOC emissions as a fixed fraction of the primary emissions.

Deleted: This is a topic for future developments of the model. ¶ In TM5-FASST_v0 the monthly perturbations are aggregated to annual emission-concentration SR matrices, as the health, climate and vegetation impact metrics used in this version are also aggregated to annual values. Surface ozone (and NO₂) fields

Deleted: ppbV

Deleted: M6M

Deleted: The -20% emission perturbation calculations were performed for the combination of emission perturbations given in Table 2.

Deleted: We note that

Deleted: HTAP1 CH₄ perturbation experiment is not a set-up that evaluates

Deleted: ozone response

Deleted: a change in CH₄ emissions which would involve large transient time-scale computations, but rather

Deleted: steady-state result of an established changed background CH₄ concentration. The change in CH₄ burden due to OH oxidation under this prescribed

Deleted: change is treated as an

Deleted: , in the case of TM5 corresponding to a sustained emission perturbation of 77Tg/year, allowing to normalize the resulting responses in O₃ concentration and metrics on a CH₄ emission basis which are then linearly scaled in the reduced-form TM5-FASST set-up.

of CO emissions on global methane and O₃ global radiative forcing, also in this case retrieved from HTAP1 dedicated CO perturbation experiments with TM5.

Deposition source-receptor matrices of nitrogen and sulfur compounds are obtained in the same way as for the pollutant ambient concentration fields, making the difference between the base and perturbation simulations. Nitrogen depositions are calculated from accumulation of the instantaneous surface budgets of all relevant nitrogen components (NO, NO₂, NO₃, 2×N₂O₅, HNO₄, organic nitrates, NH₃, NH₄) and similar for sulfur from SO₂ and SO₄, into monthly time steps. Column amounts of ozone and particulate matter are also computed using 3D monthly output of concentrations and meteorological parameters.

2.4 PM_{2.5} adjustments in urban regions for health impact evaluation

TM5-FASST is specifically aiming at providing pollutant exposure fields for further impact evaluation. For the evaluation of health impacts from outdoor air pollution, a 1°x1° horizontal resolution may not adequately represent sub-grid gradients of pollutants. Indeed, higher pollutant levels are expected to concur with high population density in urban areas, hence an area-averaged concentration for a nominally 100x100km² sized grid cell will underestimate the exposure of population located in pollution hotspots within a single grid cell. We provide a simple parameterization, generating a correction factor on the gridbox area-mean PM_{2.5} concentration, to better represent the actual mean population exposure within that grid cell. In the current approach we only consider PM_{2.5}, although also ozone and NO₂ are likely subject to sub-grid gradients. The parameterization is based on the underlying assumption that the spatial distribution of primary emitted PM_{2.5} correlates with population density. Our parameterization builds upon high-resolution population grid maps, allowing a sub-grid readjustment of the PM_{2.5} concentration within each 1°x1° grid cell. Further, it needs additional information to flag the population sub-grids as 'urban' or 'rural', e.g. population density for which an urban threshold can be defined, or more sophisticated schemes defining urban areas. We further assume that only primary PM_{2.5} from the residential and the surface transport sectors is contributing to the local (urban) increment, whereas other aerosol precursor components and other sectors are assumed to be homogeneously distributed over the 1°x1° grid cell. Indeed, secondary PM_{2.5} is formed over longer time scales and therefore deemed to be more homogeneously distributed at the regional scale, while primary PM_{2.5} emissions from other sources than the residential and transport sector are assumed to occur more remotely from urban areas. The adjusted population-weighted mean concentration within each 1°x1° grid cell (conserving the area-based grid cell mean) is then calculated as follows:

$$PM_{2.5,inc} = DU + SS + SO_4^{2-} + NO_3^- + NH_4^+ + (1-k_{BC}) BC + (1-k_{POM}) POM + INCR(k_{BC} BC + k_{POM} POM) \quad (4)$$

with DU and SS the fixed natural mineral dust and sea-salt contributions respectively; SO₄²⁻, NO₃⁻, NH₄⁺, BC and POM the 1°x1° grid cell average values resulting from TM5 or TM5-FASST; k_{BC} (k_{POM}) the fraction of (residential + transport) BC (POM) emissions in the total BC (POM) emissions within the 1°x1° grid cell and INCR the urban increment factor. This sub-grid parameterization has been applied as a part of the methodology to estimate population exposure in the Global

Deleted: Although the impact of CO on O₃ concentration is limited - based on the HTAP1 CO perturbation simulations with TM5, we estimate that anthropogenic CO emissions contribute with 1 – 1.9 ppbv in annual mean O₃ over Europe, 1.3 -19 over North-America, 0.7-1 over South Asia and 0.3 – 1.5 over East-Asia – this is an important issue for the further development of the tool.

Deleted: <#>Sub-grid PM_{2.5} gradients¶

Deleted: In the current study we only consider PM_{2.5}, although also ozone and NO₂ are likely subject to sub-grid gradients.

Deleted: while

Deleted: .

Burden of Disease assessments (Brauer et al., 2012). Supplemental Information section S4 provides details on the calculation of INCR.

The required gridded sectorial emission data may not be readily available for any assessment. A “default” set of regional population-weighted averaged increment factors for BC and POM is given in Table S4.2, based on the RCP year 2000 baseline simulations performed with TM5 for the year 2000, i.e. using year 2000 population (CIESIN GWPv3) and the RCP year 2000 gridded emissions by sector.

2.5 Health impacts

TM5-FASST provides output of annual mean PM_{2.5} and O₃ health metrics (3-monthly and 6-monthly mean of daily maximum hourly O₃ (3mDMA1, 6mDMA1), and the sum of the maximal 8-hourly mean above a threshold of 35 ppbV (SOMO35) or without threshold (SOMO0), as well as annual mean NO_x and SO₂ concentrations at grid resolution of 1°x1°. These are the metrics consistent with underlying epidemiological studies (Jerrett et al., 2009; Krewski et al., 2009; Pope et al., 2002). The population-weighted pollutant exposure metrics grid maps, in combination with any consistent population grid map, are thus available for human health impact assessment. The TM5-FASST_v0 tool provides a set of standard methodologies, including default population and health statistics, to quantify the number of air quality-related premature deaths from PM_{2.5} and O₃.

Health impacts from PM_{2.5} are calculated as the number of annual premature mortalities from 5 causes of death, following the Global Burden of Disease methodology (Lim et al., 2012): ischemic heart disease (IHD), chronic obstructive pulmonary disease (COPD), stroke, lung cancer (LC) and acute lower respiratory airways infections (ALRI) whereas mortalities from exposure to O₃ are related to respiratory disease.

Cause-specific excess mortalities are calculated at grid cell level using a population-attributable fraction approach as described in Murray et al. (2003) from $\Delta Mort = m_0 \times AF \times Pop$, where m_0 is the baseline mortality rate for the exposed population, $AF = (RR-1)/RR$ is the fraction of total mortalities attributed to the risk factor (exposure to air pollution), $RR =$ relative risk of death attributable to a change in population-weighted mean pollutant concentration, and Pop is the exposed population (adults ≥ 30 years old, except for ALRI for which infant population <5 years old was considered). RR for PM_{2.5} exposure is calculated from the Integrated Exposure-Response functions (IER) developed by Burnett et al. (2014), and first applied in e.g. the Global Burden of Disease study (Lim et al., 2012).

In order to facilitate comparison with earlier studies, TM5-FASST provides as well mortality estimates based on a log-linear exposure response function $RR = \exp^{\beta \Delta PM_{2.5}}$ where β is the concentration-response factor (CRF; i.e., the estimated slope of the log-linear relation between concentration and mortality) and $\Delta PM_{2.5}$ is the change in concentration. More details on the health impact methodologies, as well as sources for currently implemented population and baseline mortality statistics and their projections in TM5-FASST_v0 are given in section S5 of the SI.

Deleted: .

Deleted: M3M, M6M

Deleted: :

Deleted: -/

Deleted: Sources for currently implemented population and baseline mortality statistics and their projections in TM5-FASST_v0 are given in section S5 of the SI. TM5-FASST currently includes two approaches from the literature to evaluate RRs for PM_{2.5}: the first one follows methodology and outcomes of the American Cancer Society (ACS) study

Moved down [2]: based on a log-linear exposure response function $RR = \exp^{\beta \Delta PM_{2.5}}$ where β is the concentration-response factor (CRF; i.e., the estimated slope of the log-linear relation between concentration and mortality) and $\Delta PM_{2.5}$ is the change in concentration.

Deleted: The fraction of the disease burden attributable to PM_{2.5} as a risk factor, the attributable fraction (AF), is defined as $AF = \frac{RR-1}{RR} = 1 - \exp(-\beta \Delta PM_{2.5})$. A 10 $\mu\text{g}/\text{m}^3$ increase in PM_{2.5} (concentration range, 5.8–22.2 $\mu\text{g}/\text{m}^3$) was associated with 13% (95% CI, 10–16%), and 14% (95% CI, 6–23%) increases in cardiopulmonary (CP) and lung cancer (LC) mortality, corresponding to β (for a 1 $\mu\text{g}/\text{m}^3$ increase in PM_{2.5}) of 0.01213 and 0.01284 for CP and LC respectively. We also include an evaluation based on total non-accidental mortality with a RR per 10 $\mu\text{g}/\text{m}^3$ of 6.2% (95% CI, 4.0–8.3%). The second methodology uses age-averaged

Deleted: . IERs expand epidemiological studies on the long-term effects of ambient PM_{2.5} exposure to higher concentration ranges than the one available from the ACS study, making use of health impact studies for smoking and second-hand smoking. This tends to flatten off the RR function at high PM_{2.5} concentration levels compared to the traditionally-used log-lin function which, extrapolated outside the concentration range where the health impacts were determined, would lead to ...

Moved (insertion) [2]

Deleted: $RR(PM_{2.5}) = 1 + \alpha [1 - e^{-\gamma(PM_{2.5}-zcf)^{\delta}}]$ for $PM_{2.5} > zcf$

For O₃ exposure, $RR = e^{\beta(\Delta 6mDMA1)}$, β is the concentration–response factor, and $RR = 1.040$ [95% confidence interval (CI): 1.013, 1.067] for a 10 ppb increase in 6mDMA1 according to Jerrett et al. (2009). We apply a default counterfactual concentration of 33.3 ppbV, the minimum 6mDMA1 exposure level in the Jerrett et al. (2009) epidemiological study.

Deleted: $e^{\beta(\Delta 6mM)}$

Deleted: M6M

Deleted: M6M

We note that the coefficients in the IER functions used in the GBD assessments have been recently updated due to methodological improvements in the curve fitting, leading to generally higher RR and mortality estimates (Cohen et al., 2017; Forouzanfar et al., 2016). In particular, the theoretical minimum risk exposure level was assigned a uniform distribution of 2.4–5.9 $\mu\text{g}/\text{m}^3$ for PM_{2.5}, bounded by the minimum and fifth percentiles of exposure distributions from outdoor air pollution cohort studies, compared to the presently used range of 5.8 - 8.8 $\mu\text{g}/\text{m}^3$ which would increase the health impact from PM_{2.5} in relatively clean areas. Further, a recent health impact assessment (Malley et al., 2017), using updated RR estimate and exposure parameters from the epidemiological study by Turner et al. (2016), estimates 1.04–1.23 million respiratory deaths in adults attributable to O₃ exposure, compared with 0.40–0.55 million respiratory deaths attributable to O₃ exposure based on the earlier (Jerrett et al., 2009) risk estimate and parameters. These recent updates have not been included in the current version of TM5-FASST. Health impacts from exposure to other pollutants (NO₂, SO₂ for example) are currently not being evaluated in TM5-FASST-v0.

Deleted: .

Deleted: ¶
The inclusion of a theoretical minimum risk exposure level (z_{cf}) in the PM_{2.5} exposure-response functions is motivated by the lowest prevailing concentration at which an increased risk was observed in the ACS cohort studies.) argue that zero exposure is not a practical counterfactual level because it is impossible to achieve even in pristine environments, implicitly indicating that their exposure-response curves strictly apply to total PM_{2.5}, including the natural components (mineral dust, sea-salt). In impact assessment studies, evaluating the difference between two anthropogenic emission scenarios (under otherwise identical natural background conditions) is often more relevant than evaluating absolute impacts for a single scenario. Therefore, TM5-FASST includes the option to customize the value of z_{cf} , both in the IER as the log-linear shaped functions. In practice, we recommend to use $z_{cf}=0$ when evaluating anthropogenic emissions only. Because of the non-linear IER functions, Mortalities between 2 scenarios (S1, S2) with population-weighted PM_{2.5} concentrations PM_{S1} and PM_{S2} respectively are evaluated as $Mort(PM_{S2}) - Mort(PM_{S1})$, and not as $Mort(PM_{S2}-PM_{S1})$. ¶

2.6 Crop impacts

The methodology applied in TM5-FASST to calculate the impacts on four crop types (wheat, maize, rice, and soy bean) is based on Van Dingenen et al. (2009). In brief, TM5 base and -20% perturbation simulations of gridded crop O₃ exposure metrics (averaged or accumulated over the crop growing season) are overlaid with crop suitability grid maps to evaluate receptor region-averaged exposure metrics SR coefficients. Gridded crop data (length and centre of growing period, as well as a gridded crop-specific suitability index, based on average climate 1961 – 1990) have been updated compared to Van Dingenen et al. (2009) using the more recent and more detailed Global Agro-Ecological Zones (GAEZ) data set (IIASA and FAO, 2012, available at <http://www.gaez.iiasa.ac.at/>).

Deleted: although the model output does provide population-weighted mean concentrations of NO₂ and SO₂

Deleted: M_i

Deleted: .

Deleted: . The Weibull-type exposure-response functions express

Deleted: relative yield (RYL) loss

Deleted: a function of M_i:

Available crop ozone exposure metrics are 3-monthly accumulated ozone above 40 ppbV (AOT40) and seasonal mean 7 hr or 12 hr day-time ozone concentration (M7, M12) for which exposure-response functions are available from the literature (Mills et al., 2007; Wang and Mauzerall, 2004). Both metrics (M_i) are calculated as the 3-monthly mean daytime (09:00 – 15:59 for M7, 08:00 – 19:59 for M12) ozone concentration, AOT40 and M_i are evaluated over the 3 months centred on the midpoint of the location-dependent crop-growing season, provided by the GAEZ data set. Note that in the GAEZ methodology, the theoretical growing season is determined based on prevailing temperatures and water balance calculations for a reference crop, and can range between 0 and 365 days, however our approach always considers 3 months as the standard metric accumulation or averaging period.

The crop relative yield loss (RYL) is calculated as linear function from AOT40 and from a Weibull-type exposure-response as a function of M_i:

Deleted: $RYL = 1 - \frac{\exp\left[-\left(\frac{M_i}{a}\right)^b\right]}{\exp\left[-\left(\frac{c}{a}\right)^b\right]}$ ¶

$$RYL[AOT40] = a \times AOT40 \quad (5)$$

$$RYL(M_i) = \begin{cases} 1 - \frac{\exp\left[-\left(\frac{M_i}{a}\right)^b\right]}{\exp\left[-\left(\frac{c}{a}\right)^b\right]} & M_i \geq c \\ 0 & M_i < c \end{cases} \quad (6)$$

The parameter values in the exposure response functions are given in Table 3. Coefficients a and b are shape factors of the Weibull function, while c represents the lower M_i threshold for visible crop damage. Also here, the non-linear shape of the RYL(M_i) function requires the ΔRYL for 2 scenarios (S1, S2) being evaluated as $RYL(M_{i,S2}) - RYL(M_{i,S1})$, and not as $RYL(M_{i,S2} - M_{i,S1})$.

Finally, it is important to note that TM5-FASST modelled O_3 surface concentrations refer to the middle of the TM5's lower layer gridbox, i.e. 30m above surface, whereas monitoring of O_3 (from which exposure metrics are derived) actually happens at a standard altitude of 3 to 5m above the surface where, due to deposition and meteorological processes, the concentration may differ. However comparing TM5 simulated gridbox-centre ozone metrics with observations from 99 monitoring stations worldwide, Van Dingenen et al. (2009) find that, when averaged at the regional scale, TM5 simulated crop metrics obtained from the grid box centre are reproducing the observations within their standard deviations, and that the monthly 10m TM5 metric values do not significantly improve the bias between model and observations. Therefore we use the standard model output at 30m.

2.7 Climate metrics

We make use of the available 3D aerosol and O_3 fields in the -20% emission perturbation simulations with TM5 to derive the change in global forcing for each of the perturbed emitted precursors. The region-to-global radiative forcing SR for precursor j , emitted from region k ($SR_{RF_k^j}$) is calculated as the emission-normalized change in global radiative forcing between the TM5 base and the corresponding -20% emission perturbation experiment:

$$SR_{RF_k^j} = \frac{RF_PERT[j,k] - RF_BASE}{0.2E_k^j} \text{ [W/m}^2\text{]/[kg/yr]} \quad (7)$$

where RF_PERT and RF_BASE are the TM5 global radiative forcings for the perturbation and base simulations respectively, and E_k^j is the annual base emission of precursor j from region k .

For each emitted pollutant (primary and secondary) the resulting normalized global forcing responses are then further used to calculate the global warming potential (GWP) and global temperature potential (GTP) for a series of time horizons H. In this way, a set of climate metrics is calculated with a consistent methodology as the air quality metrics, health and ecosystem impacts calculated from the concentration and deposition fields. In this section we describe in more detail the applied

Deleted: and

Deleted: applied methodology are described in detail by , however gridded crop data (growing season and suitability, based on average climate 1961 – 1990) have been updated using Global Agro-Ecological Zones data set . Again we note that

Deleted: over

Deleted: horizontal resolution of the grid cells, the

Deleted: 30m monthly O_3 and O_3

Deleted: represent the observed values

Deleted: variability range

Deleted: [W/m²]/[kg/yr]

methodologies in TM5 to obtain the radiative forcing from aerosols, clouds and gases, as well as the derivation of the GWP and GTP metrics.

2.7.1 Instantaneous radiative forcing by aerosols

The base simulation and -20% perturbation response of the column-integrated aerosol mass over all 25 vertical layers of TM5 for all relevant species was calculated and stored. The calculation of the top-of-atmosphere (TOA) instantaneous forcing by aerosol is based on the radiative transfer model described by Marmer et al. (2007) using monthly average meteorological fields and surface characteristics using ECMWF monthly average meteorological fields (temperature, clouds, relative humidity, surface albedo) for the year 2001. We assume externally mixed aerosols and calculate the forcing separately for each component. The total aerosol forcing is obtained by summing up these contributions. We refer to section S6 of the SI for a more detailed description of the forcing calculations. To avoid further extensive radiative transfer calculation, monthly-mean radiative forcing efficiencies, expressed as $[W/m^2]/[μg]$, were calculated once using the $1^{\circ} \times 1^{\circ}$ gridded TM5 base simulation outputs and off-line radiative code using monthly fields of aerosol, ECMWF meteorology and surface characteristics, and stored for further use (Marmer et al., 2007). The annual TOA global forcing for each scenario is then obtained by multiplying the monthly column-integrated aerosol mass with this grid-cell specific monthly mass forcing efficiency and subsequently averaged over one year. Neglecting the aerosol mixing state and using column-integrated mass rather than vertical profiles introduces additional uncertainties in the resulting forcing efficiencies. Accounting for internal mixing may increase the BC absorption by 50 to 200% (Bond et al., 2013), whereas including the vertical profile would weaken BC forcing and increase SO_4 forcing (Stjern et al. 2016). Further, the BC forcing contribution through the impact on snow and ice is not included, nor are semi- and indirect effects of BC on clouds. Our evaluation of pre-industrial to present radiative forcing in the validation section demonstrates that, in the context of the reduced-form FASST approach, the applied method however provides useful results. Figure S6.1 (a, b, c) in the SI shows the resulting global radiative forcing fields for sulfate, POM and BC. The regional emission-normalized forcing SRs for aerosol precursors (in $W m^{-2} Tg^{-1}$) are given in Table S6.2 of the SI.

2.7.2 Indirect aerosol forcing

Aerosols modify the microphysical and radiative properties and lifetime of clouds, commonly denoted as the aerosol indirect effect (Haywood and Boucher, 2000). This forcing results from the ability of the hygroscopic particles to act as (warm) cloud condensation nuclei thus altering the size, the number and the optical properties of cloud droplets (Twomey, 1974). More and smaller cloud droplets increase the cloud albedo, which leads to cooling. Using TM5 output, indirect forcing is evaluated considering only the so far best studied first indirect effect, and using the method described by Boucher and Lohmann (1995). Fast feedbacks on cloud lifetimes and precipitation were not included in this off-line approach. This

Deleted: Enhanced aerosol scattering of solar radiation back into space increases the planetary albedo and is therefore associated with cooling. On the other hand BC is a strong absorber of solar radiation and is therefore associated with warming .

Deleted: (see section S6 of the SI for more details on the forcing calculations).

Deleted: $μg$

Deleted: Although this method has some limitations, as discussed

Deleted: , we demonstrate

Deleted: reliable

Deleted: In this study we have

Deleted: considered

Deleted: In particular

simplified method uses TM5 3D time-varying fields of SO₂ concentrations, cloud liquid water content, and cloud cover (the latter from the parent ECMWF meteorological data). The parameterization uses the cloud information (liquid water content and cloud cover) from the driving ECMWF operational forecast data (year 2001). Fast feedbacks on cloud lifetimes and precipitation were not included in this off-line approach. The cloud droplet number concentrations and cloud droplet effective radius were calculated following Boucher and Lohmann (1995) separating continental and maritime clouds. The equations are given in section S6 of the SI. The global indirect forcing field associated with sulfate aerosols is shown in Fig. S6.1(d) of the SI and regional forcing SRs are listed in Table S6.2. Indirect forcing by clouds remains however highly uncertain, and although FASST evaluates its magnitude, it is often not included in our analyses.

2.7.3 Radiative forcing by O₃ and CH₄

Using TM5 output, radiative forcing (RF) by ozone is approximated using the forcing efficiencies obtained by the STOCHEM model as described in Dentener et al. (2005), normalized by the ozone columns obtained in that study. Here we use annual averaged forcing based on the RF computations provided as monthly averages by D. Stevenson (personal communication, 2004). The radiative transfer model was based on Edwards and Slingo (1996). These forcings account for stratospheric adjustment, assuming the fixed dynamical heating approximation, which reduces instantaneous forcings by ~22%.

For CH₄ the RF associated with the base simulation was taken from the equations in the IPCC-Third Assessment Report (TAR) (Table 6.2 of Ramaswamy et al., 2001). Using the HTAP1 calculated relationship between CH₄ emission and concentration (see section S3.1 in the SI), we evaluated a globally uniform value of 2.5 mW/m² per Tg CH₄ emitted. It includes both the direct CH₄ greenhouse gas (GHG) forcing (1.8 mW/m²) as well as the long-term feedback of CH₄ on hemispheric O₃ (0.7 mW/m²). From the TM5 perturbation experiments we derive as well region-to-global radiative forcing SRs (expressed as [W m⁻²]/[Tg yr⁻¹]) for precursors NO_x, NMVOC, SO₂ and CO (the latter taken from HTAP1 experiments) through their feedback on the CH₄ lifetime and subsequently on long-term hemispheric O₃ levels. Hence, the greenhouse gas radiative forcing contribution of each ozone precursor consists of 3 components: a direct effect through the production of O₃, a contribution by a change in CH₄ through modified OH levels (including a self-feedback factor accounting for the modified CH₄ lifetime), and a long-term contribution via the feedback of CH₄ on hemispheric ozone. The details of the applied methodology for direct and indirect CH₄ forcing SRs are given in section S6.2 of the SI, including tables with the regional emission-based forcing efficiencies for all precursors (Tables S6.3 to S6.5).

In its current version, TM5-FASST_v0 provides the steady-state concentrations and forcing response of the long-term O₃ and CH₄ feedback of sustained precursor emissions, i.e. it does not include transient computations that take into account the time lag between emission and establishment of the steady-state concentration of the long-term O₃ and CH₄ responses.

Deleted: ERA

Deleted: .

Deleted: the set of equations 'A' in

Deleted: The cloud droplet effective radius is calculated from the mean volume cloud droplet radius using equation 4

Deleted: Boucher and Lohmann (1995).

Deleted: .

Deleted: was

Deleted: The effect of

Deleted: emissions on global forcing is

Deleted: by applying a

Deleted: For CH₄ the RF associated with

Deleted: base simulation was

Deleted: IPCC-Third Assessment Report (TAR).
A secondary

Deleted: through

Deleted: effect of precursors (NO_x, NMVOC, CO and SO₂) on CH₄,

Deleted: , is included as well. The CH₄ response from a perturbation in NO_x, NMVOC and SO₂ is calculated from the change in CH₄ burden due to OH oxidation under the respective perturbations. This burden perturbation is treated as an emission perturbation for CH₄ which translates in a new steady-state CH₄ and background O₃ concentration. Using the HTAP1 simulations SR1 and SR2 (1760 ppb and 1408 ppb, see we evaluated a CH₄ lifetime sensitivity coefficient $s = \partial \ln(LT) / \partial \ln(CH_4)$ of 0.33 which can be compared to a range of values between 0.25- and 0.31 in IPCC-TAR, Table 4.2). The change in steady-state methane concentrations, induced by O₃ precursor emissions, follows the method outlined by , resulting in a calculated feedback factor F=1.53.) report slightly lower F values of 1.25 to 1.43, due to the fact that they accounted for a fixed CH₄ lifetime with respect to losses to the stratosphere (120 years) and soils (160 years), which would have lowered the TM5 factor F to 1.43, and 5 % higher normalized forcing (Wm⁻²ppb⁻¹). The use of 12 model average F of 1.33 would lead to 12 % higher normalized forcing resulting from ...

Deleted: The response of O₃ forcing to CO emission changes (for which no ...

2.7.4 Calculation of GWP, GTP, delta T and CO_{2eq} emissions

The obtained emission-based forcing efficiencies (Tables S6.2 to S6.5 in the SI) are immediately useful for evaluating a set of short-lived climate pollutant climate metrics. Applying the methodology described by Fuglestedt et al. (2010) briefly outlined below, the resulting emission-normalized specific forcing responses A_x [W/m²]/[kg/year] are used to calculate the absolute global warming potential (AGWP) and absolute global temperature potential (AGTP) for various time horizons H (20, 50, 100, 500 yr), as a basis to obtain the corresponding CO_{2eq} for the actually emitted amounts.

The AGWP for emitted short-lived (exponentially decaying) species x with lifetime a_x is calculated by integrating the specific forcing over a time span H of an emission pulse at $t=0$:

$$AGWP(H) = \int_0^H A_x \exp\left(\frac{-t}{a_x}\right) dt = A_x a_x \left[1 - \exp\left(\frac{-H}{a_x}\right)\right] \quad (8)$$

AGTP of a short-lived (exponentially decaying) component is calculated as an endpoint change in temperature after H years from a one-year emission pulse at time 0.

$$AGTP(H) = \int_0^H A_x \exp\left(\frac{-t}{a_x}\right) R(H-t) dt \quad (9)$$

where $R(t)$ represents the response in global-mean surface temperature to a unit pulse in forcing. Following Fuglestedt et al. (2010) we adopt the functional form for $R(t)$ from Boucher and Reddy (2008), derived from a GCM :

$$R(t) = \sum_{j=1}^2 \frac{c_j}{d_j} \exp\left(-\frac{t}{d_j}\right) \quad (10)$$

The first term in the summation can crudely be associated with the response of the ocean mixed-layer to a forcing, the second term as the response of the deep ocean with c_j [K(Wm⁻²)⁻¹] and d_j [years] represent temperature sensitivity and response time of both compartments respectively. This leads to:

$$AGTP(H) = \sum_{j=1}^2 \frac{A_x a_x c_j}{(a_x - d_j)} \left(\exp\left(\frac{-H}{a_x}\right) - \exp\left(\frac{-H}{d_j}\right) \right) \quad (11)$$

As discussed earlier, we take into account that species such as NO_x, NMVOC and CO lead to changes in O₃ and CH₄ and consequently have a short-lived component (O₃) as well as long-lived components (CH₄ and CH₄-induced O₃) contributing to AGWP and AGTP. We refer to Appendix 2 in Fuglestedt et al., 2010 for a detailed description of the methodology and numerical values for c_j and d_j . As aerosols and directly produced O₃ from ozone precursors have a lifetime of the order of days (aerosols) to several months (O₃), the resulting integrated specific forcing is insensitive to the actual lifetime for the range of time horizons considered (decades to centuries), and in practice we use a default value of 0.02yr for aerosols and 0.27yr for short term O₃. This does however not apply to the long-term forcing contribution of CH₄ and the associated O₃ feedback from O₃ precursors for which we use a perturbation adjustment time of 14.2 years (Wild et al., 2001). Note that this adjustment time scale is larger than the total atmospheric time scale for CH₄ oxidation by OH combined with losses to soils and the stratosphere (HTAP1 model ensemble mean: 8.8 years (Fiore et al., 2009)) due to the feedback of CH₄ on atmospheric OH concentrations and thereby its own lifetime (Forster et al., 2007). Fuglestedt et al. (2010) report CH₄

adjustment times from various modelling studies between 10.2 and 16.1 years. Dimensionless metrics GWP (GTP) are obtained dividing AGWP (AGTP) by the AGWP (AGTP) of CO₂ as a reference gas for which we use values from Joos et al. (2013).

Finally, still following Fuglestedt et al. (2010), we also include a calculation of the global temperature change $\Delta T_x(H)$ between year 0 and year H for a sustained emission change $\Delta E_x(t) = E_x(t) - E_x(0)$ of component x as the sum of the delta T from one-year emission ‘pulses’ approaching the time horizon.

$$\Delta T_x(H) = \sum_{t=0}^H \Delta E_x(t) AGTP(H - t) \quad (12)$$

In this way, a set of climate metrics is obtained which is consistent with the air quality metrics, health and ecosystem impacts calculated from the concentration and deposition fields.

3 Results: validation of the reduced-form TM5-FASST

In this section we focus on the validation of regionally aggregated TM5-FASST_v0 outcomes (pollutant concentrations, exposure metrics, impacts), addressing specifically:

- (1) The additivity of individual pollutant responses as an approximation to obtain the response to combined precursor perturbations,
- (2) The linearity of the emission responses over perturbation ranges extending beyond the -20% perturbation,
- (3) The FASST outcome versus TM5 for a set of global future emission scenarios that differ significantly from the reference scenario,
- (4) FASST key-impact outcomes versus results from the literature for some selected case studies, with a focus on climate metrics, health impacts and crops.

3.1 Validation against the full TM5 model: additivity and linearity

We recall that the TM5-FASST computes concentrations and metrics based on a perturbation approach, i.e. the linearization applies only on the difference between scenario and reference emission. Therefore we focus on evaluating the perturbation response, i.e. the second term in the right hand side of Eq. 2.

The standard set of -20% emission perturbation simulations, available for all 56 continental source regions and constituting the kernel of TM5-FASST_v0 are simulations P1 (perturbation of SO₂, NO_x, BC and POM), P2 (SO₂ only), and P4 (NH₃ and NMVOC) shown in Table 2. Additional standard -20% perturbation experiments P3 (NO_x only) and P5 (NO_x and NMVOC), as well as an additional set of perturbation simulations P1’ to P5’ over the range [-80%, +100%], listed in Table S3 of the SI, have been performed for a limited selection of representative source regions (Europe, USA, China, India, Japan) due to limited CPU resources. For the same reason, no combined perturbation studies are available for (SO₂ + NH₃) and (NO_x + NH₃) for a systematic evaluation of additivity and linearity. The available [-80%, +100%] perturbations are used to validate

Deleted: validating TM5-FASST_v0,

Deleted: (1) Evaluating possible caveats related to the hypothesis of

Deleted: and linearity

Deleted: secondary

Deleted: towards single and

Deleted: by confronting extrapolated FASST SRs (obtained from

Deleted:) with TM5 simulations for an extended perturbation

Deleted: range [-80%, +100%]

Deleted: (2) Testing the validity of

Deleted: , now including all source and receptor regions in the evaluation.

Deleted: (3) Confront

Deleted: with

Deleted: and

Deleted: all precursors

Deleted: primary pollutants emissions

Deleted: Simulations

Deleted: (-20%),

Deleted: the

Deleted: %]

Deleted: set

Deleted: and listed in Annex 4 of the SI,

the linearized reduced-form approach against the full TM5 model, exploring chemical feedback mechanisms (additivity) and extrapolation of the -20% response sensitivity towards larger emission perturbation magnitudes (linearity). This is in particular relevant for the NO_x - NMVOC - O_3 chemistry and for the secondary $\text{PM}_{2.5}$ components NO_3^- - SO_4^{2-} - NH_4^+ . These mechanisms could also be important for organic aerosol, but we remind that in this study organic aerosol formation was parameterized as pseudo-emissions.

3.1.1 Additivity and linearity of secondary inorganic $\text{PM}_{2.5}$ response:

Experiment P1, where BC, POM, SO_2 and NO_x emissions are simultaneously perturbed by -20% relative to base simulation P0, delivers SR matrices for primary components BC and POM, and a first-order approximation for the precursors SO_2 and NO_x whose emissions do not only affect SO_2 and NO_x gas concentrations but also lead to several secondary products (SO_2 forms ammonium sulfate, NO_x leads to O_3 and ammonium nitrate). Experiment P2 perturbs SO_2 only, whereas experiment P3 perturbs NO_x only (in this latter case, to limit the computational cost, computed for a limited set of representative source regions only).

We first test the hypothesis that the $\text{PM}_{2.5}$ response to the combined ($\text{NO}_x + \text{SO}_2$) -20% perturbation (P1) can be approximated by the sum of the single precursor perturbations responses (P2 + P3). Figure 2 summarizes the resulting change in SO_4^{2-} , NO_3^- , NH_4^+ and total inorganic $\text{PM}_{2.5}$ respectively for the selected source regions. For Europe, the emission perturbations were applied over all European countries simultaneously, hence the responses are partly due to inter-regional transport from other countries. Following findings result from the perturbation experiments P1, P2 and P3:

- (1) Sulfate shows a minor response to NO_x emissions, and likewise nitrate responds only slightly to SO_2 emissions and both perturbations are additive. In general the response is one order of magnitude lower than the direct formation of SO_4^{2-} and NO_3^- from SO_2 and NO_x respectively (Fig. 2a, b);
- (2) NH_4 responds to NO_x and SO_2 emissions with comparable magnitudes and in an additive way (Fig. 2c);
- (3) The response of total sulfate, nitrate and ammonium to a combined NO_x and SO_2 -20% perturbation can be approximated by the sum of the responses to the individual perturbations, i.e. $\text{P1} \approx \text{P2} + \text{P3}$ (Fig. 2d). Scatterplots of P1 versus P2+P3 responses for the regional averaged individual secondary products and total inorganic $\text{PM}_{2.5}$ are shown in Fig. S7.1 of the SI.

From the combined [$\text{SO}_2 + \text{NO}_x$] perturbation (P1), and the separate SO_2 perturbation simulations (P2), both available for all source regions, the missing NO_x SR matrices have been gap-filled using (P1 - P2). By lack of simulations for combined ($\text{SO}_2 + \text{NH}_3$) or ($\text{NO}_x + \text{NH}_3$) perturbations we assume additivity for simultaneous NH_3 , SO_2 and NO_x perturbations, i.e. the response is computed from a linear combination of P2, P3 and P4.

Next we evaluate the hypothesis that the -20% perturbation responses can be extrapolated towards any perturbation range, as an approximation of a full TM5 simulation. Figure 3 shows, for the selected regions listed in Table S3 of the SI, the TM5

Deleted: in particular regarding

Deleted: issue

Deleted: issue

Deleted: with

Deleted: compared

Deleted: ,

Deleted: while

Deleted: only

Deleted: results

Deleted: Note that

Deleted: Germany as individual source region was evaluated as well, as a case-study with significant emissions and potentially large non-linearities. In general we find that P3 gives a minor response on sulfate, and similar for P2 on nitrate, in general one order of magnitude lower than the direct formation of SO_4^{2-} and NO_3^- from SO_2 and NO_x respectively (Fig. 2). We also find that the -20% perturbations of both precursors behave in an additive manner for what concerns the formation of secondary $\text{PM}_{2.5}$, i.e. $d\text{SO}_4^{2-}/d[\text{SO}_2 + \text{NO}_x] \approx d\text{SO}_4^{2-}/d\text{SO}_2 + d\text{SO}_4^{2-}/d\text{NO}_x$, and similar for NO_3^- and NH_4^+ in $\text{PM}_{2.5}$ (Fig. 2), i.e. $\text{P1} \approx \text{P2} + \text{P3}$. Scatterplots between P1 and P2+P3 for the individual secondary products and total inorganic $\text{PM}_{2.5}$ are shown in Fig. S7.1 of the SI. Hence, from the combined [$\text{SO}_2 + \text{NO}_x$] perturbation (P1), and the separate SO_2 perturbation simulations (P2), which are both available for all source regions, the missing NO_x SR matrices can be gap-filled using (P1 - P2).

Deleted: larger

Deleted: ranges

5 computed relative change in secondary PM_{2.5} concentration versus the relative change in precursor emission in the range [-80%, +100%]. The figure illustrates the general near-linear behaviour of regionally aggregated responses to single precursor emission perturbations for all regions, except for India where the linearity of the response to NO_x emissions breaks down for emission reductions beyond -50%. For India we further observe a relative strong nitrate response to NO_x emissions, with NO₃ increasing by a factor of 3 for a doubling of NO_x emissions, although the responses shown in Fig. 2 indicate that absolute changes (in µg m⁻³) in NO₃ are relatively low and that secondary PM_{2.5} in this region is dominated by SO₄. We are not aware of reliable observations or other published NO_x-aerosol sensitivity studies from that region that could corroborate this calculated sensitivity. Because such a feature may strongly affect projected future PM_{2.5} levels and associated impacts, we recommend regional multi-model studies devote attention this feature.

10 Because the TM5-FASST linearization is based on the extrapolation of the -20% perturbation slope, concave-shaped trends in Fig. 3 indicate a tendency of TM5-FASST to over-predict secondary PM_{2.5} at large negative or positive emission perturbations, and opposite for convex-shaped trends. Figure 4 illustrates the error introduced in regional secondary PM_{2.5} concentrations responses when linearly extrapolating the regional -20% perturbation sensitivities to -80% (blue dots) and +100% (red dots) perturbations respectively. While the scatter plots for the single perturbations (Fig. 4 a,b,c) evaluate the linearity of the single responses, the panel showing the combined (SO₂+NO_x) perturbation (Fig. 4d) is a test for the linearity combined with additivity of SO₂ and NO_x perturbations over the considered range. In general, the linear approximation leads to a slight over-prediction of the resulting secondary PM_{2.5} (i.e. the sum of sulfate, nitrate and ammonium) for all regions considered, in either perturbation direction. Table 4 shows regional statistical validation metrics (normalized mean bias NMB [%], mean bias MB [µg m⁻³], and correlation coefficient, definitions are given in the Table Notes) for the grid-to-grid comparison between TM5-FASST and TM5-CTM of the response to the [-80%, 100%] perturbation simulations (with Europe presented as a single region).

20 In terms of NMB, the FASST linearisation performs worst for the NO_x perturbations, with almost a factor 2 overestimate in Japan for an emission doubling. However, because of the already low NO_x emissions in this region, the absolute error (MB) remains below 0.2µg m⁻³. In all considered perturbation cases, FASST shows a positive MB, except for the NO_x perturbation in India. In general, the highest NMB are observed for the regions where secondary PM_{2.5} shows low response sensitivity to the applied perturbations and where the impact on the total PM_{2.5} is therefore relatively low. Indeed, when considering the total resulting secondary PM_{2.5} (i.e. the full right-hand side of Eq. 2, including the PM_{2.5} base-concentration term containing primary and secondary components), regional averaged FASST secondary PM_{2.5} values stay within 15% of TM5 (see Table S7.1 of the SI). A break-down for the individual receptor regions within the European zoom region of the linearisation error on the resulting total secondary PM_{2.5} from individual and combined precursor perturbations is shown in Fig. S7.3 of the SI.

Deleted: components, normalized to the base

Deleted: , as a function of

Deleted: perturbation

Deleted: [%] relative to the base emission.

Deleted: response

Deleted: towards

Deleted: Linear

Deleted: responses (i.e. the TM5-FASST approach) towards

Moved (insertion) [3]

Deleted: perturbations

Deleted: (Fig. 4).

Moved up [3]: While the scatter plots for the single perturbations (Fig. 4 a,b,c) evaluate the linearity of the single responses, the

Deleted: plot showing the combined (SO₂+NO_x) perturbation (Fig. 4d) is a test for the linearity combined with additivity of FASST. For the -80% perturbation from the base case, the linearized result is within 12%, 19% and 30% of the full TM5 outcome for the single SO₂, NO_x and NH₃ perturbations respectively, and within 21% of TM5 for the combined (SO₂ + NO_x) perturbation. The response to a doubling of the base emissions is within 13%, 45% and 12% of the full TM5 outcome for the single SO₂, NO_x and NH₃ perturbations respectively, and within 34% of TM5 for the combined (SO₂ + NO_x) perturbation.

3.1.2 Additivity and linearity of O₃ responses to combined precursor emissions

O₃ atmospheric chemistry is in general highly non-linear, displaying a response magnitude and sign depending on the concentration ratio of its two main ozone precursors NO_x and NMVOC, with high VOC/NO_x ratios corresponding to NO_x-sensitive chemistry and low VOC/NO_x ratios corresponding to VOC-sensitive chemistry (Seinfeld and Pandis, 1998; Sillman, 1999). ~~Because the NO_x/NMVOC ratio determines the O₃ response to emission changes,~~ a perturbation with simultaneous NO_x and NMVOC emission changes of the same relative size is expected to behave more linearly than single perturbations since the chemical regime remains similar. The FASST reduced-form approach builds on the assumption that the O₃ response to combined precursor perturbation can be ~~approximated~~ by the sum of the single component emission perturbations (additivity hypothesis). This is in particular relevant for combined and individual NO_x and NMVOC perturbations, and to a less extend for the (SO₂, NO_x) combination.

~~Although the impact of SO₂ chemistry on O₃ is low,~~ for gap-filling purposes we first evaluate the additivity hypothesis for the combined (SO₂ + NO_x) perturbation. Comparing experiments P1 (SO₂ + NO_x perturbation), P2 (SO₂ perturbation) and P3 (NO_x perturbation) confirms that the ozone response to SO₂ emissions is marginal and additive to the response to NO_x (P1 ≈ P2+P3) over the full range of perturbations, as shown in Fig. S7.2 in the SI, and hence we can ~~gap-fill~~ the missing NO_x perturbation SR matrix for all source and receptor regions from ~~P3 ≈ P1 - P2~~.

Next, we evaluate whether the O₃ response ~~to~~ the combined NO_x + NMVOC perturbation (P5) can be approximated by the sum of O₃ responses to individual NO_x (P3) and NMVOC (P4) perturbations, i.e. assuming P5 = P4 + P3. P5 was obtained for a limited set of representative source regions: Europe (by perturbing precursor emissions from all FASST source regions inside the EUR master zoom region simultaneously), China, India and USA. As shown in Fig. 5, ~~for the -20% perturbations~~ we find good agreement between the combined (NO_x + NMVOC) perturbation (open circles) with the sum of the individual precursor perturbation (black dots). This occurs even in situations where titration by NO₂ causes a reverse response in O₃ concentration as is the case in most of ~~Europe and the USA, indicating that a -20% perturbation in individual precursors appears not to change the prevailing O₃ regime.~~ ~~However~~ extending the O₃ (and metrics) linearized responses as a sum of scaled individual -20% precursor responses towards more extreme perturbation ranges could be a challenge, as the individual perturbation of one of the (NO_x, NMVOC) precursor may change the ozone formation regime. In particular during winter time, titration of O₃ under high NO_x conditions may reverse the slope of the NO_x emission – O₃ concentration response. ~~On the other hand,~~ the impact-relevant O₃ metrics, both health and crop related, are based on summertime and daytime values and are expected to ~~be less affected by titration and consequently to maintain a positive emission-response slope~~ (Wu et al., 2009).

Figure 6 shows that, while the response to NMVOC (with constant NO_x) is near-linear and monotonically increasing over the full range for all regions, the NO_x response (with constant NMVOC) is showing a more complex behaviour, exhibiting a negative slope for annual mean O₃ over nearly all European regions and the USA, ~~whereas the slope is~~ positive for India and

Deleted: The relative errors by region for the [-80%,+100%] perturbation range for individual and combined precursor perturbations versus total PM_{2.5} (primary +secondary) are shown in Fig. S7.2 of the SI, showing that in nearly all cases, the error on total resulting PM_{2.5} from a simultaneous perturbation on all 3 precursors is higher for a -80% emission reduction than for a doubling of emissions. In nearly all cases, the FASST linearization leads to an over-prediction of total PM_{2.5}, by between 0% and +30%. This information is relevant in view of the general tendency for further emission reduction in developed countries, compared to growing emission in developing regions. ¶

Deleted: However

Deleted: approached

Deleted: ,

Deleted: 3

Deleted: (

Deleted: -

Deleted:).

Deleted: from

Deleted: 5, also here

Deleted: Europa and the USA. ¶

Deleted: However

Deleted: behave more linearly

Deleted: Indeed, as shown in Fig.

Deleted: while

China. For the health-relevant exposure metric 6mDMA1 and the crop metric M12 the slope is positive in most regions, due to their implicit constraint to the summer season when titration plays a minor role, except in strongly NO_x-polluted North-Western European countries (Great Britain, Germany, Belgium and The Netherlands, as well as Finland) where titration in large urbanized areas remains important even during summer. The concave shapes of the response curves indicate significant non-linearities, in particular for responses of crop and health exposure metrics to strong NO_x emission perturbations.

Figure 7 illustrates the performance of the TM5-FASST approach versus TM5 for regional mean annual mean ozone, health exposure metric 6mDMA1 (both evaluated as population-weighted mean), and for the crop-relevant exposure metrics AOT40 and M12 (both evaluated as area-weighted mean) over the extended emission perturbation range. In most cases the response (i.e. the change between base and perturbed case) to emission perturbations lies above the 1:1 line across the 4 metrics, indicating that FASST tends to over-predict the resulting metric (as a sum of base concentration and perturbation).

Of the four presented metrics, AOT40 is clearly the least robust one, which can be expected for a threshold-based metric that has been linearized. Tables 5 to 7 give the statistical metrics for the grid-to-grid comparison of the perturbation term between FASST and TM5 for the health exposure metric 6mDMA1, and crop exposure metrics AOT40 and M12, respectively. Statistical metrics for the total absolute concentrations (base concentration + perturbation term) are given in Tables S7.2 to S7.4 in the SI. As anticipated, the NO_x-only perturbation terms are showing the highest deviation, in particular for a doubling of emissions, however combined NO_x-NMVOC perturbations are reproduced fairly well for all regions, staying within 33% for a -80% perturbation for all 3 exposure metrics, and within 38% for an emission doubling for 6mDMA1 and M12, while the AOT40 metric is overestimated by 76 to 126% for emission doubling. The total resulting concentration over the entire perturbation range for single and combined NO_x and NMVOC perturbation agrees within 5% for 6mDMA1 and M12, and within 64% for AOT40. The mean bias is positive for both perturbations, for all metrics and over all analysed regions, except for crop metric M12 under a doubling of NMVOC emissions over Europe showing a small negative bias. The deviations for individual European receptor regions under single and combined NMVOC and NO_x perturbations for health and crop exposure metrics are shown in Figs. S7.4 to S7.6 of the SI.

3.2 TM5-FASST_v0 versus TM5 for future emission scenarios

In this section we evaluate different combinations of precursor emission changes relative to the base scenario in a global framework. We take advantage of available TM5 simulations for a set of global emission scenarios which differ significantly in magnitude from the FASST base simulation, and as such provide a challenging test case to the application of the linear source-receptor relationships used in TM5-FASST. We assume that the full TM5 model provides valid evaluations of emission scenarios, and we test to what extent these simulations can be reproduced by the linear combinations of SRs implemented in the TM5-FASST_v0 model.

We use a set of selected policy scenarios prepared with the MESSAGE integrated assessment model in the frame of the Global Energy Assessment GEA (Rao et al., 2012, 2013; Riahi et al., 2012). These scenarios are the so called “frozen

Deleted: M6M

Deleted: reverses to

Deleted:).

Deleted: (linearly extrapolated sum of individual responses)

Deleted: the normalized

Deleted: O₃ concentration responses to combined NMVOC and NO_x perturbations for

Deleted: M6M,

Deleted: reductions down to -80% is generally underestimated by 13% – 17%

Deleted: . For a doubling of the combined precursor emissions, the

Deleted: approach

Deleted: estimates the response by 20% for annual O₃, 36% for M12, 50% for M6M and more than a factor 2 for AOT40.

Deleted: However, for

Deleted: other

Deleted: even

Deleted: strong titration effect, leading

Deleted: reduced O₃ under doubling of NO_x emissions, is still relatively-well reproduced in the reduced-form approach. Table 3 gives the relative error on the resulting estimated metrics (relative to the TM5 outcome) for individual and combined precursor perturbations. ¶ The relative errors by individual region for the evaluated NO_x emission perturbation (...)

Deleted: M6M

Deleted: are within [1%, 12%] and [-3% ...]

Deleted: , while the least robust metric (...)

Deleted: responses are solely related to (...)

Deleted: , both additivity and (...)

Deleted: annual O₃, M6M,

Deleted: and AOT40 respectively

Deleted: compare

Deleted: -FASST_v0 results with TM5 (...)

Deleted: which used the 2000 emissions

Deleted: challenge

Deleted: e

legislation” and “mitigation” emission variants for the year 2030 (named ~~FLE2030~~, ~~MIT2030~~ respectively), policy variants that describe two different policy assumptions on air pollution until 2030. These scenarios and their outcomes are described in detail in Rao et al. (2013), the scope of the present study is the inter-comparison between FASST and TM5 resulting pollutant concentration and exposure levels, as well as associated health impacts.

Major scenario features and emission characteristics are provided in section S8 of the SI. Table S8.1 shows the change in global emission strengths for the major precursors for both test scenarios, relative to the RCP2000 base, aggregated to the FASST ‘master zoom’ regions listed in Table S2.2. Emission changes for the selected scenarios mostly exceed the 20% emission perturbation amplitude from which the SRs were derived. Under the MIT2030 low emission scenario, all precursors and primary pollutants (except primary PM_{2.5} in East-Asia and NH₃ in all regions) are showing a strong decrease compared to the RCP2000 reference scenario. The strongest decrease is seen in Europe (NO_x: -83%, SO₂: -93%, BC: -89%, primary PM_{2.5} – 56%) while NH₃ is increasing by 14 to 46% across all regions. The FLE2030 scenario displays a global increase for all precursors, however with heterogeneous trends across regions. In Europe, North-America and Australia, the legislation in place, combined with use of less and cleaner fuels by 2030, leads to a decrease in pollutant emissions except for NH₃ and primary PM_{2.5}. On the other hand, very substantial emission increases are projected in East and South-East for BC, NO_x and primary PM_{2.5}. Anticipating possible linearity issues, we note that for both scenarios, in all regions, SO₂ and NO_x emissions are evolving in the same direction, although not always with similar relative changes, whereas NH₃ is always increasing, which may induce linearity issues in the ammonium-sulfate-nitrate system. Regarding O₃ metrics, NMVOC and NO_x are evolving in the same direction, but also here we observe possible issues due to a changing emission ratio (in particular in Russia and Asia). We further note that not only the emission levels of these scenarios are different from the FASST base scenario (RCP year 2000), but also the spatial distribution of the emissions, at the resolution of grid cells, may differ from the reference set.

We use FASST to compute PM_{2.5} and ozone concentrations applying Eq. (2), i.e. considering the ~~FLE2030~~ and ~~MIT2030~~ emission scenarios as a perturbation on the FASST reference emission set (RCP year 2000).

The scope of TM5-FASST is to evaluate on a regional basis the impacts of policies that affect emissions of short-lived air pollutants and their precursors. Hence we average the resulting O₃ and PM_{2.5} concentration and O₃ exposure metric ~~6mDMA1~~ over the each of the 56 FASST regions and compare them with the averaged TM5 results for the same regions.

Further, in a policy impact analysis framework, the change in pollutant concentrations between two scenarios (e.g. between a reference and policy case) is often more relevant than the absolute concentrations. We therefore present absolute concentrations, as well as the change (delta) between the two GEA scenarios, evaluating the benefit of a mitigation scenario versus the frozen legislation scenario.

Figure 8 shows the FASST versus TM5 regional scatter plots for absolute and delta population-weighted mean anthropogenic PM_{2.5} for all 56 FASST receptor regions while the population-weighted means over the 9 larger zoom areas

Deleted: FLE-2030, MIT-2030

Moved (insertion) [4]

Deleted: Major features and emission characteristics are provided in section S8 of the SI.

Deleted: equation

Deleted: FLE-2030

Deleted: MIT-2030

Deleted:) from which the TM5-FASST source-receptor matrices were derived. Table S8 in the SI shows (using larger world regions aggregated from the FASST source regions) the change in global emission strengths for the major precursors for both test scenarios, relative to the base scenario on which the SR perturbations were applied.

Moved up [4]: Emission changes for the selected scenarios mostly exceed the 20% emission perturbation amplitude from which the SRs were derived.

Deleted: Under the MIT-2030 scenario, all precursors and primary pollutants – except NH₃ and primary PM_{2.5} in Asia – are showing a strong decrease compared to the RCP year 2000 reference scenario. The FLE-2030 scenario displays a global increase for all precursors, however with heterogeneous trends across regions, with only Asia undergoing consistently increasing emissions for all pollutants. In other regions (e.g. OECD, Reforming Economies), despite stagnating air pollution controls, emissions decline due to the use of less and cleaner fuels project for 2030. (...)

Deleted: M6M

Deleted: Figure 8 and 9 show the FASST versus TM5 regional scatter plots for PM (...)

Deleted: In such a set-up, TM5-FASST_v0 is performing better: while it (...)

Deleted: PM_{2.5}

Deleted: ,

Deleted: in regional PM_{2.5}

Deleted: scenarios is underestimated by 5% on

Deleted: average, with R² of 0.97 (Table 4 and Fig. S8.1).

Deleted: O₃ metrics (annual mean O₃ concentration and M6M) are, both for th (...)

are shown in Figure 9. Similarly annual mean population-weighted O₃ and 6mDMA1 scatter plots are shown in Fig. 10, and the regional distribution in Fig. 11. The grid-cell statistics (mean, NMB, MB and R²) over larger zoom areas are given in Tables 8 and 9 for PM_{2.5} and 6mDMA1 respectively.

Figure 8 and Table 8 show that on a regional basis, the low emission scenario generally overestimates population-weighted PM_{2.5} concentrations, with the highest negative bias in Europe and Asia, while the lowest deviation is found in Latin America and Africa. The agreement between FASST and TM5 is significantly better for the high emission scenario, in line with the findings in the previous section. As shown in Table 8, averaged over the larger zoom regions, we find that the relative deviation for PM_{2.5} is within 11% for FLE2030, and within 28% for MIT2030, except for Europe where the (low) PM_{2.5} concentration is overestimated by almost a factor of 2. The policy-relevant delta between the scenarios however is for all regions reproduced within 23%.

The ozone health metric 6mDMA1 is more scattered than annual mean ozone, and also here, as expected, the low emission scenario performs worse than the high emission one. Over larger zoom areas however the agreement is acceptable for both scenarios (FASST within 22% of TM5). Contrary to PM_{2.5}, the NMB for the delta 6mDMA1 between two scenarios is higher than the NMB on absolute concentrations, with a low bias for the delta metric of -38% and -45% for Europe and North-America respectively, and a high bias of 35 to 46% in Asia. However, the MB on the delta is of the same order or lower than the absolute concentrations (Table 9). This is a consequence of the fixed background ozone in the absolute concentration reducing the weight of the anthropogenic fraction in the relative error.

Figures 9 and 11 provide a general picture of the performance of FASST: despite the obvious uncertainties and errors introduced with the FASST linear approximation for large emission changes compared to the RCP base run, at the level of regionally aggregated concentrations, a consistent result emerges both for absolute concentrations from the individual scenarios as for the policy-relevant delta.

A major issue in air pollution or policy intervention impact assessments is the impact on human health; therefore we also evaluate the TM5-FASST outcome on air pollution premature mortalities with the TM5-based outcome, applying the same methodology on both TM5 and FASST outcomes. We evaluate mortalities from PM_{2.5} using the IER functions (Burnett et al., 2014) and O₃ mortalities using the log-linear ER functions and RR's from Jerrett et al. (2009) respectively. Figure 12 (PM_{2.5}) and Fig. 13 (O₃) illustrate how FASST-computed mortalities compare to TM5, both as absolute numbers for each scenario, as well as the delta (i.e. the health benefit for MIT2030 relative to FLE2030). Regional differences in premature mortality numbers are mainly driven by population numbers. In line with the findings for the exposure metrics (PM_{2.5} and 6mDMA1) FASST in general over-predicts the absolute mortality numbers, in particular in the low-emission case. For MIT2030, global PM_{2.5} mortalities are overestimated by 19%, in Europe and North-America FASST even by 43%. In the FLE2030 case, we find a better agreement, with a global mortality over-prediction of 3% (for Europe and North-America 5% and 11% respectively). For the latter scenario, the highest deviation is found in Latin America (10 – 20%). O₃ mortalities are

Deleted: _v0

Deleted: pollution sets.

Deleted: Figures 10 and 11 show scatterplots of FASST against TM5 mortalities for PM_{2.5} and ozone respectively, as well as total mortalities for major world regions. The latter show that the difference between FASST and TM5 results is smaller than the uncertainty on the mortalities resulting from the uncertainty on RR's only.

overestimated globally by 11% (7%) with regional agreement within 20% (14%) for MIT2030 (FLE2030). However, as shown by the error bars, the difference between FASST and TM5 is smaller than the uncertainty on the mortalities resulting from the uncertainty on RR's only. The potential health benefit of the mitigation versus the non-mitigation scenario (calculated as FLE2030 minus MIT2030 mortalities) is shown in Figs. 12c and 13c. Globally, FASST underestimates the reduction in global PM_{2.5} mortalities by 17% with regional deviations ranging between -30% for Europe and North-America, and -12% for India. The global health benefit for ozone is underestimate by 2% for O₃, however as a net result of 11% overestimation in India and 12 to 59% underestimation in the other regions. The numbers corresponding to Figs. 12 and 13 are provided in Table S8.4 and S8.5 of the SI.

The error ranges presented here are obviously linked to the choice of the test scenarios and will for any particular scenario depend on the magnitude and the relative sign of the emission changes relative to RCP2000, but given the amplitude of the emission change for the currently two selected scenarios relative to RCP2000, these results support the usefulness of TM5-FASST as a tool for quick scenario screening.

3.3 Comparison of TM5-FASST_v0 impact estimates with published studies

In this section we evaluate TM5-FASST_v0 outcomes for a number of key impacts (climate metrics, human health and O₃ damage to crops) with results from earlier studies in the literature.

Deleted: confront

Deleted: and

3.3.1 Year 2000 total global anthropogenic forcing by component

The most widely published radiative forcing estimates compare the present-day with the pre-industrial time. To simulate pre-industrial, for simplicity in our TM5-FASST_v0 evaluation we set all anthropogenic in the base simulation (RCP year 2000) to zero and calculate the change in forcing compared to the base case. We include forcing from all aerosol components, as well as CH₄ (including its feedback on O₃) and the short and long term forcing impacts of NO_x, NMVOC and CO on ozone and the methane lifetime. Figure J4 shows the anthropogenic forcings derived from TM5-FASST by emitted component, together with results from AR5 (year 1750-2011). We find that, except for BC, TM5-FASST_v0 reproduces, within the uncertainties reported by IPCC AR5, the global forcing values by emitted component. Only our estimated BC forcing (0.15 W/m²) falls just outside the AR5 90% confidence interval (0.23, 1.02) W/m², which can be partly explained by the different emission years used in the inter-comparison (also explaining the relatively low estimate for CH₄). However, comparing to another widely used literature source (Bond et al., 2013), the TM5-FASST_v0 BC forcing estimate still falls within the 90% CI (0.08, 1.27) W/m² direct radiative forcing given for the year 2005, with a comparable global BC emission rate. Our low-end BC forcing estimate can be partly explained by the simplified treatment as externally mixed aerosol, without accounting for the enhancement of the mass absorption cross-section when BC particles become mixed or coated with scattering components. Not-included snow albedo and indirect cloud effects would contribute with +0.13 (+0.04 to +0.33) W/m² and +0.23 (-0.47 to +1.0) W/m² respectively (Bond et al., 2013).

Deleted: 12

Deleted: by

Deleted: (Bond et al., 2013).

A break-down of the forcing contributions of each emitted pollutant to aerosol, ozone (including immediate and long-term response modes) and methane (when applicable) forcing is given in Table S6.6 of the SI, together with the respective AR5 central values. **Although** there are very large uncertainties associated with the estimates of the indirect aerosol effect due to the strong approximations made in this work, the calculated magnitude (-0.81 W/m²) is in agreement with the published literature range -0.55 W/m² 90% CI (-1.33, -0.06) W/m².

Deleted: While

Table 10 compares the contribution of anthropogenic O₃ precursors CH₄, NO_x, NMVOC and CO to the O₃ and CH₄ radiative forcing with earlier work (Shindell et al., 2005, 2009; Stevenson et al., 2013). Except for NO_x which shows a large scatter across the studies, the FASST computed contributions to global O₃ and CH₄ forcing - using the same year 1850 to 2000 emission changes as in Stevenson et al. (2013) - are in good agreement with the model ensemble range in the latter study. FASST NO_x forcing contributions are a factor 3 lower than in the Stevenson et al. study and more in line with Shindell et al. (2005, 2009) values (based on the period 1750 – 2000), however the latter obtain a NMVOC contribution to O₃ forcing which is a factor of 5 to 6 lower than the other estimates. Differences across the studies are likely due to differences in oxidation chemistry and lifetimes across models.

Deleted: 5

Deleted: , who used different emission sets than RCP. Our O₃ and CH₄ forcing values from CH₄ and NO_x coincide particularly well with the values obtained by Shindell et al. (2005, 2009)

Deleted: the O₃ forcing derived from CH₄ obtained by Shindell et al. (2009) which is 37% higher in their study. In contrast, our estimates of the (less important) CO and NMVOC

Deleted: O₃ forcing result to be higher by a factor 1.9 and 1.5 for CO and NMVOC respectively compared to and by a factor 2.3 and 7.6 respectively compared to Shindell et al. (2009). The same observation can be made for the contribution of CO and NMVOC to CH₄ forcing, where we find excellent

Deleted: between our results and the two earlier studies by Shindell et al., while our estimates of the

Deleted: from CO and NMVOC

Deleted: a factor 1.5 and 2.2 higher compared to , essentially due to difference in OH levels

3.3.2 Regional forcing efficiencies by emitted component

Earlier work in the frame of HTAP1 (Fry et al., 2012; Yu et al., 2013) and HTAP2 (Stjern et al., 2016) evaluated regional forcing efficiencies for larger regions than the ones defined for FASST. For a comparison we aggregate the FASST forcing efficiencies (as listed in section S6.3 of the SI) by making an emission-weighted averages over Europe (EUR), North-America (NAM), South-Asia (SAS), East-Asia (EAS), Mediterranean and Middle East (MEA) and Russia, Belarus and Ukraine (RBU). Tables 11 (PM precursors) and 12 (NO_x, NMVOC and CO) show the earlier studies along with the FASST results. The FASST forcing efficiencies for PM precursors confirm our earlier observation that FASST is particularly biased low for BC, in particular compared to Stjern et al. (2016), but further compares relatively well with the earlier work, in particular with Yu et al. (2013) which was based on a year 2001 baseline, similar to conditions of our base scenario. A similar observation is made for the regional O₃ precursors for which FASST forcing efficiencies correspond within 1 standard deviation to the study by Fry et al. (2012) except for South- and East-Asia where FASST falls within 2 standard deviations.

3.3.3 Direct radiative forcing of short-lived climate pollutants by sector

The segregation of the RCP reference emission inventory by sector enables the evaluation of the contribution of individual sectors to the global instantaneous forcing. This is achieved by ‘switching off’ the respective sectorial emissions in the base emission scenario one by one, and comparing the resulting ΔForcing with the reference case. In Fig. 15 we compare the total

and sector-attributed direct radiative forcing with Unger et al. (2010) who made a similar evaluation for the year 2000 based on the EDGAR Fast Track 2000 emission inventory (Olivier et al., 2005). Figure 15b shows the break-down by forcing component, including the direct contributions by aerosols, by short-lived precursors to O₃ (SLS S-O₃), their indirect effect on CH₄ (SLS I-CH₄) and associated long-term O₃ (SLS M-O₃), as well as CH₄ forcing from direct CH₄ emissions and its associated feedback on background ozone (CH₃ O₃). Fig. 15a separates the contributions by emission sector. Since different inventories are used, we do not expect a perfect match between the two analyses, however the emerging picture, in terms of over-all contribution by emitted component, as well as the contribution by sector is very similar, underlining the applicability of the TM5-FASST tool for this type of analysis in a consistent framework with other types of impacts. In general, BC forcing as well as the short-term O₃ forcing by NO_x and NMVOC (SLS-O₃) are consistently lower for FASST, while the indirect feedbacks on CH₄ and long-term O₃ are corresponding well. This is also the case for the direct forcing by inorganic aerosols and POM. The higher direct CH₄ forcing and its feedback on O₃ by Unger et al. (2010) can be attributed to higher emissions in particular in the agricultural and waste – landfills sectors.

3.3.4 GWP and GTP

We use the methodology described in section 2.7.4 to evaluate global GTP and GWP for different time horizons H (20y and 100y) and compare with the range of values given in IPCC AR5 (Myhre et al., 2013). We recall that the forcings used to compute the FASST metrics, based on the meteorological year 2001 and RCP year 2000 emissions, are region-specific and take into account differences in atmospheric life time and surface albedo. As shown in Table 13 we find an over-all good agreement with AR5 values. TM5-FASST BC metrics are at the low end of the IPCC range, in line with the previously made observation regarding the low FASST BC forcing. For the NO_x metrics we have separately reported the strongly different ranges from Fuglestvedt et al. (2010) and Shindell et al. (2009). Our values for NO_x appear to be more in line with the former study, except for GWP20 where FASST gives a negative value (-31), whereas AR5 reports a range (12, 26) from Fuglestvedt et al. (2010) and (-440, -220) from Shindell et al. (2009).

3.3.5 Health impacts

Present-day health impacts

Table 14 gives an overview of recent global PM_{2.5} health impact studies, together with FASST estimates for the year 2000 (RCP) and year 2010 (HTAP2 scenario). The studies differ in emission inventories and year evaluated, in applied methodologies to estimate PM_{2.5} exposure, in model resolution, as well as in the choice of the exposure response functions, the value of the minimum exposure threshold, and mortality statistics. Studies excluding natural dust from the exposure are mostly applying the log-lin exposure response function and RR from Krewski et al. (2009), and estimate between 1.6 and 2.7 million annual premature mortalities from PM_{2.5} in scenario years 2000 to 2004. FASST returns 2.1 and 2.5 million deaths

Deleted: 13b

Deleted: (where we separated

Deleted: and indirect

Deleted: and

Deleted:), while the

Deleted: 13a shows

Deleted: 6

Deleted: were

Deleted: and

Field Code Changed

using the GBD and log-lin exposure functions respectively. Studies including mineral dust are mostly applying the GBD integrated exposure-response functions and a non-zero threshold to avoid unrealistically high relative risk rates at high PM_{2.5} levels in regions frequently exposed to dust. Depending on the choice of the exposure-response function and scenario year, FASST obtains 2.6 to 4.1 million global deaths, comparable with the range 1.7 to 4.2 million from previous studies.

Global ozone mortalities reported in Table 15 have been commonly based on the Jerrett et al. (2009) methodology, implemented in FASST. FASST obtains 197 thousand and 340 thousand deaths for RCP 2000 and HTAP2 2010 scenarios respectively, while the earlier studies find 380 to 470 thousand deaths in 2000, and 140 to 250 thousand in 2010 – 2015. Differences can be attributed to model chemical and meteorological processes, emission inventories, and the use of different sources for respiratory base mortality statistics.

Both for PM_{2.5} and O₃, the difference between the different studies falls within the combined RR uncertainty and model variability range.

Health impacts in future scenarios: intercomparison with ACCMIP model ensemble

The health impact analysis of the RCP scenarios performed with the Atmospheric Chemistry and Climate Model Intercomparison Project (ACCMIP) model-ensemble (Silva et al., 2016), provides a useful test case for the ability of TM5-FASST to reproduce trends derived from emission scenarios. The ACCMIP ensemble consisted of 14 state-of-the-art global chemistry climate models with spatial resolution from 1.9°x1.2° to 5°x5°. The ACCMIP models simulated future air quality for specific periods through 2100, for four global greenhouse gas and air pollutant emission scenarios projected in the Representative Concentration Pathways (RCPs). The analysis by Silva et al. (2016) used the same methodology implemented in FASST for estimating premature mortalities from PM_{2.5} and O₃ (i.e. Burnett et al., 2014 as in the Global Burden of Disease study and Jerrett et al., 2009 respectively), with the small difference that it does not include Acute Lower Respiratory Infections (ALRI) as a cause of death (in FASST applicable to age group below 5 years only) and the evaluated age group is >25 years old while in TM5-FASST this was done for population older than 30 years. Further, the ACCMIP health impact analysis uses scenario-specific projections for population and cause-specific base mortalities while FASST uses the same population projections and mortality rates, as described in the methods section, across all scenarios.

Following the approach of Silva et al. (2016), we compare the global population-weighted annual mean PM_{2.5} concentration change and ozone exposure metric $\int \text{mDMA1}$ relative to year 2000 concentrations for RCP scenarios 2.6, 4.5 and 8.5 for the years 2030 and 2050, with year 2000 exposure evaluated over the population of the respective scenario years (Tables S2 and S3 in Silva et al., 2016). Figure 16 shows the results from the ACCMIP model ensemble as well as individual model results along with TM5-FASST outcome. We make the evaluation with and without the urban increment parameterization included (using the generic increment factors from Table S4.2). We find that TM5-FASST qualitatively reproduces PM_{2.5} trends between 2030 and 2050 for the selected RCP scenarios although in only 2 of the 6 considered scenarios the TM5-FASST

Deleted: as

Deleted: as in TM5-FASST

Deleted: death

Deleted: ,

Deleted: M6M

Deleted: .

Deleted: 14

Deleted: (i.e. the slope)

concentration relative to year 2000 falls within the ACCMIP ensemble range. Even without urban increment correction, TM5-FASST consistently gives higher PM_{2.5} exposure levels than ACCMIP (higher by 0.9, 1.5 and 1.0 µg m⁻³ in 2030 and 0.7, 1.3 and 0.9 µg m⁻³ in 2050 for RCP 2.6, 4.5 and 8.5 respectively). **Apart from our previous finding that FASST tends to overestimate PM_{2.5} levels compared to a full chemistry-transport model, an additional** plausible explanation is the underlying higher spatial resolution in FASST (1°x1°) than any of the ACCMIP models. Including the urban increment increases the global mean change in exposure relative to year 2000 with an additional 0.1 to 0.6 µg m⁻³.

Deleted: A

The ozone exposure metric **6mDMA1** falls within the range of the ACCMIP model ensemble for 2030 - 2050, but the slope between 2030 and 2050 is lower than for the ACCMIP ensemble mean, **i.e. FASST shows a lower response sensitivity for O₃ to changing emissions between 2030 and 2050 than the ACCMIP models (-1ppb from 2030 to 2050 in FASST, versus -3ppb for the ACCMIP mean).** Given our previous observation that FASST reproduces TM5 relatively well, this indicates that inter-model variability is a stronger factor in the model uncertainty than the reduced-form approach.

Deleted: M6M

Deleted: . In the light of the previously demonstrated satisfactory performance of

The trends from 2000 to 2050 in global mortality burden from PM_{2.5} and O₃ are shown in Figure **J7**. Assuming that the relative error for the year 2000 – the only uncertainty range given by Silva et al. (2016) – can be applied on the other cases, we find that TM5-FASST reproduces the ACCMIP health impacts from PM_{2.5} within the ACCMIP range. Including the urban increment correction increases the mortality by 26% in 2000, 24%, 22% and 17% in 2030, and 32%, 31% and 25% in 2050 for RCP2.6, 4.5 and 8.5 respectively.

Deleted: 15

While **calculated** O₃ mortalities for years 2000 and 2030 are within the ACCMIP range, TM5-FASST does not confirm the strongly increasing O₃ mortalities in the ACCMIP ensemble by 2050. However this difference can be attributed to the use of different baseline mortality statistics, in particular for the year 2050 where FASST, by lack of WHO projections for 2050, assumes year 2030 WHO projected mortality rates whereas Silva et al. (2016) use International Futures (IFs) projections up till 2100. Indeed, the IFs projections (Fig. S7 in the SI of Silva et al., 2016) foresee relative constant global mortality rates (deaths per 1000 people) between 2030 and 2050 for all air pollution-related death causes, except for respiratory disease (on which O₃ mortality estimates are based) which increases with a factor 2.5 globally from 2030 to 2050. An acceptable agreement with the ACCMIP model ensemble outcome is achieved when this effect is included as a simple adjustment factor on the FASST RCP year 2050 O₃ mortalities, as shown by the dot-symbols (year 2050) in Fig. **J7**. **Respiratory mortality is not considered as a cause of death for PM_{2.5}, which explains why a similar disagreement is not observed in the PM_{2.5} mortality trend in Fig. 17b.**

Deleted: also

Deleted: to a large extend

Deleted: and population

A regional break-down of mortality burden from PM_{2.5} in 2030 and 2050, relative to exposure to year 2000 concentrations, for major world regions and for the globe is shown in **Figures S9.1 and S9.2 of the SI. Compared to Fig. 17 which shows the global mortality trends as a combined effect of changing population, mortality rates and pollution level, here the effect of changing population and baseline mortality is eliminated by exposing the evaluated year's population to pollutant levels of the relevant year and to RCP year 2000 levels respectively, and calculating the change between the two resulting mortality**

Deleted: 15.

Deleted: Figure S9. The results demonstrate that FASST has the capacity to deliver the essential regional features. In line with the conclusions drawn from the comparison with the full TM5 model, the results in Figure S9 confirm that FASST

5 numbers. FASST reproduces the over-all observed trends across the regions: we see substantial reductions in North America and Europe in 2030, whereas in East Asia significant improvements in air quality impacts are realized after 2030. For the India region, all scenarios project a worsening of the situation. The global trend is dominated by the changes in East Asia. The observed differences between FASST and ACCMIP ensemble are not insignificant and partly due to different mortality and population statistics in particular for the year 2050, still they are consistent with the findings in the previous section: FASST tends to overestimate absolute PM_{2.5} concentrations for emission scenarios different from RCP2000, and consequently tends to under-predict the benefit of emission reductions, while over-predicting the impact of increasing emissions.

Deleted: pollution

3.3.6 Present day O₃ – crop losses

10 Avnery et al. (2011) evaluate year 2000 global and regional O₃-induced crop losses for wheat, maize and soy bean, based on the same crop ozone exposure metrics as used in FASST, obtained with a global chemical transport model at 2.8°x2.8° resolution. Figure 18 compares their results (in terms of relative yield loss) with FASST (TM5) results based on RCP year 2000 for the globe and 3 selected key regions (Europe, North-America and East Asia). Despite the less-robust quantification of crop impacts from O₃ in a linearized reduced-form model set-up, we find that FASST reproduces the major features and trends across regions and crop varieties. Differences may be attributed to a variety of factors, including model resolution, model O₃ chemistry processes, emissions, definition of crop growing season and crop spatial distribution.

4 Discussion

20 Although the methodology of a reduced-form air quality model, based on linearized emission – concentration sensitivities is not new and has been successfully applied in earlier studies (Alcamo et al., 1990), the concept of directly linking pollutant emission scenarios to a large set of impacts across various policy fields, in a global framework, have made TM5-FASST a highly requested tool in a broad field of applications. HTAP1 showed that TM5 source-receptor results (for the large HTAP1 regions) were in most cases similar to the median model results of more than 10 global models, lending additional trust to the model performance (e.g. Anenberg et al., 2014; Dentener et al., 2010; Fiore et al., 2009). The results in the previous sections have outlined its strengths and weaknesses. The major strength of the tool is its mathematical simplicity allowing for a quick processing of large sets of scenarios or scenario ensembles. An extreme example is the full family of SSP scenarios delivered by all participating Integrated Assessment Models, for decadal time slices up to 2050, constituting a batch of 594 scenarios of which a selection of 124 scenarios was analysed with TM5-FASST in the study by Rao et al. (2017). Further, the tool is unique in having a broad portfolio of implemented impact modules which are evaluated consistently over the global domain from the same underlying pollutant field which creates a basis for a balanced evaluation of trade-offs and benefits attached to policy options.

Deleted: analyzed

On the other hand, the reduced-form approach inevitably encompasses a number of caveats and uncertainties that have to be considered with care and which are discussed in the following sections.

Deleted: .

4.1 Issues related to the reduced-form approach

The reliability of the model output in terms of impacts depends critically on the validity of the linearity assumption for the relevant exposure metrics (in particular secondary components), which becomes an issue when evaluating emission scenarios that deviate strongly from the base and -20% perturbation on which the current FASST SRs are based. The evaluation exercise indicated that non-linearity effects in PM_{2.5} and O₃ metrics in general lead to a higher bias for stringent emission reductions (towards -80% and beyond) than for strong emission increases compared to the RCP2000 base case, but over-all remain within acceptable limits when considering impacts. Indeed, because of the thresholds included in exposure-response functions, the higher uncertainty on low (below-threshold) pollutant levels from strong emission reductions has a low weight in the quantification of most impacts. In future developments the available extended-range (-80%, +100%) emission perturbation simulations could form the basis of a more sophisticated parameterization including a bias correction based on second order terms following the approach by Wild et al. (2012) both for O₃ and secondary PM_{2.5}. The break-down of the linearity at low emission strengths is relevant for O₃ and O₃ exposure metrics as the implementation of control measures in Europe and the US has already substantially lowered NO_x levels over the past decade, gradually modifying the prevailing O₃ formation regime from NO_x-saturated (titration regime) to NO_x-limited (Jin et al., 2017).

Deleted: simulations from

Deleted: SR have been established.

Deleted: previous sections have shown

Deleted: when aggregated at the regional level,

Deleted: .

Ozone impact on agricultural crop production is deemed to be the least robustly quantified impact category included in FASST, in particular when evaluated from the threshold-based AOT40 metric, and has to be interpreted as indicative order-of-magnitude estimate. In an integrated assessment perspective of evaluating trade-offs and benefits of air pollutants scenarios, the dominant impact category however appears to be human health (Kitous et al., 2017; OECD, 2016; UNEP, 2011) where TM5-FASST provides reliable estimates.

Moved (insertion) [5]

Deleted: emissions for arbitrary scenarios analysed with FASST. Having established

Deleted: 'once and for all', the underlying emissions

Deleted: patterns are implicitly fixed

Deleted: source

Deleted: . In other words, for the analysis of arbitrary emission scenarios of the past or the future, the FASST

Deleted: will scale the emissions in each grid cell by the ratio of total region scenario emissions to year 2000 emissions for that region, but it

Deleted: shifting emission patterns of a specific compound compared to the base simulation year 2000 within a single source region

Deleted: be

Another issue for caution relates to the FASST analysis of emission scenarios with spatial distribution that differs from the FASST reference scenario (RCP year 2000). The definition of the source regions when establishing the SR matrices implicitly freezes the spatial distribution of pollutant emissions within each region, and therefore the reduced-form model cannot deal with intra-regional spatial shifts in emissions. In practice this is not expected to introduce large errors as anthropogenic emissions are closely linked to populated areas and road networks of which the extent may change, but much less so the spatial distribution. It can be a problem when going far back in time, when large patterns of migration and land development occurred, while in RCP scenarios relatively simple expansions of emissions into the future did not assume huge shifts in regional emission patterns.

Deleted: It can be expected that newer generation scenarios with dynamic allocation of emission across countries and macro-regions, for which FASST errors will be larger.

The implicitly fixed emission spatial distribution may also become relevant when making a sector apportionment of pollutant concentrations and impacts. Source-Receptor relations are indeed particularly useful to evaluate the apportionment of emission sources (in terms of economic sector as well as source regions) to pollutant levels in a given receptor. However, as

Deleted: is

the TM5-FASST_v0 source-receptor matrices were not segregated according to economic sectors, an emission reduction of 20% for a given source region is implicitly considered as a 20% reduction in all sectors simultaneously. ~~Although~~ the atmospheric chemistry and transport of emissions is in principle independent of the specific source, a difference in the sector-specific SR matrices may occur due to differences in temporal and spatial (horizontal/vertical) distribution of the sources. Therefore apportionment studies on sectors which have a significantly different emission spatial distribution than other sectors in the same region should be interpreted with care. In particular impacts of off-shore flaring cannot be assessed with TM5-FASST because those emissions were not included in the RCP base emissions. ~~This limitation however does not apply to international shipping and aviation for which specific SR matrices have been established.~~

Deleted: While

Comparing to earlier studies and reference data, the performance of TM5-FASST with respect to climate metrics is satisfactory, with the exception of BC forcing which is at the low side of current best estimates. In fact, earlier TM5-FASST assessments where climate metrics were provided (UNEP, 2011; UNEP and CCAC, 2016) applied ~~a uniform~~ adjustment factor of 3.6 on BC forcing, in line with the observation by that many models underestimate atmospheric absorption attributable to BC with a factor of almost 3. In TM5-FASST, an adjustment factor of 3.6 leads to a global forcing by anthropogenic BC of 600 mW m⁻². ~~This tuning factor implicitly accounts for not-considered BC forcing contributions and for a longer BC atmospheric lifetime than implemented in the TM5 model and the resulting FASST SR coefficients.~~

Deleted: an

The current version of TM5-FASST is missing some source-receptor relations which may introduce a bias in estimated PM_{2.5} and O₃ responses upon emission changes. The omission of secondary organic PM in TM5 is estimated to introduce a low bias in the base concentration of the order of 0.1 µg m⁻³ as global mean however with regional levels in Central Europe and China up to 1 µg m⁻³ in areas where levels of primary organic matter are reaching 20 µg m⁻³ (Farina et al., 2010) indicating a relatively low contribution of SOA to total PM_{2.5}. O₃ formation from CO is included in the TM5 base simulations, but no SR matrices for the FASST source region definition are available. Based on the HTAP1 CO perturbation simulations with TM5, we estimate that a doubling of anthropogenic CO emissions contributes with 1 – 1.9 ppb in annual mean O₃ over Europe, 1.3 -1.9 ppb over North-America, 0.7-1.0 ppb over South Asia and 0.3 – 1.5 ppb over East-Asia. Development of CO-O₃ SRs is an important issue for the further development of the tool.

4.2 Inter-annual meteorological variability

A justified critique on the methodology applied to construct the FASST SRs relates to the use of a single and fixed meteorological year 2001, implying possible unspecified biases in pollutant concentrations and source-receptor matrices compared to using a 'typical meteorological/climatological year'. We followed the choice of the meteorological year 2001 made for the HTAP1 exercise. As the North-Atlantic Oscillation (NAO) is an important mode of the inter-annual variability in pollutant concentrations and long range transport (Christoudias et al., 2012; Li et al., 2002; Pausata et al., 2013; Pope et al., 2018), the HTAP1 expectation was that this year was not an exceptional year for long-rang pollutant transport - e.g. for the North-Atlantic region, as indicated by a North Atlantic Oscillation (NAO) index close to zero for that year

(<https://www.ncdc.noaa.gov/teleconnections/nao/>). The HTAPI report (Dentener et al., 2010) also suggested that “Inter-annual differences in SR relationships for surface O₃ due to year-to-year meteorological variations are small when evaluated over continental-scale regions. However, these differences may be greater when considering smaller receptor regions or when variations in natural emissions are accounted for”. The role of spatial and temporal meteorological variability can thus be reduced by aggregating resulting pollutant levels and impacts as regional and annual averages or aggregates, the approach taken in TM5-FASST.

The impact of the choice of this specific year on the TM5-FASST model uncertainty or possible biases in base concentrations and SR coefficients is not easily quantified. For what concerns the pollutant base concentrations, some insights in the possible relevance of meteorological variability can be found in the literature. For example, Anderson et al., (2007) showed that in Europe, the meteorological component in regional inter-annual variability of pollutant concentrations ranges between 3% and 11% for airborne pollutants (O₃, PM_{2.5}), and up to 20% for wet deposition. On a global scale, Liu et al. (2007) demonstrated that the inter-annual variability in PM concentrations, related to inter-annual meteorological variability can even be up to a factor of 3 in the tropics (e.g. over Indonesia) and in the storm track regions. A sample analysis (documented in section S2.2 of the SI) of the RCP year 2000 emission scenario with TM5 at 6°x4° resolution of 5 consecutive meteorological years 2001 to 2005 indicates a year-to-year variability on regional PM_{2.5} within 10% (relative standard deviation) and within 3% for annual mean O₃. We find a similar variability on the magnitudes of 20% emission perturbation responses within the source region for 6 selected regions (India, China, Europe, Germany, USA and Japan). The relative share of source regions to the pollutant levels within a given receptor region shows a lower inter-annual variability (typically between 2 and 6% for PM_{2.5}) than the absolute contributions.

4.3 Impact of the native TM5 grid resolution on pollutant concentration and SRs

FASST base concentrations and SRs have been derived at a 1°x1° resolution which is a relatively fine grid for a global model, but still not optimal for population exposure estimates and health impact assessments. Previous studies have documented the impact of grid resolution on pollutant concentrations. The effect of higher grid resolution in global models is in general to decrease ozone exposure in polluted regions and to reduce O₃ long-range transport, while PM_{2.5} exposure – mainly to primary species - increases (Fenech et al., 2018; Li et al., 2016; Pungert and West, 2013). Without attempting a detailed analysis, a comparison of TM5 available output for PM_{2.5} and O₃ at 6°x4°, 3°x2° and 1°x1° resolution confirms these findings, as illustrated in Fig. S2.6 of the SI. Although FASST is expected to better represent population exposure to pollutants than coarser resolution models, a resolution of 1°x1° may not adequately capture urban scale pollutant levels and gradients when the urban area occupies only a fraction of the grid cell. The developed sub-grid parameterization for PM_{2.5}, providing an order-of-magnitude correction which is consistent with a high-resolution satellite product, is subject to improvement and to extension to other primary pollutants (NO₂, e.g. Kieseewetter et al., 2014, 2015) and O₃. To our

knowledge a workable parametrization to quantify the impact of sub-grid O₃ processes on population exposure – in particular titration due to local high NO_x concentrations in urban areas - has not been addressed in global air quality models.

The impact of grid resolution on the within-region source-receptor coefficients can be significant, in particular for polluted regions where the coarse resolution includes ocean surface, like Japan. Table S2.3 in the SI shows as an example within-region and long-range SR coefficients for receptor regions Germany, USA and Japan. A higher grid resolution increases the within-region response and decreases the contribution of long-range transport (where the contribution of China to nearby Japan behaves as a within-region perturbation). In the case of Japan, the within-region PM_{2.5} response magnitude increases with a factor of 3, and the sign of the within-region O₃ response is reversed when passing from 6°x4° to higher resolution. Also over the USA, the population-weighted within-region response sensitivity upon NO_x perturbation increases with a factor of 5. Further, we find that in titration regimes, the magnitude of the O₃ response to NO_x emissions increases with resolution (i.e. ozone increases more when NO_x is reduced using a fine resolution) whereas the in-region ozone response is reduced in non-titration regimes (India and China, Fig. 2.7d). These indicative results are in line with more detailed studies (e.g. Wild and Prather, 2006).

5 Conclusions and way forward

The FASST_v0 version of TM5 is a trade-off between accuracy and applicability. TM5-FASST_v0 enables immediate “what-if” and sensitivity calculations, and, by means of the available source-receptor coefficients, the extraction of this information down to the level of individual regions, economic sectors and chemical compounds. In this paper we have extensively documented the embedded methodology and validated the tool against the full chemistry transport model as well as against selected case studies from the literature. In conclusion, provided that the TM5-FASST_v0 is considered as a screening tool, the simplifications introduced in order to generate immediate results from emission scenarios are not compromising the validity of the output and as such TM5-FASST_v0 has been proven to be a useful tool in science-policy analysis.

The native set of TM5-FASST region-to-grid source-receptor grid maps is sufficiently detailed, both in terms of spatial and temporal resolution as well as number of pollutant species and metrics, to include additional impact categories not included so far. Some examples are BC deposition to snow-covered surfaces, combined nitrogen fertilization and O₃ feedbacks on Carbon-sequestration by vegetation from NO_x emission, both relevant as additional climate forcing, population exposure to NO₂ and SO₂ as additional health effects.

The regional 58x56 region-to-region source-receptor matrices aggregated from the high-resolution (region-to-gridmap) SRs are easily implemented in a spreadsheet-type environment. A user-friendly web-based interactive **stable** version based on the latter is available at <http://tm5-fasst.jrc.ec.europa.eu/>. This version offers the possibility to explore built-in as well as user-defined scenarios, using static default urban increment correction factors and crop production data. A more sophisticated in-

Moved up [5]: Ozone impact on agricultural crop production is deemed to be the least robustly quantified impact category included in FASST, in particular when evaluated from the threshold-based AOT40 metric, and has to be interpreted as indicative order-of-magnitude estimate. In an integrated assessment perspective of evaluating trade-offs and benefits of air pollutants scenarios, the dominant impact category however appears to be human health

Deleted: where TM5-FASST provides reliable estimates.¶

Deleted: , ...

house research version with gridded output and flexibility in the choice of gridded ancillary data (population grid maps, scenario-specific urban increment factors, crop distribution) is under continuous development and has been applied for the assessments listed in table S1.

Some foreseen further developments of the TM5-FASST tool, making use of readily available SRs include:

- Using the available extended-range perturbation simulations to develop a correction algorithm on the current simple linear extrapolation procedure, in particular for the regions where the O₃ or secondary PM_{2.5} regimes are non-linear, e.g. following the approach by Wild et al (2010) and Turnock et al. (2018)
- Update the health impact modules with recent findings in literature, specifically on the long-term O₃ impact (Turner et al., 2016), adjusted IER function parameters and age-specific exposure – response functions for PM_{2.5} mortalities (Cohen et al., 2017), as well as including different health metrics (DALYS, life years lost) and improved projections for base mortalities and other health statistics.
- Including a transient O₃ response function to CH₄ emission changes
- Including cryosphere forcing via BC deposition
- Stomatal approach for crop ozone impacts and extension of vegetation types considered
- Higher temporal resolution exploiting the available native monthly source-receptor maps.

Even with these further developments, an important limitation of TM5-FASST_v0 remains that it is based on a single meteorological year (2001), on source-receptor relations computed by a single underlying Chemistry-Transport model, based on the reference year 2000, and using fixed fields for natural PM_{2.5}. The HTAP phase 2 modelling exercise addresses these issues: it has been designed in line with the FASST philosophy (albeit with a larger aggregation of source region definitions), with an *ensemble* of chemistry-transport or climate-chemistry models providing source-receptor simulations, based on an updated and harmonized common anthropogenic pollutant emission inventory for the years 2008 - 2010 (Janssens-Maenhout et al., 2015; Koffi et al., 2016). The FASST architecture allows for an implementation of new or additional SR matrices, for instance new HTAP2 model ensemble mean matrices, each one accompanied by an ensemble standard deviation matrix to include the model variability in the results. Efforts are now underway to create a new web-based and user-friendly HTAP-FASST version, operating under the same principles as TM5-FASST, but based on an up-to-date reference simulation and underlying meteorology, thus creating a link between the knowledge generated by the HTAP scientific community and interested policy-oriented users.

Deleted: implement the HTAP2 ensemble of source-receptor relations in the FASST architecture, resulting in

References

- Alcamo, J., Shaw, R. and Hordijk, L., Eds.: *The RAINS Model of Acidification - Science and Strategies in Europe*, 1st ed., Springer Netherlands., 1990.
- 5 Amann, M., Bertok, I., Borken-Kleefeld, J., Cofala, J., Heyes, C., Höglund-Isaksson, L., Klimont, Z., Nguyen, B., Posch, M., Rafaj, P., Sandler, R., Schöpp, W., Wagner, F. and Winiwarter, W.: Cost-effective control of air quality and greenhouse gases in Europe: Modeling and policy applications, *Environ. Model. Softw.*, 26(12), 1489–1501, doi:10.1016/j.envsoft.2011.07.012, 2011.
- 10 Andersson, C., Langner, J. and Bergström, R.: Interannual variation and trends in air pollution over Europe due to climate variability during 1958–2001 simulated with a regional CTM coupled to the ERA40 reanalysis, *Tellus B*, 59(1), 77–98, doi:10.1111/j.1600-0889.2006.00196.x, 2007.
- Anenberg, S. C., West, J. J., Fiore, A. M., Jaffe, D. A., Prather, M. J., Bergmann, D., Cuvelier, K., Dentener, F. J., Duncan, B. N., Gauss, M., Hess, P., Jonson, J. E., Lupu, A., Mackenzie, I. A., Marmer, E., Park, R. J., Sanderson, M. G., Schultz, M., Shindell, D. T., Szopa, S., Vivanco, M. G., Wild, O. and Zeng, G.: Intercontinental impacts of ozone pollution on human mortality, *Environ. Sci. Technol.*, 43(17), 6482–6487, doi:10.1021/es900518z, 2009.
- 15 Anenberg, S. C., Horowitz, L. W., Tong, D. Q. and West, J. J.: An estimate of the global burden of anthropogenic ozone and fine particulate matter on premature human mortality using atmospheric modeling, *Environ. Health Perspect.*, 118(9), 1189–1195, doi:10.1289/ehp.0901220, 2010.
- 20 Anenberg, S. C., West, J. J., Yu, H., Chin, M., Schulz, M., Bergmann, D., Bey, I., Bian, H., Diehl, T., Fiore, A., Hess, P., Marmer, E., Montanaro, V., Park, R., Shindell, D., Takemura, T. and Dentener, F.: Impacts of intercontinental transport of anthropogenic fine particulate matter on human mortality, *Air Qual. Atmosphere Health*, 7(3), 369–379, doi:10.1007/s11869-014-0248-9, 2014.
- Anon: Estimates of global mortality attributable to particulate air pollution using satellite imagery, *Environ. Res.*, 120, 33–42, doi:10.1016/j.envres.2012.08.005, 2013.
- 25 Avnery, S., Mauzerall, D. L., Liu, J. and Horowitz, L. W.: Global crop yield reductions due to surface ozone exposure: 1. Year 2000 crop production losses and economic damage, *Atmos. Environ.*, 45(13), 2284–2296, doi:10.1016/j.atmosenv.2010.11.045, 2011.
- 30 Bond, T. C., Doherty, S. J., Fahey, D. W., Forster, P. M., Berntsen, T., DeAngelo, B. J., Flanner, M. G., Ghan, S., Kärcher, B., Koch, D., Kinne, S., Kondo, Y., Quinn, P. K., Sarofim, M. C., Schultz, M. G., Schulz, M., Venkataraman, C., Zhang, H., Zhang, S., Bellouin, N., Guttikunda, S. K., Hopke, P. K., Jacobson, M. Z., Kaiser, J. W., Klimont, Z., Lohmann, U., Schwarz, J. P., Shindell, D., Storelvmo, T., Warren, S. G. and Zender, C. S.: Bounding the role of black carbon in the climate system: A scientific assessment, *J. Geophys. Res. Atmospheres*, 118(11), 5380–5552, doi:10.1002/jgrd.50171, 2013.
- Boucher, O. and Lohmann, U.: The sulfate-CCN-cloud albedo effect: a sensitivity study with two general circulation models, *Tellus Ser. B*, 47 B(3), 281–300, 1995.
- 35 Brauer, M., Amann, M., Burnett, R. T., Cohen, A., Dentener, F., Ezzati, M., Henderson, S. B., Krzyzanowski, M., Martin, R. V., Van Dingenen, R., Van Donkelaar, A. and Thurston, G. D.: Exposure assessment for estimation of the global burden of disease attributable to outdoor air pollution, *Environ. Sci. Technol.*, 46(2), 652–660, doi:10.1021/es2025752, 2012.

- Burnett, R. T., Pope, C. A., III, Ezzati, M., Olives, C., Lim, S. S., Mehta, S., Shin, H. H., Singh, G., Hubbell, B., Brauer, M., Anderson, H. R., Smith, K. R., Balmes, J. R., Bruce, N. G., Kan, H., Laden, F., Prüss-Ustün, A., Turner, M. C., Gapstur, S. M., Diver, W. R. and Cohen, A.: An Integrated Risk Function for Estimating the Global Burden of Disease Attributable to Ambient Fine Particulate Matter Exposure, *Environ. Health Perspect.*, doi:10.1289/ehp.1307049, 2014.
- 5 Christoudias, T., Pozzer, A. and Lelieveld, J.: Influence of the North Atlantic Oscillation on air pollution transport, *Atmospheric Chem. Phys.*, 12(2), 869–877, doi:<https://doi.org/10.5194/acp-12-869-2012>, 2012.
- Cohen, A. J., Brauer, M., Burnett, R., Anderson, H. R., Frostad, J., Estep, K., Balakrishnan, K., Brunekreef, B., Dandona, L., Dandona, R., Feigin, V., Freedman, G., Hubbell, B., Jobling, A., Kan, H., Knibbs, L., Liu, Y., Martin, R., Morawska, L., Pope, C. A., III, Shin, H., Straif, K., Shaddick, G., Thomas, M., van Dingenen, R., van Donkelaar, A., Vos, T., Murray, C. J. L. and Forouzanfar, M. H.: Estimates and 25-year trends of the global burden of disease attributable to ambient air pollution: an analysis of data from the Global Burden of Diseases Study 2015, *The Lancet*, 389(10082), 1907–1918, doi:10.1016/S0140-6736(17)30505-6, 2017.
- 10 Dentener, F., Stevenson, D., Cofala, J., Mechler, R., Amann, M., Bergamaschi, P., Raes, F. and Derwent, R.: The impact of air pollutant and methane emission controls on tropospheric ozone and radiative forcing: CTM calculations for the period 1990-2030, *Atmos Chem Phys*, 5(7), 1731–1755, doi:10.5194/acp-5-1731-2005, 2005.
- 15 Dentener, F., Kinne, S., Bond, T., Boucher, O., Cofala, J., Generoso, S., Ginoux, P., Gong, S., Hoelzemann, J. J., Ito, A., Marelli, L., Penner, J. E., Putaud, J.-P., Textor, C., Schulz, M., Van, D. W. and Wilson, J.: Emissions of primary aerosol and precursor gases in the years 2000 and 1750 prescribed data-sets for AeroCom, *Atmospheric Chem. Phys.*, 6(12), 4321–4344, 2006a.
- 20 Dentener, F., Stevenson, D., Ellingsen, K., Van Noije, T., Schultz, M., Amann, M., Atherton, C., Bell, N., Bergmann, D., Bey, I., Bouwman, L., Butler, T., Cofala, J., Collins, B., Drevet, J., Doherty, R., Eickhout, B., Eskes, H., Fiore, A., Gauss, M., Hauglustaine, D., Horowitz, L., Isaksen, I. S. A., Josse, B., Lawrence, M., Krol, M., Lamarque, J. F., Montanaro, V., Müller, J. F., Peuch, V. H., Pitari, G., Pyle, J., Rast, S., Rodriguez, J., Sanderson, M., Savage, N. H., Shindell, D., Strahan, S., Szopa, S., Sudo, K., Van Dingenen, R., Wild, O. and Zeng, G.: The global atmospheric environment for the next generation, *Environ. Sci. Technol.*, 40(11), 3586–3594, doi:10.1021/es0523845, 2006b.
- 25 Dentener, F., Keating, T., Akimoto, H., Pirrone, N., Dutchak, S., Zuber, A., Convention on Long-range Transboundary Air Pollution, United Nations and UNECE Task Force on Emission Inventories and Projections, Eds.: Hemispheric transport of air pollution 2010: prepared by the Task Force on Hemispheric Transport of Air Pollution acting within the framework of the Convention on Long-range Transboundary Air Pollution, United Nations, New York ; Geneva., 2010.
- 30 Edwards, J. M. and Slingo, A.: Studies with a flexible new radiation code. I: Choosing a configuration for a large-scale model, *Q. J. R. Meteorol. Soc.*, 122(531), 689–719, 1996.
- Eickhout, B., Den Elzen, M. G. J. and Kreileman, G. J. J.: The Atmosphere-Ocean System of IMAGE 2.2. A global model approach for atmospheric concentrations, and climate and sea level projections, RIVM, Bilthoven, The Netherlands. [online] Available from: <http://rivm.openrepository.com/rivm/handle/10029/8936> (Accessed 10 January 2017), 2004.
- 35 Fang, Y., Naik, V., Horowitz, L. W. and Mauzerall, D. L.: Air pollution and associated human mortality: the role of air pollutant emissions, climate change and methane concentration increases from the preindustrial period to present, *Atmospheric Chem. Phys.*, 13(3), 1377–1394, doi:<https://doi.org/10.5194/acp-13-1377-2013>, 2013.

- Farina, S. C., Adams, P. J. and Pandis, S. N.: Modeling global secondary organic aerosol formation and processing with the volatility basis set: Implications for anthropogenic secondary organic aerosol, *J. Geophys. Res. Atmospheres*, 115(D9), doi:10.1029/2009JD013046, 2010.
- 5 Fiore, S., Doherty, R. M., Heaviside, C., Vardoulakis, S., Macintyre, H. L. and O'Connor, F. M.: The influence of model spatial resolution on simulated ozone and fine particulate matter for Europe: implications for health impact assessments, *Atmospheric Chem. Phys.*, 18(8), 5765–5784, doi:10.5194/acp-18-5765-2018, 2018.
- Fiore, A. M., West, J. J., Horowitz, L. W., Naik, V. and Schwarzkopf, M. D.: Characterizing the tropospheric ozone response to methane emission controls and the benefits to climate and air quality, *J. Geophys. Res. Atmospheres*, 113(8), doi:10.1029/2007JD009162, 2008.
- 10 Fiore, A. M., Dentener, F. J., Wild, O., Cuvelier, C., Schultz, M. G., Hess, P., Textor, C., Schulz, M., Doherty, R. M., Horowitz, L. W., MacKenzie, I. A., Sanderson, M. G., Shindell, D. T., Stevenson, D. S., Szopa, S., Van Dingenen, R., Zeng, G., Atherton, C., Bergmann, D., Bey, I., Carmichael, G., Collins, W. J., Duncan, B. N., Faluvegi, G., Folberth, G., Gauss, M., Gong, S., Hauglustaine, D., Holloway, T., Isaksen, I. S. A., Jacob, D. J., Jonson, J. E., Kaminski, J. W., Keating, T. J., Lupu, A., Marmer, E., Montanaro, V., Park, R. J., Pitari, G., Pringle, K. J., Pyle, J. A., Schroeder, S., Vivanco, M. G., Wind, P., Wojcik, G., Wu, S. and Zuber, A.: Multimodel estimates of intercontinental source-receptor relationships for ozone pollution, *J. Geophys. Res. Atmospheres*, 114(D4), doi:10.1029/2008JD010816, 2009.
- 15 Foley, K. M., Napelenok, S. L., Jang, C., Phillips, S., Hubbell, B. J. and Fulcher, C. M.: Two reduced form air quality modeling techniques for rapidly calculating pollutant mitigation potential across many sources, locations and precursor emission types, *Atmos. Environ.*, 98, 283–289, doi:10.1016/j.atmosenv.2014.08.046, 2014.
- 20 Forouzanfar, M. H., Alexander, L., Anderson, H. R., Bachman, V. F., Biryukov, S., Brauer, M., Burnett, R., Casey, D., Coates, M. M., Cohen, A., Delwiche, K., Estep, K., Frostad, J. J., KC, A., Kyu, H. H., Moradi-Lakeh, M., Ng, M., Slepak, E. L., Thomas, B. A., Wagner, J., Aasvang, G. M., Abbafati, C., Ozgoren, A. A., Abd-Allah, F., Abera, S. F., Aboyans, V., Abraham, B., Abraham, J. P., Abubakar, I., Abu-Rmeileh, N. M. E., Aburto, T. C., Achoki, T., Adelekan, A., Adofo, K., Adou, A. K., Adsuar, J. C., Afshin, A., Agardh, E. E., Al Khabouri, M. J., Al Lami, F. H., Alam, S. S., Alasfoor, D., Albittar, M. I., Alegretti, M. A., Aleman, A. V., Alemu, Z. A., Alfonso-Cristancho, R., Alhabib, S., Ali, R., Ali, M. K., Alla, F., Allebeck, P., Allen, P. J., Alsharif, U., Alvarez, E., Alvis-Guzman, N., Amankwaa, A. A., Amare, A. T., Ameh, E. A., Ameli, O., Amini, H., Ammar, W., Anderson, B. O., Antonio, C. A. T., Anwari, P., Cunningham, S. A., Arnlöv, J., Arsenijevic, V. S. A., Artaman, A., Asghar, R. J., Assadi, R., Atkins, L. S., Atkinson, C., Avila, M. A., Awuah, B., Badawi, A., Bahit, M. C., Bakfalouni, T., Balakrishnan, K., Balalla, S., Balu, R. K., Banerjee, A., Barber, R. M., Barker-Collo, S. L., Barquera, S., Barregard, L., Barrero, L. H., Barrientos-Gutierrez, T., Basto-Abreu, A. C., Basu, A., Basu, S., Basulaiman, M. O., Ruvalcaba, C. B., Beardsley, J., Bedi, N., Bekele, T., Bell, M. L., Benjet, C., Bennett, D. A., et al.: Global, regional, and national comparative risk assessment of 79 behavioural, environmental and occupational, and metabolic risks or clusters of risks in 188 countries, 1990–2013: a systematic analysis for the Global Burden of Disease Study 2013, *The Lancet*, 386(10010), 2287–2323, doi:10.1016/S0140-6736(15)00128-2, 2015.
- 30 Forouzanfar, M. H., Afshin, A., Alexander, L. T., Biryukov, S., Brauer, M., Cercy, K., Charlson, F. J., Cohen, A. J., Dandona, L., Estep, K., Ferrari, A. J., Frostad, J. J., Fullman, N., Godwin, W. W., Griswold, M., Hay, S. I., Kyu, H. H., Larson, H. J., Lim, S. S., Liu, P. Y., Lopez, A. D., Lozano, R., Marczak, L., Mokdad, A. H., Moradi-Lakeh, M., Naghavi, M., Reitsma, M. B., Roth, G. A., Sur, P. J., Vos, T., Wagner, J. A., Wang, H., Zhao, Y., Zhou, M., Barber, R. M., Bell, B., Blore, J. D., Casey, D. C., Coates, M. M., Cooperrider, K., Cornaby, L., Dicker, D., Erskine, H. E., Fleming, T., Foreman, K., Gakidou, E., Haagsma, J. A., Johnson, C. O., Kemmer, L., Ku, T., Leung, J., Masiye, F., Millea, A., Mirarefin, M., Misganaw, A., Mullany, E., Mumford, J. E., Ng, M., Olsen, H., Rao, P., Reinig, N., Roman, Y., Sandar, L., Santomauro, D. F., Slepak, E. L., Sorensen, R. J. D., Thomas, B. A., Vollset, S. E., Whiteford, H. A., Zipkin, B., Murray, C. J. L., Mock, C.
- 35
- 40

- N., Anderson, B. O., Futran, N. D., Anderson, H. R., Bhutta, Z. A., Nisar, M. I., Akseer, N., Krueger, H., Gotay, C. C., Kisson, N., Kopec, J. A., Pourmalek, F., Burnett, R., Abajobir, A. A., Knibbs, L. D., Veerman, J. L., Lalloo, R., Scott, J. G., Alam, N. K. M., Gouda, H. N., Guo, Y., McGrath, J. J., Charlson, F. J., Erskine, H. E., Jeemon, P., Dandona, R., Goenka, S., Kumar, G. A., et al.: Global, regional, and national comparative risk assessment of 79 behavioural, environmental and occupational, and metabolic risks or clusters of risks, 1990–2015: a systematic analysis for the Global Burden of Disease Study 2015, *The Lancet*, 388(10053), 1659–1724, doi:10.1016/S0140-6736(16)31679-8, 2016.
- 5 Forster, P., Ramaswamy, V., Artaxo, P., Bernsten, T., Betts, R., Fahey, D. W., Haywood, J., Lean, J., Lowe, D. C., Myhre, G., Nganga, J., Prinn, R., Raga, G., Schulz, M. and Van Dorland, R.: Changes in Atmospheric Constituents and in Radiative Forcing., in *Climate Change 2007: The Physical Science Basis. Contribution of Working Group I to the Fourth Assessment Report of the Intergovernmental Panel on Climate Change*, Cambridge University Press, Cambridge, United Kingdom and New York, NY, USA. [online] Available from: http://inis.iaea.org/Search/search.aspx?orig_q=RN:39002468 (Accessed 30 November 2017), 2007.
- 10 Fry, M. M., Naik, V., West, J. J., Schwarzkopf, M. D., Fiore, A. M., Collins, W. J., Dentener, F. J., Shindell, D. T., Atherton, C., Bergmann, D., Duncan, B. N., Hess, P., MacKenzie, I. A., Marmer, E., Schultz, M. G., Szopa, S., Wild, O. and Zeng, G.: The influence of ozone precursor emissions from four world regions on tropospheric composition and radiative climate forcing, *J. Geophys. Res. Atmospheres*, 117(7), doi:10.1029/2011JD017134, 2012.
- 15 Fuglested, J. S., Shine, K. P., Bernsten, T., Cook, J., Lee, D. S., Stenke, A., Skeie, R. B., Velders, G. J. M. and Waitz, I. A.: Transport impacts on atmosphere and climate: Metrics, *Atmos. Environ.*, 44(37), 4648–4677, doi:10.1016/j.atmosenv.2009.04.044, 2010.
- 20 Grewe, V., Dahlmann, K., Matthes, S. and Steinbrecht, W.: Attributing ozone to NOx emissions: Implications for climate mitigation measures, *Atmos. Environ.*, 59, 102–107, doi:10.1016/j.atmosenv.2012.05.002, 2012.
- Haywood, J. and Boucher, O.: Estimates of the direct and indirect radiative forcing due to tropospheric aerosols: A review, *Rev. Geophys.*, 38(4), 513–543, doi:10.1029/1999RG000078, 2000.
- Höglund-Isaksson, L. and Mechler, R.: The GAINS model for greenhouse gases-version 1.0: Methane (CH₄), IIASA Interim Report, International Institute for Applied Systems Analysis, Laxenburg, Austria. [online] Available from: <http://pure.iiasa.ac.at/7784/> (Accessed 10 January 2017), 2005.
- 25 Huang, Y., Wu, S., Dubey, M. and French, N. H. F.: Impact of aging mechanism on model simulated carbonaceous aerosols, *Atmospheric Chem. Phys. Print*, 12, 10.5194/acpd-12-28993–2012, doi:10.5194/acpd-12-28993-2012, 2012.
- Huijnen, V., Williams, J., van Weele, M., van Noije, T., Krol, M., Dentener, F., Segers, A., Houweling, S., Peters, W., de Laat, J., Boersma, F., Bergamaschi, P., van Velthoven, P., Le Sager, P., Eskes, H., Alkemade, F., Scheele, R., Nédélec, P. and Pätz, H.-W.: The global chemistry transport model TM5: description and evaluation of the tropospheric chemistry version 3.0, *Geosci. Model Dev.*, 3(2), 445–473, doi:10.5194/gmd-3-445-2010, 2010.
- 30 IIASA and FAO: Global Agro-Ecological Zones V3.0, [online] Available from: <http://www.gaez.iiasa.ac.at/> (Accessed 11 November 2016), 2012.
- Janssens-Maenhout, G., Crippa, M., Guizzardi, D., Dentener, F., Muntean, M., Pouliot, G., Keating, T., Zhang, Q., Kurokawa, J., Wankmüller, R., Denier van der Gon, H., Kuenen, J. J. P., Klimont, Z., Frost, G., Darras, S., Koffi, B. and Li, M.: HTAP_v2.2: a mosaic of regional and global emission grid maps for 2008 and 2010 to study hemispheric transport of air pollution, *Atmos Chem Phys*, 15(19), 11411–11432, doi:10.5194/acp-15-11411-2015, 2015.
- 35

- Jerrett, M., Burnett, R. T., Arden, P. I., Ito, K., Thurston, G., Krewski, D., Shi, Y., Calle, E. and Thun, M.: Long-term ozone exposure and mortality, *N. Engl. J. Med.*, 360(11), 1085–1095, doi:10.1056/NEJMoa0803894, 2009.
- 5 Jin, X., Fiore, A. M., Murray, L. T., Valin, L. C., Lamsal, L. N., Duncan, B., Folkert, B., De, S., Abad, G. G., Chance, K. and Tonnesen, G. S.: Evaluating a Space-Based Indicator of Surface Ozone-NO_x-VOC Sensitivity Over Midlatitude Source Regions and Application to Decadal Trends, *J. Geophys. Res. Atmospheres*, 122(19), 10439–10461, doi:10.1002/2017JD026720, 2017.
- 10 Joos, F., Roth, R., Fuglestedt, J. S., Peters, G. P., Enting, I. G., von Bloh, W., Brovkin, V., Burke, E. J., Eby, M., Edwards, N. R., Friedrich, T., Frölicher, T. L., Halloran, P. R., Holden, P. B., Jones, C., Kleinen, T., Mackenzie, F. T., Matsumoto, K., Meinshausen, M., Plattner, G.-K., Reisinger, A., Segsneider, J., Shaffer, G., Steinacher, M., Strassmann, K., Tanaka, K., Timmermann, A. and Weaver, A. J.: Carbon dioxide and climate impulse response functions for the computation of greenhouse gas metrics: a multi-model analysis, *Atmospheric Chem. Phys.*, 13(5), 2793–2825, doi:10.5194/acp-13-2793-2013, 2013.
- 15 Kanakidou, M., Seinfeld, J. H., Pandis, S. N., Barnes, I., Dentener, F. J., Facchini, M. C., Dingenen, R. V., Ervens, B., Nenes, A., Nielsen, C. J., Swietlicki, E., Putaud, J. P., Balkanski, Y., Fuzzi, S., Horth, J., Moortgat, G. K., Winterhalter, R., Myhre, C. E. L., Tsigaridis, K., Vignati, E., Stephanou, E. G. and Wilson, J.: Organic aerosol and global climate modelling: a review, *Atmospheric Chem. Phys.*, 5(4), 1053–1123, doi:10.5194/acp-5-1053-2005, 2005.
- Kiesewetter, G., Borken-Kleefeld, J., Schöpp, W., Heyes, C., Thunis, P., Bessagnet, B., Terrenoire, E., Gsella, A. and Amann, M.: Modelling NO₂ concentrations at the street level in the GAINS integrated assessment model: projections under current legislation, *Atmospheric Chem. Phys.*, 14(2), 813–829, doi:https://doi.org/10.5194/acp-14-813-2014, 2014.
- 20 Kiesewetter, G., Borken-Kleefeld, J., Schöpp, W., Heyes, C., Thunis, P., Bessagnet, B., Terrenoire, E., Fagerli, H., Nyiri, A. and Amann, M.: Modelling street level PM₁₀ concentrations across Europe: source apportionment and possible futures, *Atmospheric Chem. Phys.*, 15(3), 1539–1553, 2015.
- 25 Kitous, A., Keramidas, K., Vanduyck, T., Saveyn, B., Van Dingenen, R., Spadaro, J. and Holland, M.: Global Energy and Climate Outlook 2017: How climate policies improve air quality, Joint Research Centre, Luxembourg: Publications Office of the European Union., 2017.
- Koffi, B., Dentener, F., Janssens-Maenhout, G., Guizzardi, D., Crippa, M., Diehl, T., Galmarini, S. and Solazzo, E.: Hemispheric Transport Air Pollution (HTAP): Specification of the HTAP2 experiments, Publications Office of the European Union, Luxembourg. [online] Available from: <http://publications.jrc.ec.europa.eu/repository/bitstream/JRC102552/lbna28255enn.pdf> (Accessed 14 December 2017), 2016.
- 30 Krewski, D., Jerrett, M., Burnett, R. T., Ma, R., Hughes, E. and Shi, Y.: Extended Follow-Up and Spatial Analysis of the American Cancer Society Study Linking Particulate Air Pollution and Mortality., Research Report, Health Effects Institute, Boston., 2009.
- 35 Krol, M., Houweling, S., Bregman, B., van den Broek, M., Segers, A., van Velthoven, P., Peters, W., Dentener, F. and Bergamaschi, P.: The two-way nested global chemistry-transport zoom model TM5: algorithm and applications, *Atmos Chem Phys*, 5(2), 417–432, doi:10.5194/acp-5-417-2005, 2005.
- Lamarque, J., Bond, T., Eyring, V., Granier, C., Heil, A., Klimont, Z., Lee, D., Lioussé, C., Mieville, A., Owen, B., Schultz, M., Shindell, D., Smith, S., Stehfest, E., Van Aardenne, J., Cooper, O., Kainuma, M., Mahowald, N., McConnell, J., Naik, V., Riahi, K. and van Vuuren, D.: Historical (1850-2000) gridded anthropogenic and biomass burning emissions of reactive

- gases and aerosols: methodology and application, *Atmospheric Chem. Phys.*, 10, 7017–7039, doi:10.5194/acp-10-7017-2010, 2010.
- 5 Lamarque, J.-F., Shindell, D. T., Josse, B., Young, P. J., Cionni, I., Eyring, V., Bergmann, D., Cameron-Smith, P., Collins, W. J., Doherty, R., Dalsoren, S., Faluvegi, G., Folberth, G., Ghan, S. J., Horowitz, L. W., Lee, Y. H., MacKenzie, I. A., Nagashima, T., Naik, V., Plummer, D., Righi, M., Rumbold, S. T., Schulz, M., Skeie, R. B., Stevenson, D. S., Strode, S., Sudo, K., Szopa, S., Voulgarakis, A. and Zeng, G.: The Atmospheric Chemistry and Climate Model Intercomparison Project (ACCMIP): overview and description of models, simulations and climate diagnostics, *Geosci Model Dev*, 6(1), 179–206, doi:10.5194/gmd-6-179-2013, 2013.
- 10 Lelieveld, J., Barlas, C., Giannadaki, D. and Pozzer, A.: Model calculated global, regional and megacity premature mortality due to air pollution, *Atmospheric Chem. Phys.*, 13(14), 7023–7037, doi:https://doi.org/10.5194/acp-13-7023-2013, 2013.
- Li, J., Yang, W., Wang, Z., Chen, H., Hu, B., Li, J., Sun, Y. and Huang, Y.: A modeling study of source–receptor relationships in atmospheric particulate matter over Northeast Asia, *Atmos. Environ.*, 91, 40–51, doi:10.1016/j.atmosenv.2014.03.027, 2014.
- 15 Li, Q., Jacob, D. J., Bey, I., Palmer, P. I., Duncan, B. N., Field, B. D., Martin, R. V., Fiore, A. M., Yantosca, R. M., Parrish, D. D., Simmonds, P. G. and Oltmans, S. J.: Transatlantic transport of pollution and its effects on surface ozone in Europe and North America, *J. Geophys. Res. Atmospheres*, 107(D13), ACH 4-1-ACH 4-21, doi:10.1029/2001JD001422, 2002.
- Li, Y., Henze, D. K., Jack, D. and Kinney, P. L.: The influence of air quality model resolution on health impact assessment for fine particulate matter and its components, *Air Qual. Atmosphere Health*, 9(1), 51–68, doi:10.1007/s11869-015-0321-z, 2016.
- 20 Liang, C.-K., West, J. J., Silva, R. A., Bian, H., Chin, M., Davila, Y., Dentener, F. J., Emmons, L., Flemming, J., Folberth, G., Henze, D., Im, U., Jonson, J. E., Keating, T. J., Kucsera, T., Lenzen, A., Lin, M., Lund, M. T., Pan, X., Park, R. J., Pierce, R. B., Sekiya, T., Sudo, K. and Takemura, T.: HTAP2 multi-model estimates of premature human mortality due to intercontinental transport of air pollution and emission sectors, *Atmospheric Chem. Phys.*, 18(14), 10497–10520, doi:https://doi.org/10.5194/acp-18-10497-2018, 2018.
- 25 Lim, S. S., Vos, T., Flaxman, A. D., Danaei, G., Shibuya, K., Adair-Rohani, H., Amann, M., Anderson, H. R., Andrews, K. G., Aryee, M., Atkinson, C., Bacchus, L. J., Bahalim, A. N., Balakrishnan, K., Balmes, J., Barker-Collo, S., Baxter, A., Bell, M. L., Blore, J. D., Blyth, F., Bonner, C., Borges, G., Bourne, R., Boussinesq, M., Brauer, M., Brooks, P., Bruce, N. G., Brunekreef, B., Bryan-Hancock, C., Bucello, C., Buchbinder, R., Bull, F., Burnett, R. T., Byers, T. E., Calabria, B., Carapetis, J., Carnahan, E., Chafe, Z., Charlson, F., Chen, H., Chen, J. S., Cheng, A. T.-A., Child, J. C., Cohen, A., Colson, K. E., Cowie, B. C., Darby, S., Darling, S., Davis, A., Degenhardt, L., Dentener, F., Des Jarlais, D. C., Devries, K., Dherani, M., Ding, E. L., Dorsey, E. R., Driscoll, T., Edmond, K., Ali, S. E., Engell, R. E., Erwin, P. J., Fahimi, S., Falder, G., Farzadfar, F., Ferrari, A., Finucane, M. M., Flaxman, S., Fowkes, F. G. R., Freedman, G., Freeman, M. K., Gakidou, E., Ghosh, S., Giovannucci, E., Gmel, G., Graham, K., Grainger, R., Grant, B., Gunnell, D., Gutierrez, H. R., Hall, W., Hoek, H. W., Hogan, A., Hosgood III, H. D., Hoy, D., Hu, H., Hubbell, B. J., Hutchings, S. J., Ibeanusi, S. E., Jacklyn, G. L., Jassrasaria, R., Jonas, J. B., Kan, H., Kanis, J. A., Kassebaum, N., Kawakami, N., Khang, Y.-H., Khatibzadeh, S., Khoo, J.-P., Kok, C., et al.: A comparative risk assessment of burden of disease and injury attributable to 67 risk factors and risk factor clusters in 21 regions, 1990-2010: A systematic analysis for the Global Burden of Disease Study 2010, *The Lancet*, 380(9859), 2224–2260, doi:10.1016/S0140-6736(12)61766-8, 2012.

- Liu, X., Penner, J. E., Das, B., Bergmann, D., Rodriguez, J. M., Strahan, S., Wang, M. and Feng, Y.: Uncertainties in global aerosol simulations: Assessment using three meteorological data sets, *J. Geophys. Res.*, 112(D11), doi:10.1029/2006JD008216, 2007.
- 5 Liu, Y., Hong, Y., Fan, Q., Wang, X., Chan, P., Chen, X., Lai, A., Wang, M. and Chen, X.: Source-receptor relationships for PM_{2.5} during typical pollution episodes in the Pearl River Delta city cluster, China, *Sci. Total Environ.*, 596–597, 194–206, doi:10.1016/j.scitotenv.2017.03.255, 2017.
- Maione, M., Fowler, D., Monks, P. S., Reis, S., Rudich, Y., Williams, M. L. and Fuzzi, S.: Air quality and climate change: Designing new win-win policies for Europe, *Environ. Sci. Policy*, 65, 48–57, doi:10.1016/j.envsci.2016.03.011, 2016.
- 10 Malley, C. S., Henze, D. K., Kuylensstierna, J. C. I., Vallack, H., Davila, Y., Anenberg, S. C., Turner, M. C. and Ashmore, M.: Updated Global Estimates of Respiratory Mortality in Adults ≥ 30 Years of Age Attributable to Long-Term Ozone Exposure., *Environ. Health Perspect.*, 125(8), 087021, doi:10.1289/EHP1390, 2017.
- Marmer, E., Langmann, B., Hungershöfer, K. and Trautmann, T.: Aerosol modeling over Europe: 2. Interannual variability of aerosol shortwave direct radiative forcing, *J. Geophys. Res. Atmospheres*, 112(D23), D23S16, doi:10.1029/2006JD008040, 2007.
- 15 Mills, G., Buse, A., Gimeno, B., Bermejo, V., Holland, M., Emberson, L. and Pleijel, H.: A synthesis of AOT₄₀-based response functions and critical levels of ozone for agricultural and horticultural crops, *Atmos. Environ.*, 41(12), 2630–2643, doi:10.1016/j.atmosenv.2006.11.016, 2007.
- Ming, Y. and Russell, L. M.: Predicted hygroscopic growth of sea salt aerosol, *J. Geophys. Res. Atmospheres*, 106(D22), 28259–28274, 2001.
- 20 Murray, C. J., Ezzati, M., Lopez, A. D., Rodgers, A. and Vander Hoorn, S.: Comparative quantification of health risks: conceptual framework and methodological issues, *Popul. Health Metr.*, 1(1), 1, 2003.
- Myhre, G., Fuglestedt, J. S., Berntsen, T. K. and Lund, M. T.: Mitigation of short-lived heating components may lead to unwanted long-term consequences, *Atmos. Environ.*, 45(33), 6103–6106, doi:10.1016/j.atmosenv.2011.08.009, 2011.
- 25 Myhre, G., Shindell, D., Bréon, F.-M., Collins, W., Fuglestedt, J., Huang, J., Koch, D., Lamarque, J.-F., Lee, D. and Mendoza, B.: Anthropogenic and natural radiative forcing, in *Climate Change 2013: The Physical Science Basis. Contribution of Working Group I to the Fifth Assessment Report of the Intergovernmental Panel on Climate Change* [Stocker, T.F., D. Qin, G.-K. Plattner, M. Tignor, S.K. Allen, J. Boschung, A. Nauels, Y. Xia, V. Bex and P.M. Midgley (eds.), vol. 423, pp. 658–740, Cambridge University Press, Cambridge, United Kingdom and New York, NY, USA., 2013.
- 30 OECD: The Economic Consequences of Outdoor Air Pollution, OECD Publishing. [online] Available from: http://www.oecd-ilibrary.org/environment/the-economic-consequences-of-outdoor-air-pollution_9789264257474-en (Accessed 10 January 2017), 2016.
- Olivier, J. G. J., Aardenne, J. A. V., Dentener, F. J., Pagliari, V., Ganzeveld, L. N. and Peters, J. A. H. W.: Recent trends in global greenhouse gas emissions: regional trends 1970–2000 and spatial distribution of key sources in 2000, *Environ. Sci.*, 2(2–3), 81–99, doi:10.1080/15693430500400345, 2005.

- Pausata, F. S. R., Pozzoli, L., Dingenen, R. V., Vignati, E., Cavalli, F. and Dentener, F. J.: Impacts of changes in North Atlantic atmospheric circulation on particulate matter and human health in Europe, *Geophys. Res. Lett.*, 40(15), 4074–4080, doi:10.1002/grl.50720, 2013.
- 5 Pope, C. A., III, Burnett, R. T., Thun, M. J., Calle, E. E., Krewski, D., Ito, K. and Thurston, G. D.: Lung Cancer, Cardiopulmonary Mortality, and Long-term Exposure to Fine Particulate Air Pollution, *JAMA*, 287(9), 1132–1141, doi:10.1001/jama.287.9.1132, 2002.
- Pope, R. J., Chipperfield, M. P., Arnold, S. R., Glatthor, N., Feng, W., Dhomse, S. S., Kerridge, B. J., Latter, B. G. and Siddans, R.: Influence of the wintertime North Atlantic Oscillation on European tropospheric composition: an observational and modelling study, *Atmospheric Chem. Phys.*, 18(11), 8389–8408, doi:10.5194/acp-18-8389-2018, 2018.
- 10 Porter, P. S., Rao, S. T., Hogrefe, C. and Mathur, R.: A reduced form model for ozone based on two decades of CMAQ simulations for the continental United States, *Atmospheric Pollut. Res.*, 8(2), 275–284, doi:10.1016/j.apr.2016.09.005, 2017.
- Punger, E. M. and West, J. J.: The effect of grid resolution on estimates of the burden of ozone and fine particulate matter on premature mortality in the United States, *Air Qual. Atmosphere Health*, 6(3), doi:10.1007/s11869-013-0197-8, 2013.
- 15 Ramaswamy, V., Boucher, O., Haigh, J., Hauglustaine, D., Haywood, J., Myhre, G., Nakajima, T., Shi, G., Solomon, S., Betts, R. E., Charlson, R., Chuang, C. C., Daniel, J. S., Del Genio, A. D., Feichter, J., Fuglestedt, J., Forster, P. M., Ghan, S. J., Jones, A., Kiehl, J. T., Koch, D., Land, C., Lean, J., Lohmann, U., Minschwaner, K., Penner, J. E., Roberts, D. L., Rodhe, H., Roelofs, G.-J., Rotstayn, L. D., Schneider, T. L., Schumann, U., Schwartz, S. E., Schwartzkopf, M. D., Shine, K. P., Smith, S. J., Stevenson, D. S., Stordal, F., Tegen, I., van Dorland, R., Zhang, Y., Srinivasan, J. and Joos, F.: Radiative Forcing of Climate Change, Pacific Northwest National Laboratory (PNNL), Richland, WA (US). [online] Available from: <https://www.osti.gov/scitech/biblio/899821> (Accessed 27 January 2017), 2001.
- 20 Rao, S., Chirkov, V., Dentener, F., Van Dingenen, R., Pachauri, S., Purohit, P., Amann, M., Heyes, C., Kinney, P., Kolp, P., Klimont, Z., Riahi, K. and Schoepp, W.: Environmental Modeling and Methods for Estimation of the Global Health Impacts of Air Pollution, *Environ. Model. Assess.*, 17(6), 613–622, doi:10.1007/s10666-012-9317-3, 2012.
- 25 Rao, S., Pachauri, S., Dentener, F., Kinney, P., Klimont, Z., Riahi, K. and Schoepp, W.: Better air for better health: Forging synergies in policies for energy access, climate change and air pollution, *Glob. Environ. Change*, 23(5), 1122–1130, doi:10.1016/j.gloenvcha.2013.05.003, 2013.
- Rao, S., Klimont, Z., Smith, S. J., Van Dingenen, R., Dentener, F., Bouwman, L., Riahi, K., Amann, M., Bodirsky, B. L., van Vuuren, D. P., Aleluia Reis, L., Calvin, K., Drouet, L., Fricko, O., Fujimori, S., Gernaat, D., Havlik, P., Harmsen, M., Hasegawa, T., Heyes, C., Hilaire, J., Luderer, G., Masui, T., Stehfest, E., Strefler, J., van der Sluis, S. and Tavoni, M.: Future air pollution in the Shared Socio-economic Pathways, *Glob. Environ. Change*, doi:10.1016/j.gloenvcha.2016.05.012, 2016.
- 30 Rao, S., Klimont, Z., Smith, S. J., Van Dingenen, R., Dentener, F., Bouwman, L., Riahi, K., Amann, M., Bodirsky, B. L., van Vuuren, D. P., Aleluia Reis, L., Calvin, K., Drouet, L., Fricko, O., Fujimori, S., Gernaat, D., Havlik, P., Harmsen, M., Hasegawa, T., Heyes, C., Hilaire, J., Luderer, G., Masui, T., Stehfest, E., Strefler, J., van der Sluis, S. and Tavoni, M.: Future air pollution in the Shared Socio-economic Pathways, *Glob. Environ. Change*, 42, 346–358, doi:10.1016/j.gloenvcha.2016.05.012, 2017.
- 35 Riahi, K., Grübler, A. and Nakicenovic, N.: Scenarios of long-term socio-economic and environmental development under climate stabilization, *Technol. Forecast. Soc. Change*, 74(7), 887–935, doi:10.1016/j.techfore.2006.05.026, 2007.

- 5 Riahi, K., Dentener, F., Gielen, D., Grubler, A., Jewell, J., Klimont, Z., Krey, V., McCollum, D., Pachauri, S., Rao, S., van Ruijven, B., van Vuuren, D. P. and Wilson, C.: The Global Energy Assessment - Chapter 17 - Energy Pathways for Sustainable Development, in *Global Energy Assessment - Toward a Sustainable Future*, pp. 1203–1306, Cambridge University Press, Cambridge, UK and New York, NY, USA and the International Institute for Applied Systems Analysis, Laxenburg, Austria. [online] Available from: www.globalenergyassessment.org, 2012.
- Russ, P., Wiesenthal, T., Van Regemorter, D. and Ciscar, J.: Global Climate Policy Scenarios for 2030 and beyond. Analysis of Greenhouse Gas Emission Reduction Pathway Scenarios with the POLES and GEM-E3 models., European Commission, Joint Research Centre, IPTS, Seville, Spain., 2007.
- 10 Seinfeld, J. H. and Pandis, S. N.: *Atmospheric Chemistry and Physics: From Air Pollution to Climate Change*, 1st Edition., Wiley, Hoboken, New Jersey. [online] Available from: <http://www.wiley.com/WileyCDA/WileyTitle/productCd-1118947401.html> (Accessed 11 August 2017), 1998.
- 15 Shindell, D., Kuylenstierna, J., Vignati, E., van Dingenen, R., Amann, M., Klimont, Z., Anenberg, S., Muller, N., Janssens-Maenhout, G., Raes, F., Schwartz, J., Faluvegi, G., Pozzoli, L., Kupiainen, K., Hoglund-Isaksson, L., Emberson, L., Streets, D., Ramanathan, V., Hicks, K., Oanh, N., Milly, G., Williams, M., Demkine, V. and Fowler, D.: Simultaneously Mitigating Near-Term Climate Change and Improving Human Health and Food Security, *Science*, 335(6065), 183–189, doi:10.1126/science.1210026, 2012.
- Shindell, D. T., Faluvegi, G., Bell, N. and Schmidt, G. A.: An emissions-based view of climate forcing by methane and tropospheric ozone: EMISSIONS-BASED CLIMATE FORCING, *Geophys. Res. Lett.*, 32(4), n/a-n/a, doi:10.1029/2004GL021900, 2005.
- 20 Shindell, D. T., Faluvegi, G., Koch, D. M., Schmidt, G. A., Unger, N. and Bauer, S. E.: Improved Attribution of Climate Forcing to Emissions, *Science*, 326(5953), 716–718, doi:10.1126/science.1174760, 2009.
- Sillman, S.: The relation between ozone, NO(x) and hydrocarbons in urban and polluted rural environments, *Atmos. Environ.*, 33(12), 1821–1845, doi:10.1016/S1352-2310(98)00345-8, 1999.
- 25 Silva, R. A., West, J. J., Zhang, Y., Anenberg, S. C., Lamarque, J.-F., Shindell, D. T., Collins, W. J., Dalsoren, S., Faluvegi, G., Folberth, G., Horowitz, L. W., Tatsuya Nagashima, Naik, V., Rumbold, S., Skeie, R., Sudo, K., Takemura, T., Daniel Bergmann, Cameron-Smith, P., Cionni, I., Doherty, R. M., Eyring, V., Josse, B., MacKenzie, I. A., Plummer, D., Righi, M., Stevenson, D. S., Strode, S., Szopa, S. and Zeng, G.: Global premature mortality due to anthropogenic outdoor air pollution and the contribution of past climate change, *Environ. Res. Lett.*, 8(3), 034005, doi:10.1088/1748-9326/8/3/034005, 2013.
- 30 Silva, R. A., West, J. J., Lamarque, J. F., Shindell, D. T., Collins, W. J., Dalsoren, S., Faluvegi, G., Folberth, G., Horowitz, L. W., Nagashima, T., Naik, V., Rumbold, S. T., Sudo, K., Takemura, T., Bergmann, D., Cameron-Smith, P., Cionni, I., Doherty, R. M., Eyring, V., Josse, B., MacKenzie, I. A., Plummer, D., Righi, M., Stevenson, D. S., Strode, S., Szopa, S. and Zeng, G.: The effect of future ambient air pollution on human premature mortality to 2100 using output from the ACCMIP model ensemble, *Atmospheric Chem. Phys.*, 16(15), 9847–9862, doi:10.5194/acp-16-9847-2016, 2016.
- 35 Stevenson, D. S., Dentener, F. J., Schultz, M. G., Ellingsen, K., Noije, T. P. C. van, Wild, O., Zeng, G., Amann, M., Atherton, C. S., Bell, N., Bergmann, D. J., Bey, I., Butler, T., Cofala, J., Collins, W. J., Derwent, R. G., Doherty, R. M., Drevet, J., Eskes, H. J., Fiore, A. M., Gauss, M., Hauglustaine, D. A., Horowitz, L. W., Isaksen, I. S. A., Krol, M. C., Lamarque, J.-F., Lawrence, M. G., Montanaro, V., Müller, J.-F., Pitari, G., Prather, M. J., Pyle, J. A., Rast, S., Rodriguez, J. M., Sanderson, M. G., Savage, N. H., Shindell, D. T., Strahan, S. E., Sudo, K. and Szopa, S.: Multimodel ensemble

- simulations of present-day and near-future tropospheric ozone, *J. Geophys. Res. Atmospheres*, 111(D8), doi:10.1029/2005JD006338, 2006.
- 5 Stevenson, D. S., Young, P. J., Naik, V., Lamarque, J.-F., Shindell, D. T., Voulgarakis, A., Skeie, R. B., Dalsoren, S. B., Myhre, G., Berntsen, T. K., Folberth, G. A., Rumbold, S. T., Collins, W. J., MacKenzie, I. A., Doherty, R. M., Zeng, G., Van, N., Strunk, A., Bergmann, D., Cameron-Smith, P., Plummer, D. A., Strode, S. A., Horowitz, L., Lee, Y. H., Szopa, S., Sudo, K., Nagashima, T., Josse, B., Cionni, I., Righi, M., Eyring, V., Conley, A., Bowman, K. W., Wild, O. and Archibald, A.: Tropospheric ozone changes, radiative forcing and attribution to emissions in the Atmospheric Chemistry and Climate Model Intercomparison Project (ACCMIP), *Atmospheric Chem. Phys.*, 13(6), 3063–3085, doi:10.5194/acp-13-3063-2013, 2013.
- 10 Stjern, C. W., Samset, B. H., Myhre, G., Bian, H., Chin, M., Davila, Y., Dentener, F., Emmons, L., Flemming, J., Haslerud, A. S., Henze, D., Jonson, J. E., Kucsera, T., Lund, M. T., Schulz, M., Sudo, K., Takemura, T. and Tilmes, S.: Global and regional radiative forcing from 20 % reductions in BC, OC and SO₄ - An HTAP2 multi-model study, *Atmospheric Chem. Phys.*, 16(21), 13579–13599, doi:10.5194/acp-16-13579-2016, 2016.
- 15 Tang, I. N.: Chemical and size effects of hygroscopic aerosols on light scattering coefficients, *J. Geophys. Res. Atmospheres*, 101(14), 19245–19250, 1996.
- The World Bank, The International Cryosphere Climate Initiative: On Thin Ice, Washington DC. [online] Available from: <http://iccinet.org/thinicepubfinal>, 2013.
- 20 Turner, M. C., Jerrett, M., Pope, C. A., Krewski, D., Gapstur, S. M., Diver, W. R., Beckerman, B. S., Marshall, J. D., Su, J., Crouse, D. L. and Burnett, R. T.: Long-Term Ozone Exposure and Mortality in a Large Prospective Study, *Am. J. Respir. Crit. Care Med.*, 193(10), 1134–1142, doi:10.1164/rccm.201508-1633OC, 2016.
- Turnock, S., Wild, O., Dentener, F., Davila, Y., Emmons, L., Flemming, J., Folberth, G., Henze, D., Jonson, J., Keating, T., Kengo, S., Lin, M., Lund, M., Tilmes, S. and O'Connor, F.: The Impact of Future Emission Policies on Tropospheric Ozone using a Parameterised Approach, *Atmospheric Chem. Phys. Discuss.*, 1–41, doi:https://doi.org/10.5194/acp-2017-1220, 2018.
- 25 Twomey, S.: Pollution and the planetary albedo, *Atmospheric Environ.* 1967, 8(12), 1251–1256, doi:10.1016/0004-6981(74)90004-3, 1974.
- UNEP: Near-term climate protection and clean air benefits: Actions for controlling short-lived climate forcers, Report, United Nations Environment Programme, Nairobi, Kenya. [online] Available from: <http://researchrepository.murdoch.edu.au/id/eprint/15325/> (Accessed 10 January 2017), 2011.
- 30 UNEP and CCAC: Integrated Assessment of Short-Lived Climate Pollutants for Latin America and the Caribbean: improving air quality while mitigating climate change. Summary for decision makers., United Nations Environmental Programme, Nairobi, Kenya. [online] Available from: http://www.ccacoalition.org/sites/default/files/resources/UNEP_Assessment%20A%20SINGLE.pdf (Accessed 14 December 2017), 2016.
- 35 Unger, N., Bond, T. C., Wang, J. S., Koch, D. M., Menon, S., Shindell, D. T. and Bauer, S.: Attribution of climate forcing to economic sectors, *Proc. Natl. Acad. Sci. U. S. A.*, 107(8), 3382–3387, doi:10.1073/pnas.0906548107, 2010.

- Van Aardenne, J., Dentener, F., Van Dingenen, R., Maenhout, G., Marmer, E., Vignati, E., Russ, P., Szabo, L. and Raes, F.: Climate and air quality impacts of combined climate change and air pollution policy scenarios, JRC Scientific and Technical Reports, Ispra, Italy., 2007.
- 5 Van Dingenen, R., Dentener, F. J., Raes, F., Krol, M. C., Emberson, L. and Cofala, J.: The global impact of ozone on agricultural crop yields under current and future air quality legislation, *Atmos. Environ.*, 43(3), 604–618, doi:10.1016/j.atmosenv.2008.10.033, 2009.
- van Vuuren, D. P., Elzen, M. G. J. den, Lucas, P. L., Eickhout, B., Strengers, B. J., Ruijven, B. van, Wonink, S. and Houdt, R. van: Stabilizing greenhouse gas concentrations at low levels: an assessment of reduction strategies and costs, *Clim. Change*, 81(2), 119–159, doi:10.1007/s10584-006-9172-9, 2007.
- 10 Wang, X. and Mauzerall, D. L.: Characterizing distributions of surface ozone and its impact on grain production in China, Japan and South Korea: 1990 and 2020, *Atmos. Environ.*, 38(26), 4383–4402, doi:10.1016/j.atmosenv.2004.03.067, 2004.
- Wild, O., Fiore, A. M., Shindell, D. T., Doherty, R. M., Collins, W. J., Dentener, F. J., Schultz, M. G., Gong, S., MacKenzie, I. A., Zeng, G. and others: Modelling future changes in surface ozone: a parameterized approach, *Atmospheric Chem. Phys.*, 12(4), 2037–2054, 2012.
- 15 Wu, S., Duncan, B. N., Jacob, D. J., Fiore, A. M. and Wild, O.: Chemical nonlinearities in relating intercontinental ozone pollution to anthropogenic emissions, *Geophys. Res. Lett.*, 36(5), doi:10.1029/2008GL036607, 2009.
- 20 Yu, H., Chin, M., West, J. J., Atherton, C. S., Bellouin, N., Bergmann, D., Bey, I., Bian, H., Diehl, T., Forberth, G., Hess, P., Schulz, M., Shindell, D., Takemura, T. and Tan, Q.: A multimodel assessment of the influence of regional anthropogenic emission reductions on aerosol direct radiative forcing and the role of intercontinental transport, *J. Geophys. Res. Atmospheres*, 118(2), 700–720, doi:10.1029/2012JD018148, 2013.
- Zhang, L., Liu, L., Zhao, Y., Gong, S., Zhang, X., Henze, D. K., Capps, S. L., Fu, T.-M., Zhang, Q. and Wang, Y.: Source attribution of particulate matter pollution over North China with the adjoint method, *Environ. Res. Lett.*, 10(8), 084011, 2015.

Table 1: Relevant precursor-pollutant relationships included in TM5-FASST. ●: direct emission or immediate product; ○: effect via thermodynamic equilibration; ◇ effect via first order oxidation products (OH) affecting the lifetime of other precursors.

Pollutant \ Precursor	SO ₂ (g)	NO _x (g)	NH ₃ (g)	O ₃	CH ₄	SO ₄ (PM _{2.5})	NO ₃ (PM _{2.5})	NH ₄ (PM _{2.5})	EC (PM _{2.5})	POM (PM _{2.5})	SOx (dep)	NOy (dep)	Rad. forcing
SO ₂ (g)	●	◇	○	◇	◇	●	○	○			●		●
NO _x (g)	◇	●	○	●	◇	○	●	○			◇	●	●
NH ₃ (g)	◇	◇	●	◇	◇	○	○	●			◇		●
BC (pm)									●				●
POM (pm)										●			●
NMVOC (g)	◇	◇	◇	●	◇	◇	◇	◇			◇		●
CO (g)*				●	◇								●
CH ₄ (g)*	◇	◇	◇	◇	●	◇	◇	◇			◇		●

* From HTAP phase 1 (Dentener et al., 2010)

Table 2: Overview of TM5-CTM perturbation simulations (20% emission reduction) for the calculation of the source-receptor (SR) matrices*comparing to the same zoom regions as in P0.

Simulation	Emission perturbations	Applied on source regions	Scope
P0	No perturbations	Master zoom regions with 1°x1° resolution: AFR, AUS, EAS, EUR, MAM, MEA, NAM,RSA, RUS, SAM, SAS, SEA and PAC (3°x2°)	Base simulation
P1	SO ₂ , NO _x , BC, POM	All 56 continental regions* + international shipping + aviation	SR matrices for BC and POM and first order approximation for SO ₂ and NO _x , assuming negligible chemical interaction
P2	SO ₂	All 56 source regions* + shipping	Independent SR for SO ₂ , to be compared to P1 to quantify potential interference between SO ₂ and NO _x in the formation of sulfate and ozone
P3	NO _x	Representative source regions* (China, Europe, Japan, India, Germany, South-Africa, USA)	Independent SR for NO _x , to verify the additivity of P1 = P2 + P3 and justify the use of (P1 – P2) as a proxy for NO _x perturbation for all other regions
P4	NH ₃ , NMVOC	All 56 continental source* regions + international shipping	SR matrices for NH ₃ and NMVOC emissions, assuming little chemical interaction between the selected precursors in the formation of NH ₄ and O ₃
P5	NMVOC, NO _x	Representative source regions* (Europe, China, India, USA)	Quantify chemical feedbacks in O ₃ formation between NO _x and NMVOC (P5 = P3 + P4) additivity

*See list of regions and their definition in Table S2.2 of the SI.

Table 3. Overview of air quality indices used to evaluate crop yield losses. The a, b and c coefficients refer to the exposure-response equations given in the equations 5 and 6. Source: Van Dingenen et al. (2009), Mills et al. (2007), Wang and Mauzerall (2004)

	Wheat			Rice			Soy			Maize		
Metric:	a	b	c	a	b	c	a	b	c	a	b	c
AOT40 (ppm.h)	0.0163	-	-	0.00415	-	-	0.0113	-	-	0.00356	-	-
Mi (ppbV)	137	2.34	25	202	2.47	25	107	1.58	20	124	2.83	20

5

- Deleted: Table 3: Median (95% CI) ...
- Deleted: $\frac{c_{FASST} - c_{TMS}}{c_{TMS}}$ (%)
- Inserted Cells ...
- Inserted Cells ...
- Deleted: Precursor
- Deleted: PERTURBATION
- Deleted: Annual O₃
- Deleted: M6M
- Deleted: M12
- Deleted: AOT40
- Inserted Cells ...
- Deleted: NO_x ...
- Moved down [7]: -80%
- Deleted: -80%
- Inserted Cells ...
- Inserted Cells ...
- Deleted: 4 (0.2, 1.6)
- Inserted Cells ...
- Inserted Cells ...
- Deleted: 6 (0.2, 2.8)
- Inserted Cells ...
- Inserted Cells ...
- Deleted: 5 (0.1, 1.3)
- Deleted: 2.3 (-7.5, 6.5)
- Inserted Cells ...
- Deleted: ¶
- Moved down [6]: -80%
- Deleted: 4 (-2.2, 5.4)
- Inserted Cells ...
- Inserted Cells ...
- Deleted: 5 (-1.0, 4.4)
- Inserted Cells ...
- Inserted Cells ...
- Inserted Cells ...
- Inserted Cells ...
- Deleted: 1 (0.3, 4.4)
- Deleted: 28 (0.9, 69)
- Deleted: ¶
- Deleted: -----Page Break-----

Table 4: Statistical metrics describing the correspondence between the linearized FASST and TM5 computed change in secondary PM_{2.5} upon -80% and 100% emission perturbation in its precursors (SO₂, NO_x, NH₃ and combined SO₂ + NO_x), relative to the RCP2000 base scenario. Statistics are calculated over all 1°x1° grid cells in each region. Statistics for total concentrations are given in annex S7 of the SI.

Region	FASST MEAN (µg m ⁻³)		TM5 MEAN (µg m ⁻³)		NMB ^(a) (%)		MB ^(b) (µg m ⁻³)		R ^{2(c)}	
	↓80%	↓100%	↓80%	↓100%	↓80%	↓100%	↓80%	↓100%	↓80%	↓100%
Precursor: SO ₂										
EUR	-1.0	1.2	-1.1	1.1	-11.8	12.8	0.13	0.14	0.99	1.00
USA	-0.8	1.1	-0.9	1.0	-8.2	10.8	0.08	0.10	1.00	1.00
JPN	-0.3	0.4	-0.3	0.4	-5.0	6.8	0.02	0.02	1.00	1.00
CHN	-1.5	1.8	-1.7	1.6	-13.3	17.7	0.22	0.28	1.00	1.00
IND	-2.1	2.7	-2.2	2.5	-4.6	8.3	0.10	0.20	1.00	1.00
Precursor: NO _x										
EUR	-0.9	1.2	1.1	0.8	-13.7	44.4	0.15	0.36	0.9	0.9
USA	-0.5	0.6	0.6	0.4	-25.1	60.9	0.15	0.21	0.8	0.87
JPN	-0.3	0.4	0.4	0.2	-27.3	93.2	0.11	0.17	0.9	0.91
CHN	-0.8	1.0	0.9	0.7	-11.9	35.5	0.11	0.26	0.9	0.90
IND	-0.6	0.7	0.6	0.8	6.8	-9.3	0.04	0.08	0.9	0.94
Precursor: NH ₃										
EUR	-1.1	1.4	1.6	1.2	-29.0	12.8	0.45	0.16	0.9	0.92
USA	-0.6	0.8	0.8	0.6	-20.2	28.6	0.16	0.17	0.9	0.94
JPN	-0.4	0.4	0.4	0.4	-16.9	28.2	0.07	0.10	0.9	0.99
CHN	-0.8	1.0	1.0	0.7	-25.5	43.8	0.26	0.30	0.8	0.98
IND	-0.2	0.3	0.4	0.2	-47.6	48.4	0.18	0.08	0.8	0.94
Precursor: SO ₂ +NO _x										
EUR	-1.9	2.4	2.3	1.8	-17.5	33.5	0.40	0.60	0.9	0.95
USA	-1.3	1.6	1.6	1.2	-16.1	31.2	0.25	0.39	0.9	0.97
JPN	-0.6	0.7	0.7	0.5	-16.5	44.9	0.11	0.22	0.9	0.96

^(a) Normalized Mean Bias = (FASST - TM5)/TM5

- Deleted: FLE
- Deleted: MIT
- Inserted Cells
- Moved (insertion) [6]
- Moved (insertion) [7]
- Deleted: Slope
- Deleted: R²
- Deleted: Slope
- Deleted: R²
- Inserted Cells
- Moved down [8]: 0.97
- Deleted: Total PM_{2.5}
- Deleted: 11
- Deleted: 54
- Inserted Cells
- Deleted: 85
- Inserted Cells
- Deleted: Primary PM_{2.5}
- Inserted Cells
- Deleted: 20
- Deleted: 96
- Deleted: 62
- Deleted: 91
- Inserted Cells
- Inserted Cells
- Inserted Cells
- Deleted: Secondary PM_{2.5}
- Deleted: 93
- Deleted: 95
- Deleted: 46
- Deleted: 0.42
- Deleted: Annual mean O₃
- Deleted: 04
- Deleted: 0.90
- Deleted: 03
- Inserted Cells
- Inserted Cells
- Inserted Cells
- Inserted Cells

5

^(b) Mean Bias = $\overline{(FASST - TM5)}$

^(c) Correlation coefficient

\bar{Y} = average of all grid cells in region

Table 5: Statistical metrics describing the correspondence between the linearized FASST and TM5 computed change in O₃ exposure metric 6mDMA1 upon -80% and 100% emission perturbation in its precursors (NMVOC, NO_x and combined NO_x + NMVOC), relative to the RCP2000 base scenario. Statistics are calculated over all 1°x1° grid cells in each region. Statistics for total concentrations are given in annex S7 of the SI.

Region	FASST MEAN (ppb)		TM5 MEAN (ppb)		NMB ^(a) (%)		MB ^(b) (ppb)		R ^{2(c)}	
	-80%	100%	-80%	100%	-80%	100%	-80%	100%	-80%	100%
Precursor: NMVOC										
EUR	-1.5	1.8	-1.7	1.3	-11	36	0.2	0.5	0.55	0.41
USA	-1.1	1.4	-1.3	1.2	-10	23	0.1	0.3	0.98	0.99
JPN	-0.9	1.1	-1.0	0.8	-14	30	0.1	0.3	0.99	0.98
CHN	-0.9	1.1	-1.3	0.6	-30	93	0.4	0.5	0.98	0.96
IND	-0.9	1.1	-1.2	0.7	-25	59	0.3	0.4	0.99	0.99
Precursor: NO _x										
EUR	-2.7	3.3	-4.5	1.2	-41	169	1.9	2.1	0.87	0.77
USA	-4.5	5.7	-6.8	3.3	-33	70	2.3	2.3	0.79	0.85
JPN	-1.1	1.4	-2.7	-0.4	-58	-499	1.6	1.8	0.59	0.59
CHN	-4.3	5.4	-6.1	3.3	-29	64	1.7	2.1	0.96	0.82
IND	-7.3	9.1	-9.6	6.4	-25	41	2.4	2.7	0.98	0.96
Precursor: NO _x + NMVOC										
EUR	-4.1	5.2	-5.1	3.8	-18	38	0.9	1.4	0.89	0.97
USA	-5.7	7.1	-7.1	5.2	-20	36	1.4	1.9	0.97	0.95
CHN	-5.2	6.5	-6.0	5.2	-13	26	0.8	1.3	0.99	0.99
IND	-8.1	10.1	-9.6	8.4	-15	21	1.5	1.7	0.99	0.99

^(a) Normalized Mean Bias = $(FASST - TM5)/TM5$

^(b) Mean Bias = $(FASST - TM5)$

^(c) Correlation coefficient

\bar{Y} = average of all grid cells in region

5

Table 6: Statistical metrics describing the correspondence between the linearized FASST and TM5 computed change in O₃ crop exposure metric AOT40 upon -80% and 100% emission perturbation in its precursors (NMVOC, NO_x and combined NO_x + NMVOC), relative to the RCP2000 base scenario. Statistics are calculated over all 1°x1° grid cells in each region.

Region	FASST MEAN (ppm.h)		TM5 MEAN (ppm.h)		NMB ^(a) (%)		MB ^(b) (ppm.h)		R ^{2(c)}	
	-80%	100%	-80%	100%	-80%	100%	-80%	100%	-80%	100%
Precursor: NMVOC										
EUR	-1.1	1.4	-1.3	1.2	-11	24	0.1	0.3	0.87	0.75
USA	-1.0	1.3	-1.1	1.0	-10	26	0.1	0.3	0.98	0.99
JPN	-0.7	0.8	-0.8	0.6	-13	38	0.1	0.2	0.98	0.98
CHN	-0.7	0.8	-0.9	0.4	-29	95	0.3	0.4	0.98	0.96
IND	-0.6	0.8	-0.8	0.4	-27	70	0.2	0.3	0.98	0.96
Precursor: NO _x										
EUR	-2.1	2.6	-3.1	1.3	-34	102	1.1	1.3	0.93	0.84
USA	-4.6	5.7	-6.3	3.7	-27	57	1.7	2.1	0.82	0.86
JPN	-0.7	0.9	-1.7	-0.2	-56	-498	0.9	1.1	0.83	0.63
CHN	-3.0	3.7	-3.5	2.5	-14	50	0.5	1.3	0.92	0.87
IND	-4.5	5.6	-5.3	3.9	-15	44	0.8	1.7	0.93	0.91
Precursor: NO _x + NMVOC										
EUR	-3.2	4.0	-4.2	1.8	-23	126	1.0	2.2	0.94	0.91
USA	-5.6	7.0	-6.9	3.8	-18	86	1.3	3.2	0.95	0.90
CHN	-3.7	4.6	-4.3	2.4	-15	90	0.6	2.2	0.87	0.89
IND	-5.1	6.3	-5.8	3.6	-12	76	0.7	2.7	0.89	0.90

^(a) Normalized Mean Bias = $(\overline{FASST} - \overline{TM5}) / \overline{TM5}$

^(b) Mean Bias = $(\overline{FASST} - \overline{TM5})$

^(c) Correlation coefficient

\bar{Y} = average of all grid cells in region

5

Table 7: Statistical metrics describing the correspondence between the linearized FASST and TM5 computed change in O₃ crop exposure metric M12 upon -80% and 100% emission perturbation in its precursors (NMVOC, NO_x and combined NO_x + NMVOC), relative to the RCP2000 base scenario. Statistics are calculated over all 1°x1° grid cells in each region

Region	FASST MEAN (ppb)		TM5 MEAN (ppb)		NMB ^(a) (%)		MB ^(b) (ppb)		R ^{2(c)}	
	-80%	100%	-80%	100%	-80%	100%	-80%	100%	-80%	100%
Precursor: NMVOC										
EUR	-0.9	1.1	-1.6	1.3	-43	-16	0.7	-0.2	0.50	0.37
USA	-1.0	1.3	-1.2	1.0	-11	27	0.1	0.3	0.98	0.99
JPN	-0.7	0.9	-0.8	0.6	-16	38	0.1	0.2	0.98	0.97
CHN	-0.8	0.9	-1.1	0.5	-33	102	0.4	0.5	0.98	0.95
IND	-0.6	0.8	-0.9	0.5	-28	76	0.7	0.3	0.98	0.95
Precursor: NO _x										
EUR	-1.6	2.0	-3.2	0.4	-49	392	1.6	1.6	0.87	0.78
USA	-4.3	5.4	-6.4	3.2	-33	66	2.1	2.2	0.82	0.84
JPN	0.5	-0.6	-0.6	-1.9	-188	-67	1.1	1.3	0.92	0.80
CHN	-3.4	4.3	-4.9	2.5	-30	68	1.5	1.7	0.95	0.81
IND	-4.8	6.0	-6.8	3.9	-29	54	2.0	2.1	0.94	0.98
Precursor: NO _x + NMVOC										
EUR	-2.5	3.2	-3.8	2.7	-33	16	1.2	0.4	0.88	0.88
USA	-5.3	6.7	-6.6	5.0	-19	34	1.3	1.7	0.96	0.94
CHN	-4.2	5.2	-4.8	4.2	-13	25	0.6	1.1	0.98	0.96
IND	-5.5	6.9	-6.6	5.6	-18	23	1.2	1.3	0.96	0.94

^(a) Normalized Mean Bias = $(\overline{FASST} - \overline{TM5}) / \overline{TM5}$

^(b) Mean Bias = $(\overline{FASST} - \overline{TM5})$

^(c) Correlation coefficient

\bar{Y} = average of all grid cells in region

5

Table 8: Regional grid cell mean anthropogenic PM_{2.5} concentration (including primary and secondary components) and performance statistics for FASST vs. TM5, for the high (FLE2030) and low (MIT2030) emission scenarios and for the delta. See Table S2.2 in the SI for the region legend.

REG	PM _{2.5} FASST (µg m ⁻³)	PM _{2.5} TM5 (µg m ⁻³)	NMB	MB(µg m ⁻³)	R ²
FLE2030					
EUR	9.2	8.7	6%	0.56	0.94
NAM	4.7	4.2	11%	0.47	0.95
EAS	30.2	27.5	10%	2.75	0.93
SAS+SEA	26.4	26.8	-2%	-0.42	0.84
RUS	5.8	5.7	1%	0.07	0.91
SAM	5.0	4.9	1%	0.07	0.77
MEA	8.9	9.2	-3%	-0.23	0.88
AFR	8.5	9.4	-10%	-0.90	0.77
MIT2030					
EUR	4.0	2.1	86%	1.84	0.83
NAM	2.8	2.2	28%	0.63	0.78
EAS	10.1	8.5	19%	1.58	0.94
SAS+SEA	8.8	7.1	24%	1.72	0.73
RUS	2.6	2.1	24%	0.51	0.85
SAM	4.4	4.3	1%	0.04	0.74
MEA	3.6	3.2	11%	0.36	0.74
AFR	4.9	4.7	5%	0.21	0.93
FLE2030 - MIT2030					
EUR	5.3	6.6	-20%	-1.28	0.97
NAM	1.8	2.0	-8%	-0.16	0.93
EAS	20.1	18.9	6%	1.17	0.93
SAS+SEA	17.6	19.7	-11%	-2.14	0.85
RUS	3.2	3.6	-12%	-0.44	0.85
SAM	0.6	0.6	6%	0.03	0.13
MEA	5.4	6.0	-10%	-0.59	0.77
AFR	3.6	4.8	-23%	-1.11	0.47

Table 9: Regional grid cell mean anthropogenic ozone health exposure metric 6mDMA1 and performance statistics for FASST vs. TM5, for the high (FLE2030) and low (MIT2030) emission scenarios, and for the delta. See Table S2.2 in the SI for the region legend.

REG	6mDMA1 FASST (ppb)	6mDMA1 TM5 (ppb)	NMB	MB (ppb)	R ²
FLE2030					
EUR	55	53	4%	2	0.98
NAM	57	53	7%	4	0.96
EAS	69	57	21%	12	0.93
SAS+SEA	92	76	20%	15	0.96
RUS	53	50	6%	3	0.98
SAM	42	38	9%	3	0.92
MEA	72	70	4%	3	0.95
AFR	59	55	7%	4	0.94
MIT2030					
EUR	49	43	13%	6	0.95
NAM	50	41	22%	9	0.95
EAS	50	44	13%	6	0.94
SAS+SEA	51	46	11%	5	0.90
RUS	44	40	11%	4	0.99
SAM	35	31	12%	4	0.90
MEA	55	51	9%	4	0.89
AFR	48	44	8%	3	0.96
FLE2030 - MIT2030					
EUR	6	9	-38%	-4	0.89
NAM	7	12	-45%	-5	0.67
EAS	19	13	46%	6	0.89
SAS+SEA	40	30	35%	10	0.94
RUS	8	10	-15%	-1.4	0.89
SAM	6	7	-5%	-0.3	0.47
MEA	17	19	-9%	-1.8	0.89
AFR	11	10	4%	0.4	0.72

Table 10: Contributions of emissions of CH₄, NO_x, CO and NMVOC to O₃ and CH₄ radiative forcing. Stevenson et al. (2013): for the period 1850-2000; Shindell et al. (2005, 2009) for the period 1750-2000. **FASST: emission changes from Stevenson et al. (2013) multiplied with FASST global forcing efficiencies**

	Stevenson et al., 2013	Shindell et al., 2005	Shindell et al., 2009	TM5-FASST
Contribution to O ₃ forcing (mWm ⁻²)				
CH ₄	166 ± 46	200 ± 40	275	211
NO _x	119 ± 33	60 ± 30	41	35
CO	58 ± 13		48	67
NMVOC	35 ± 9		7	39
Contribution to CH ₄ forcing (mWm ⁻²)				
CH ₄	533 ± 39	590 ± 120	530	528
NO _x	-312 ± 67	-170 ± 85	-130	95
CO	57 ± 9			58
NMVOC	22 ± 18			38

Deleted: FASST: anthropogenic emissions RCP year 2000

Deleted: 200

Deleted: 61

Deleted: 108

Deleted: 53

Deleted: 500

Deleted: 167

Deleted: 83

Deleted: 49

Deleted: -----Page Break-----
¶
Table 6

Table 11. Regional-to-global direct radiative forcing efficiencies for PM_{2.5} precursors (mW/m²/Tg of annual emissions) for the larger source-receptor regions in earlier studies, and from FASST, aggregated to similar regional definitions. Values in brackets represent 1 standard deviation from the respective reported model ensembles.

		NAM	EUR	SAS	EAS	RUS	MEA
Stjern et al., 2016	BC	52 (±21)	55 (±22)	94 (±38)	55 (±16)	78 (±47)	202 (±323)
	POM	-8 (±6)	-7 (±4)	-10 (±6)	-5 (±3)	-2 (±5)	-18 (±7)
	SO ₄ (SO ₂)	-5 (±2)	-6 (±2)	-8 (±4)	-4 (±1)	-4 (±1)	-10 (±7)
Yu et al., 2013	BC	27 (±15)	37 (±19)	25 (±15)	28 (±20)		
	POM	-4 (±2)	-4 (±2)	-4 (±2)	-4 (±2)		
	SO ₄ (SO ₂)	-4 (±1)	-4 (±1)	-4 (±1)	-3 (±1)		
FASST (RCP2000)	BC	17	19	19	16	25	43
	POM	-6	-4	-6	-5	-4	-9
	SO ₄ (SO ₂)	-3	-3	-4	-2	-2	-7

Table 12. Regional-to-global direct radiative forcing efficiencies for O₃ precursors (mW/m²/Tg of annual emissions) for the larger source-receptor regions in earlier work, and from FASST, aggregated to similar regional definitions, including direct O₃ forcing, feedbacks on CH₄ and long-term O₃ forcing from the latter. Values in brackets represent reported 1 standard deviation from the model ensemble in Fry et al., 2012.

		East-Asia	Europe	N-America	South-Asia
Fry et al., 2012	NO _x	-0.31 (±0.6)	-0.80 (±0.5)	-0.53 (±0.6)	-1.17 (±2.2)
	NMVOC	0.50 (±0.2)	0.45 (±0.2)	0.47 (±0.2)	0.72 (±0.2)
	CO	0.15 (±0.02)	0.13 (±0.02)	0.16 (±0.02)	0.15 (±0.02)
FASST (RCP200)	NO _x	-0.44	-0.33	-0.35	-1.43
	NMVOC	0.60	0.57	0.61	0.74
	CO	0.18	0.15	0.15	0.19

5

Table 13: Global GWP and GTP values 95% CI range (excluding Indirect Radiative Effects) from IPCC AR5 (Forster et al., 2007), and from FASST based on RCP year 2000 emissions and the regional forcing efficiencies listed in Table A6.2 of the SI (all numbers rounded to 2 significant figures).

	GWP20		GWP100		GTP20		GTP100	
	AR5	FASST	AR5	FASST	AR5	FASST	AR5	FASST
CH ₄	(70, 98)	78	(24, 33)	29	(56, 79)	66	(3.6, 5.0)	3.9
BC	(940, 4100)	880	(257, 1100)	240	(270, 1200)	340	(35, 150)	37
OC	(-410, -89)	-280	(-114, -25)	-77	(-120, -26)	-110	(-16, -3)	-12
SO ₂	(-210, -70)	-150	(-58, -19)	-40	(-61, -20)	-57	(-8, 38)	-6.2
VOC	(8.3, 20)	21	(2.7, 6.3)	7	(4.4, 11)	11	(0.4, 0.9)	1.2
NO _x	(12, 26) ^a (-220, -440) ^b	-31	(-15, -7) ^a (-130, -64) ^b	-14	(-120, -57)	-100	(-3.9, -1.9)	-8
CO	(6.0, 7.8)	7.9	(2, 3)	2.6	(3.7, 6.1)	6.3	(0.27, 0.55)	0.42

a Fuglestvedt et al. (2010)

b Shindell et al., (2009)

Deleted:

b . . , excluding indirect aerosol effects

5

Table 14 Overview of previous studies on health impact of PM_{2.5}, together with FASST results for 2 different scenarios. Uncertainty ranges are as reported in the respective studies. The uncertainty range on FASST results includes the RR uncertainty only (Fig. S5.1 in the SI)

Reference	Year evaluated	Method	threshold	Exposure - response function	Global deaths (millions)
Excluding mineral dust					
Fang et al., 2013	2000	CTM	no	K2009 ^(a)	1.6 (1.2 – 1.9)
Silva et al., 2013	2000	CTM	no	K2009	2.1 (1.3 -3.0)
Anenberg et al., 2010	2000	CTM	5.8µg m ⁻³	K2009	2.7 (2.0 -3.4)
Evans et al., 2013	2004	SAT	5.8µg m ⁻³	K2009	2.7 (1.9 - 3.5)
Lelieveld et al., 2013	2005	CTM	no	K2009	2.2 (2.1 - 2.3)
FASST (RCP)	2000	FASST	~7.3µg m⁻³	K2009	2.5 (1.2 – 3.6)
FASST (RCP)	2000	FASST	~7.3µg m⁻³	B2014^(b)	2.1 (1.0 – 3.0)
Including mineral dust					
Silva et al., 2016	2000	ACCMIP CTM ensemble	~7.3µg m ⁻³	B2014	1.7 (1.3 – 2.1)
Evans et al. 2013	2004	SAT	5.8µg m ⁻³	K2009	4.3 (2.9 – 5.4)
Lelieveld et al., 2015	2010	CTM	~7.3µg m ⁻³	B2014	3.2 (1.5 - 4.6)
GBD2010 (Lim et al., 2012)	2010	Fused (FASST + SAT + ground based)	~7.3µg m ⁻³	B2014	3.2 (2.8 -3.6)
GBD2013 (Forouzanfar et al., 2015)	2013	Fused (FASST + SAT + ground based)	~7.3µg m ⁻³	B2014	2.9 (2.8 – 3.1)
GBD2015 (Cohen et al., 2017)	2015	Fused (FASST + SAT + ground based)	~4.1µg m ⁻³	B2014	4.2 (3.7 – 4.8)
FASST (RCP)	2000	FASST	~7.3µg m⁻³	K2009	3.6 (2.7 -4.5)
FASST (RCP)	2000	FASST	~7.3µg m⁻³	B2014	2.6 (1.2 – 3.8)
FASST (HTAP2)	2010	FASST	~7.3µg m⁻³	B2014	4.1 (2.0 - 5.9)

(a) Krewski et al., 2009

(b) Burnett et al., 2014

5

Table 15 Overview of previous studies on long-term health impact of ozone, together with FASST results for 2 different scenarios

Ref	year	Method	threshold	Exposure-response function	Global deaths (thousands)
Anenberg et al., 2010	2000	CTM	33.3	J2009 ^(a)	470 (182 - 758)
Silva et al., 2013	2000	ACCMIP CTM ensemble	33.3	J2009	380 (117 - 750)
Lelieveld et al., 2015	2010	CTM	~37.6	J2009	142 (90 - 208)
GBD 2010 (Lim et al., 2012)	2010	FASST	~37.6	J2009	152 (52 - 270)
GBD 2013 (Forouzanfar et al., 2015)	2013	FASST	~37.6	J2009	217 (161 - 272)
GBF 2015 (Cohen et al., 2017)	2015	FASST	~37.6	J2009	254 (97 - 422)
FASST (RCP)	2000	FASST	33.3	J2009	197 (66 - 315)
FASST (HTAP2)	2010	FASST	33.3	J2009	340 (116 - 544)

(a) Jerrett et al., 2009

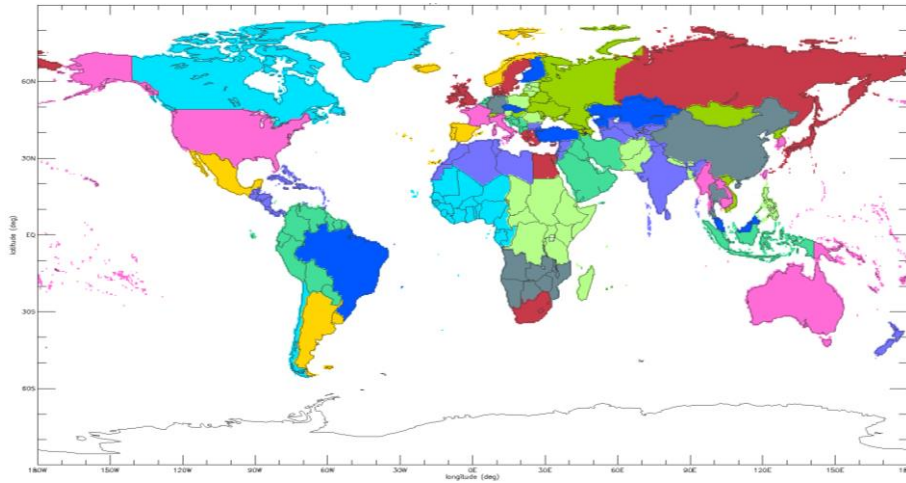


Figure 1: 56 continental emission source regions in TM5-FASST. See Table S2.2 in the SI for the mapping between regions and countries

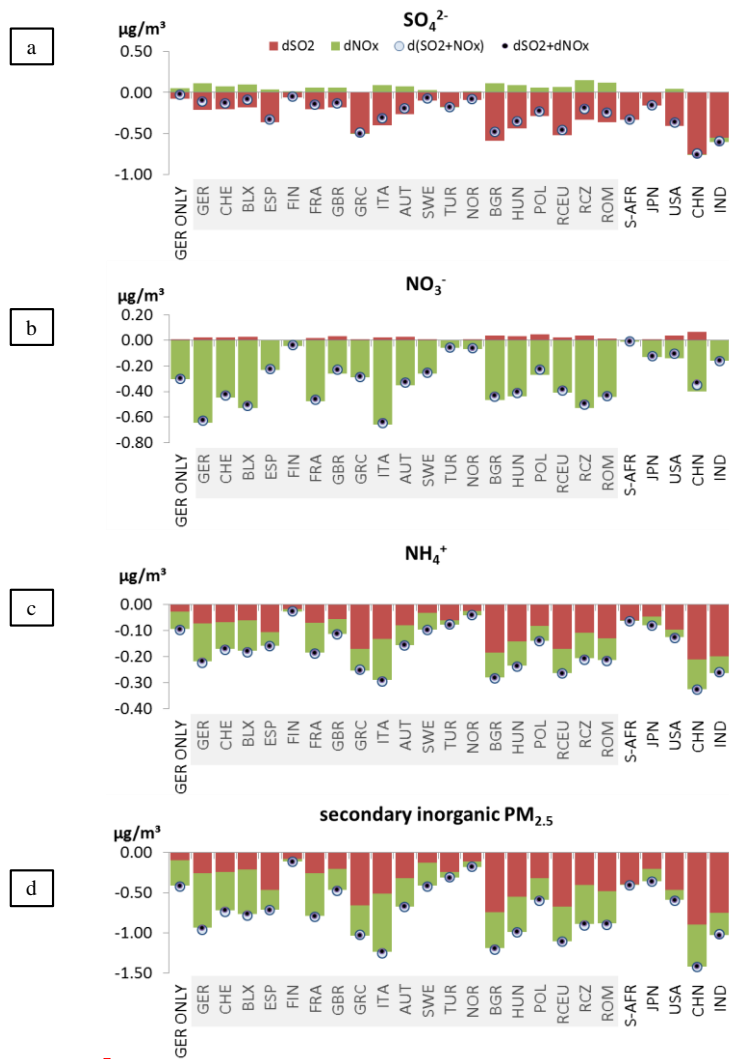


Figure 2: TM5-CTM response in annual population-weighted mean sulfate (a), nitrate (b), ammonium (c) and total inorganic secondary $\text{PM}_{2.5}$ (d) (as sum of the 3 components) upon emitted precursor perturbation of -20% for selected source regions (see SI table S2.2 for the region codes legend). Only the concentration change inside each source region is shown. Red bars: SO_2 -only perturbation (simulation P2); green bars: NO_x -only perturbation (simulation P3). Open circles: simultaneous ($\text{SO}_2 + \text{NO}_x$) perturbation (simulation P1). Black dots: P2 + P3. Shaded regions are perturbed simultaneously as one European region.

Deleted:

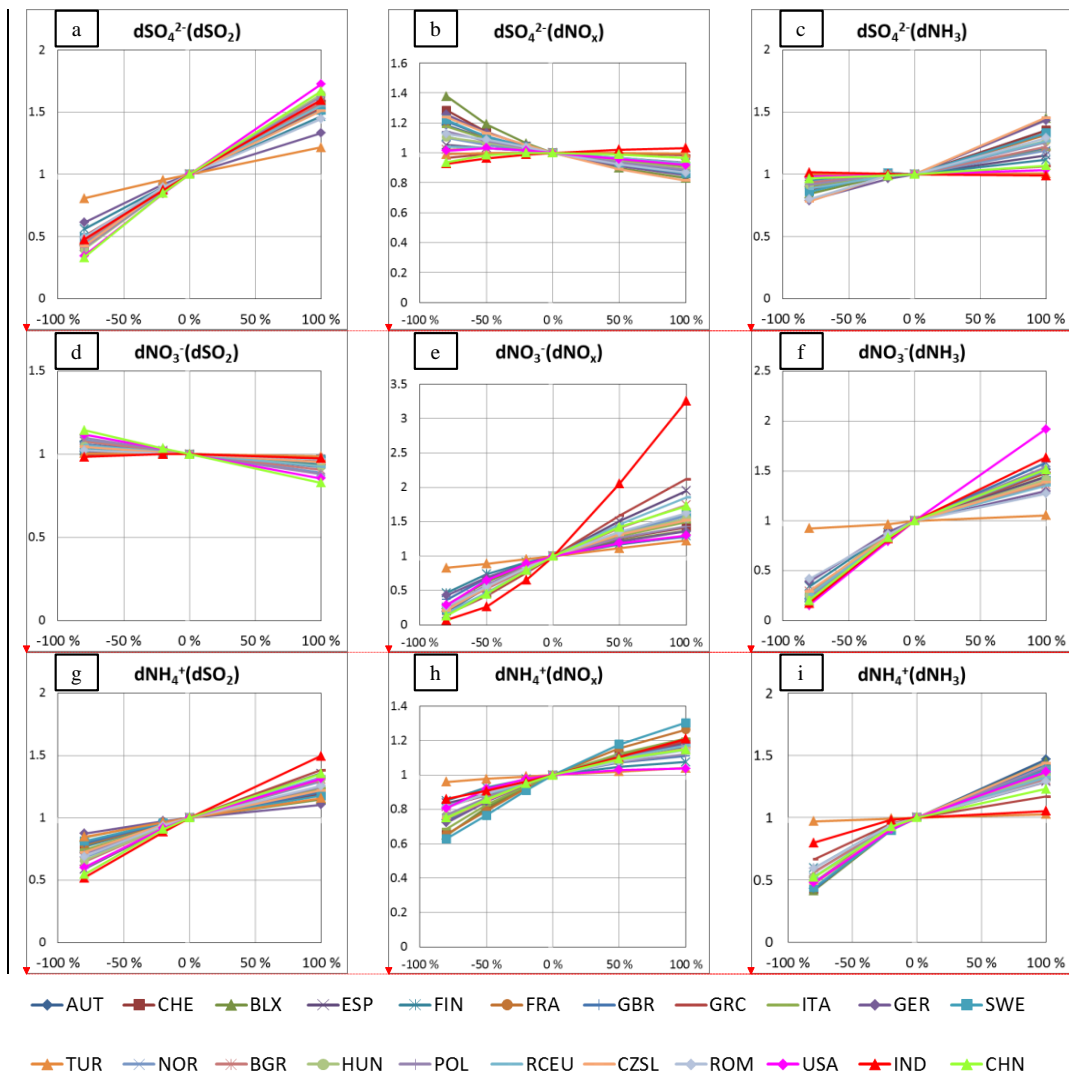
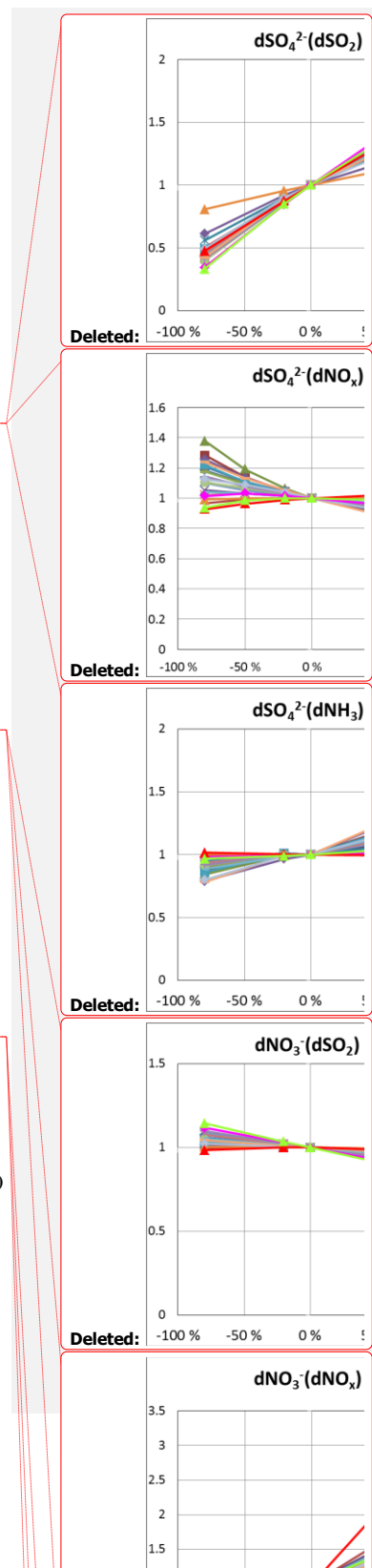
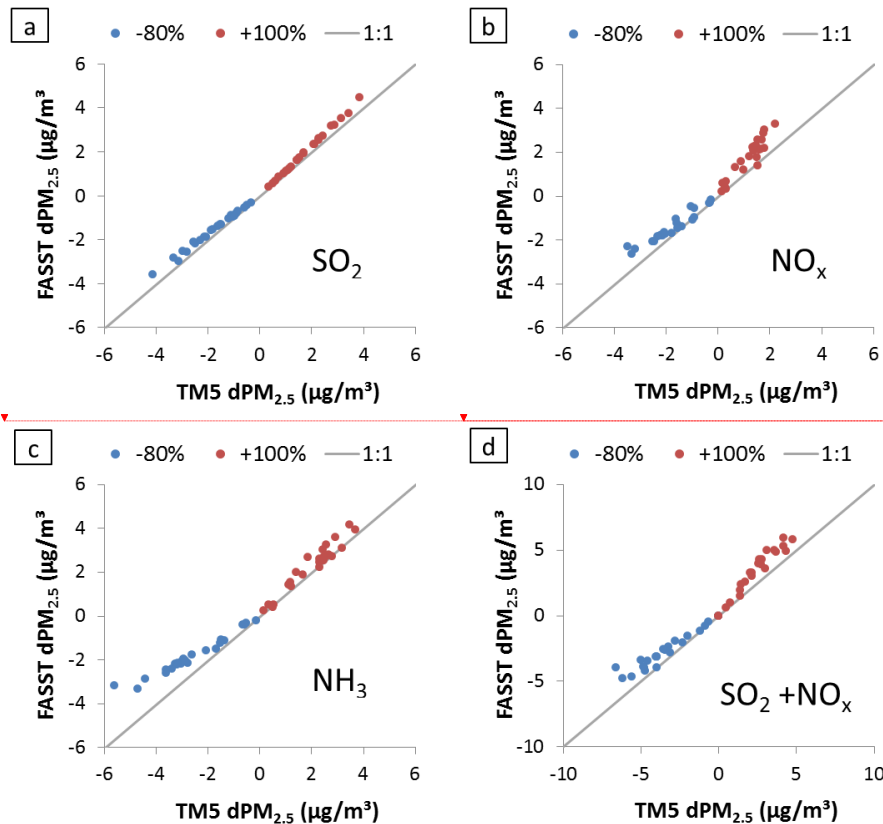


Figure 3: TM5-CTM change in population-weighted regional mean secondary $PM_{2.5}$ components SO_4^{2-} (a to c), NO_3^- (d to f), NH_4^+ (g to i), relative to their respective base scenario concentration, as a function of precursor SO_2 (a, d, g), NO_x (b, e, h) and NH_3 (c, f, i) emission perturbation strength for European receptor regions, USA, India and China. Perturbations were applied over all European regions simultaneously.

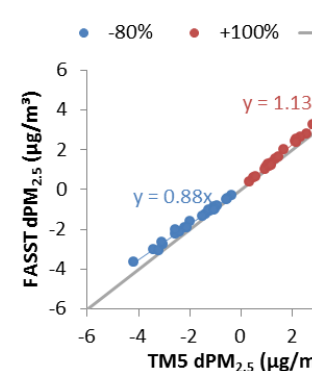


Linearity of SO₂, NO_x and NH₃ perturbation response



Deleted: PM2.5

Deleted: <object>



Deleted: <object><object><object>

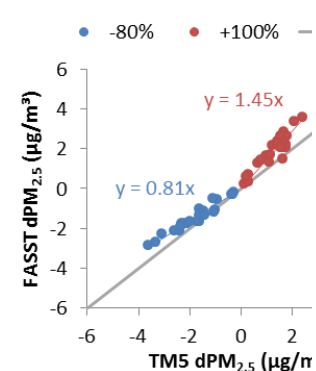


Figure 4: Regional Secondary PM_{2.5} (SO₄²⁻+NO₃⁻+NH₄⁺) response to -80% and +100% single precursor emission perturbations for SO₂ (a), NO_x (b), NH₃ (c) as well as the combined SO₂ + NO_x perturbation (d). X-axis: Full TM5 model; Y-axis: Linear extrapolation of -20% perturbation (FASST approach). Each point corresponds to the population-weighted mean concentrations over a receptor region.

Deleted: <object>

Deleted: <object><object><object>

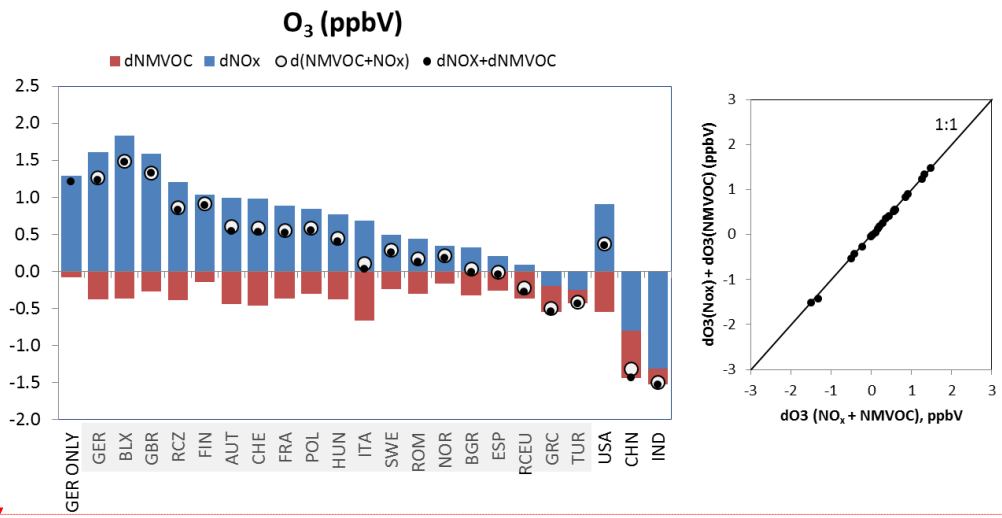
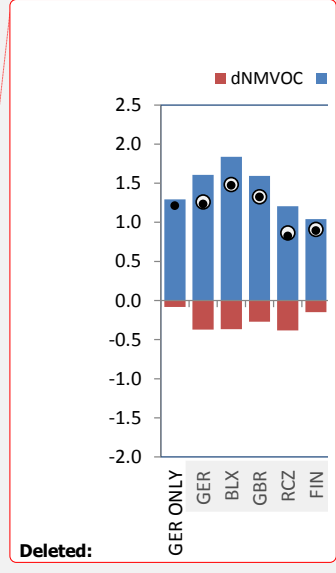


Figure 5: TM5-CTM response in annual mean population-weighted O₃ concentration (in ppbV) upon emitted precursor perturbation of -20% for selected source receptor regions. European regions were perturbed simultaneously. Red bar: **response from NMVOC-only perturbation (simulation P4)**; blue bar: **response from NO_x-only perturbation (simulation P3)**. Open circles: **response from simultaneous (NMVOC + NO_x) perturbation (simulation P5)**. Black dots: **sum of individual responses**. Shaded regions are perturbed simultaneously as one European region. **Right panel: scatter plot between O₃ response to combined and summed individual responses.**



Deleted:

Deleted: P3 + P4.

5

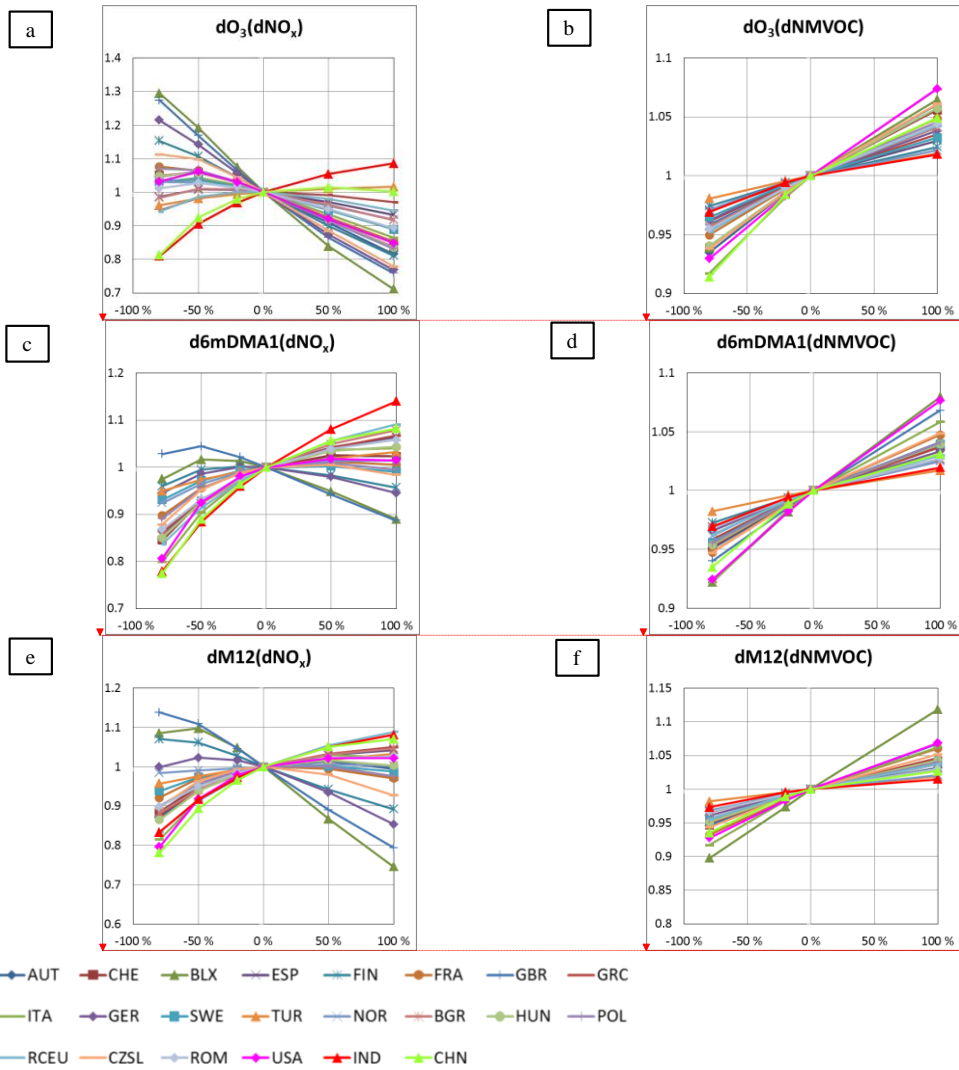
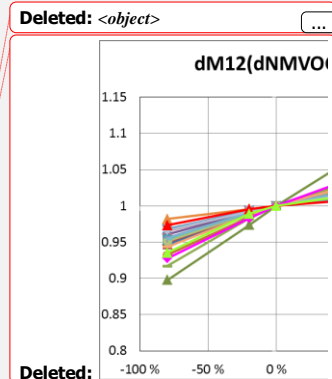
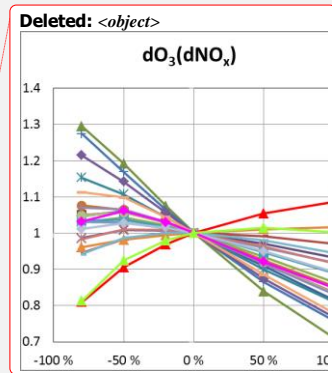


Figure 6: TM5-CTM response in population weighted annual mean O_3 (a, b) and health exposure metric 6mDMA1 (c, d), and in grid cell-area-weighted crop exposure metric M12 (e, f), relative to their respective base simulation values, as a function of precursors NO_x (a, c, e) and NMVOC (b, d, f) emission perturbation strength. European regions are perturbed simultaneously as one region.



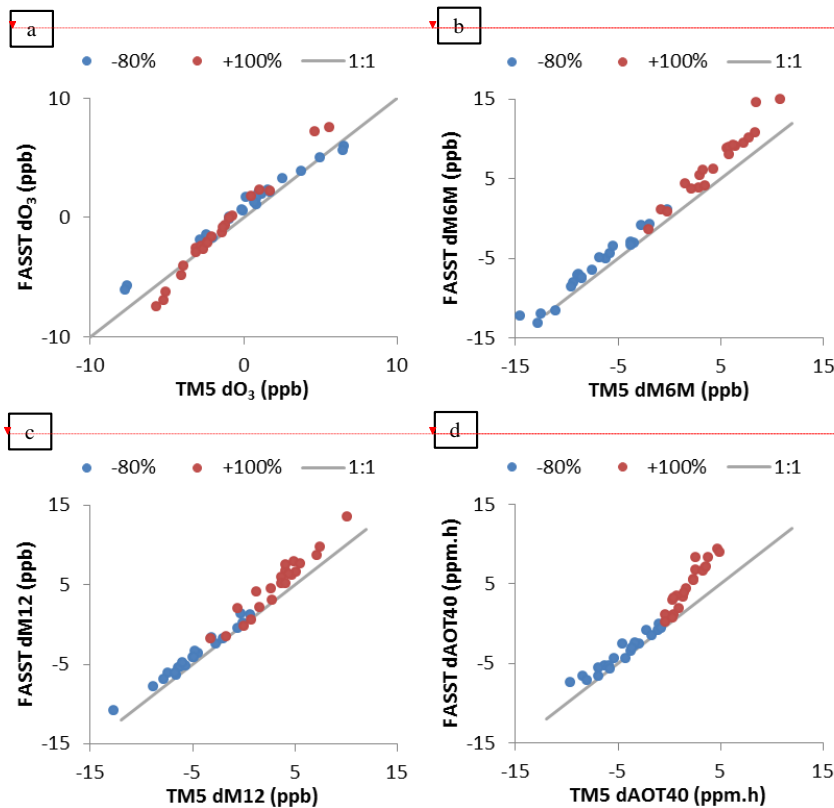
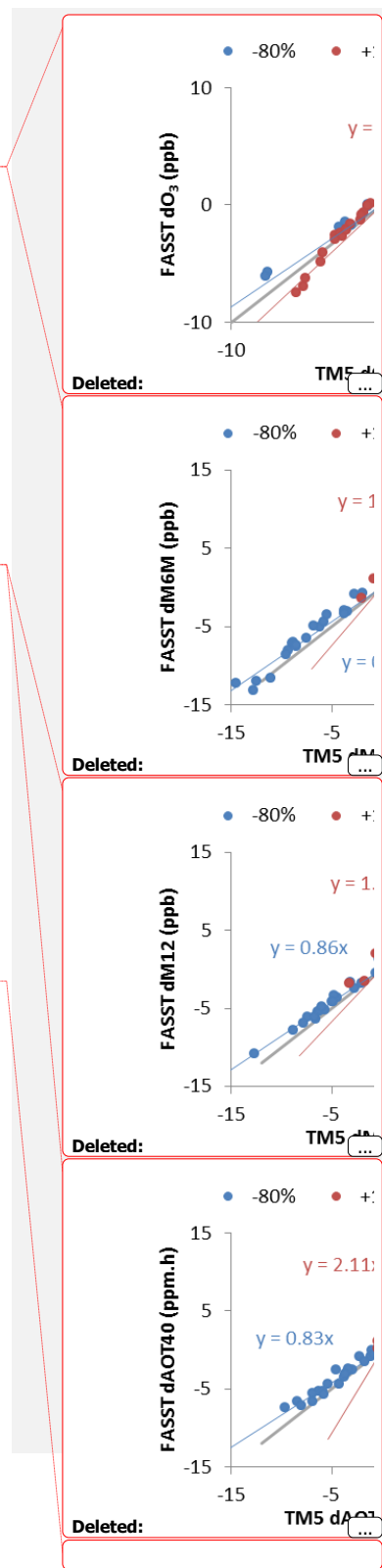


Figure 7: Regional O₃ and O₃ exposure metrics responses to combined -80% and +100% precursor emission perturbations of NO_x and NMVOC. (a) annual mean population-weighted O₃; (b) population-weighted ϕ mDMA1; (c) area-mean M12; (d) area-mean AOT40 X-axis: Full TM5 model; Y-axis: Linear extrapolation of -20% perturbation (FASST approach). Each point corresponds to the mean metric over a source region.



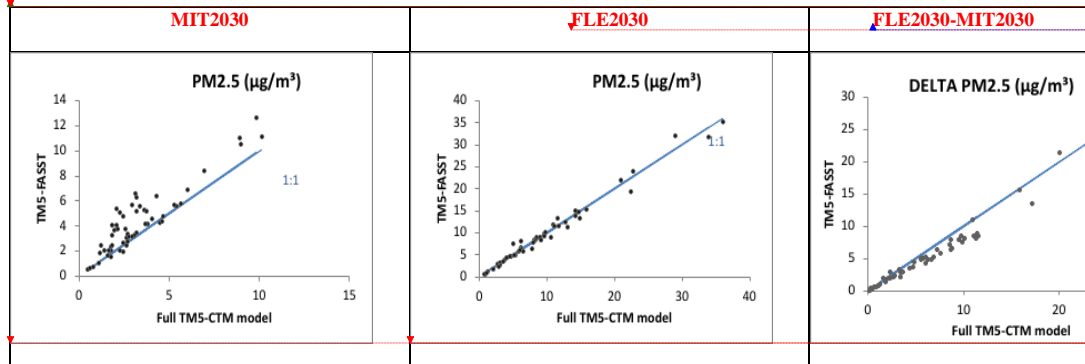
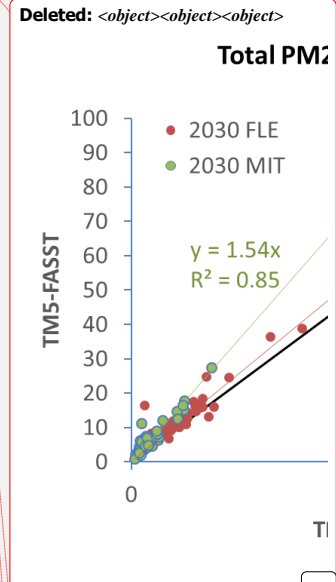


Figure 8: Population-weighted mean $PM_{2.5}$ concentration computed with TM5-FASST versus TM5-CTM for low emission scenarios MIT2030 (left), high emission scenario FLE2030 (middle) and the change between the two. Each point represents the population-weighted mean over a TM5-FASST receptor region. Blue line: 1:1 relation.

Moved down [10]: Each point represents the population-weighted mean over a TM5-FASST receptor region.



Deleted: Black line: 1:1 relation. breakdown for (b) primary (BC+POM+other primary $PM_{2.5}$) and ...

Deleted: <object>

Inserted Cells

Deleted: <object>

Deleted: <object>

Deleted: 9: Scatter plot of

Deleted: ozone (a, b) and exposure metric M6M (c, d) obtained by

Deleted: chemistry transport model (

Deleted:),

Deleted: a

Deleted: (MIT,

Deleted:) and

Deleted: (FLE, right)

Deleted: .

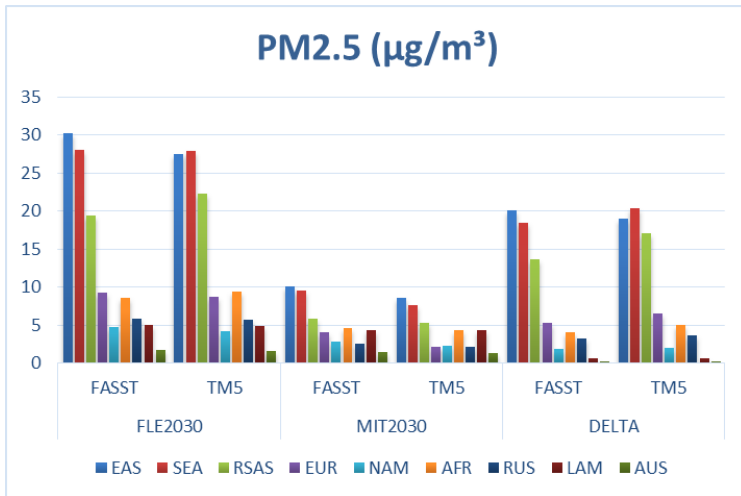


Figure 9 Total population-weighted anthropogenic $\text{PM}_{2.5}$ over larger FASST zoom areas, for the high (FLE2030) and low (MIT2030) emission scenarios, and the difference (delta) between both, computed with the full TM5 model and with FASST

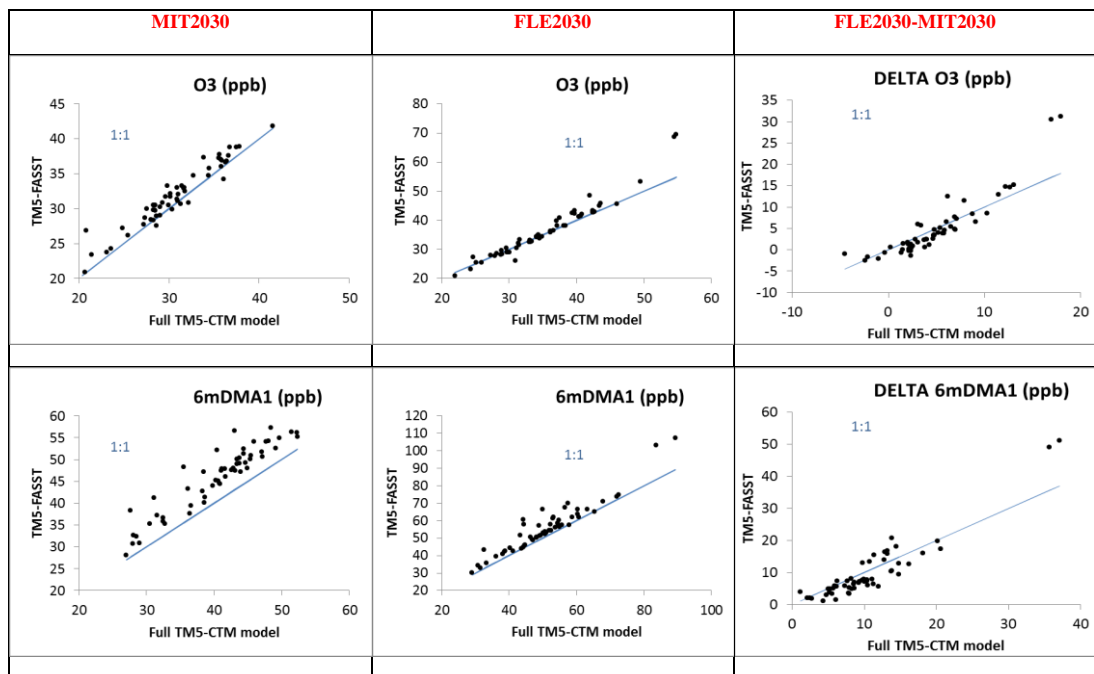


Figure 10: Population-weighted mean annual ozone (top) and ozone exposure metric 6mDMA1 (bottom) computed with TMS-FASST versus TMS-CTM for low emission scenarios MIT2030 (left), high emission scenario FLE2030 (middle) and the change between the two (right). Each point represents the population-weighted mean over a TMS-FASST receptor region. Blue line: 1:1 relation.

Moved (insertion) [10]

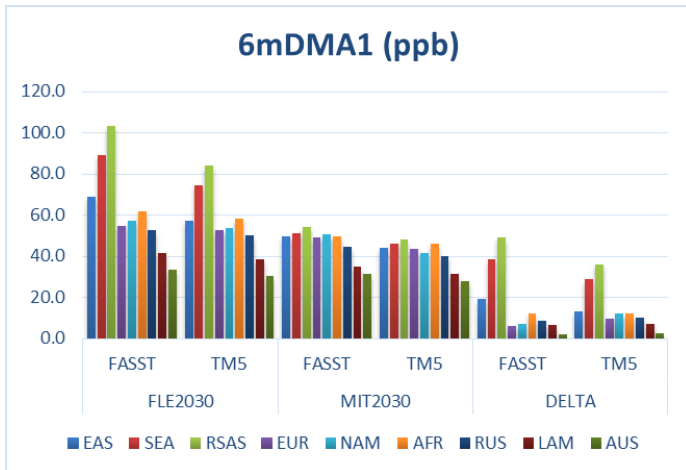


Figure 11: Total population-weighted anthropogenic PM_{2.5} over larger FASST zoom areas, for the high (FLE2030) and low (MIT2030) emission scenarios, and the difference (delta) between both, computed with the full TM5 model and with FASST

Premature mortalities from PM_{2.5}

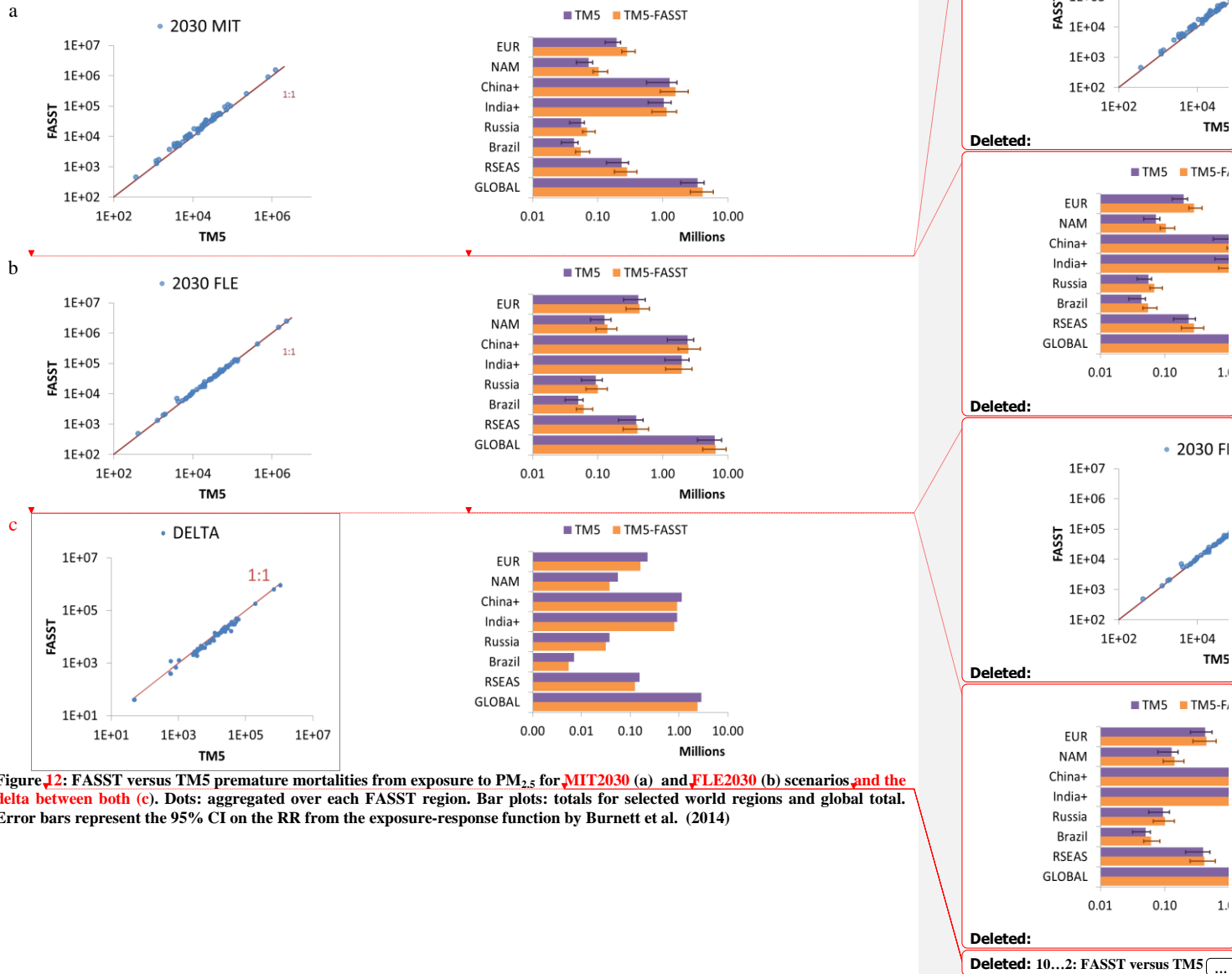


Figure J2: FASST versus TM5 premature mortalities from exposure to PM_{2.5} for MIT2030 (a) and FLE2030 (b) scenarios and the delta between both (c). Dots: aggregated over each FASST region. Bar plots: totals for selected world regions and global total. Error bars represent the 95% CI on the RR from the exposure-response function by Burnett et al. (2014)

Premature mortalities from O₃

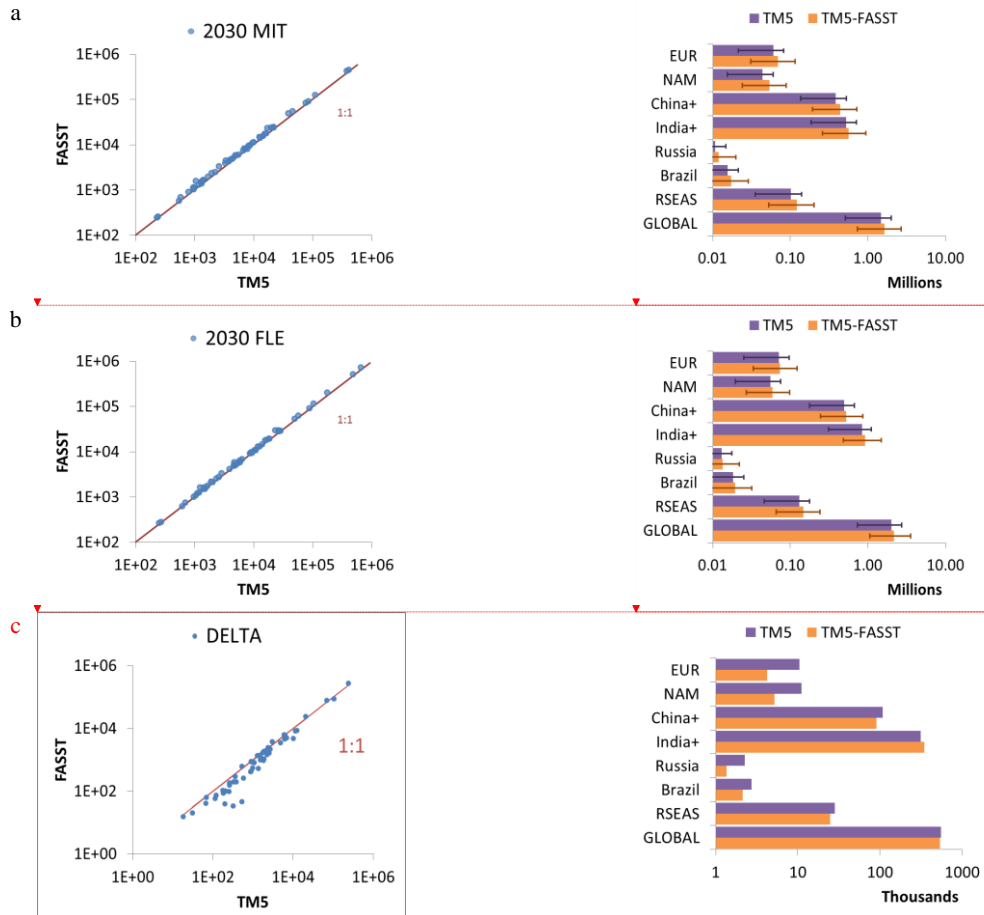


Figure J3: FASST versus TM5 premature mortalities from exposure to O₃ for **MIT2030** (a) and **FLE2030** (b) scenarios and the **delta between both** (c). Dots: aggregated over each FASST region. Bar plots: totals for selected world regions and global total. Error bars represent the 95% CI on the exposure-response function (Jerrett et al., 2009).

2030 M

Deleted:

2030 FI

Deleted:

Deleted: 11...3: FASST versus TMS

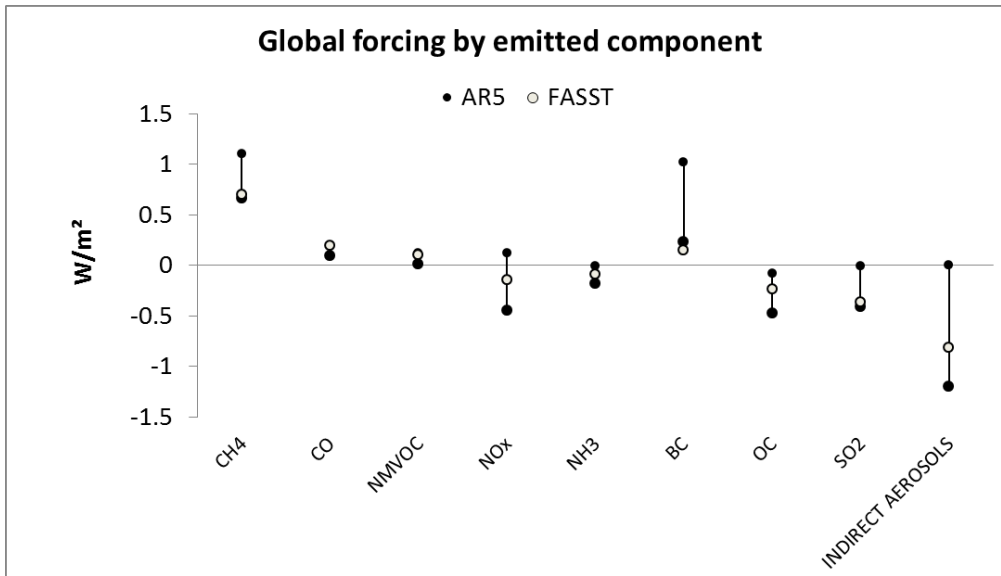


Figure 14: Global anthropogenic radiative forcing by emitted component, from TM5-FASST forcing efficiencies applied on RCP (year 2000 anthropogenic emissions), and range of best anthropogenic forcings from AR5 (change over period 1750 – 2011)

Deleted: 12

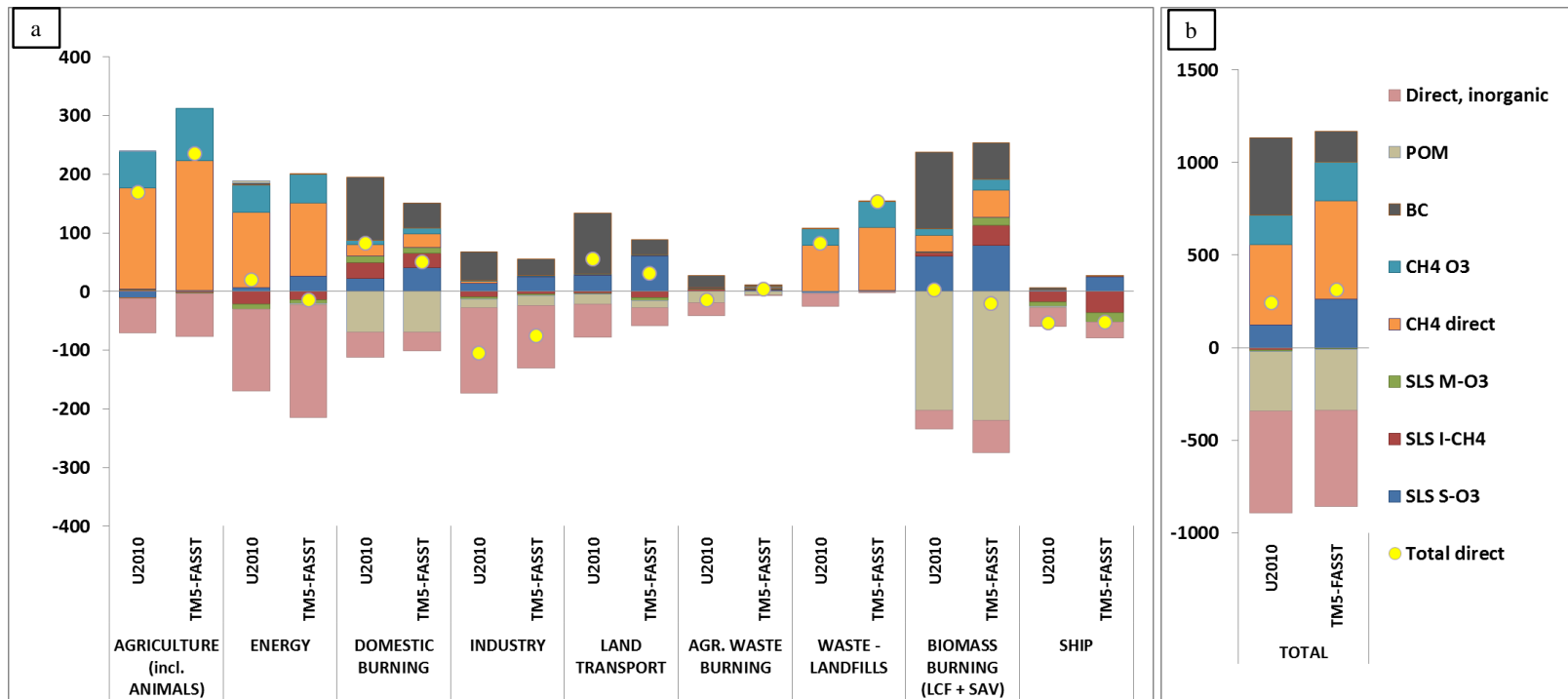


Figure 15: Year 2000 radiative forcing from Unger et al. (2010), based on EDGAR year 2000 emissions and from TM5-FASST applied to RCP year 2000 (a) break-down by sector and by forcing component, Biomass burning includes both large scale fires and savannah burning; (b) total over all sectors. SLS S-O₃: direct contribution of short-lived species (SLS) to O₃; SLS I-CH₄: indirect contribution from SLS to CH₄; SLS M-O₃: indirect feedback from SLS on background ozone via the CH₄ feedback. CH₄ O₃: feedback of emitted CH₄ on background O₃

Deleted: 13

Deleted: ; (b) total over all

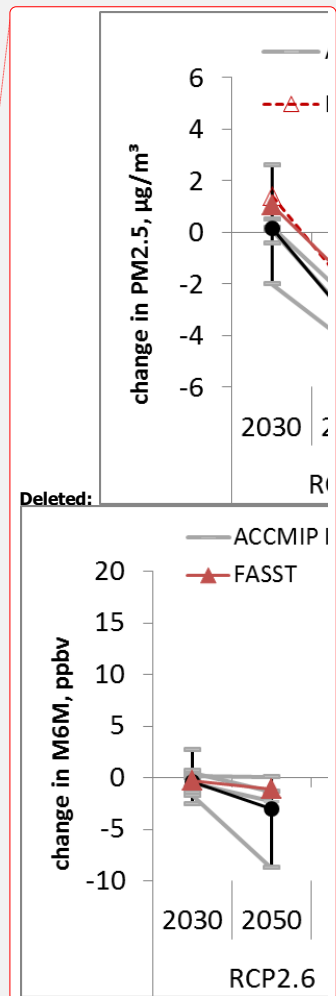
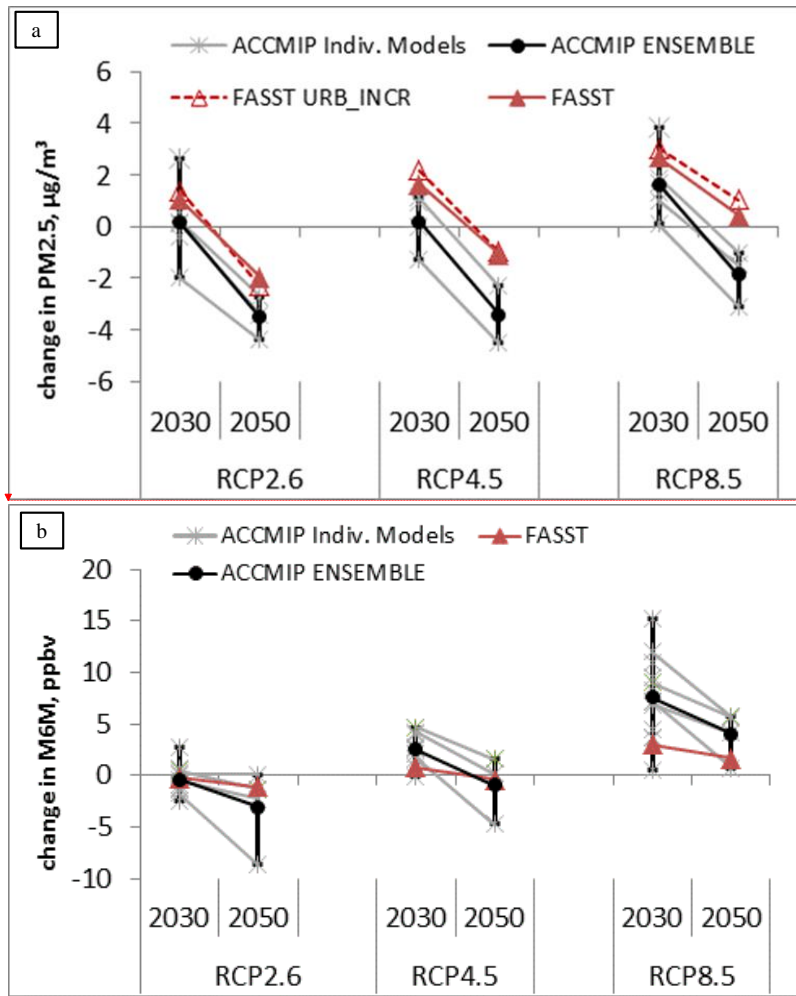


Figure 16: Global population-weighted differences (scenario year minus year 2000) (a) in annual mean PM_{2.5} concentrations and (b) in O₃ exposure metric **6mDMA1** for 3 RCP scenarios in each future year, from the ACCMIP model ensemble (Silva et al., 2016) (black symbols and lines) and TM5-FASST_v0 (red symbols and lines). FASST URB_INCR: including the urban increment correction. Grey symbols: results from individual ACCMIP models. Grey lines connect results from a single model. Not all models have provided data for all scenarios. ACCMIP error bars represent the range (min, max) across the ACCMIP ensemble.

Deleted: 14
Deleted: M6M

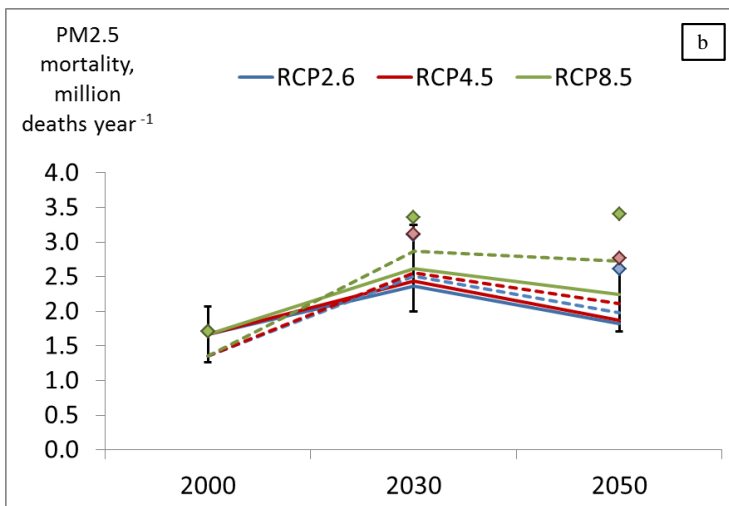
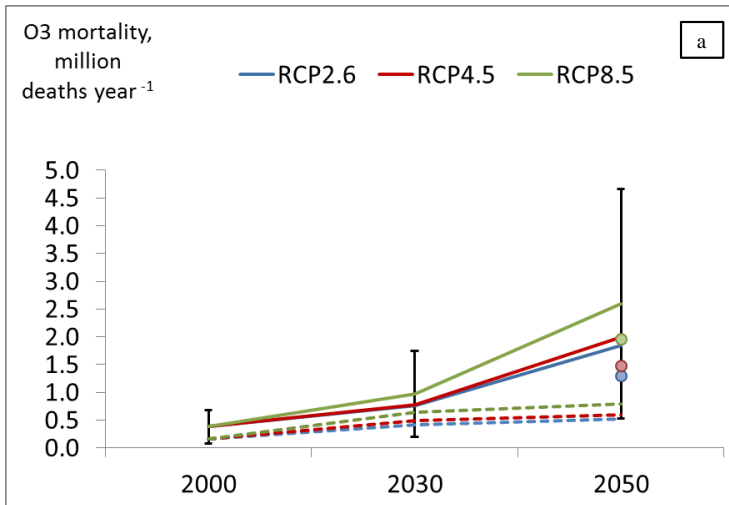


Figure 17. Trends in global burden on mortality of ozone (a) and PM_{2.5} (b) from year 2000 to 2050 from the ACCMIP multi-model ensemble (Silva et al., 2016) (full lines) and TM5-FASST (dashed lines) for 3 RCP scenarios. The error bar on the year 2000 is the ACCMIP 95% CI including uncertainty in RR and across models. CI for 2030 and 2050 were not provided by ACCMIP, we use here the same relative error as for year 2000. Dots (O₃ mortality): adjusted TM5-FASST ozone mortalities for RCP 2050, using baseline respiratory mortalities consistent with Silva et al. (2016). Diamonds (PM_{2.5} mortality): TM5-FASST estimate including the urban increment parameterization

Deleted: 15

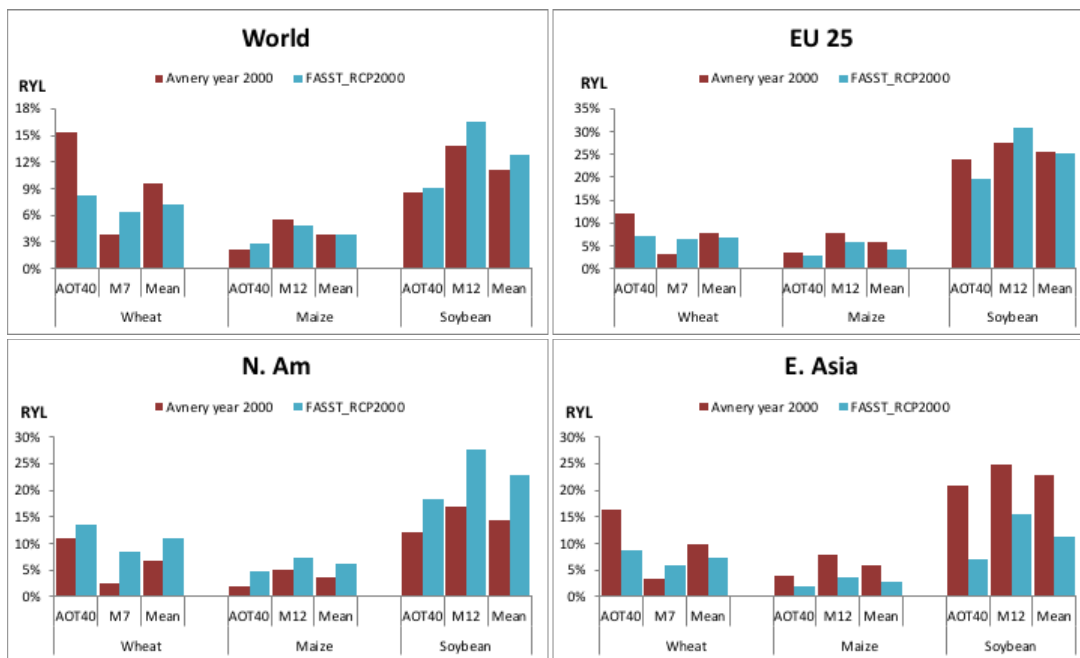


Figure 18: Year 2000 global and regional ozone-induced relative yield losses in 4 world regions for 3 major crops, from Avnery et al. (2011) and from TM5-FASST (RCP year 2000), estimated from the 2 common exposure metrics M7 and AOT40 (see text), as well as the mean of both.